Molecular Characterization of Biological Rhythms in the beach amphipod *Talitrus saltator* (Montagu)

Laura Sophie Hoelters 2018

As thesis submitted at the Institute of Biological, Environmental and Rural Sciences (Aberystwyth University), for the degree of Doctor of Philosophy.

Declaration

Word count of thesis: 39.837

This work has not previously been accepted in substance for any degree and is not being concurrently submitted in candidature for any degree.

Signed……...(candidate) Date: 07.10.2018

STATEMENT 1

This thesis is the result of my own investigations, except where otherwise stated. Where correction services have been used, the extent and nature of the correction is clearly marked in a footnote(s).

Other sources are acknowledged by footnotes giving explicit references. A bibliography is appended.

Signed……...(candidate) Date: 07.10.2018

STATEMENT 2

I hereby give consent for my thesis, if accepted, to be available for photocopying and for inter-library loan, and for the title and summary to be made available to outside organisations.

Signed…….. (candidate) Date: 07.10.2018

Acknowledgements

My first and foremost thanks goes to Dr David Wilcockson for supervision, project development and experimental ideas. The supervision was characterized by constant fair support, freedom of work and ideas, teaching in rational thinking and science practice as well as a deeply rooted knowledge in the field. I highly appreciate the guidance on treading the path of a researcher.

I also thank Prof. Dr Karl Hoffman for secondary supervision and inspiring science conversations.

During my collaboration with Università degli Studi di Firenze (Florence University, Italy), Prof. Dr Alberto Ugolini provided friendly guidance and support, which I am thankful for. I was impressed with his inventive genius and his lifelong dedication to his research and deep knowledge in his field. Here, special thanks also goes to Alice, Anna-Maria and Linda for help with collecting sandhoppers.

Thank you Eli, Alun, Rory, Joseph, Martin, Martin, Andrew, Nathan and Joanna for being such excellent colleagues, teachers and co-workers.

Naturally, I am also grateful to my peer IBERS PhD students, the great people in my office(s) who made my everyday work even more fun and easy.

I also thank the ISTM (Karlsruhe Institute of Technology) for being my friends and office mates while writing the thesis.

Obviously, I also want to thank DCDS and Aberystwyth University for funding my thesis and for giving me the possibility to work in their laboratories.

I thank my extended family for substantial interest in my work, continuous encouragement and support. Especially I thank my mother for taking care of my daughter Sophia during the time while I completed writing.

My very personal gratitude is also due to my husband Tobias, who was my ‘rock in the waves’. Thank you for never stopping to believe in me.

To my daughter.

Summary

The supralittoral sandhopper, *Talitrus saltator* (Montagu, 1808) exhibits prominent circadian behavioural phenotypes such as locomotor activity rhythm and time-compensated celestial navigation. To investigate the molecular underpinnings of these behaviours, a circadian transcriptome was assembled from time-series RNA-seq data with template from brain tissue samples. Rhythmically expressed clock and clock- associated genes were identified and compared to homologous sequences in the literature. Investigating the time-compensation aspect of *Talitrus* navigation, evidence for an anatomically discrete antennal moon compass clock was discovered while solar orientation was found to be antennae independent. Further, the time-compensation mechanism of solar navigation and rhythmic locomotor activity is likely linked to clock gene expression as molecular and behavioural phenotypes agree. Immunohistochemical staining indicated at least four neurons as potential central pacemaker cells in the cerebral ganglia. The circadian clock output was also researched through analysing 'crustacean hyperglycaemic hormone' (CHH) which was- contrary to other crustaceans- not expressed rhythmically in the brain. Immunolocalisation of CHH protein and mRNA confirm distinct staining patterns in agreement with findings in the literature. The present thesis connects molecular data with behavioural phenotypes and provides clear progress in the research of biological rhythms in arthropods.

Table of contents

Declaration ii
Acknowledgements iii
Summary v
List of Abbreviations 9
List of Figures 12
List of Tables 14
CHAPTER 1: GENERAL INTRODUCTION 1
1.1 BIOLOGICAL CLOCKS 1
1.2 BIOLOGICAL RHYTHMS IN MARINE ENVIRONMENTS 2
1.3 MOLECULAR BASIS OF CIRCADIAN CLOCKS 7
1.4 *TALITRUS SALTATOR* BIOLOGY 9
1.5 OBJECTIVES 11
CHAPTER 2: GENERAL METHODS 13
2.1 ANIMAL HUSBANDRY 13
2.2 LOCOMOTOR ACTIVITY MEASUREMENT 13
2.3 RNA EXTRACTION 14
2.4 REVERSE TRANSCRIPTION (RT) 14
2.5 POLYMERISE CHAIN REACTION (PCR) 15
2.6 AGAROSE GEL ELECTROPHORESIS 15
2.7 5' AND 3' RAPID AMPLIFICATION OF CDNA ENDS (RACE) PCR 15
2.8 CLONING 17
2.9 SEQUENCING 17
2.10 SEQUENCE ANALYSIS 18
2.11 QUANTITATIVE REAL-TIME PCR (qRT-PCR) 18
2.12 IMMUNOLOCALISATION OF PEPTIDES 20
CHAPTER 3: CIRCADIAN TRANSCRIPTOME AND CLOCK GENE SEQUENCING 22
3.1 ABSTRACT 22
3.2 INTRODUCTION 22
3.2.1 Circadian transcriptome sequencing 22
3.2.2 The invertebrate circadian clock 23
3.2.3 Objective 31
3.3 MATERIALS AND METHODS 31
3.3.1 Locomotor activity measurement 31
3.3.2 Tissue harvest and RNA extraction 31
3.3.3 Sequencing 33
3.3.4 Sequence confirmation 33
3.3.5 De novo transcriptome assembly 34
3.3.6 Full length sequence confirmation of core clock genes 35
3.3.7 Functional annotation with Blast2GO 36
3.3.8 Quantification of mRNA transcripts 36
3.3.9 Identification of rhythmically expressed transcripts 37
3.3.10 Sequence analysis software 37
3.4 RESULTS 38
3.4.1 Locomotor activity rhythm 38
3.4.2 Transcriptome sequencing and assembly 39
3.4.3 Functional annotation of contigs 39
3.4.4 Analysis of putative clock gene protein sequences 49
3.4.5 Identification of rhythmically expressed transcripts 59
3.5 DISCUSSION 65
3.5.1 The *T. saltator* circadian transcriptome 65
3.5.2 Identified clock and clock-associated genes 65
3.5.3 Rhythmically expressed transcripts 70

3.6 SUMMARY 71
CHAPTER 4: CELESTIAL NAVIGATION AND CLOCK GENE EXPRESSION 72
4.1 ABSTRACT 72
4.2 INTRODUCTION 72
4.2.1 Solar navigation in *T. saltator* 72
4.2.2 Lunar orientation in *T. saltator* 75
4.2.3 Objective 76
4.3 MATERIALS AND METHODS 76
4.3.1 Animal collection 77
4.3.2 Activity measurement 77
4.3.3 Escape (orientation) behavior 77
4.3.4 Antennal manipulation 79
4.3.5 Clock gene expression analysis 79
4.4 RESULTS 81
4.4.1 Locomotor activity 81
4.4.2 Orientation behaviour 82
4.4.3 Clock gene mRNA expression 85
4.5 DISCUSSION 88
4.5.1 Clock gene expression and orientation shifts 88
4.5.2 A putative extra-cerebral lunar clock in the antennae 89
4.6 SUMMARY 93
CHAPTER 5: IMMUNOLOCALISATION OF CENTRAL PACEMAKER CELLS IN *T. SALTATOR* BRAINS 94
5.1 ABSTRACT 94
5.2 INTRODUCTION 94
5.2.1 The core clock component Period 94
5.2.2 Invertebrate central pacemaker 95
5.2.3 T. saltator core clock component Period 97
5.3 MATERIALS AND METHODS 98
5.3.1 Production of the TalPER antiserum 98
5.3.2 Animal sampling protocol 99
5.3.3 Whole mount immunofluorescent staining of *T. saltator* brains 99
5.3.4 Image acquisition and analysis 100
5.4 RESULTS 100
5.4.1 Production of antisera 100
5.4.2 Immunofluorescent labelling of TalPER cerebral ganglia 101
5.4.3 Diurnal rhythm of TalPER immunoreactivity 103
5.5 DISCUSSION 104
5.5.1 TalPER immunohistochemical staining of cerebral ganglia 104
5.5.2 Diurnal rhythms of Period transcript and protein abundance 105
5.6 SUMMARY 107
CHAPTER 6: CHARACTERISATION AND TEMPORAL EXPRESSION OF CRUSTACEAN HYPERGLYCAEMIC HORMONE 108
6.1 ABSTRACT 108
6.2 INTRODUCTION 108
6.2.1 Crustacean hyperglycaemic hormone 108
6.2.2 Characteristics of the CHH transcript and protein sequences 109
6.2.3 CHH release and receptor mechanism 110
6.2.4 CHH physiological effects 111
6.2.5 CHH as a circadian clock controlled gene? 112
6.2.6 Objective 113
6.3 MATERIALS AND METHODS 113
6.3.1 Animal behaviour 113
6.3.2 Obtaining *T. saltator* neural RNA 113
6.3.3 *Talchh* full length sequencing 114

6.3.4 Quantification of *Talchh* mRNA transcripts 115
6.3.5 Histological description of *Talchh* transcripts though *in situ* hybridization 116
6.3.6 Immunolocalisation of CHH 118
6.4 RESULTS 119
6.4.1 CHH transcript characterization 119
6.4.2 Locomotor activity analysis 121
6.4.3 Temporal expression of neural CHH mRNA 121
6.4.4 Histological description of CHH mRNA and protein 122
6.5 DISCUSSION 125
6.5.1 CHH transcript sequencing 125
6.5.2 CHH immunoreactivity in cerebral ganglia 127
6.5.3 Temporal expression of CHH mRNA in the brain 129
6.6 SUMMARY 131
CHAPTER 7: GENERAL DISCUSSION 132
7.1 CIRCADIAN CLOCK GENE EXPRESSION IN *T. SALTATOR* 132
7.2 CLOCK PROTEINS IN *T. SALTATOR* 136
7.3 CLOCK CONTROLLED GENES IN *T. SALTATOR* 137
7.4 LOCOMOTOR ACTIVITY RHYTHM 137
7.5 CELESTIAL COMPASS NAVIGATION 138
7.6 SUMMARY 139
References 141
APPENDIX A 174
Additional Figures and Tables 174
APPENDIX B 187
Buffers and Solutions 187
APPENDIX C 189
List of Origins (consumables) 189

List of Abbreviations

aa	amino acid(s)
ANOVA	analysis of variance
ATP	adenosine-5’-triphosphate
BCIP	5-bromo-4-chloro-3-indolyl phosphate
bHLH	basic helix-loop-helix
BLAST	basic local alignment search tool
bp	base pair(s)
cAMP	cyclic adenosine monophosphate
CCD	charge coupled device
ccg	clock controlled gene(s)
CCP	clock controlled protein(s)
cDNA	complementary DNA
CHH	crustacean hyperglycaemic hormone
°C	degrees celsius
cm	centimetre
CNS	central nervous system
CPRP	CHH precursor related peptide
cRNA	complementary RNA
CT	circadian time
C-terminus	carboxyl-terminus
CTFT	corrected total cellular fluorescence
CTP	cytidine-5’-triphosphate
d	days
DA	dopamine
DAB	Diaminobenzidine
DAM	drosophila activity monitor
DC	deuterocerebrum
DD	constant darkness
DEPC	diethylpyrocarbonate
DNA	deoxyribonucleic acid
dNTP	nucleoside triphosphate
DTT	dithiothreitol
DVM	diel vertical migrations
EDTA	ethylenediaminetetraacetic acid
ELISA	enzyme-linked immunosorbent assay
EP	eye peduncle
EtOH	ethanol
FAD	flavin adenine dinucleotide
g	gram
g	gravitational force
Gb	gigabase

gDNA	genomic DNA
GO	gene ontology
GPCR	G-protein-coupled peptide receptor
GSP	gene specific primer
GSP N	Nested GSP
GTP	guanosine-5’-triphosphate
HiFi	high fidelity (proof-reading) DNA polymerase
HP	hepatopancreas
HPLC	high performance liquid chromatography
hr	hour
hrs	hours
Hz	Hertz
IHC	immunohistochemistry
IPTG	isopropyl β-D-1-thiogalactopyranoside
kb	kilobases
kDa	kilodaltons
L	litre
LB	Luria broth
LD	light / dark
LL	constant light
l-LNV	large ventral lateral neuron
LND	dorsal lateral neuron
max	maximum
µ	micro
min	minutes
mL	millilitre
mm	millimetre
mM	millimolar
mRNA	messenger RNA
NBT	nitro blue tetrazolium
NCBI	National Centre for Biotechnology Information
NES	nuclear export signal
ng	nanogram
NGS	next generation sequencing
NLS	nuclear localisation signal
nm	nanometre
nt	nucleotide
N-terminus	amino-terminus
Oes	oesophageal orifice
ON	over night
PAGE	polyacrylamide gel electrophoresis
PAS	Per-Arnt-Sim
PBS	phosphate buffered saline

PC	personal computer
PCR	polymerase chain reaction
PCRM	protocerebrum
PDF	pigment-dispersing factor
PDH	pigment-dispersing hormone
PPRP	PDH precursor related peptide
PTX	PBS with Triton X-100 (see APPENDIX B)
qRT-PCR	quantitative real-time, reverse transcription
R^2	coefficient of determination
RACE	rapid amplification of cDNA ends
RLM-RACE	RNA ligase-mediated RACE
RNA	ribonucleic acid
RNA-seq	RNA-sequencing
rpm	revolutions per minute
RT	reverse transcription
SBS	sequencing by synthesis
ssRNA	singel stranded RNA
SCN	suprachiasmatic nucleus
SCNi	suprachiasmatic nuclei
SDS	sodium dodecyl sulphate
sec	seconds
SEM	standard error of the mean
SG	sinus gland
s-LNV	small ventral lateral neuron
SNP	single nucleotide polymorphism
SOC	super optimal broth with catabolite repression
t	period length
Taq	*Thermus aquaticus*
temp	temperature
U	enzyme unit
UTP	uridine-5'-triphosphate
UTR	untranslated region
V	volts
v/v	volume / volume
W	watt
w/v	weight / volume
X-gal	5-bromo-4-chloro-indolyl-β-D galactopyranoside
XO	X-organ
XOSG	X-organ sinus gland complex
ZT	Zeitgeber time

List of Figures

Figure 1.1: Basic model of the circadian core clock feedback-loop…..... 8
Figure 2.1*:* Activity monitor for *T. saltator*.……...….. 14
Figure 3.1: Model of the *Drosophila* central feedback-loop……..….. 24
Figure 3.2: Mechanism of CRY1 induced TIM degradation……..….. 25
Figure 3.3: Regulation of PER:TIM subcellular location…..……..….. 26
Figure 3.4: PDP1 and VRI feedback loop……..……..… 26
Figure 3.5: Overview of the mechanism of clock-associated gene functions..... 38
Figure 3.6: Schematic drawing of the *D. plexxippus* clock feedback-loop…… 30
Figure 3.7: Sampling scheme with the circadian and the external (local) solar time of tissue collection…..…….. 32
Figure 3.8: Sampling scheme for RNA extraction……..…..... 33
Figure 3.9: Trinity processing pipeline.……..….. 35
Figure 3.10: Locomotor activity rhythms of *T. saltator* in DD.…….. 39
Figure 3.11: Species distribution chart.…….…….. 40
Figure 3.12: Sequence similarity distribution of the Blast2GO analysis…. 41
Figure 3.13: E-value distribution chart.……... 42
Figure 3.14: GO-level distribution.……...……...… 43
Figure 3.15: Distribution of GO level 2 terms for the category “Molecular Function……. 44
Figure 3.16: Distribution of GO level 2 terms for the category “Biological Process”…….……... 44
Figure 3.17: Distribution of GO level 2 terms for the category “Cellular Component”……...……..…… 45
Figure 3.18: Direct GO Count “Molecular Function” (MF).……... 46
Figure 3.19: Direct GO Count for “Biological Process” (BP).…… 47
Figure 3.20: Direct GO count for “Cellular Component” (CC)……... 48
Figure 3.21: Schematic representation of the *T. saltator* core clock protein sequences…….……. 52
Figure 3.22: TalCRY2 sequence…….……. 52
Figure 3.23: TalPER sequence derived from the Blast2GO analysis.……. 53
Figure 3.24: Translated *Taltim* contig identified via Blast2GO analysis.… 54
Figure 3.25: TalBMAL1/CYC sequence.……..…….. 55
Figure 3.26: TalCLK partial sequence……. 55
Figure 3.27: Heat maps of the circadian transcriptome……... 62
Figure 3.28: Expression dynamics of core clock and clock associated gene transcripts over a 24 hr DD period…….……..…… 65
Figure 4.1: Setup of orientation experiments…….…….. 79
Figure 4.2: Tissue collection scheme and experimental pipeline……..... 81

Figure 4.3: Orientation behaviour of *T. saltator* at solar midday……... 84
Figure 4.4: Lunar orientation behaviour under antennal manipulation….. 85
Figure 4.5: Cock gene mRNA levels in behaviourally rhythmic *T. saltator* brains……... 86
Figure 4.6: Clock gene mRNA levels in antennae of behaviourally rhythmic *Talitrus*…….. 88
Figure 5.1: Schematic, simplified drawing of the *Drosophila* brain with clock cells and respective neuronal projections……..... 97
Figure 5.2: TalPER positive neurons in the *T. saltator* brain…….. 103
Figure 5.3: Schematic drawing of TalPER positive neurons in *T. saltator* cerebral ganglia……. 105
Figure 5.4: Analysis of diurnal TalPER staining intensity in cerebral ganglia……... 106
Figure 5.5: Period mRNA and protein levels in *T. saltator* brains……..... 108
Figure 6.1: Schematic depiction of the *T. saltator* CHH mRNA transcript 122
Figure 6.2: *T. saltator* CHH cDNA sequence..…….…….. 123
Figure 6.3: *T. saltator* activity rhythms……... 124
Figure 6.4: CHH transcript abundance in the brain quantified with qRT-PCR……..... 125
Figure 6.5: Immunolocalisation of the CHH peptide in *Talitrus* cerebral ganglia……... 126
Figure 6.6: Alignment of mature CHH peptide sequences of *T. saltator* and *E. pulchra*……..…. 128
Figure 6.7: Phylogenetic analysis of CHH peptide sequences determined from brain or eyestalk tissue.…… 130
Figure 7.1: Schematic drawing of the *T. saltator brain*..…… 140

List of Tables

Table 2.1: PCR cycling conditions……. 15
Table 3.1: Summary of Blast2GO results……..... 49
Table 3.2: Contigs coding for clock genes in *T. saltator*…… 51
Table 3.3: Proportion of rhythmically expressed mRNA contigs in *the T. saltator* transcriptome according to JTK_cycle analysis…….. 60
Table 3.4: Summary of the core clock and clock associated gene transcripts rhythmicity analyses……..…….. 64
Table 5.1: Peptide sequences used for production of antisera…… 99
Table 5.2: Immunization protocol the rabbits were treated with to receive TalPER antisera.……... 99
Table 5.3: Quality and quantity assessment of the two TalPER antisera…… 102

Wer von einer echten Liebe zum Naturstudium, und von der erhabenen Würde desselben beseelt ist, kann durch nichts entmutigt werden, was an eine künftige Vervollkommnung des menschlichen Wissens erinnert. Ein Versuch, die Natur lebendig und in ihrer erhabenen Größe zu schildern, in dem wellenartig wiederkehrenden Wechsel physischer Veränderlichkeit das Beharrliche aufzuspüren, wird daher auch in späteren Zeiten nicht ganz unbeachtet bleiben.

Alexander von Humboldt (1769–1859), Kosmos- Entwurf einer physischen Weltbeschreibung

The one who is ensouled by a true love for the study of nature and the sublime dignity of the very same, can not be discouraged to achieve what bears resemblance of a future completion of human knowledge. An attempt to describe nature in its lively and exalted greatness, to trace the persistent in its wave like reoccurring change in physical variability, will not be completely disregarded in later times.

Alexander von Humboldt (1769–1859), Cosmos- A Sketch of the Physical Description of the Universe

CHAPTER 1: GENERAL INTRODUCTION

1.1 BIOLOGICAL CLOCKS

The diverse and vast marine and coastal habitat is characterised by rhythmic changes of the environment that impose remarkable challenges on organisms living there. For example inundation, hydrostatic pressure, humidity and salinity can dramatically differ over a tidal cycle. Superimposed on these tidal changes are daily differences in temperature and light intensity. Moreover, intertidal habitats in temperate regions are further complicated by seasonal fluxes in photoperiod and temperature as well as other climatic variables (Tessmar-Raible *et al.*, 2011; Bulla *et al.*, 2017). Organismal adaptations to these changes are vital and the anticipation of reoccurring environmental changes seems to be a crucial requirement for survival which is thought to be the driving factor for the evolution of biological clocks (Dodd *et al.*, 2005; Vaze and Sharma, 2013; Kaiser *et al.*, 2016; Pollak *et al.*, 2017).

Biological clocks pervade all life and are thought to have evolved as an energy storage mechanism in photosynthetic organisms. Photosynthetic activity is tightly coupled with the clock to optimally utilize the period of sunlight (Reitzel *et al*., 2013, Rothschild, 1994; Axmann *et al.*, 2014). Over the course of a solar day, energy storages are progressively filled up and depleted during the night when no sunlight is available for energy production. This leads to rhythmic, solar-driven molecular changes in the cell. Biological clocks can be set 'in phase' (entrained) to external environmental cues through so called Zeitgeber (German: Zeit~time; geber~giver)(Aschoff, 1954) -such as light, temperature and food availability. In constant conditions, a biological clock will free-run with a period closely resembling natural entrainment conditions and continue to do so resembling a self-sustained oscillator (Dunlap, 1999). As almost everywhere on the planet, light availability changes with earth rotation and temperature rises and falls with sunrise and sunset. Following this, biological clocks in the terrestrial realms tend to run with a 24 hour (hr) rhythm which are deemed circadian clocks (latin: circa~ about; diem~ a day) (Halberg *et al.*, 2003) whilst in the intertidal of the marine environment, both daily and circatidal and lunar derived rhythmic phenotypes are observed.

Circadian rhythms are the most prominently researched. Internally, rhythmic

behaviour is governed by a central clock reflecting a self-sustained oscillator that can be entrained by environmental factors and is governed by expression and degradation patterns of so called 'clock genes'. These orchestrate a transcriptional-translational feedback loop, resulting in rhythmic patterns of transcript abundance(Tomioka and Matsumoto, 2010). The core oscillatory system further orchestrates the expression of so called "clock controlled genes" (ccg) that regulate physiological functions thereby driving rhythmic behaviour (Taghert and Shafer, 2006). Under constant conditions, one cycle is called a period, or tau (t). Clock genes are highly conserved among phylogeny with the major invertebrate clock genes (derived from the fruit fly model) are *period (per), cryptochrome (cry), cycle (cyc), clock (clk) and timeless (tim)* (Stanewsky, 2002). Clock gene homologues from other taxa have been identified and their involvement in behavioural and physiological output is under investigation (Young and Kay, 2001; Sandrelli *et al.*, 2008; Tomioka and Matsumoto, 2010).

Moreover, and apart from the prominent circadian rhythms, lunar rhythms have lately come into focus. Endogenous rhythms in accordance with the lunar day (24.8 hours), lunar or synodic month (29.5 days) are now being intensely investigated. Circatidal rhythms have been reported for many inhabitants of the intertidal zone reoccurring with a 12.4 hours (hrs) period and which are strongly interlinked with lunar constellations (Naylor, 2013). Further, circannual rhythms occur with a period of 365 days and are very prominent in the animal and plant kingdoms (Strauss and Dircksen, 2010; Hut and Beersma, 2011; Naylor, 2013).

1.2 BIOLOGICAL RHYTHMS IN MARINE ENVIRONMENTS

The terrestrial realm is replete with examples of overt daily phenotypes, both nocturnal and diurnal. In contrast to terrestrial habitats where the predominant, rhythmic abiotic factors are light and temperature that invariably cycle with a 24 hr period, marine habitats are also prone to changes in water levels, hydrostatic pressure, humidity, salinity, oxygen tension, pH etc. that drastically differ depending on the tidal state (Morgan, 1991). For photosynthetic marine organisms, circadian regulation of behaviour is closely linked to energy extraction and the related cellular components are regulated accordingly. The Marine dinoflaggelate *Gonyaulax polyedra* exhibits a circadian rhythm in the catalytic activity of nitrate reductase with peak activity at

midday (Ramalho *et al*., 1995). Similarly, green algae and diatoms, synchronize their cell division in a circadian manner (Harding and Heinbokel, 1984; Escande, 2010). Even in comparably simple organisms such as the bioluminescent *Gonyaulax* biological rhythms and underlying clocks can be complex. Here, two separate circadian oscillators are present; a circadian rhythm in luciferase activity driven bioluminescence (blue light responder) is separate from swimming behaviour where both features are responding to different electromagnetic wavelengths and can be manipulated by according light regimes (Bae and Hastings, 1994; Roenneberg and Taylor, 1994; Roenneberg, 1995). More complex metazoans from plankton to megafauna display rhythmic phenotypes that occur on a 24 hr cycle, phased to the solar (or possibly lunar) day (Naylor, 1985; Aguzzi *et al.*, 2011; van Ooijen *et al.*, 2013; Bulla *et al.*, 2017). However, more tractable species, particularly intertidal molluscs and arthropods are the staple for chronobiologists attempting to unravel the basis and evolution of biological clocks, further expedited by recent developments in gene sequencing technology that abrogates the necessity for a fully annotated genome (Tessmar-Raible *et al.*, 2011).

One famous example of lunar rhythms is the reproductive cycle of the worm *Eunice viridis* inhabiting the south Pacific. In Samoan waters, the worms gametes ripen twice a year on the second and third day after the third moon quarter in October and exactly one month after. On these days, the abdomen and gametes of *E. viridis* rise to the ocean surface and inhabitants of the Samoan islands collect them as they are seen as a delicacy (Hauenschild *et al*., 1968; Caspers, 1984). One other example of circatidal rhythms is the behaviour of the planarian *Symsagitiffera roscoffensis*, which harbours endosymbiotic microalgae (Gamble and Keeble, 1903). At low tides, the worm migrates through the substrate to achieve maximal solar exposure, thus promoting photosynthesis. At high water, the host worm descends into the sediment to avoid predation and dislodgement. The 12.4 hrs emergence rhythm of the flatworm from the sea bed is anticipatory and persists under constant conditions in the laboratory (Gamble and Keeble, 1903; Tessmar-Raible *et al.*, 2011). Many intertidal animals utilize circatidal clock systems to anticipate food availability during low or high tides. Endogenous clock-controlled behaviour has been shown to control the tidal migrations of the brown shrimp *Crangon crangon* (Adhub-Al and Naylor, 2009) and the tidal activity rhythms of the intertidal crab *Liocarcinus holsatus* (Abelló *et al*.,

1991), as well as the shore crab *Carcinus maenas* (Naylor and Atkinson, 1972). *Carcinus* seeks refuge on the mid-shore, at low tide, and becomes active when inundated by the rising tide. When removed from the field and divorced from external cues in the laboratory, these crabs show persistent, locomotor activity with a tidal period and in phase with the home shore (Naylor, 1958). *Carcinus* shows circatidal locomotor activity rhythms but a circadian rhythm of chromatophore intensity (Powell, 1962). *Carcinus* also shows halokinesis behaviour and can be entrained to rhythmically occurring changes in salinity (Naylor, 1985). In the drive to explain the basis of non-circadian rhythms in organisms that inhabit complex environments, such as the intertidal region, a long standing debate emerged about the very nature of tidal oscillators (Reid and Naylor, 1989; Naylor, 1997). Naylor surmised that the circatidal clock suppresses the circadian clock which in life leads to regular 12.4 hr activity rhythms with different heights (Naylor, 1996, 1997). This hypothesis was supported by observations that circadian phenotypes in this crab could be experimentally uncoupled from the dominating circatidal oscillations. When chilled, *Carcinus* displays no circadian but a circatidal activity rhythm which is interpreted as hint for the deep anchoring of a circatidal clock in the animal (Naylor, 1963). The speckled sea louse, *Eurydice pulchra* is found several centimetres buried in sand at the mean high water mark on surf-washed North West European coasts. Incoming tides disinter these isopods which become active, swimming in the surf-line to feed and breed. Before the tide recedes they re-bury at their preferred position on the shore. This anticipatory behaviour maintains their position on the beach and is persistent even when held in constant laboratory conditions (Alheit and Naylor, 1976; Hastings and Naylor, 1980; Naylor and Rejeki, 1996). *Eurydice* has circatidal swimming behaviour and as *Carcinus*, circadian chromophore dispersion rhythm (Zhang *et al.*, 2013).

The most prominent lunar controlled marine biological rhythms are reproductive rhythms. The synchronicity of mass spawning of some reef inhabitants needs an anticipation of gamete ripening to allow external fertilization (Takemura, 2001; Ando *et al.*, 2013). A broad study analysing reef fish spawning at Kimbe Bay (Papua New Guinea) observed 41 fish species spawning mainly between December and April around new moon coincident with higher tides. These spawning rhythms are species specific as diel spawning times last for less than 1 hr and dawn, afternoon

and dusk spawning species were classified (Claydon *et al.*, 2014). A figurative example of plasticity in rhythmic phenotypes is the gamete release of the marine algae *Dictyotales.* Rhythms in this behaviour are remarkably different depending on which Zeitgeber the algae are exposed to. In Europe where they are subjected to large and regular semilunar tides gamete release occurs on a semilunar cycle. However, in North Carolina (USA), gametes are released only once each month as the monthly spring tide is much greater than regular high tides. Thirdly, in Jamaican waters where tides are irregular no tidal periodicity in gamete release was observed (Hoyt, 1927). The small intertidal teleost fish, *Leuresthes tenuis,* the Californian grunion, is a prominent example for tidally rhythmic behaviour clearly supporting the survival of a species (Nardi *et al*., 2003). Females beach themselves aided by the momentum from an incoming wave where they deposits eggs about 200 mm deep in wet sand. Oviposition, which takes place up to four nights after a full or new moon, when the tidal range is maximal, is performed 3-4 h after high water to ensure that eggs are not washed away by the incoming tide. Undisturbed until the next spring tide, eggs develop during the next 12 days and are washed out of the sand with the following spring-tide high water (Marsden *et al*., 2003). Another example for the interplay between different clocks with different periodicity are the reproduction rhythms of the intertidal dipteran midge *Clunio marinus*. Adult flies deposit their eggs on seaweed at the low water mark during spring tides. Detritivorous larvae develop on these algae until eclosion takes place at low water, approximately 15 d later on consecutive spring tides. This unique timing mechanism seems to be result of an interplay between multiple clocks (circadian, circatidal, circalunar) and breeding studies have shown that it is controlled genetically (Burnet, 1965; Neumann, 1966; Kaiser *et al*., 2011; Kaiser and Heckel, 2012). Experiments with three *Clunio* populations naturally differing in period and phase relationship with the lunar month could be synchronised by artificial moonlight and the laboratory (Neumann, 1989). Lunar reproduction rhythms were also found in several deep-sea dwelling species (Mercier *et al.,* 2011). How the moonlight can act as a Zeitgeber in more than 200 meter depth, is still under investigation. Deep-tidal currents or lunar fluctuations of surface- produced organic mass are discussed as Zeitgeber (Mercier *et al.*, 2011).

Vast masses of zooplankton seek refuge from predation in deep water during the day but swim upwards to feed in the phytoplankton rich surface water at night.

This mass migration is referred to as diel vertical migration (DVM) (Lampert, 1989; Liu *et al*., 2003; Gaten *et al.*, 2008). In the Arctic, this behaviour even continues during the winter and polar night when the light is extremely low (Berge *et al.*, 2009). With a shift in the seasons, a shift in oscillation period from a 24 hr solar driven DVM rhythm to a 24.8 hr lunar day rhythm occurs as well as rhythmic movement following the 29.5 days of a synodic month (Last *et al.*, 2016). The copepod *Calanus finmarchius* expresses a circadian rhythm of DVM and classical clock gene cycling coincides with that rhythm (Häfker *et al.*, 2017). In the krill, *Euphausia superba*, this behaviour is equally governed by a daily clock (De Pittà *et al.*, 2013). Migrations of large masses of prey are correspondingly followed by predators for which the food availability can serve as a Zeitgeber. For example, in summer months, southern elephant seals switch feeding strategies to following these DVM in pelagic waters (Biuw *et al.*, 2010). Similarly, a variety of deep diving odontocetes, including many whale and dolphin species follow the mesopelagic boundary community throughout the night to optimize their foraging effort around the islands of Hawaii (Au and Benoit-Bird, 2008; Benoit-Bird *et al*., 2009; Au *et al.*, 2013). In the Atlantic ocean, foraging dives of short-finned whales *Globicephala macrorhynchus* off Tenerife adapt to diurnal rhythms of their prey, with 'flatter' nocturnal dives (Aguilar Soto *et al.*, 2008).

A relatively recent advance in chronobiology is the finding of a relationship of clock genes and navigational abilities in long as well as short distance travelling animals. In the chinook salmon (*Oncorhynchus tshawytscha*), a latitudinal cline in the average allele length and frequency (polyglutamine repeats) of the *OtsClockb* gene was determined (O'Malley *et al.*, 2013). From a clock gene architecture perspective the time of migration onset explains a large part of the genetic diversity between the populations (O'Malley and Banks, 2008). In the Monarch butterfly, *Danaus plexxippus*, clock genes have proven to exert control over its long distance navigation behaviour (Guerra *et al.*, 2014). Animals were shown to exhibit a circadian master clock in the dorsolateral protocerebrum (pars lateralis) of the brain where clock cells express at least *per, tim and cry1/2* as well as an antennae clock, where clock genes oscillate in abundance even when dislocated from the butterfly (Reppert, 2007; Merlin *et al*., 2009).

1.3 MOLECULAR BASIS OF CIRCADIAN CLOCKS

Research on the biological basis of circadian clocks began with mutation studies in the invertebrate model organism *Drosophila melanogaster*. In mutants with altered rhythms of eclosion behaviour the gene responsible was named *period (per)* (Konopka and Benzer, 1971). The altered behavioural phenotypes could later be directly correlated with *per* messenger ribonucleic acid (mRNA) expression levels and protein abundance (Zerr *et al.*, 1990). Circadian rhythms of the Period protein (PER) were identified in brain and eyes of the fly (Siwicki *et al.*, 1988) and a circadian rhythm in *per* mRNA expression was subsequently shown (Hardin, Hall and M. Rosbash, 1990). Protein sequence analysis of PER revealed a Per- Arnt- Sim (PAS) domain which is common for transcription factors and allows protein-protein interactions (Huang *et al*., 1993). These PAS domains were found to be necessary for the dimerization with another clock protein named TIM (Vosshall *et al.*, 1994; Darlington *et al.*, 1998). Drosophila *tim* mutants, exhibit similar behavioural phenotypes as the *per* mutants (Sehgal *et al.*, 1994; Sehgal, 1995) and their mRNA expression rhythm is the same (Sehgal, 1995). As the PER protein had a high abundance in the nucleus and its protein sequence showed motifs typical for transcription factors it was hypothesized that PER and TIM dimerize and translocate into the nucleus (Vosshall *et al.*, 1994) where they regulate their own transcription (Saez and Young, 1996). Further mutation studies in mice, identified *clock (clk)* as part of the circadian oscillator, as mutants show disrupted circadian rhythms in locomotor activity (Vitaterna *et al.*, 1994). Protein sequence analysis revealed a basic helix-loop-helix (bHLH) deoxyribonucleic acid (DNA) binding domain which binds to enhancer (E-) boxes. E-box consensus sequences are short DNA sequences (CANNTG) located upstream of the promoter. Binding of a transcription factor strongly facilitates the transcription of the associated gene (Kyriacou and Rosato, 2000). The CLK sequence further contains a PAS domain and was shown to dimerize with CYCLE (CYC), another core clock protein. Together the two promote the transcription of *per* and *tim* as well as other clock genes in the nucleus, establishing a positive feedback-loop (Rutila *et al.*, 1998). The expression of *clk* and *cyc* was shown to be inhibited by the PER:TIM heterodimer, thus deploying a negative feedback loop (Darlington *et al.*, 1998) with one round of expression/repression lasting about 24 hrs (Figure 1.1). The core oscillator is regulated on several levels by a multitude of proteins, via transcription factors, kinases and phosphatases as well as

ubiquitinases which are further introduced in chapter 2.

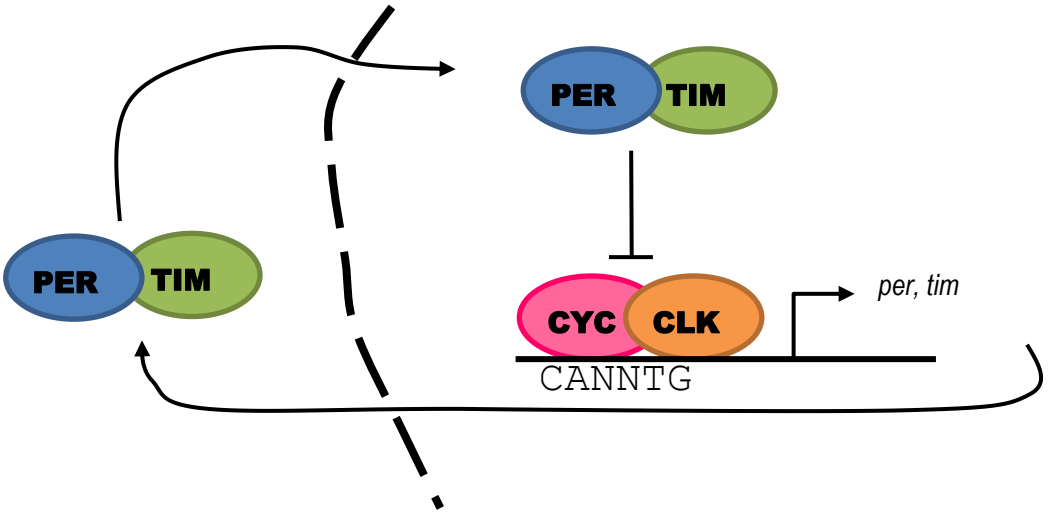

Figure 1.1: Basic model of the circadian core clock feedback-loop. The expression of *per* and *tim* mRNA is driven by the CLK: CYC heterodimer. Upon translation, PER:TIM in turn form a heterodimer to relocate into the nucleus (dotted line) and inhibit their own transcription. The dotted line represents the nuclear membrane.

It is well established that circadian clock mechanisms are temperature compensated and that this facet has evolved to meet the particular thermal demands of the environment. For example, in *drosophila*, a *Per* gene threonine-glycine repeat region is polymorphic with the repeat length shows significant latitudinal distribution. It was shown that this polymorphism is related to the ability of the clock to compensate for different temperatures (Costa *et al.*, 1992).

In most animals, clock input is processed via a central 'pacemaker' which synchronizes other body parts to the outside phase. However, body parts can have individual oscillators, peripheral clocks, for example hepatic clocks for animals and root clocks for plants (Green *et al.*, 2008; Albrecht, 2012). The conventional fruit fly master clock consists of about 150 neurons. They are groups of cells which are connected but have specific functions to govern distinct circadian activity behaviour which consists of morning (M) and evening (E) bouts of activity (Helfrich-Förster *et al.*, 2007). These are a ventrolateral group of neurons (LN_V) and a dorsolateral group of neurons (LNd) which, with help of some dorsal neurons (DN), orchestrate the circadian activity patterns in *Drosophila* (Grima *et al.*, 2004; Stoleru *et al.*, 2004). In

mammals, the suprachiasmatic nucleus (SCN), a collection of neurons above the optic chiasm in the hypothalamus hosts the master circadian clock. It consist of 20,000 neurons entrained by light (Ralph *et al.*, 1990), which can oscillate in cell culture in a self- sustained manner (Welsh *et al.*, 1995). Arrhythmic hamsters, with ablated SCNs could regain behavioural rhythmicity with SCNs transplanted from healthy animals (Ralph *et al.*, 1990). The SCN hierarchically coordinates secondary oscillators in other body parts which are not entrained through photic cues and not self-sustained (Reppert and Weaver, 2002).

1.4 TALITRUS SALTATOR BIOLOGY

T. saltator (Montagu, 1808) is a small amphipod crustacean, commonly known as the sandhopper, inhabiting the supralittoral zone in coastal regions of the North Atlantic, the Mediterranean sea, the Baltic and the North sea (Williams, 1978; Rainbow *et al*., 1998; Jankauskienė and Safonovienė, 2009). *Talitrids* are important detritivores (Olabarria *et al.*, 2009) and represent a protein source for many predatory members of the ecosystem (Marques *et al.*, 2003; Jankauskienė and Safonovienė, 2009). Sensitive to environmental perturbation, *T. saltator* serves as a biomonitor for pollution (Rainbow *et al*., 1998; Fialkowski *et al.*, 2009; Ungherese *et al.*, 2010, 2012; Ugolini, Perra, *et al.*, 2012) and as a bioindicator for human encroachment of beaches (Barca-Bravo *et al.*, 2008; Ugolini *et al.*, 2008). They exhibit a bivoltine life cycle where females breed twice with two generations present in each breeding season (Marques *et al.*, 2003) and the numbers of females in a population exceeds the males (Scapini, Campacci and Audoglio, 1999). A light regime of 14 hrs of light and 10 hrs of darkness is needed for the onset of breeding (Williams, 1978). Temperature has only limited effect on this behaviour (Williams, 1985). During the winter with temperatures, below 10°C, sandhoppers stay buried in the sand and remain inactive (Palluault, 1954). *T. saltator* has a haploid genome with n=25 chromosomes (2n=50) and a size of 2.15 Gb (±0.067) (Libertini *et al.*, 2008). Locomotor activity rhythms are, as the orientation behaviour, influenced by trace metals and can thus be used as a biomonitor for environmental contamination (Ugolini *et al.*, 2004). Gut microbes of *T. saltator* are species specific reflecting the amphipods microhabitat (Abdelrhman *et al.*, 2017).

During the light phase, *T. saltator* avoid desiccation (Williams, 1995) by burrowing in the moist sand (up to 50 cm deep). At the onset of dusk, they migrate down- shore to forage and return back to their burrows before daybreak (Williamson, 1951; Geppetti and Tongiorgi, 1967a). In captivity, *T. saltator* continues to expresses robust circadian rhythms of nocturnal activity. In constant darkness, these activity rhythms are persistent for several weeks in the laboratory (Bregazzi and Naylor, 1972; Jelassi *et al.*, 2015). Population density significantly changes the individuals phase of activity (Bregazzi and Naylor, 1972). Nightly activity peaks can be modulated by temperature but are independent from this factor in naturally occurring temperature ranges (Bregazzi, 1972). Accordingly, a circadian rhythm of oxygen consumption with higher rates during the night is persistent in constant conditions for even 50 days (Williams, 1982). The locomotor activity rhythm exhibits a period of 24.5 (±0.4) hrs and can be entrained with light (Williams, 1980b). Males and females do not differ in their locomotor activity rhythm (Williams, 1980a) and no circatidal patterns were observed in the locomotor activity rhythm (Williams, 1983).

Numerous compass mechanisms have been reported for the sandhopper from solar to lunar navigation as well a magnetic compass (Arendse and Kruyswijk, 1981; Ugolini, 2006; Meschini *et al*., 2008). If released under sunlight, Mediterranean *T. saltator* clearly orients towards the cardinal direction of their home beach independent from their current position (Pardi and Papi, 1952). The direction of escape is inherited but prone to modulation especially in young *Talitrus* (Pardi, 1960; Gambineri and Scapini, 2008). This sun compass can be modulated by the light regime (Pardi and Grassi, 1955; Ugolini *et al*., 2002; Ugolini, 2014) so the circadian clock and the chronometric mechanism aiding the solar orientation behaviour were hypothesised to share a common mechanism (Naylor and Rejeki, 1996; Ugolini *et al.*, 2007). Another additional behaviour that aids sandhoppers to relocate towards suitable conditions on the beach is its tendency to move towards the foot of an incline and positive scototaxis (Scapini, 1997; Nardi *et al.*, 2000; Gambineri and Scapini, 2008). Further, they exhibit a circadian rhythm of orientation towards light dark boundary. This is thought to help the animals to move towards the water (light/dark boundary by day) after they have been accidentally dislocated from their burrows (Edwards and Naylor, 1987).

Preliminary, sequencing experiments by O'Grady (2013) allowed the

identification of classical core clock genes in the *T. saltator* brain and quantitative mRNA measurements showed that some of these, change their expression level in constant conditions following the subjective day night cycle. This result provides a promising basis for further circadian clock analysis in this species.

1.5 OBJECTIVES

Until relatively recently, biologists have relied on elegant behavioural analyses to postulate how marine organisms cope with multiple temporal changes in physiochemical conditions. This has limited our grasp of the nature of time-keeping mechanisms in these species. Recent advances in molecular biology and genetics, together with a renewed interest in chronobiology of non-model species is starting to give insight to the molecular mechanisms of biological clocks in marine organisms. The availability, easy husbandry, clear circadian behavioural phenotypes and preliminary clock gene sequencing data lay ideal working ground for researching *T. saltator* as a crustacean clock model organism.

The current Ph.D. project aimed to dissect the biological clock of *T. saltator* on molecular and behavioural levels. The first challenge was the full identification and characterization of the circadian components in *T. saltator*. Several clock genes were already identified using Roche 454 Titanium FLX sequencing and homology cloning (O'Grady, 2013). Now, generation of full-length complementary DNA (cDNA) for all canonical clock genes was aimed to be accomplished via a combination of homology cloning, transcriptome mining and RACE polymerase chain reaction (PCR).

Further, a circadian transcriptome was assembled to assess circadian gene expression patterns. Next, brain tissue from light-entrained animals with robust daily rhythms were harvested at 3 hr intervals and used to assess temporal expression patterns of clock genes by qRT-PCR using Taqman assays. This clock gene expression data was linked to behavioural experiments on the timing of solar orientation mechanism to determine if the mechanisms of time compensation of solar orientation and locomotor activity are both entrained by the circadian clock gene network.

Further, the sun and moon compass behaviour were both morphologically

dissected following the example of *D. plexxippus* solar orientation analysis which harbours sun compass clocks in the antennae with clock genes cycling in expression independent from the central circadian oscillator in the brain (Merlin *et al.*, 2009).

The circadian clock output was researched focusing on the determination of the *T. saltator* clock controlled genes (ccgs) or clock controlled proteins (ccps). In the crayfish, the Crustacean hyperglycaemic hormone (CHH) rhythmically oscillates in a circadian fashion. Beside others, it is well studied for its hyperglycaemia inducing function, when cycling in the haemolymph, which follows a circadian rhythm as well (Kallen *et al*., 1988; Kallen *et al*., 1990; Nelson-Mora *et al.*, 2013). This puts CHH as a probable candidate for a directly clock controlled gene or protein.

CHAPTER 2: GENERAL METHODS

If not stated otherwise all reactions using kits were carried out according to manufacturer's instructions. Recipes for all buffers and solutions are shown in the Appendix B.A list of consumables with companies names and registered offices are found in Appendix C.

2.1 ANIMAL HUSBANDRY

Animals were collected from the beach at Ynyslas Nature Reserve (Ynyslas, UK) and kept in glass tanks (40 x 20 x 30 cm) filled with damp sand from the sampling site. Sandhoppers were fed fish food *ad libitum* (TetraMin fish flakes, Tetra). The ambient temperature was 17°C and a 12:12 LD schedule was applied centred on the middle of the day of the natural light cycle.

2.2 LOCOMOTOR ACTIVITY MEASUREMENT

Locomotor activity was measured using bespoke activity monitors (TriKinetics Inc., see Figure 2.1). An array of infra-red light beams was arranged around a glass tank filled with sand. The tank was compartmented with Plexiglas into individual measuring areas. Each arena carried 5 individuals as animals change their activity rhythms when kept individually (Bregazzi and Naylor, 1972). When an animal emerged from the sand, it broke an infra-red beam. These incidents were processed by a connected personal computer using the DAM system software (TriKinetics Inc.). A Chi Square periodogram was calculated using ClockLab (ActiMetrics).

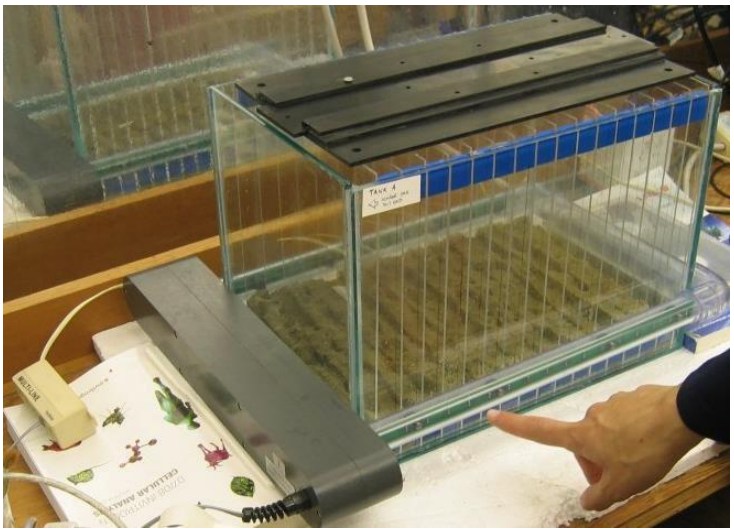

Figure 2.1: Activity monitor for *T.saltator*. When animals emerge above sand level they break an infra-red which was recorded and processed by a personal computer attached. Photograph taken by Laura Schumm.

2.3 RNA EXTRACTION

The detailed sample collection scheme is described in the methods of the corresponding chapter. A general overview is given here. Before the extraction of RNA, the head, brain or antennae tissue was homogenized using the Qiagen TissueLyser II bead mill (Qiagen) at 50 Hertz (Hz) for 7-10 minutes with 7 mm stainless steel beads. Total RNA was extracted from *Talitrus* tissue using the RNeasy® Mini Kit (Qiagen) following the protocol: *Purification of Total RNA from Animal Tissues* in the handbook. In the final step, the RNA was eluted into RNAse-free water and quantity and quality determined spectrometrically with the Nanodrop ND2000 (Thermo Fisher Scientific).

2.4 REVERSE TRANSCRIPTION (RT)

To enhance stability in downstream processing, the extracted RNA was reverse transcribed into cDNA. Depending on the downstream applications, different enzymes were utilised to reverse transcribe total RNA into cDNA. When used for qRT-PCR, 500 ng of total RNA was incubated with random primers and the High-Capacity cDNA Reverse Transcription Kit (Applied Biosystems®) following instructions. cDNA for sequencing work was reverse transcribed with the Superscript™ III First-Strand Synthesis System (Invitrogen™) following the

manuals instructions.

2.5 POLYMERISE CHAIN REACTION (PCR)

PCR was used for several experiments and will be mentioned in the respective segments of the methods in each chapter. Two master mixes were used to run PCRs, the MyTaq™ Red PCR Mix (Bioline Reagents) and AmpliTaq Gold™ 360 PCR Mix (Applied Biosystems®). The reaction times and temperatures were displayed in the Table below (Table 2.1).

Table 2.1: PCR cycling conditions. Protocols for both master mixes used throughout the work differ slightly and temperature and incubation times are given for each step.

	MyTaq™ Red PCR Mix (Bioline Reagents)			AmpliTaq™ Gold 360 PCR Mix (Applied Biosystems®)		
PCR step	**Temp. [°C]**	**Time [sec]**		**Temp. [°C]**	**Time [sec]**	
Initialisation	95	240		95	300	
Denaturation	94	30	30 cycles	95	30	30 cycles
Annealing	55	45		55	30	
Extension	72	45		72	60	
Final extension	72	420		72	420	

2.6 AGAROSE GEL ELECTROPHORESIS

PCR products were analysssed through gel electrophoresis. If not stated otherwise, all agarose gels used were 1.5% w/v gels. The appropriate amount of agarose (Sigma-Aldrich) was dissolved in TAE buffer. SYBR™ safe DNA gel stain (Invitrogen™) was added before pouring. The PCR products were mixed with DNA loading Buffer Blue (5x) (Bioline Reagents) before being pipetted into the gel pockets. Depending on the expected band size the respective HyperLadder (Bioline Reagents, see Figure A.1) was used. The gel was run at 110 V and 250 mA (4-10V/cm) in TAE and afterwards imaged under UV light.

2.7 5’ AND 3’ RAPID AMPLIFICATION OF CDNA ENDS (RACE) PCR

To determine the 5’ and 3’ untranslated regions (UTRs) of a transcript contig sequence, RACE-PCR was performed using the GeneRacer™ cDNA kit (Life

Technologies™) following the kits instructions.

Briefly, high quality cDNA was synthesised from 1 µg of the total RNA with the GeneRacer™ cDNA kit (Life Technologies™) and SuperScript™ III Reverse Transcriptase system (Invitrogen™). The cDNA was incubated with a gene specific 3'RACE primer and the kit supplied GeneRacer 3' primer in a PCR reaction using the AmpliTaq Gold™ 360 Master Mix (Applied Biosystems®) for the first reaction. All primers sequences used are indicated in the relevant chapter. The second PCR used the result of the first PCR as template but with nested primers. In the same fashion, the third PCR was conducted with a gene specific 3'RACE nested forward primer and GeneRacer 3'N as reverse primer and template from the first nested PCR but with only 30 PCR cycles run to insure sequence integrity. Resulting amplicons were checked on an 1.5% agarose gel, bands of expected size cut out, cleaned with the Isolate II PCR and Gel Kit (Bioline Reagents) and cloned and sequenced as described in 2.8.

A similar approach was used for the 5' RACE PCR with the modification that specific 5'RACE mRNA was produced with the GeneRacer™ Oligo Kit and first strand synthesis was conducted with SuperScript III and random primers. For the 5'RACE cDNA synthesis, a gene specific primer (GSP) can be used in the outward facing direction but modifications were necessary to generate a priming site for a forward primer. The procedure was known as RNA ligase mediated RACE (RLM-RACE). A T4 RNA ligase was used to attach an artificial RNA oligo to the 5' end of the mRNA. Before that, non-mRNA and truncated RNAs excluded from the experiment though removing their 5' phosphates with calf intestinal phosphatase (CIP) only leaving mRNAs intact. To enable manipulation, the 5' cap was removed with help of the tobacco acid pyrophosphatase (TAP) leaving a 5' phosphate residue for the ligation with the artificial oligo. Frist strand synthesis can be conducted with random primers followed by PCR with the reverse GSP and forward primer that hybridizes the attached oligo on the 5'end.

A first round PCR using the GeneRacer 5' primer and the reverse gene specific 5' RACE primer was followed by a second round PCR using a nested reverse gene specific primer (GSP) and the GeneRacer 5' N primer as well as first round PCR as starting material for the reaction. Resulting amplicons were separated on an agarose

gel, bands of the expected size were cut out, cleaned and sequenced as described above for the 3'RACE PCR.

2.8 CLONING

For sequencing, a given DNA fragment was inserted into a sequencing vector to introduce established priming sites. The gel-purified DNA fragments were cloned into the pCR™4-TOPO® Vector (Invitogen™; Figure A.2) using the TOPO™ TA Cloning™ Kit for Sequencing (Invitogen™). For the ligation reaction, 4 µL of PCR product, 1 µL of salt solution (supplied in kit) was mixed with 1 µL vector and incubated at room temperature for 5 min and then left on ice.

One Shot ®TOP10 chemically competent *E.coli* cells (Invitogen™) were subsequently transformed via heat shock .2 µL of the vector mix was added to one supplied aliquot of cells and incubated on ice for 30 min. The heat shock was performed in a water bath at 42°C for 45 sec and the reaction mix then kept on ice for another 2 min. Following this, 250 µL of kit supplied SOC medium was added and the cells incubated at 37°C for 30 min. The cells were then plated on agarose plates (with 100 µg/mL ampicillin, 0.2 mM IPTG and 40 µg X- Gal/plate) to grow over night at 37°C. The vector contained an ampicillin resistance gene only allowing transformed cells to survive.

Recombinant bacterial colonies were identified via blue-white screening. Suitable colonies (white) were picked with a sterile pipette tip and incubated with kit supplied M13 primers in 10 µL MyTaq™ Red mix (Bioline Reagents) PCR master mix and run as described in Table 2.2. The PCR results were analysed on an agarose gel, were colonies containing the vector insert in the appropriate direction were identified. These were grown over night in 5 mL Luria broth (LB) medium (with 50 µg/mL ampicillin) on a shaker at 37°C and plasmids harvested with the Isolate II Plasmid Mini Kit (Bioline Reagents) ready for sequencing.

2.9 SEQUENCING

Sequencing of the plasmids was performed in house at the Aberystwyth

University Core Genomics facilities. Again, M13 primers were used as sequencing primers with 250 ng vector as sample.

2.10 SEQUENCE ANALYSIS

Chromas Version 2.4.4 was used to visualise raw sequencing results (https://technelysium.com.au/wp/). MEGA 5-7.0.14 was used for sequence alignments (Tamura *et al.*, 2011, 2013; Kumar *et al.*, 2016).

For translation the EXPASY translate online tool was used (Gasteiger *et al.*, 2003).

Primer design for all PCRs (apart from the qRT-PCRs) was accomplished through the Thermo Fisher Scientific Oligo Perfect primer design web tool (https://www.thermofisher.com/de/de/home/products-and-services/product-types/primers-oligos-nucleotides.html).

Vector contamination in sequencing results were identified with NCBI online tool VecScreen (https://www.ncbi.nlm.nih.gov/tools/vecscreen/).

For Basic Local Alignment Searches the NCBI BLAST online search tools were used (https://blast.ncbi.nlm.nih.gov/Blast.cgi). Mainly, the tblastp and the tblastp searches were used. In the first, a nucleotide sequence is used as search query in a nucleotide sequence database. The second was used with the translated transcript sequences as protein query to search a protein database.

For local BLAST searches in the *T. saltator* transcriptome Bioedit version 7.2.6 was used (Hall, 1999).

2.11 QUANTITATIVE REAL-TIME PCR (qRT-PCR)

To allow an absolute quantification of a transcript via qRT-PCR, known amounts of cRNA standard molecules were used and run alongside with the sample reactions. These cRNA standards were produced from cDNA which is transcribed into cRNA which is then diluted into aliquots of a predetermined concentration.

In a first round PCR a T7 promoter was incorporated into the sequence in question by using GSP primers with the T7 sequence attached. The AmpliTaq Gold™ 360 Master Mix (Applied Biosystems®) was used for running the PCR. To maximise the amount of PCR product, a second round PCR (two separate reactions) was done using the first round PCR result as template. Afterwards, reactions were analysed on an agarose gel, cleaned with the Isolate II PCR and Gel Kit (Bioline Reagents) and quantified on a Nanodrop ND2000 (Thermo Fisher Scientific). The resulting T7 flanked amplicon was used as starting material for a transcription reaction using the MEGAshortscript™ Kit (Ambion™) following manufacturer's instructions apart from the fact that the reaction was left over night. The resulting cRNA was then treated with DNAse using the TURBO DNA-free™ Kit (Ambion™) to remove template DNA and was purified over a polyacrylamide gel electrophoresis (PAGE). The gel was made 6% PAGE/Urea Solution (19:1 Acrylamide/Bis, 6 M Urea) (Ambion™) with 10% ammonium persulfate (Sigma-Aldrich). A volume of 2 µL of sample and marker (RNA Century- Plus Marker (Ambion™) was denatured with 95°C heat for 5 minutes with 5 µL loading buffer and then run on the PAGE gel. The gel was stained with 0.015% Ethidium bromide solution (in TBE (0.5x)), washed with TBE (0.5x) for 5 minutes and visualised on a UV table. The band of expected size was excised and incubated in RNA elution buffer at room temperature for 8- 12 hrs. The RNA was then precipitated with Ethanol (100%) at -80°C for 20 minutes and spun at 12 000 rpm at 4°C for 15 minutes. The RNA pellet was washed with 75% v/v Ethanol, dissolved in water and quantified on the Nanodrop ND2000 (Thermo Fisher Scientific) in serial dilutions in water (1:10- 1:2 in water). The copy number was calculated according to the following formula, where m=amount of amplicon [ng] and l=amplicon length, 340 g/mole=average mass of 1 base pair (bp) single stranded RNA (ssRNA).

$$number\ of\ copies\ (molecules) = \frac{m\,ng\ \times 6.0221\ \times 10^{23}\ molecules/_{mole}}{(l\ \times 340\ {}^{g}/_{mole}\ \times 1 \times 10^{9}\ {}^{ng}/_{g}}$$

Standards were tested in an initial qRT-PCR reaction (described below) to insure correct reaction set up, efficiency and robustness. The corresponding standard curves are shown in the Appendix A.5 –A.15.

For quantification of transcripts 500 ng of total RNA was reverse transcribed with the High-Capacity cDNA Reverse Transcription Kit (Applied Biosystems®). The serial dilutions of cRNA standards were treated the same alongside. For the PCR the SensiMix™ Probe II Kit (Bioline Reagents) was used on the QuantStudio™ 12K Flex Real-Time PCR System (Applied Biosystems®). Standards were measured in serial 10-fold dilutions between 10^9-10^3 copies for each reaction. *T. saltator* Arginine kinase (*Talak*) was used as a house keeping gene as previously described (established by O'Grady, 2013). All samples and standards were measured in triplets.

When plotting the resulting cycle threshold (C_T) against the given copies of standard molecules the slope of the resulting curve estimates the PCR reaction efficiency. A value of -3.3 represents 100% efficiency. The efficiency can be determined with the formula:

$$qPCR\ efficiancy = 10^{\frac{-1}{slope}} - 1$$

The absolute amounts of transcripts were then calculated through regression analysis of the standard curve and normalised with the housekeeping gene.

2.12 IMMUNOLOCALISATION OF PEPTIDES

Neural proteins were visualised through immunohistochemical staining. For these experiments, whole brains were used. They were quickly dissected form the carapace in ice-cold physiological saline and fixed at 4°C overnight in Stephanini's fixative (Stefanini *et al*., 1967). Following fixation, the tissue was washed with PTX, first 3 times for 10 minutes then 2 times for 30 minutes and finally for 2 hrs. The tissue was incubated with primary antibody (target specified in respective chapter) in PTX over night at 4°C. The next day, the brains were washed in PTX 3 times for 10 minutes and then 3 times for 30 minutes to remove residual antibody. As a secondary antibody, the Alexa Flour 488 coupled goat-α-rabbit AB (Molecular Probes) was used diluted 1:500 in PTX and incubated with the brains over night at 4°C in the dark. Following,

the brains were washed again with PTX as after primary antibody incubation and mounted in Vectashield Antifade Mounting Medium (Vector Laboratories Inc., Burlingame, CA, UK).

Staining was visualised on a Leica TCS SP5 II confocal microscope. Mainly, a HCX PL APO CS 20.0x0.70 IMM UV and a HCX PL APO lambda blue 1.25 OIL UV objectives (40.0x magnification) were used. Z-stack images of 15-25 optical sections were obtained at 1-2 µm intervals and images were analysed with the software suite Leica LAS AF Lite 2.6.3 (Leica Microsystems) and were edited with Adobe Photoshop CS6 (Adobe Systems Incorporated).

CHAPTER 3: CIRCADIAN TRANSCRIPTOME AND CLOCK GENE SEQUENCING

3.1 ABSTRACT

Information on gene or transcript sequences in non-model organisms especially crustaceans is very limited. To fill this gap and to hold a reference for future molecular genetic work a transcriptome was generated from time-course sampled brain tissue harvested from animals held in constant darkness following entrainment in 12:12 LD. The transcriptome was assembled *de novo* using Trinity and functionally annotated using Blast2GO. The homologs of core clock and clock-associated gene transcripts were determined and their temporal expression profiles were analysed with JTK_cycle. These data show that ~7% of the *Talitrus* transcriptome cycles with a circadian period. Most of the expected invertebrate canonical core clock and clock- associated genes were identified in the transcriptome. Of these, *Talcry2*, *Talper*. *Talbmal1*, *Talpdh*, *Talck2ß*, *Talpp1*, *Talsgg*, *Talslimb*, *Talebony*, *Talsirt1*, *Talsirt7* and *Taljetlag* were determined to cycle with a 24 hrs period by JTK_cycle and or one-way ANOVA. The current findings lay the foundations for further explorations of the model arthropod *T. saltator* circadian molecular biology. They provide an invaluable contribution to the field by increasing the taxonomic coverage of invertebrate sequence information and of their biological clock constituents specifically.

3.2 INTRODUCTION

3.2.1 Circadian transcriptome sequencing

By definition, for non- model organisms, the genetic, transcriptomic and proteomic information is often limited. Our knowledge of the molecular biology of crustaceans and the genetic underpinnings of the biological clock specifically are now reaping the benefits of sequencing technologies, such as next generation sequencing (NGS). For an increasing number of species the molecular elements of the biological clock have been identified from *de novo* assembled transcriptome studies (Tilden *et al.*, 2011; Christie *et al.*, 2013; Stahl *et al.*, 2015; Biscontin *et al.*, 2017; Sales *et al.*, 2017). Putative homologs of the core clock genes *period (per), timeless (tim), clock*

(clk), cycle/baml1 (cyc/baml1) and *cryptochrome2* (*cry2*) have been identified for a number of crustaceans among which are copepods, *Tigiropus californicus* (Nesbit and Christie, 2014), *C. finmarchicus* (Christie *et al.*, 2013; Häfker *et al.*, 2017), Decapods, *E. superba* (Biscontin *et al.*, 2017), the Norway lobster *Nephros norvegicus* (Sbragaglia *et al.*, 2015) and the Cladoceran, *Daphnia plurex* (Tilden *et al.*, 2011).

When the tissue samples from which the transcriptome information is derived are collected over a time course, further information about the timing of clock-controlled physiology can be inferred. For instance, in the Antarctic krill, *E. superba*, about 40% of mRNA is transcribed rhythmically with a 24 hr period and 60% of this 'rhythmic transcriptome' is expressed with a 12 hr period under natural conditions (Teschke *et al.*, 2011; De Pittà *et al.*, 2013). This gene expression dynamic resonates with cyclic exposure to 24 hr LD cycles days but also reflects the diel vertical migrations (DVM) the animals exhibit in nature. The differentially expressed transcripts crudely assigned functional categories including proteolysis, energy and metabolic processes, redox regulation, visual response and stress response, which were also found to change in response to rhythmic environmental changes (De Pittà *et al.*, 2013). Further, detailed deduced functional annotation of the transcript sequences provides a background for further research on the biological action of the transcripts and their interaction.

3.2.2 The invertebrate circadian clock

The central clock is based on a transcription-translation autoregulatory feedback loop (TTFL) is described for the invertebrate model organism *D. melanogaster* (Tomioka and Matsumoto, 2010), (Figure 1.1). Very briefly, the expression of the core clock genes *per* and *tim* genes is activated by the CLK/CYC transcription factor protein complexes towards the onset of evening. Once translated, PER and TIM proteins form a cytosolic heterodimer and relocate to the nucleus where they inhibit CLK/CYC duplex activity during the late night, thus effectively regulating their own transcription in an autoregulatory feedback loop. This process is highly regulated on several levels (transcription, translation, protein activation, protein localisation, ubiquitination) by clock associated genes and their protein products to allow an accurate sequence cascade of events to repeat itself about every 24 hrs

(Giebultowicz, 2000; Meyer-Bernstein and Sehgal, 2001; Allada and Chung, 2010).

To be able to synchronise to changes in external light stimuli the fruit fly processes photonic stimuli through the blue light receptor protein CRYPTOCHROME1 (CRY1). Upon activation, CRY1 undergoes conformational change and binds to the core clock gene TIM. PER and TIM are then separately degraded in the proteasome and a new TTFL can begin (Figure 3.1).

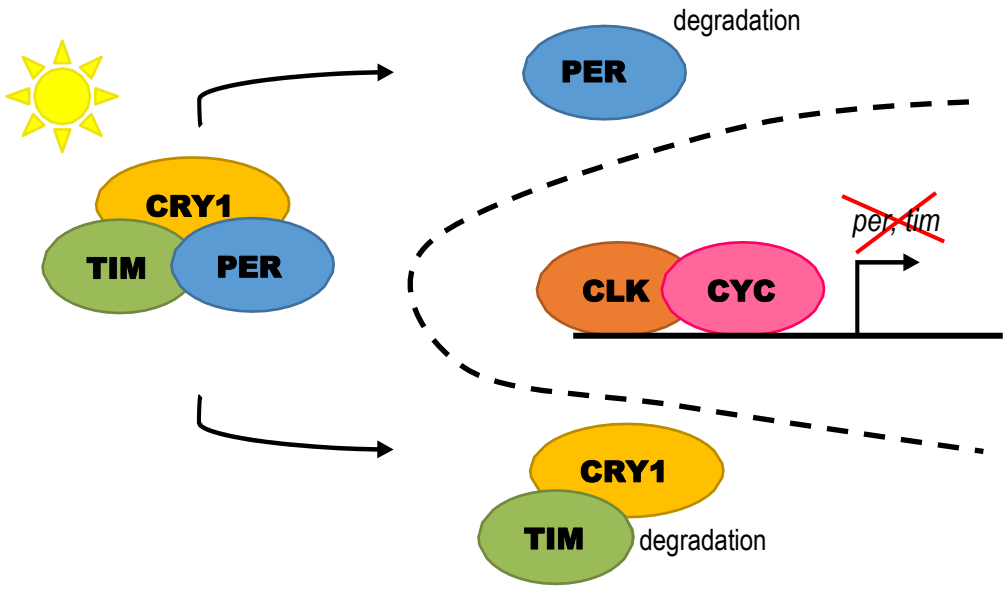

Figure 3.1: Model of the *Drosophila* central feedback-loop. Upon blue light stimulation, CRY1 is able to bind to TIM which is then subject to proteasomal degradation. Free PER is degraded via DBT and SLIMB (see text below). In this way, light functions as a Zeitgeber in the *Drosophila* circadian clock. Modified after (Yuan *et al.*, 2007; Lam, 2017).

TIM is then degraded through the proteasome allowing another transcription/translation cycle to begin (Dubruille and Emery, 2008). This proteasomal degradation is mediated via the E3 ligase JETLAG (Koh *et al.*, 2006; Peschel *et al.*, 2009) (Figure 3.2).

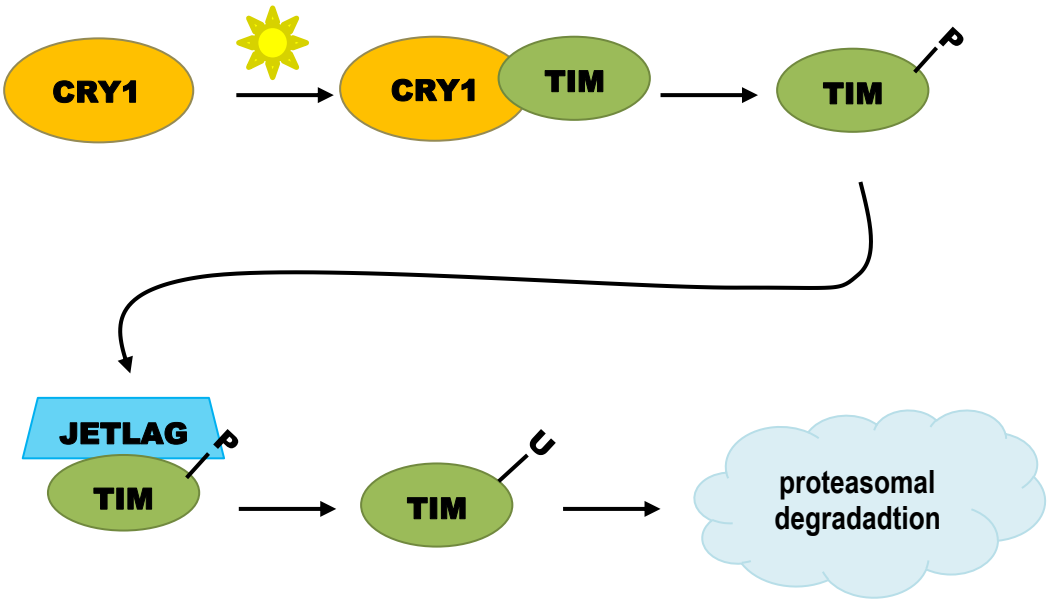

Figure 3.2: Mechanism of CRY1 induced TIM degradation. The blue light sensitive CRY1 is activated by light and is then able to bind TIM. The latter is then phosphorylated which makes it a target for the ubiquitin ligase JETLAG. After ubiquitination by JETLAG, the TIM protein is readily degraded in the proteasome.

The TIM protein is also a substrate to the phosphorylase SHAGGY (SGG) and the Ser/Thr-specific kinase Casein kinase 2 (CK2) which lead to the nuclear translocation of TIM. *Shaggy* overexpression leads to a shortened circadian period in *Drosophila* due to the premature nuclear localization of the TIM/PER complex (Martinek *et al.*, 2001; Meissner *et al.*, 2008; Bandyopadhyay *et al.*, 2016). Likewise, both PER and TIM are substrates of the protein phosphatases 1 (PP1) and 2A (PP2A). The PP2A regulatory subunits TWINS (TWS) and WIDERBORST (WDB) both stabilise the dPER protein in *Drosophila* cell culture (Sathyanarayanan *et al.*, 2004). Research in *Drosophila* cell culture also shows that PP1 stabilises TIM by dephsorphorylation (antagonising SGG action) and plays a role in regulating cyclic PER/TIM levels and PP2A seems to be involved in the relocation of the PER/TIM protein complex into the nucleus (Fang *et al.*, 2007). PER phosphorylation is further regulated by an array of enzymes. For example by CASEIN KINASE1 ε/DOUBLE TIME (CK1 ε /DBT) and CK2 which furthers the repressor function of PER (Kivimäe *et al.*, 2008).

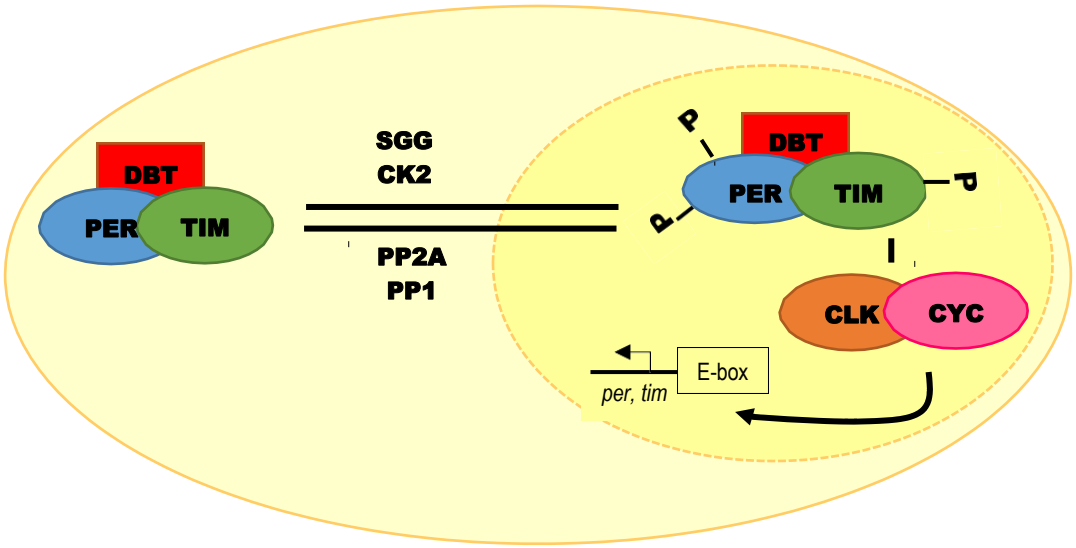

Figure 3.3: Regulation of PER:TIM subcellular location. In *Drosophila*, several kinases and phosphatases have the PER:TIM:DBT protein complex as a target and regulate its phosphorylation status and the nuclear translocation. In the nucleus, PER:TIM inhibits the CLK:CYC protein complex and thus its own transcription.

In the nucleus, PER:DBT phosphorylates CLK marking it for degradation. The phosphorylation of PER by DBT allows PER to form a complex with the E3 ubiquitin ligase SUPERNUMARY LIMBS (SLIMB) leading to its proteasomal degradation during the morning /early day. The PER degradation in turn allows the transcription activation of CLK/CYC and thus the release of PER/TIM inhibition marks the completion of the feedback loop (see Figure 3.3).

The basic zipper activator PER DOMAIN PROTEIN 1 (Pdp1) and the bZip transcriptional repressor VRILLE both are activated by CLK/CYC and they influence expression of CLK. *Vri* mRNA has to be rhythmically transcribed for cellular molecular rhythms in *Drosophila* (Cyran *et al.*, 2003). A loss of function Pdp1 mutation (specifically pdp1ε) lowers the *clk* expression in *Drosophila* and leads to a behaviourally arrhythmic phenotype (Cyran *et al.*, 2003; Zheng *et al.*, 2009) (Figure 3.4).

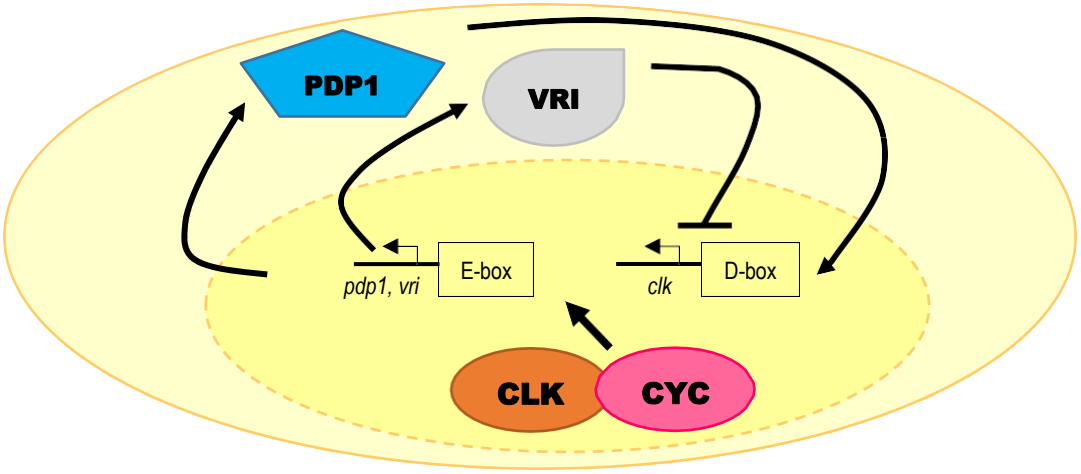

Figure 3.4: PDP1 and VRI feedback loop. The CLK:CYC complex targets the *pdp1* and *vri* genes to promote their expression. The mature VRI protein can relocate to the nucleus and in turn inhibit clock expression. The PDP1 protein on the other hand facilitates *clk* expression.

The CLK/CYC complex activates the transcription factor CLOCKWORK ORANGE (CWO) which mediates CLK/CYC induced transcription during the late night (Kadener *et al.*, 2007; Lim *et al.*, 2007; Matsumoto *et al.*, 2007; Richier *et al.*, 2008). A loss of *cwo* leads to a low amplitude, prolonged circadian period and molecular and behavioural rhythms. The CWO protein targets clock gene expression through repressor and activator mechanisms (Kadener *et al.*, 2007; Lim *et al.*, 2007; Matsumoto *et al.*, 2007; Richier *et al.*, 2008; see Figure 3.5). Another player in the *Drosophila* circadian clock is the N-β-alanyl-biogenic amine synthase EBONY. It is an enzyme specific for glial cells, which conjugates β-alanine to biogenic amines. Besides a darker body colour, *ebony* mutant flies have altered circadian rhythms (Newby and Jackson, 1991; Suh and Jackson, 2007). More specifically, *ebony* is expressed in a subgroup of glia cells which also express *per* with proximal location to circadian pacemaker neurons in the *Drosophila* brain. Mutation studies suggest, that ebony mediated dopaminergic neurotransmission is responsible for locomotor activity rhythms in *Drosophila* (Suh and Jackson, 2007).

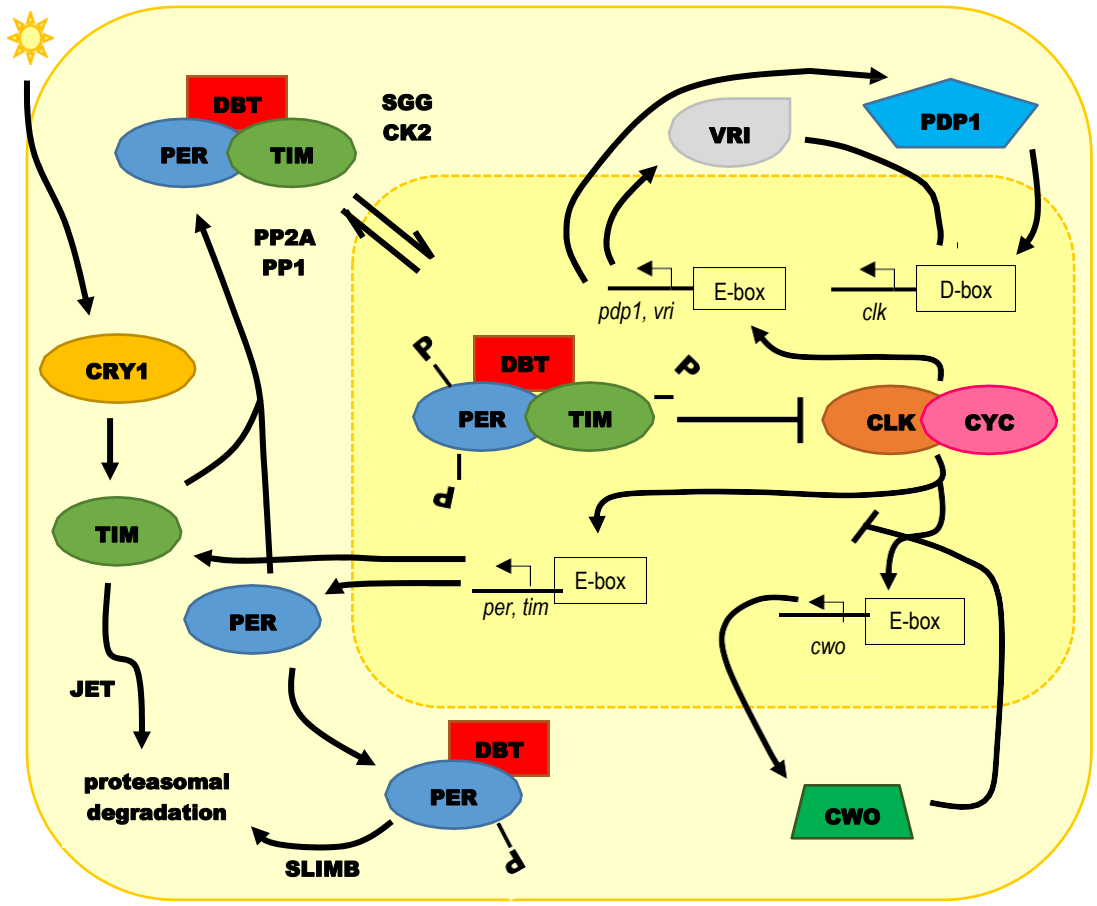

Figure 3.5: Overview of the mechanism of clock-associated gene functions. The nuclear translocation of PER:TIM:DBT is regulated by several different kinases and phosphatases. In the nucleus, PER:TIM inhibits the inductive activity of CLK:CYC on the *vri* and *pdp1* and their own gene expression. The latter is also inhibited by CWO which binds to E-box elements of *per* and *tim*. *Cwo* expression is facilitated by CLK:CYC as well. VRI and PDP1 compete to either repress or activate CLK expression. Modified after (Allada and Chung, 2010; Zordan and Sandrelli, 2015).

Sirtuins have been recently associated with the mammalian circadian clock so most of the information available on their biology is derived from research in mammals or yeast. Besides others, sirtuins exert deacetylase function and thus influence chromatin remodelling (Masri and Sassone-Corsi, 2014). Through histone modifications SIRT1 specifically modulates CLOCK-mediated chromatin remodelling (Belden and Dunlap, 2008). SIRT1 was found to modulate clock gene expression through binding to CLK-BMAL1 and promoting the deacetylation and degradation of PER2 in mammals (Asher *et al.*, 2008). Many of the physiological effects of sirtuins are linked to energy metabolism (Laurent *et al.*, 2013; Nakagawa and Guarente, 2014). SIRT1 is nicotinamide adenine dinucleotide (NAD^+)-

dependent and hence hypothesised to function as a sensor for the cellular redox and metabolic state through sensing the NAD^+ concentration (Nakahata *et al.*, 2008). The nuclear receptor and transcription factors REV-ERB and RORα (retinoic acid receptor–related orphan) both render regulatory functions in the molecular clock and also regulate lipid metabolism (Solt *et al.*, 2011; Solt *et al.*, 2012).

The last clock-associated protein to mention here is the pigment-dispensing factor (pdf) which has been first described in crustaceans (where it is called pigment-dispensing hormone (pdh)). Here, it has been shown to be involved in pigment dispersion in the retia and melanophores in several crustaceans such as the shrimp *Pandalus borealis* (Fernlund, 1976), isopod *E. pulchra* (Wilcockson *et al.*, 2011) and the sand fiddler *Uca pugilator* (Rao *et al.*, 1985). The *Drosophila* clock network is dispersed along about 150 neurons which exhibit cyclic clock gene expression (Shafer *et al.*, 2006). A subgroup of these cells, the lateral ventral neurons (LVN) express PDF and can be found proximal to projections of other neuronal clock cells (Helfrich-Förster and Homberg, 1993; Nässel *et al.*, 1993). Functional PDF is necessary for behavioural locomotor activity rhythms. A loss of function mutation (Pdf^{01}) has a drastic effect on the activity rhythm as animals become arrhythmic in constant conditions (Renn *et al.*, 1999). PDF functions as a synchronising factor in the drosophila neuronal clock network (Shafer and Yao, 2014). Apart from a role in circadian physiology, *D. melanogaster* PDF is involved in sleep (Chung and Zmora, 2008; Parisky *et al.*, 2008; Sheeba *et al.*, 2008; Kunst *et al.*, 2014), arousal (Shang *et al.*h, 2008; Sheeba *et al.*, 2008), flight (Agrawal *et al.*, 2013), geotaxis (Toma *et al.*, 2002), mating (Kim *et al.*, 2013), excretion (Talsma *et al.*, 2012) and tracheal branching (Linneweber *et al.*, 2014). The PDH isoforms in crustaceans are classified into α- and ß-PDH (Rao, 2009). Further, different isoforms of, for example ß-PDH, can exist in one animal (Rao *et al.*, 1985; Rao and Riehm, 1989; Klein *et al.*, 1994; Yang *et al.*, 1999; Fu *et al.*, 2005). For example *Cancer productus* expresses ß-PDH I and II in brain and eyestalks (Hsu *et al.*, 2008; Beckwith *et al.*, 2011). The multitude of isoforms allows the hypothesis that it might have more functions than in insects (Strauss and Dircksen, 2010; Wilcockson *et al.*, 2011). Morphological expression patterns of β-PDH I in *Drosophila* brains is similar to the one of its orthologue in the red rock crab *Cancer producuts* where neurons expressing *pdhI* co- express the canonical core clock gene *cyc*.Heterologous *Drosophila pdf* null mutants display an

arrhythmic behaviour circadian phenotype which can be rescued with *Cancer* ß-PDH I thus indicating conserved function (Beckwith *et al.*, 2011; Shafer and Yao, 2014).

In *Drosophila*, PER takes a central role in circadian timing as the main negative repressor of the CLK:CYC complex (Allada and Chung, 2010). With the elucidation of other invertebrate clocks and their components, it seems as if CRY2 has taken over the role of the primary CLK-CYC repressor in the feedback loop in some other insects and crustaceans (Robinson, 2008; Lam, 2017). Given that insects such as the monarch butterfly and the mosquito *Anopheles gambiae* for example express two distinct cryptochrome proteins (Zhu *et al.*, 2005), the blue light sensitive CRY1 and the mammalian-like CRY2. It has been hypothesised that the Cry2-clock is an ancestral form (Reppert, 2007; Robinson, 2008). Thus, in drosophilids, a loss of CRY2 was compensated with PER functioning as the major repressor component (Yuan *et al.*, 2007).

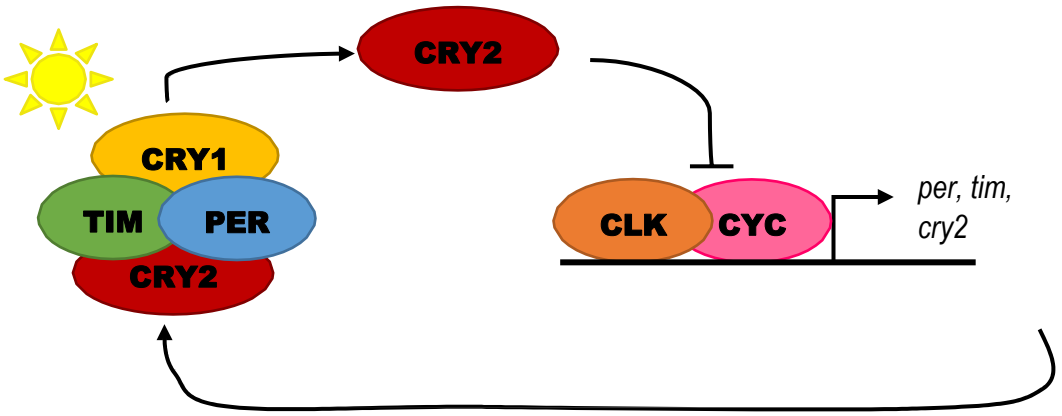

Figure 3.6: Schematic drawing of the *D. plexxippus* clock feedback-loop. CRY2 functions as the main repressor of CLK:CYC. The latter proteins drive *per, tim* and *cry2* expression.

Between evolutionarily distant phyla, biological clocks share striking conservation in terms of commonalities in key molecules and their structural hierarchy (Pegoraro and Tauber, 2011). The biological clocks have evolved for an optimal survival strategy in a biological niche. The ability to anticipate cyclic changes maximises biological fitness (Wilcockson and Zhang, 2008; Tessmar-Raible *et al.*, 2011). Thus, it is not surprising that many molecules of the biological circadian clock share sequence homology and functional similarity between different organisms

(Young and Kay, 2001; Sandrelli *et al.*, 2008).

3.2.3 Objective

T. saltator displays striking circadian locomotor rhythmicity and has long been studied on a behavioural level (Bregazzi and Naylor, 1972; Williams, 1980b; Edwards and Naylor, 1987); their abundance in nature and easy husbandry make them ideal research subject for exploring the crustacean circadian clock but, as a non-model organism, little is known of the molecular framework of the *T. saltator* chronobiology. The work detailed in this chapter was out to identify and determine key molecular elements of the *T. saltator* biological clock. To address the paucity of molecular data on crustacean clocks and the almost complete absence of any in *Talitrus*, a transcriptome was considered a primary objective and of paramount importance. A high quality, circadian transcriptome was assembled and subsequently mined for sequences homologous to known clock genes or transcripts. The identified *Talitrus* clock transcripts were analysed for their expression patterns over the circadian cycle. The transcriptome not only serves to identify potential clock genes but also as a reference for further molecular research in the non-model organism.

3.3 MATERIALS AND METHODS

If not stated otherwise, when working with kits all reactions were carried out according to manufacturer's instructions.

3.3.1 Locomotor activity measurement

The locomotor activity was measured to ensure that used for the experiments were expressing a rhythmic phenotype. For an exact description of the experimental setup, see general methods section 2.2.

3.3.2 Tissue harvest and RNA extraction

To analyse the neural transcripts of *T. saltator* at different times of the day,

head tissue was collected throughout a circadian cycle. A subset of animals that were entrained LD 12:12 and released into DD for 24 hrs were monitored for behavioural locomotor rhythmicity as explained in 2.2. This, was too ensure that potentially observed differences in transcript abundance over the time are intrinsically induced (i.e. endogenous control and not light induced). From the remaining sample of animals (equally in DD for 24 hrs prior to sampling), head tissues were harvested every 3 hrs for eight sampling time points to cover 24 hrs (Figure 3.7).

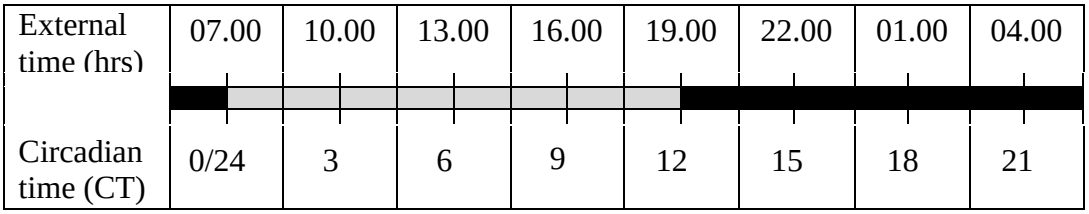

Figure 3.7*:* Sampling scheme with the circadian and the external (local) solar time of tissue collection.

To ensure sufficient material was available for extraction, the heads of 5 individuals were pooled into one sample. Six replicates were generated at each time point.

Animals were quickly decapitated with sharp scissors and the heads immediately put into ice-cold RNA*later*™ Stabilization Solution (Ambion™). To allow full perfusion, the tissue was kept at 4°C for 12-24 hrs and then processed or stored at -20°C. At harvesting, primary and secondary antennae were carefully removed and stored and processed separately. Total RNA was extracted with the RNeasy Mini Kit (Qiagen) the process of which is described in detail in 2.3. Brain and antennal cDNA was obtained from total RNA using the High-Capacity cDNA Reverse Transcription Kit (Applied Biosystems®) using random primers.

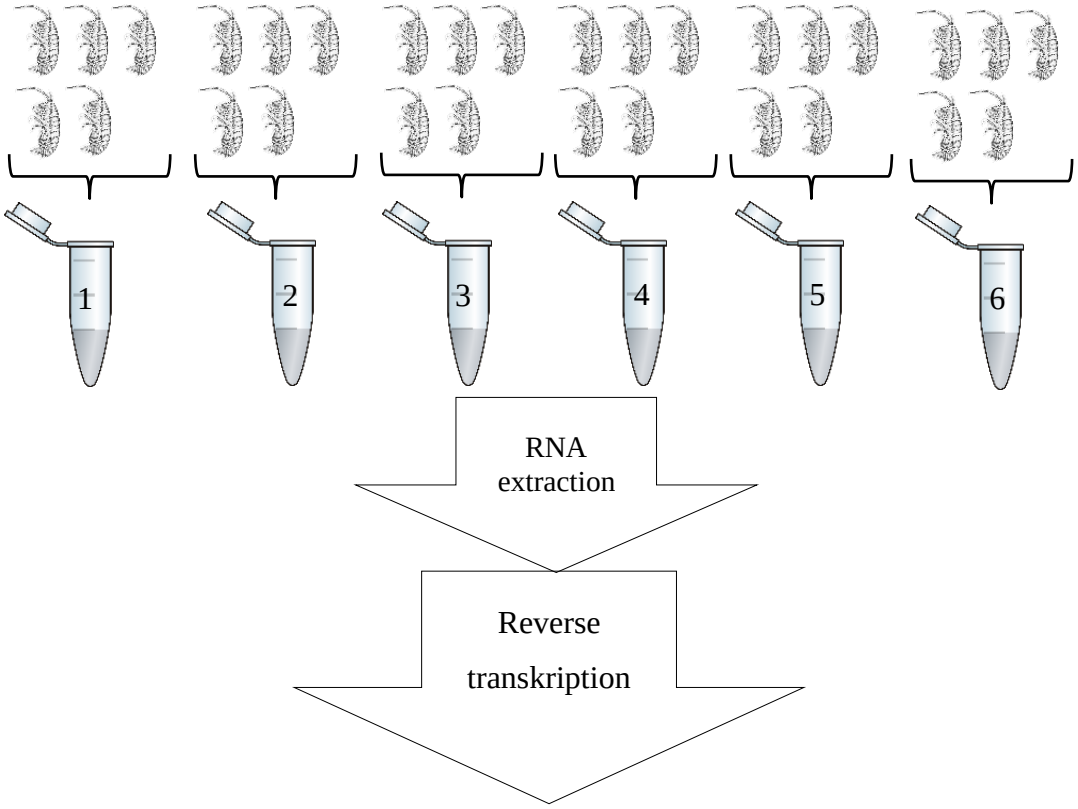

Figure 3.8: Sampling scheme of RNA extraction. At each sampling time point, (Figure 3.7) 5 animals were decapitated and the tissue pooled into one sample. Six samples were generated at each time point. Antennae and heads were processed separately. Reaction tube, free resource image: https://pixabay.com/en/vial-tube-fluid-laboratory-41375/; *T. saltator* body, side view, (public domain image) (Calman, 1911).

3.3.3 Sequencing

Illumina HiSeq2500 sequencing was performed in the Aberystwyth University Core Genomics facilities using its llumina TruSeq sequencing platform (Illumina®, Inc.) by Dr Mathew Hegarty. For each time point, four biological replicates were submitted to the sequencing process. Indexed TruSeq cDNA libraries were prepared for each sample using kit-supplied adaptors (Illumina® Inc.) and library size was verified on a 1% w/v agarose gel. Result quality of the raw sequence data was evaluated with FastQC (Andrews, 2010).

3.3.4 Sequence confirmation

To confirm the sequence identity of the core clock transcripts (*Talper*,

Talcry2, *Talclk*, *Taltim* and *Talbmal1/cyc*), PCRs were run with gene specific primers for each of the clock genes using brain cDNA. The gene specific sequencing primers can be found in Table A.2 and the PCR procedure was conducted as described in 2.5. The resulting PCR products were checked for size on an agarose gel (section 2.6), cut out from the gel and cleaned with the ISOLATE PCR & Gel Kit (Bioline Reagents). The cleaned fragments were cloned into a sequencing vector as described in 2.2 and sequenced in house (2.3). The following sequence analysis was conducted with the computer programs mentioned in 2.10.

3.3.5 *De novo* transcriptome assembly

Sequencing technologies have advanced enormously over the last decade and with the depth of sequencing and volume of data produced, the computational reassembly of the fragmented sequenced information yet remains a considerable challenge, particularly in the absence of reference genomes. Trinity is a software that assembles short-read sequences from platforms such as Illumina® RNA-seq raw data reads (Grabherr *et al.*, 2011).

Assembly proceeds through sequential application of three software modules, namely *Inchworm*, *Chrysalis* and *Butterfly* as shown in Figure 3.9. First, the software sorts the sequencing reads into k-mers (sequence with the length=k) and finds overlapping k-mers. The most abundant k-mer is taken as a seed sequence, which is elongated with help of the other overlapping k-mers. For example if most overlapping k-mers in the library contain a G at the position of interest a G will be added to the seed sequence. This process continues until all overlapping k-mers are used up and the contig is considered finished and a new seed k-mer is elongated until all k-mers are assembled into contigs. In case of splice variants, Inchworm only reports the most abundantly expressed one and the unique region of a splice variant is reported as a small separate contig. To overcome that problem, Chrysalis groups contigs that are related due to alternative splicing. Even though these small sequences do not exhibit complete identical k-mers, they still partially overlap with their larger splice variants. Thus, overlapping ends are utilized to regroup related contigs. Chrysalis then clusters contigs and builds de Bruijn graphs for each cluster (representing the translational complexity at a given locus) and lastly, Butterfly processes the de Bruijn graphs into

alternative spice variants and sorts out transcripts from paralogous genes (Haas *et al.*, 2013).

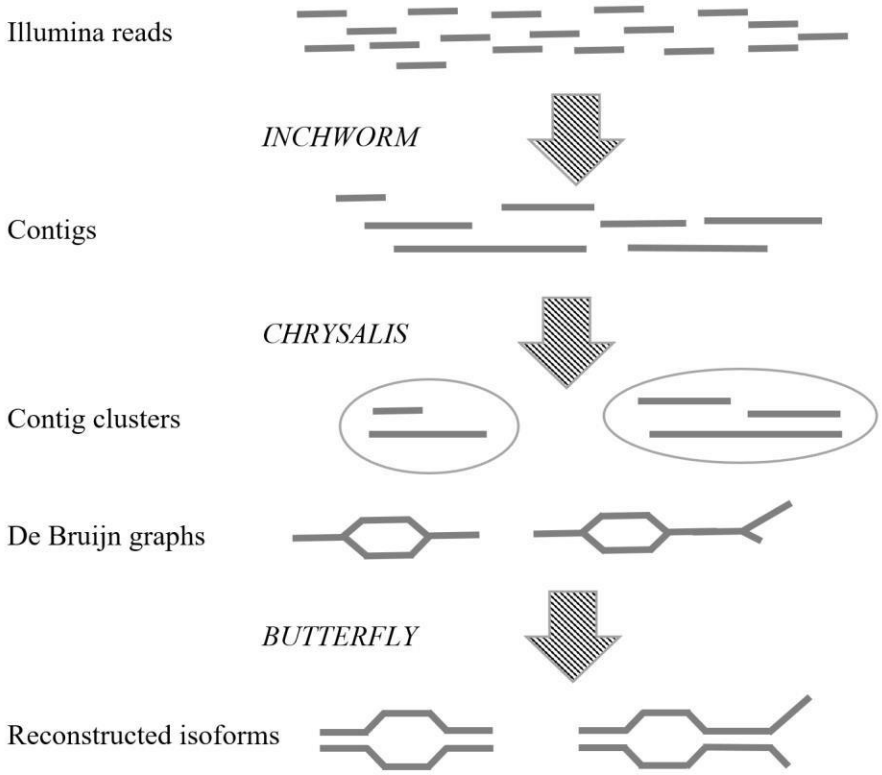

Figure 3.9: Trinity processing pipeline. Raw Illuminia reads were assembled into contigs by the inchworm algorithm. The contigs were then organised by chrysalis into clusters from which De Bruijn graphs were made. The butterfly algorithm then reconstructs isoforms of the transcripts. Image modified after Haas *et al*. (2013).

The transcriptome assembly was performed using the Trinity software version 2012-10-05 with standard settings with help of Dr Martin Swain. Prior to annotation, the entries were 'cleaned' in two steps. At first, transcripts smaller than 300 bases were removed from the assembly and possible misassembles were removed by excluding very similar splice variants using the CD-Hit-EST software (version 4.5.4) with default settings and a sequence identity threshold of 95% (Li *et al.*, 2001; Li and Godzik, 2006).

3.3.6 Full length sequence confirmation of core clock genes

Previous PCR and cloning attempts by O'Grady (2013) revealed full or partial putative sequences for the clock genes: *period, timeless, clock, cryptochrome2* and

bmal1/cycle. These were used as a foundation for the current work in terms of oligonucleotide design to determine the full-length sequence of the clock genes mentioned above. Sequence information of the UTRs (untranslated regions) was obtained via 5' and 3' rapid amplification of cDNA ends (RACE) PCR, cloning and sequencing of the resulting fragments. The methodology is detailed in general methods sections 2.5- 2.10 and the primers used for each clock transcript are displayed in Table A.2 in Appendix A.

3.3.7 Functional annotation with Blast2GO

Reads of the assembled transcriptome were functionally annotated with the Blast2GO software (Conesa *et al.*, 2005; Conesa and Götz, 2008; Gotz *et al.*, 2008) at the Aberystwyth University computing facilities using High Performance Computing Wales computing cluster with initial help of Dr Martin Vickers. This software was used to identify the newly assembled mRNA transcript contigs using the NCBI BLAST algorithm and databases. A functional annotation with an individual seven digits number (evidence codes) representing the path how the contig was annotated was assigned. The functional properties were represented with Gene Ontology (GO) terms which are categorised in either "Molecular Function", "Cellular Component" or "Biological Process". The level of ontology (GO level) depends on the classification defining the relationships between the GO terms and the GO level increasing with increasing specificity (for example: cell, nucleus, integral to membrane etc). The GO vocabulary was composed to be species independent mirroring the biochemical properties functions and special distribution of a molecule. To exclude poor quality hits from the annotation the Blast2GO cut-off parameters were the following: annotation rule cut- off=55, e-value=$1e^{-6}$, Hit-HSP overlap=0 and GO weight=5.

3.3.8 Quantification of mRNA transcripts

To quantify the newly assembled and annotated transcripts, the RSEM (RNA-Seq by Expectation-Maximization) software tool developed by Li and Dewey, (2011) was used. RSEM estimates expression levels of transcripts from RNA-seq data and

is used for *de novo* assemblies as it does not need a reference genome. Fragments per kilo base of exon per million reads mapped (FPKM) values represent the number of cDNA fragments that are assigned to a transcript. They are a numerical representation of the relative expression level of a sequence (Mortazavi *et al.*, 2008). Reporting FPKM values excludes two experimental biases. Firstly, it normalises the read counts for sequencing coverage as experiments with greater sequencing depth may have more mapping reads to each gene. Secondly, it normalises for gene length as longer transcript sequences will have more reads mapped to them. From FPKM values, TPM values (transcripts per million) were calculated following (Pachter, 2011; Wagner *et al.*, 2012). The advantage for TPM values is, that the sum of all values in each sample are the equal. This is important when comparing read numbers within an experiment. As all raw reads from all sampling time points were pooled to form a "master transcriptome" the use of TPM values to express and compare abundance of a given transcript between the single time points is the appropriate unit (Wagner *et al.*, 2012). A subset of transcripts was analysed by One-way Analysis of Variance (ANOVA) to assess differences in the mean expression levels over time. Analysis was performed with SPSS version 2.1 (IBM Corporation).

3.3.9 Identification of rhythmically expressed transcripts

Transcripts that rhythmically cycle in abundance throughout the day, were identified using the JTK_cycle software (Hughes *et al.*, 2010; Miyazaki *et al.*, 2011). It measures the period, phase and amplitude of cycling transcripts and reports permutation-based p-values (ADJ.P) and Benjamini–Hochberg q-values (BH.Q). The TPM values were subjected to the JTK_CYCLE algorithm version 2 following the user's guidelines (v2). JTK_CYCLE can not process datasets with unequal sample sizes per time point. As such, missing values at CT18 were averaged from the three data sets available. JTK was run through R (R_Core_Team, 2013).

3.3.10 Sequence analysis software

NEStradamus was used to identify nuclear localisation signals in the predicted clock protein sequences (Nguyen Ba *et al.*, 2009). NetNES 1.1 was used to identify

nuclear export signal motifs (La Cour *et al.*, 2004).

SIM – Local Similarity program was used to determine sequence identity of translated clock gene transcripts with published invertebrate clock protein sequences using standard settings (Huang and Miller, 1991). Amino acid sequence identity and similarity were also determined by EMBOSS Pairwise Alignment Algorithms (EMBL-EBI) (Rice *et al.*, 2000; McWilliam *et al.*, 2013; Li *et al.*, 2015).

Heat maps representing the changes in abundance of the transcript contigs over the measured period were comprised with Excel, Microsoft Office Professional Plus 2013 (Microsoft).

3.4 RESULTS

To receive a circadian transcriptome, brain tissue of behaviourally rhythmic animals was collected through the circadian cycle. The samples were sequenced and the resulting reads were assembled *de novo.* Functional annotation was performed before rhythmically expressed transcripts were identified to broaden the knowledge about the *T. saltator* biological clock components.

3.4.1 Locomotor activity rhythm

To ensure that animals used in these experiments display behaviourally rhythmic phenotypes, locomotor activity was measured and analysed using suitable circadian software. A subset of the animals was tested in an activity monitor in constant conditions (DD). The measured activity of 5 representative animals can be seen in the periodogram in Figure 3.10 A. It can be clearly seen that these animals exhibited free-running circadian activity rhythms with a calculated locomotor activity period of τ=24.15 h, (Chi Sq Periodogram) and activity during expected night time. The remaining sample was used in parallel for gene expression analysis.

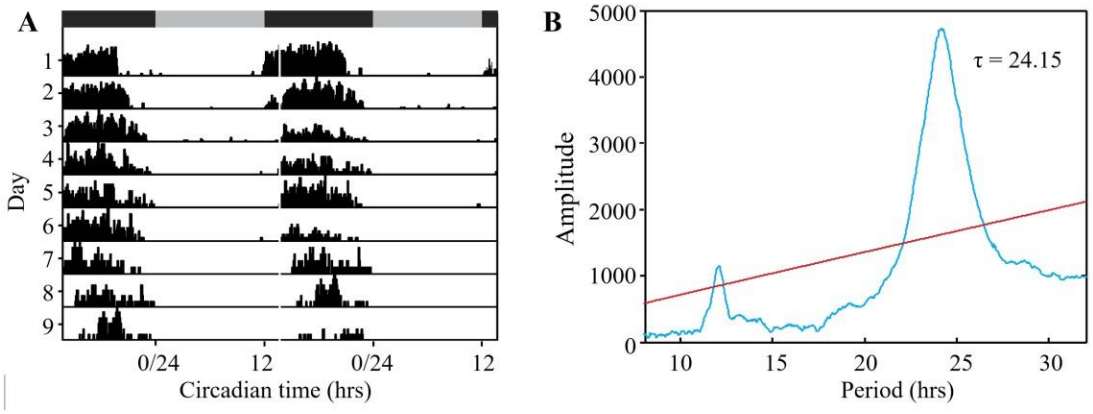

Figure 3.10: Locomotor activity rhythms of *T. saltator* in DD. (A) Actogram shows the averaged activity events of 5 representative animals for nine days; grey bars indicate the subjective day/night. (B) Chi Square Periodogram of data shown in (A). The calculated activity period is reported as τ=24.15 with the red line indicating significance level at $p < 0.001$.

3.4.2 Transcriptome sequencing and assembly

A transcriptome was composed to provide a reference for future molecular work and to widen the knowledge about the *T. saltator* biological clock machinery. This was achieved through sequencing brain mRNA samples and de novo assembly of the resulting reads into a transcriptome. Illumina HiSeq runs on the pooled RNA samples generated 141,769,456 reads. Of these reads 128,386,193 were assembled into 156,766 contigs with mean length of 1,534 bp and an N50 statistic of 968 bp. The pooled assembly is available at the DDBJ/EMBL/GenBank under the Accession No. GDUJ00000000.

3.4.3 Functional annotation of contigs

Transcriptome sequences were submitted to the Blast2GO algorithm to allow functional annotation. The first part of the Blast2GO results comprises descriptive information about the *T. saltator* transcriptome. Of the submitted contigs 126,728 sequences did not result in sequence alignments (singletons). Of the 'blasted' query sequences 7091 could not be assigned a Gene Ontology term (GO term). In total 12,464 sequences were successfully annotated.

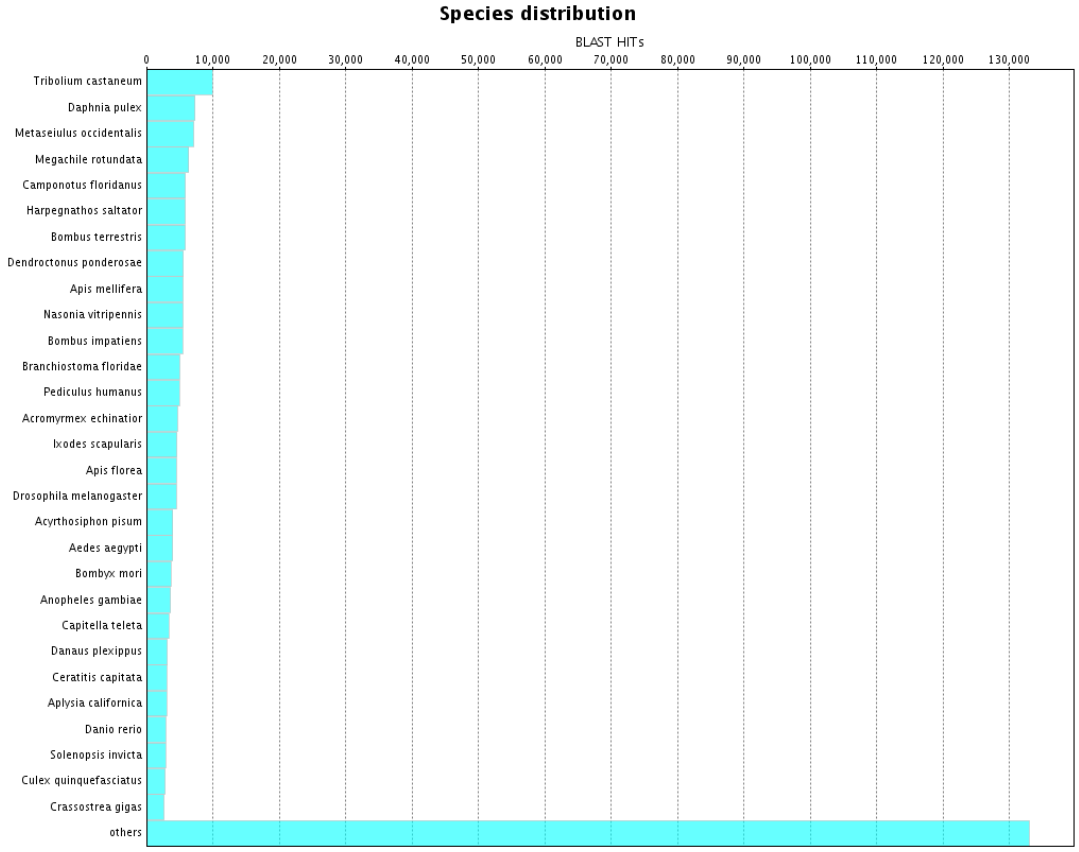

Figure 3.11: Species distribution chart. The number of BLAST hits per species is shown. The top 29 species with the most hits are displayed with *T. castaneum* and *Daphina pulex* harboring the majority of hits.

The majority of contigs aligned best to sequences of the red flour beetle *Tribolium castaneum* (about 10,000 BLAST hits; Figure 3.11). Interestingly, the second most frequently 'hit' species was the cladoceran crustacean *Daphnia pulex* with about 7500 BLAST hits, which is probably a reflection of the large number of annotated genes species the genome for which is publicly available (www.waterfleabase.org). The mite *Metaseiulus occidentalis*, the leafcutter bee *Megachile rotundata* and the carpenter ant *Camponotus floridanus* also returned more than 5,000 hits to the *Talitrus* transcriptome. All top 29 species shown in the species distribution graph are invertebrates apart from the cephalochoradate lancet *Branchiostoma floridae* (ranking number 12).

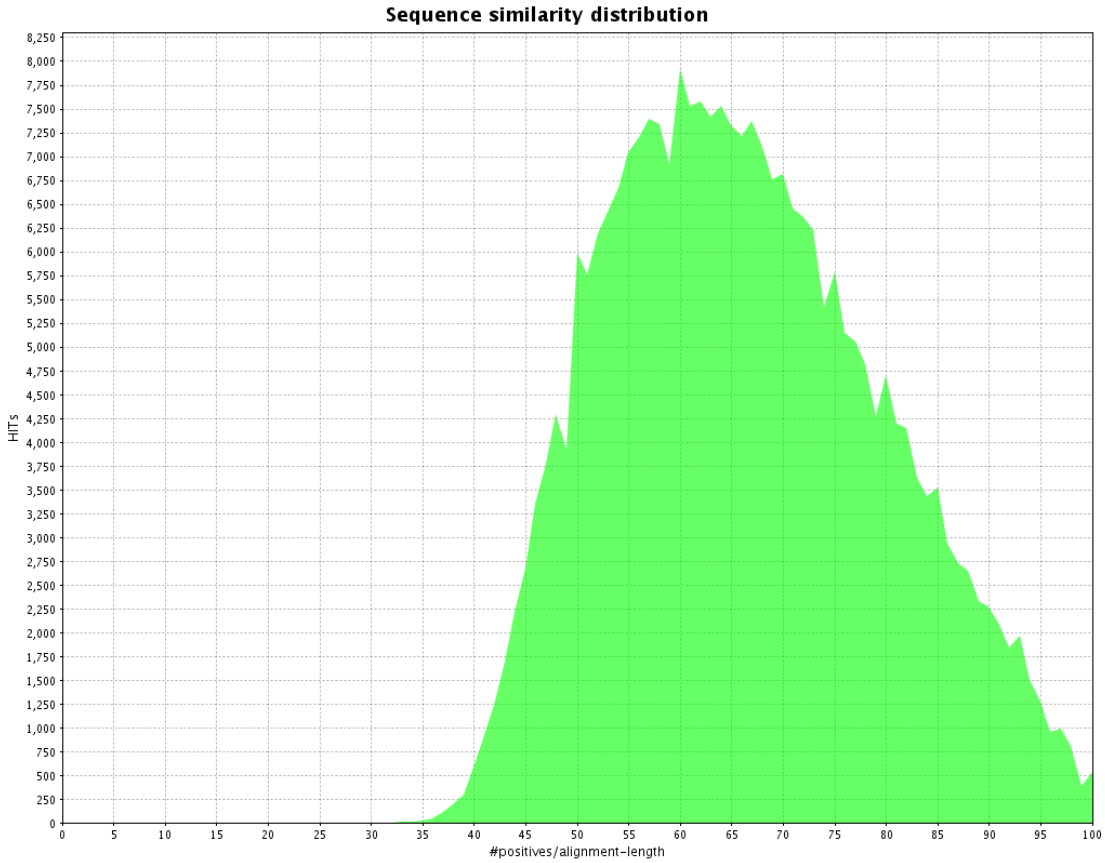

Figure 3.12: Sequence similarity distribution of the Blast2GO analysis. The number of hits is plotted against the respective alignment length.

The sequence similarity distribution is shown in Figure 3.12. The distribution of the positive alignment length of the hits is displayed. The sequence similarity within the sequence comparisons ranges between 35% and 100% with a small proportion of hits (about 500) resembling 100% sequences similarity. Most of the contigs, about 7875, hits have 60% sequence similarity with their respective hit sequences.

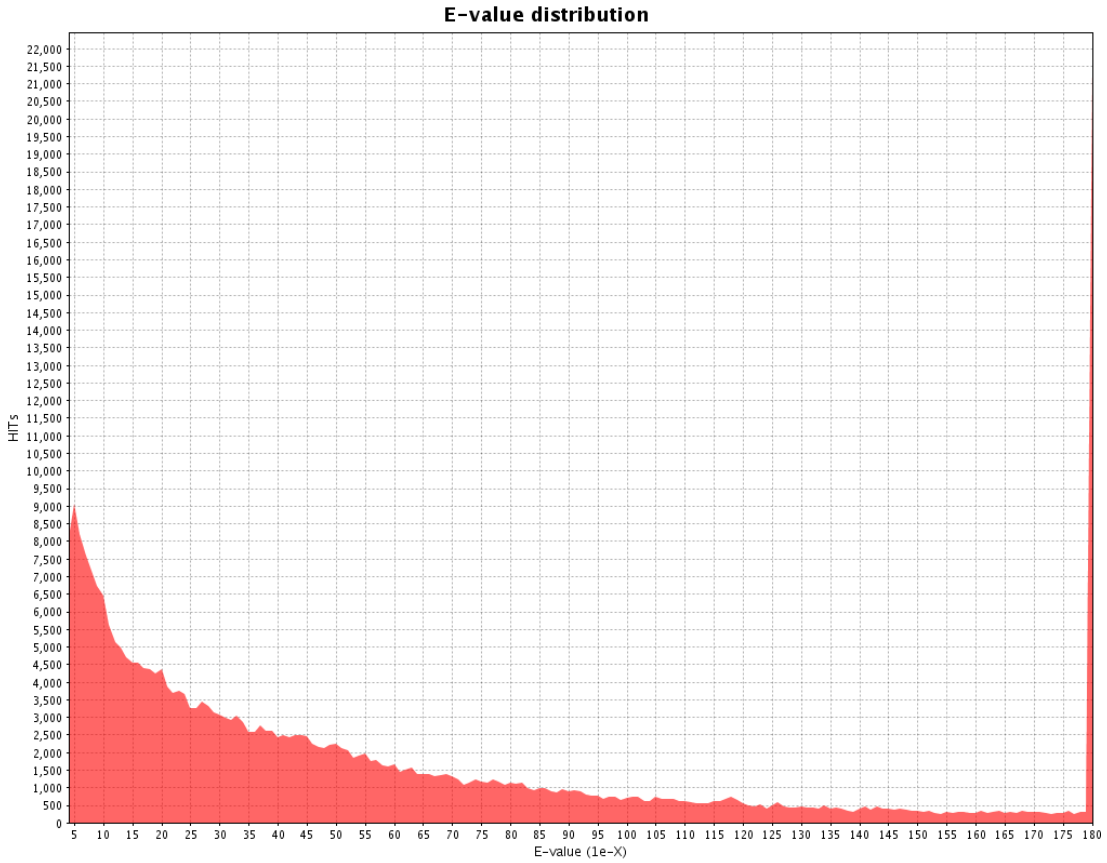

Figure 3.13: E-value distribution chart. The e-values ($1e^{-X}$) are plotted against the respective number of hits.

Figure 3.13 shows the distribution of e-values (expect-values) in the set of sequence comparisons. The data distribution indicates a high number of hits with lower similarity and thus a higher possibility for type one errors (false positive matches). Thus, fewer hits had a stronger alignment. The e-value distribution confirms the reliability of transcript identification in the reassembled transcriptome.

Following the descriptive analysis of the mRNA transcriptome, the GO analysis results are presented. The distribution of the assigned GO levels for the transcriptome contigs is shown in Figure 3.14.

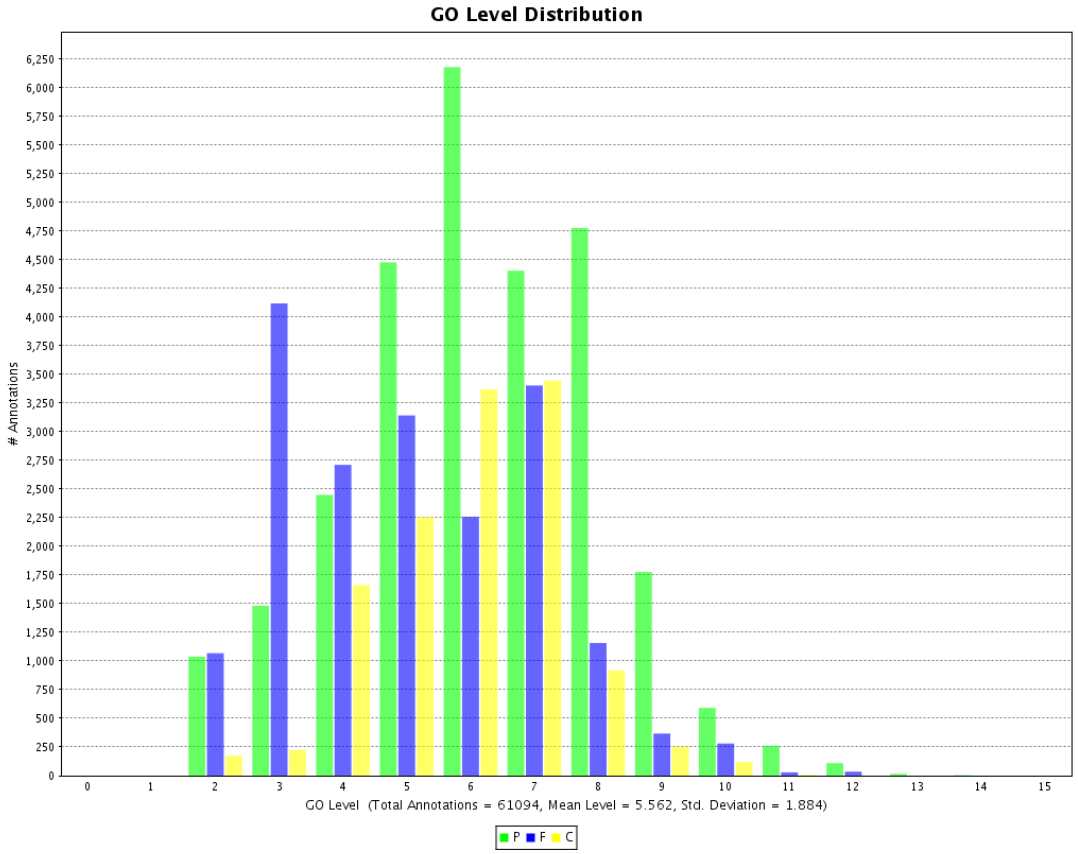

Figure 3.14: GO-level distribution. The number of annotations is plotted for each GO-level. (P=Biological Process (green), F=Molecular Function (blue) and C=Cellular Component (yellow)). In addition the total number of annotations of 61094, the mean GO-level=5.562 and the Standard Deviation=1.884 is given.

More than 60,000 GO terms were found for the *T. saltator* transcripts with a mean GO level of 5.562 and a standard deviation of 1.884. The majority of the 61,094 annotations have a GO-level between 3 and 8. "Molecular Functions" has the most annotations between 3 (maximum) and 7 (depicted in blue). For "Biological Processes" the most annotations are at a GO-level of 6. With over 6,000 GO terms the largest category (green). "Cellular Component" has been assigned GO-levels mostly between 4 and 7 (marked in yellow).

To look into the results in more detail the data for all three categories at the GO level 2 is shown in figures 3.15- 3.17. The GO level 2 terms of the category, "Molecular Function" are displayed in Figure 3.15. 43% of the annotated sequences were assigned a binding functionality, closely followed by catalytic activity with 42%. Between 1-5%, smaller percentages of contigs were assigned to "transporter

activity", "structural molecule activity", receptor activity", "nucleic acid binding transcription factor activity", enzyme regulator activity" and "molecular transducer activity".

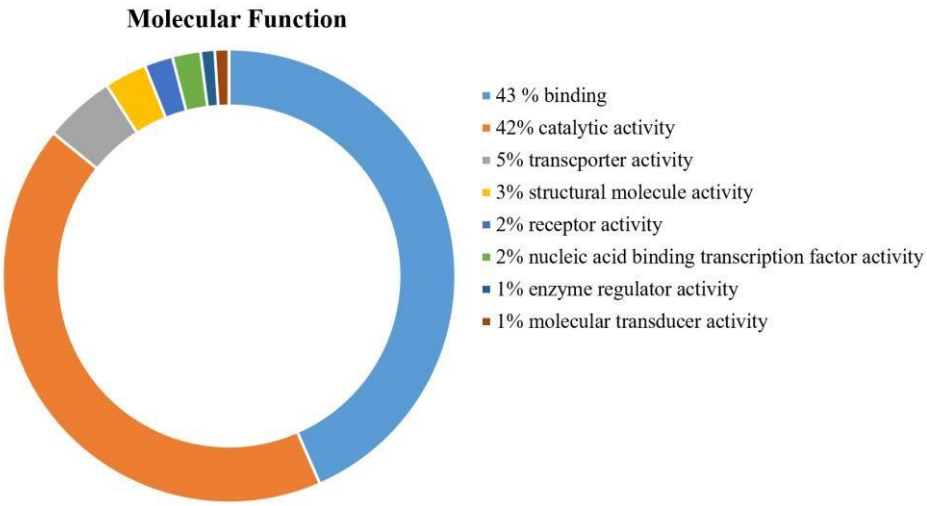

Figure 3.15: Distribution of GO level 2 terms for the category "Molecular Function". Binding and catalytic activity occupy the largest percentage of assigned qualities.

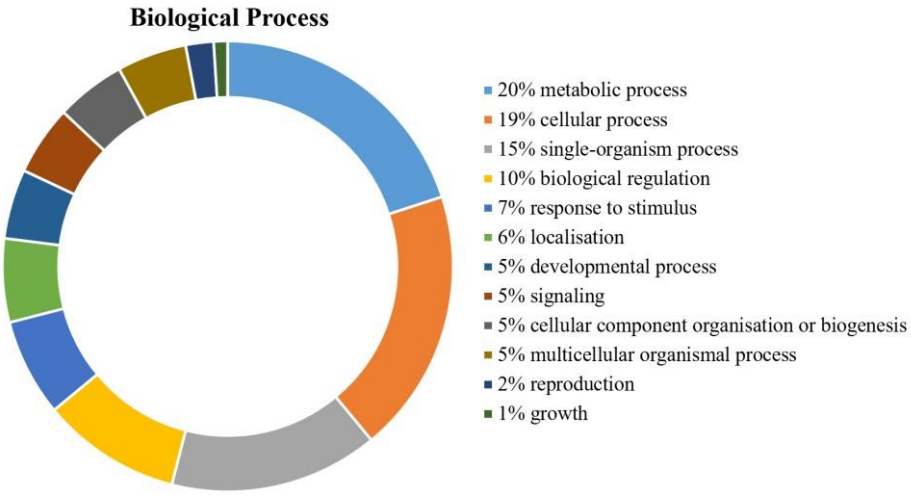

Figure 3.16: Distribution of GO level 2 terms for the category "Biological Process". Most of the annotated sequences are found to be involved in metabolic processes (20%) when considering the "Biological Process" classification.

The corresponding data for "Biological process" is shown in Figure 3.16, where the largest percentage of annotated sequences are determined to be involved in "metabolic processes" (20%). This is closely followed by very general category of

"cellular process" with 19% and "single-organism process" with 15%. The category "response to stimulus" was assigned 7% of the hits. A proportion of 5% of transcript hits were assigned to the categories "developmental process", "signalling", "cellular", "cellular component organisation or biogenesis" and "multicellular organismal process" each. A very small subset of contigs is assigned to "reproduction" and "growth" with 2% and 1% respectively.

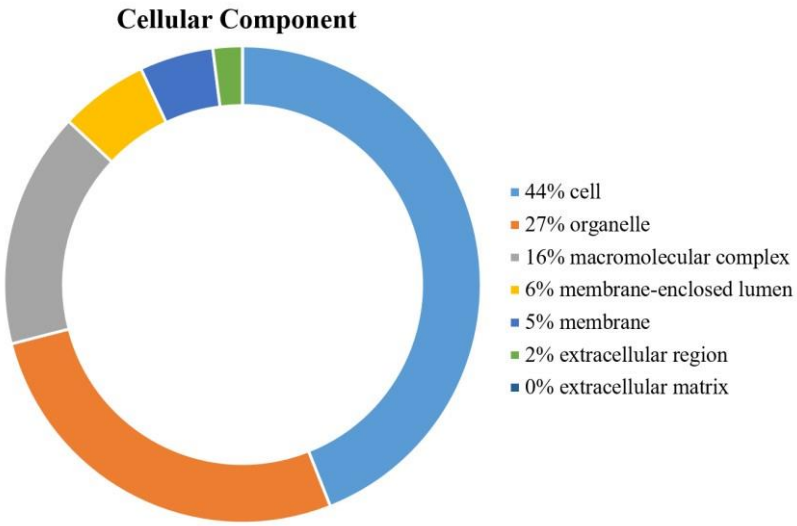

Figure 3.17: Distribution of GO level 2 terms for the category "Cellular Component". The vast majority of annotations were classified to be in the cell (44%), as opposed to 2% of the annotated contigs were assigned to the extracellular region.

For "Cellular Component" 44% of annotations fall into the "cell" category (Figure 3.17). The Blast2GO annotation associates 27% of the contigs with an "organelle" and 16% with the category "macromolecular complex". A lower proportion (6%) were assigned "membrane-enclosed lumen" and 5% of assignments were associated with the "membrane" category. A very small subset of assigned contigs, namely 2% were assigned to "extracellular region".

In Figures 3.18- 3.20 the direct GO counts for the three GO categories "Molecular Function", "Cellular Component" and "Biological Process" are given. The direct GO counts are summaries of the most abundantly assigned GO terms in the transcriptome ignoring the GO hierarchy.

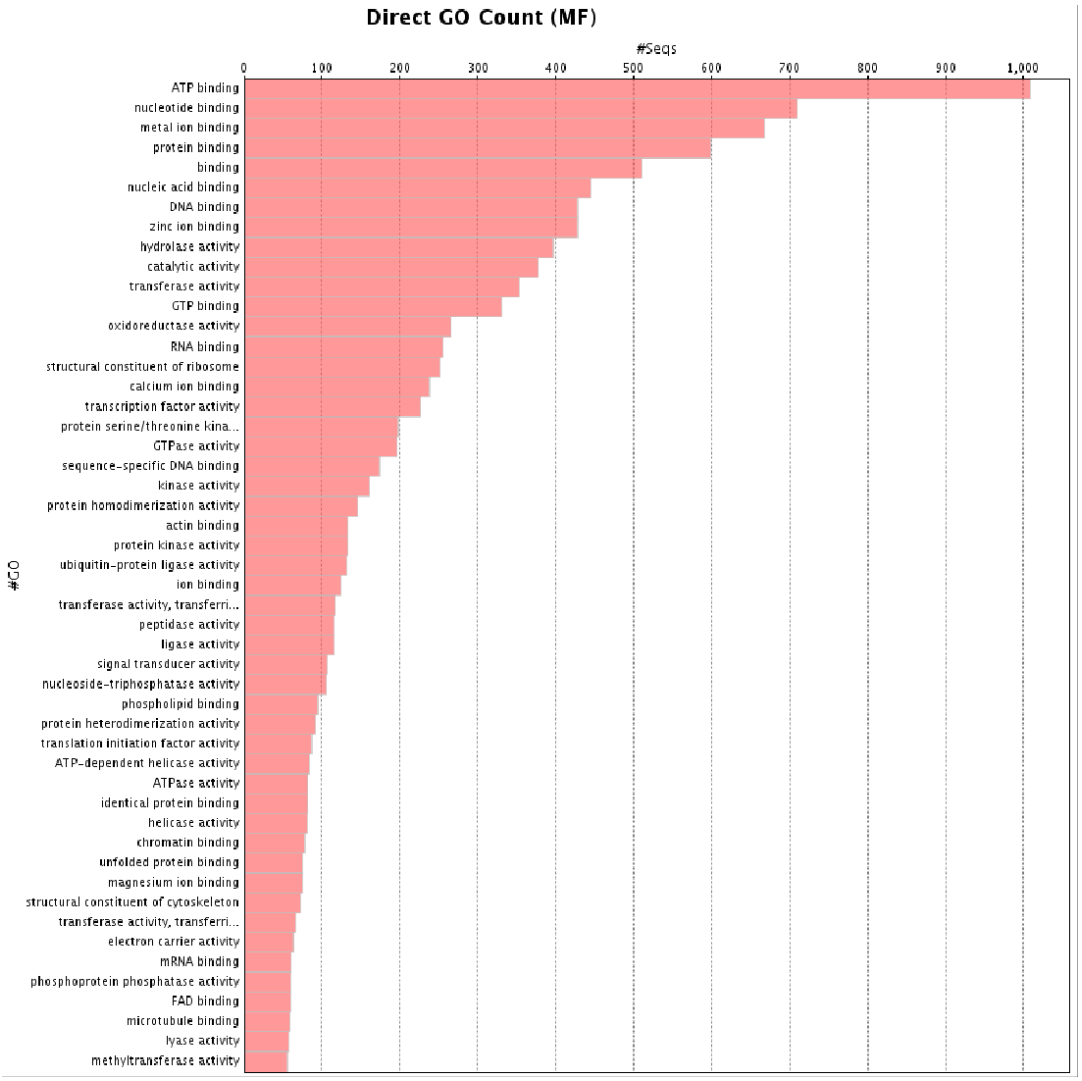

Figure 3.18: Direct GO Count "Molecular Function" (MF). By far most of the GO Counts (more than 1000) for the category of Molecular Function are ATP binding. But also nucleotide binding, metal binding and protein binding are the most common molecular functions assigned.

GO counts for "Molecular Function" are displayed in Figure 3.18. The vast majority of annotations were assigned a GO term associated with a function relating to "binding" properties. The largest number of sequences are assigned "ATP binding" with more than 1000 contigs. Second frequently used GO term is "nucleotide binding" containing about 700 sequences. This is followed by approximately 660 sequences that got assigned the GO term "metal ion binding". For the category "Biological Process" a block of GO terms is very often assigned. In order of frequency these are "oxidation reduction", "serine family amino acid metabolism activity", "signal transduction", "regulation of transcription", "metabolic process" and "protein amino acid

phosphorylation".

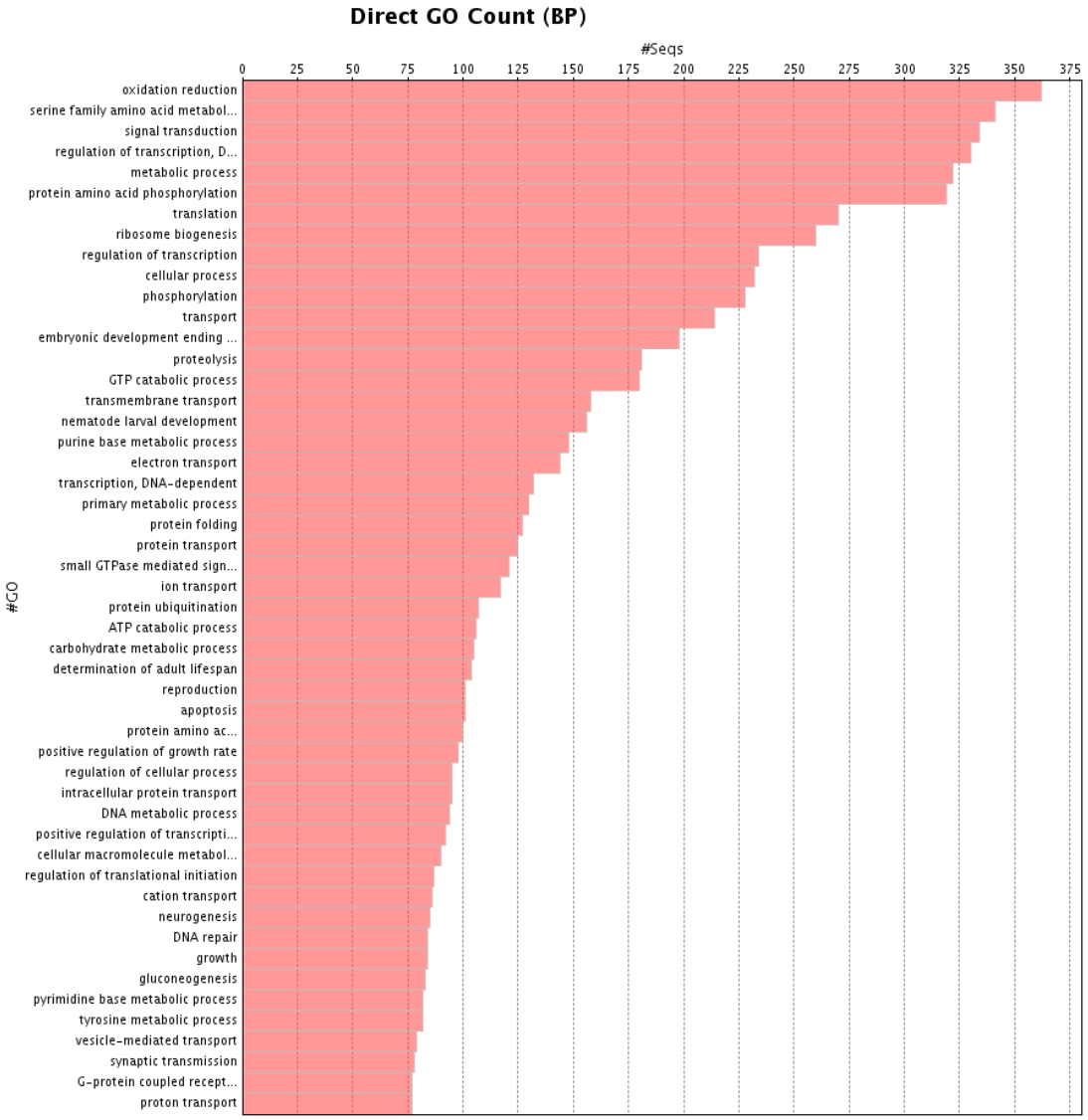

Figure 3.19: Direct GO Count for "Biological Process" (BP). Most of the sequences are classified into the oxidation reduction, are serine family amino acid metabolism, signal transduction, regulation of transcription and metabolic process and protein amino acid Phosphorylation category.

Most of the sequences, (more than 950) were categorized into the nucleus "Cellular Component" category but "cytoplasm", "membrane" and "integral to membrane" are assigned very frequently for about 700 sequences each (see Figure 3.20).

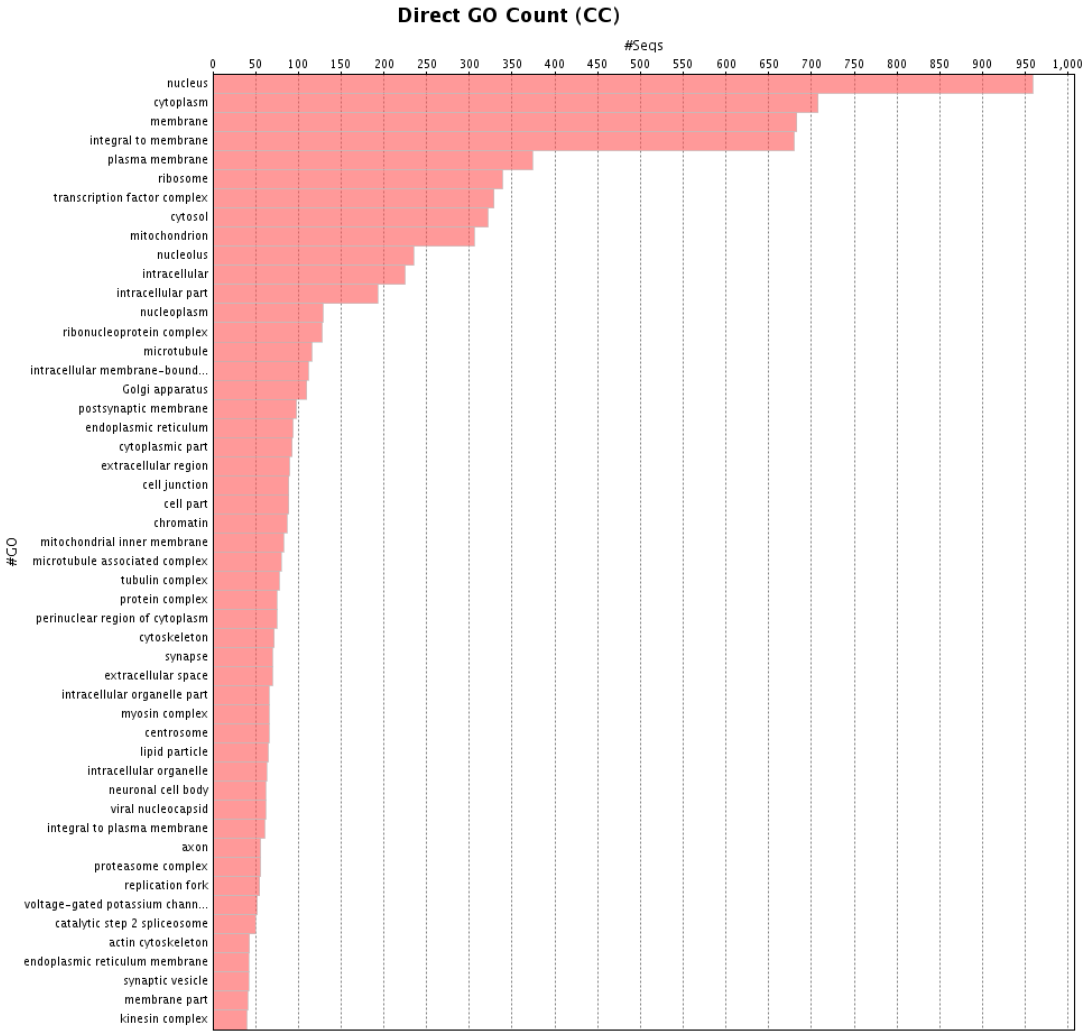

Figure 3.20: Direct GO count for "Cellular Component" (CC). The number of sequences for a specific GO are plotted for the "Cellular Component" category. Most of them, about 950 sequences have nucleic association followed by cytoplasm (about 700 sequences) and membrane (about 650 sequences).

Following in the Blast2GO pipeline, the data treatment 'Annex' (Myhre *et al.*, 2006) is hereafter performed to improve and refine annotations after Blast2GO to provide additional annotations and confirmation of GO terms. Annex analysis of the current dataset is summarized in Table 3.1. In brief, Annex analysis created 4809 new annotations and replaced 726 annotations and a total of 1815 annotations made by Blast2GO were confirmed. From the annotated transcriptome, 1.35 % of annotations were replaced. A number of 8.54% of annotations were newly added to the transcriptome with Annex analysis. This indicates that the initial annotation, done by Blast2GO were largely very accurate and reliable. However, it should be noted that this could also be a consequence of the low number of reference genomes or

transcriptomes for related crustacean species available to date.

Table 3.1: Summary of Blast2GO results. number of 8.54% of new annotations were made in process of the annex analysis. Only 1.35% annotations were replaced. Bar graph representing respective data is shown in Appendix Figure A.3.

Annex results category	**# of annotations**	**% of original annotations**
Total original annotations	56285	100%
New annotations added via Annex	4809	8.54%
General annotations replaced by more specific Annex annotations	726	1.35%
Annotations confirmed by Annex	1815	3.22%

3.4.4 Analysis of putative clock gene protein sequences

To shed light on the *T. saltator* clock composition on a transcript level, the Blast2GO annotated contigs were mined for homologs of classical core clock genes and clock associated genes. Together with information from previous analysis (O'Grady, 2013) and similarity search with clock gene homologs, entries from the FlyBase, the mRNA contig sequences for the core clock genes *Talcry2*, *Talclk*, *Talper*, *Taltim*, and *Talbmal1* were revealed. The corresponding contig identification numbers and their length in nucleotide numbers are summarised in Table 3.2. In the same Table the deduced, putative clock proteins, their length (amino acids) and names are given. Apart from the core clock genes, 22 further mRNA contigs were identified that are putative clock associated genes thought to contribute to clock function and entrainment (Table 3.2). For most of the clock genes, the coding DNA sequence (CDS) is known due to additional manual sequence confirmation done by PCR, cloning and Sanger sequencing (as described in 2.5, 2.8, and 2.9). The agarose gel electrophoresis images showing the respective PCR products are shown in A.11-A.18. The putative clock gene sequences were analysed through tblastn and tblastp searches on the NCBI website. The resulting top hit species, accession numbers and e-values are displayed in Table A.7

The translated protein queries of the core clock genes are shown in Figures 3.22-3.26 and schematically summarised in Figure 3.21.

The protein domains were predicted with the web tool Simple Modular

Architecture Research Tool (SMART) (Schultz *et al.*, 1998; Letunic *et al.*, 2015) and are printed in coloured letters.

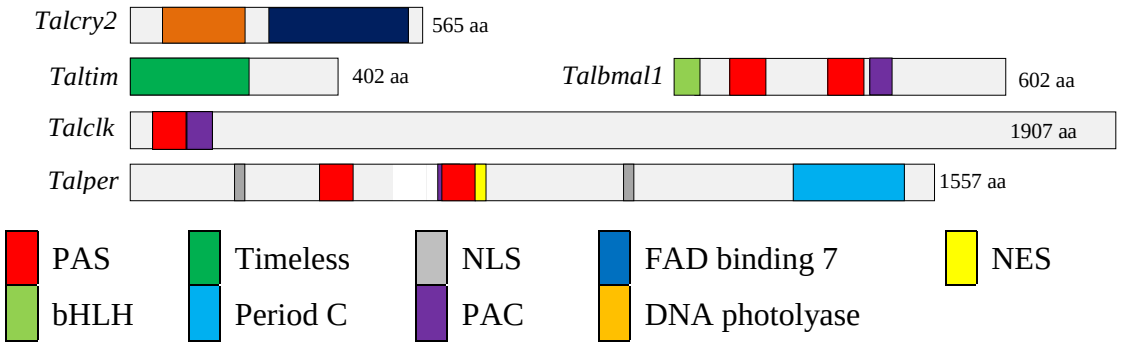

Figure 3.21: Schematic representation of the *T. saltator* core clock protein sequences. Functional motives are color-coded. The length of sequences is proportional.

The *Talcry2* mRNA sequence is represented in two separate contigs. Both were annotated as *cryptochrome2* during the Blast2GO analysis. In the correct orientation, both contigs combine to form one single *Talcry2* sequence the identity of which was confirmed by manual sequencing (see Table A.2 for primers). The combined contig covers the full CDS of the 565 amino acid putative TalCRY2 and is 1,843 nucleotides long. TalCRY2 shares 46.4% identity with the *D. plexxippus* CRY2 protein (Accession No. ABA62409; (Zhu *et al.*, 2005)) and a 78.2% high sequence identity with the CRY2 of *E. pulchra* (Accession No. AGV28717; (Zhang *et al.*, 2013)). It comprises a DNA photolyase domain (orange) and a FAD binding 7 domain (blue) as visualised in Figure 3.22.

MSPNKIASPGERSIHRTILGDNNLTFSESGSSSGLAFTAEKKNTSKVVSGKH**VVHWFRRGLRLHDN**
PALRDAIVNCETFRCIYILDPWFAGSSNVGVNKWRFLLQCLEDVDNSLRNLNSRLFVVRGQPANAL
PQLFKEWNTTVLSFEEDPEPFGRARDASIIGIAQEMGIEVIVRTSHTLYELDKIIKKKGGKPPLTY
KTFQNILAMMDPPPPPVAPIEASDLKHAYTPLQHDHDDKYGVPNLEHLGFETEHLPPAVWKGGETE
ALSRLKHHLERKAWVASFGRPKMTPQSLFA**CPTGLSPYLRFGCLSARKFYTELNVLYTKIKKVPAP**
VSLHGHLLWREFFYTAATNNPKFDHMKGNPICVQIPWDKNPEALAKWAHGQTGFPWIDAIMTQLRT
EGWIHNVARHAVACFLTRGNLWVSWEEGMKVFDELLLDADWSVNAGSWMWLSCSSFFQQFFHCYCP
VRYGRKADPNGDFIRTYLPVLKNFPTKYIHEPWMAPESVQRNARCIIGQHYPLPMVDHGTQSQNNI
ERMKQVYQQLAHYRANISTRPCGDSKLRCKYPLHSTA

Figure 3.22*:* TalCRY2 sequence. Determined by homology cloning by (O'Grady, 2013) and confirmed by the Blast2GO analysis. A DNA photolyase domain is displayed in orange and the FAD binding 7 domain is highlighted in blue which were identified by SMART analysis.

MVLGDHRTSNGSSCTQEAMEVLPPKLEEAGNQSLPSGVPTDQHVSNSPPESQEDTAAASAIESDP
EGRRQQPQNGQDPTNPCSQADQGYGSTESSFNGQSRKSSSYSGGGSLTKSRNSGSSQSSGFGEQH
KKDAHTASITSSDKESATRAPHIDTQHSNDGNTEELTDNLAAISCKSKSSSVGVDKLHDGAHYGS
STPREKRTKEQKLRDFKRKKVEESHYQTYDSFPRPPESYSFAAAAARASDLPDKHVENFTAPLIS
LQTQKDEFREPLRNFSGPSCSKNDYAIGSKATCLQSASMPSASGVKRSLDSSVVPGAQQSFFSQC
AASTSYTVSSSCRVKNEITDQPTLIYTQALNYIRRIKEGFTNKGQVFQSPEREHLSSNQSEAIA**D**
FIKSFGSNQRGFTMVLSIRDGTIIRVSTNISEVLGFPEDMVVGHSFIDFVYPRDSVHFSSKIVSG
MSLFTKNSSTRAESLMPPFYCRVRENKCYQASAFDMRGKNSYKPCKITLKFNDTLTPLEEEVMAP
ISPFHLPTSDVLLAEVIPVP**SFYQVPDEVINGGNFVIRHSASCNFSEYDPDAIPFLGHLPQDLTG**
NSIFDCYHPEDLPLLKTIYREIIREEGKPFR**SESYRFRTFNGSWVVLETEWLCFVNPWTRKIDSI**
IGQHKVIKGPRDISIYMEQCEGSLSTYSEEVCIIARKARREIIDLLSRPVAASLAEVLRHETRHP
TVSPMQHENCVGIKVPASKRRRTLAEMMSCLVNDIHAQGMKNLTSAAKISTLPTSGISTSTSTAV
TTSSAAINNSMAVQTSAPARNAVEPSASAAVTQAAKGESLLSSSESPSTYSRLNYSATMLRFFQS
NPRTASTDASAESKMESSIRGSVDEAKSSSPKQQYCKFSNSVPSGVNKSLYMSGYGSGSGDTIYL
TRKYGSKDVTDSGSGESASGPSSASGGAGSANYRHVPLTEEVLSRHNQEMQMLFMERQKKNTVAI
TTPSRQRERLSRQKLKQVKKASRKPPSKCALKRPNSGSQRGDNRAHKFPFIEKTSAKQSEQTGPS
HLPGPLHTTHGNKLTINSFHSGSGSRADHVTRRTDLAVPVIPATCSSEQPQAPYFFPGHPLPTPS
NGFQNTSLPSNPSTSLSQEPQLPSNPHPYPMTPMMMGPHQTHFMTPQGLALPLHYMGAYPGMYIP
HPSFNQAMYGAGPLMMSNMMMPHPFIQQSTSADPLHVSPTNLNTPSRQADNQSYIAQVAPVERSS
QSLQQRHTDHHHTHSHHQQQAQLQQPLPHPKSPHGVVHLRKRSDSRATSVKVEPGSVRGSVASAS
GQLRCSMSHRPESLRSETDEPGHAEQGLVYVP**RVASHASHFSRSTSVLGEAESIASPDKRPSGME**
DQHAENSSDTVMSDSSPAQDSMPMLSEFSVDTSESIGVIQPPCDDRPVLHDPAWLDHIEVTPQLL
FRYQLHTKELVDVLKNDMAALKTLNQPALVEDQLSSLYQELEIDGEQLQLDEGITSSSGEEMLDV
STKTSSEAGAARGAKKARSSRYFDKQAILHEVEAAIPPPDLSISHISPYSVARRLPNKHKS

Figure 3.23: TalPER sequence derived from the Blast2GO analysis. Two PAS domains revealed by SMART analysis are shown in red, the PAC domain in purple and the Period C domain in blue. NLS identified by NEStradamus are highlighted in grey. Amino acids that, according to NetNES analysis, are likely to contribute to a nuclear export signal are highlighted in dark blue.

A putative *Talper* mRNA sequence was determined in one contig (comp102279_c0_seq7) which was made up from 8,001 nucleotides. As was the case for *Talcry2*, the full CDS was confirmed by manual sequencing with the primers used available in Table A.2. The translated TalPER sequence is composed of 1,557 aa and the sequence contains two PAS domains (Figure 3.23). Additionally, a PAC domain and a Period C domain was found. Characteristic nuclear export signal and nuclear localisation signal motifs were also found. The translated putative TalPER sequence most shared the highest similarity with the PER sequence of *E. pulchra* (Accession No. AGV28#714; (Zhang *et al.*, 2013)) in the NCBI database.

Table 3.2: Contigs coding for clock genes in *T. saltator*. Core clock gene contigs and clock related gene contigs are shown together with the derived putative protein names and length in amino acids. P=Partial CDS sequence, F=full CDS sequence

Clock genes	**mRNA transcript**		**Protein**		
	Trinity contig ID	**Length**	**Name**	**Length (aa)**	**SMART identified domains**
Cryptochrome2	comp100937_c0_seq1 comp102609_c0_seq3	1,843	TalCRY2	565^{F}	DNA photolyase domain, FAD binding 7 domain
Clock	comp100688_c1_seq1	5,723	TalCLK	1,907^{P}	PAS domain, PAC domain
Period	comp102279_c0_seq7	8,001	TalPER	1,557^{F}	two PAS domains, PAC domain, Period C domain
Timeless	comp849619_c0_seq1	1,209	TalTIM	402^{P}	Timeless domain
Cycle/Bmal1	comp12103_c0_seq1 comp939723_c0_seq1	1,807	TalBMAL1	602^{F}	bHLH domain, PAS domain, PAC domain
Pdh I *Pdh II*	comp92607_c0_seq2 comp97165_c0_seq3		TalPDH I TalPDHII	129^{F} 89^{F}	PDH domain
Casein kinase 2α	comp102480_c0_seq1	5,147	TalCK2α	353^{F}	Serine/threonine protein kinase catalytic domain
Casein kinase 2ß	comp99101_c0_seq3	1,567	TalCK2ß	220^{F}	Casein kinase regulatory subunit domain
Clockwork orange	comp1009591_c0_seq1	503	TalCWO	167^{P}	bHLH domain, Orange of the Hairy/E(SPL) family domain
Doubeltime/Cl1ε	comp87763_c0_seq1	1,092	TalDBT	310^{F}	Serine/threonine protein kinase catalytic domain
Pdp1ε	comp98345_c0_seq1	3,423	TalPDP1ε	508^{F}	basic region leucine zipper domain
Pp1	comp97405_c0_seq1	1,725	TalPP1	357^{F}	protein phosphatase 2Ac catalytic domain (ser/thr phosphatase family)
PP2A-su mts	comp98380_c0_seq1	2,981	TalMTS	309^{F}	protein phosphatase 2Ac catalytic domain (ser/thr phosphatase family)
PP2A-su wbt	comp102157_c1_seq1	2,474	TalWBT	458^{F}	B56 domain
PP2A-su tws	comp99704_c0_seq3	1,633	TalTWS	445^{F}	seven WD40 domain
Shaggy	comp99811_c0_seq7	4,413	TalSGG	418^{F}	serine/threonine protein kinase catalytic domain
Supernumerary limbs	comp98870_c0_seq1	2,121	TalSLIMB	588^{F}	D domain of beta-TrCP, F box domain, 7 WD40 domains
Vrille	comp100474_c0_seq6	3,949	TalVRI	509^{F}	basic region leucin zipper domain
Ebony	comp99283_c0_seq2	4,380	TalEBONY	974^{F}	AMP binding domain, AMP binding C domain, PP binding domain
Rorα	comp99654_c0_seq3	2,217	TalRORα	599^{P}	C4 zinc finger domain, HOLI ligand binding domain
Rev-erb	comp101252_c0_seq2	5,385	TalREV-ERB	1,110^{F}	C4 zinc finger domain, HOLI ligand binding domain
Sirt1	comp101818_c1_seq1	4,033	TalSIRT1	955^{P}	SIR2 domain
Sirt2	comp97450_c0_seq4	2,275	TalSIRT2	376^{P}	SIR2 domain
Sirt4	comp92313_c0_seq2	2,977	TalSIRT4	354^{P}	SIR2 domain
Sirt6	comp69157_c0_seq1	1,209	TalSIRT6	402^{P}	SIR2 domain
Sirt7	comp95761_c0_seq1	5,180	TalSIRT7	948^{P}	SIR2 domain
Jetlag	comp100423_c0_seq4	2,454	TalJET	458^{P}	F-box domain, leucine-rich repeat domain

The contig comp849619_c0_seq1, was annotated by Blast2GO as “timeless protein”. The sequence is 1,209 nucleotides long and only partly covers the complete coding region. The translated protein sequence spans 402 aa (Figure 3.24). One 228 amino acid long Timeless domain was found by in the protein sequence as depicted in Figure 3.24. From the NCBI database the partial TalTIM sequence most closely aligned to the termite *Zootermopsis nevadensis* Timeless-like protein (Accession No. KDR17447; (Terrapon *et al.*, 2014)).

RVLQTDWLPLLREHHSDSALLDLVLRLLVNLTTPALLVFHQEIPEDKAGREMYLRLVSQQQGFKE
AFTDAGVWASVAGVLGSRLQQGSERDDDANLIIEMCLVLLRNVLAVAPGHQDTTRTSDDADLHDQ
VLWSLHLAGIPDLLLYLSTSTDESDLSLHTLEIISLMLRQQDPQNLAGSALHRSAEEQRKDAEAL
VQVRQAEKARRQQQVRKHYNARHSRFTYYVQNMKSISDRDVIAHKPVADVNSFNFDQNKRGKKIP
KNRAPLPDSAVTRRSTLAIRLFLQEFCVEFLNGAYNNIMSIVKDNLNRARVQEHDESYYLWAMKF
FMEFNRHHEFKVELVTETLSIQSVHYVQTNIETYHEMMTTEKKKIPLWSRRRHNGLRAYQEIMMS
LSAMDKSPDQ

Figure 3.24: Translated partial *Taltim* contig identified via Blast2GO analysis. The Timeless domain is accentuated in green, which was revealed by SMART analysis.

A putative *Talbmal1/cyc* mRNA sequence information was split over two different contigs. One of which was annotated by Blast2GO as “*circadian protein clock arnt bmal pas*”. Using the *D. melanogaster* CYC (dCYC) sequence (Accession No. AAF49107; (Adams *et al.*, 2000)) as a search input two contigs were identified in the *T. saltator* transcriptome (similarity search conducted by (O’Grady, 2013)). The contigs potentially coding for TalCYC/BMAL1 aligned to different regions of the dCYC sequence. The two contigs, assembled in different orientation can, however be reoriented and joined to form one continuous sequence the sequence identity of which was confirmed by manual sequencing as described in 2.8- 2.9 (oligonucleotide primer sequences in Table A.2). The resulting sequence spans 1,807 nucleotides and when translated results in a 602 amino acids (aa) long protein. The full CDS is available including 5’ and 3’ ends identified by RACE-PCR described in 2.7. The protein domains found in the TalBMAL1/CYC sequence (Figure 3.25) are a bHLH domain (shown in blue) and two PAS domains as well as a PAC domain and also comprises a C-terminal transactivation domain. The latter is characteristic for mammalian-like BMAL1 sequences and taken together with the Blast2GO annotation result it was determined that *T. saltator* harbours a mammalian-like

BMAL1 instead of a fly-like CYCLE. In the NCBI database the putative protein TalCYC/BMAL1 sequence most closely aligned to the signal crayfish *Pacifasticus leniusculus* BMAL1 sequence (Accession No. AFV39705).

SVASLSSDGVNIKKKLPTLGESHNDEDLDCSKNNRSSAEWNKRQNH**SEIEKRRRDKMNTYISEL**
SRMIPQCQSRKLDKLSVLRMAVQHIKMLRGSINSYTETGQYKPSFVSD**EQVQQLLQQQCTEGFL**
FVVGCDRGKILFVSESVSHILQYSQCELLGLSWFDILHPKDLTKVKEQLSCGDISRRERLVDAK
TLLPVHHSPNSSSSSSCGNYPSLPQDLTRLCPGSRRAFYARIRRPNVHKAPADDASDDASAMTG
DKRYMSIHFTGYLKSWHGAFRPAGVGDEDHDSGDAACLVAIGRL**HRPLSCASVPLKFVAKLSPE**
AKYNYVDQRMSVVLGWLPQEVLGASVFELSHPSDHCRLAAAHRALLSKTTVVE**SLQHRCRHKDG**
RWVRLEGSWKLFINPWTNELEYIVASNTVFSDDKLSSTDDSSQRNSLLQYGDSVPPDPSLSPSL
PSLTPSLGATLQQNGGGSAVPDAPASTCGSDVTDSYTVIQGQAVGSSSLASIQMARAVSGDGSD
DTASQCRASGAGEMVSDQPSTEGKDASSGDGNPLQLNLDVPARLPFLHHYNARSESEASGVGEA
TSDSDEAAMAIIMSLLEADAGLGGPAD

Figure 3.25: Putative TalBMAL1/CYC sequence. The sequence was split on two separate contigs. For the combined sequence a bHLH domain was identified which is accentuated in light green. The two PAS domains identified by SMART analysis are red and the PAC domain purple.

Blast2GO analysis annotated one contig as "*clock1-7*". When translated the sequence does not contain a stop codon and thus does not cover the complete CDS, or represents an incomplete or misassembled sequence. In this partial sequence (Figure 3.26), one PAS domain, a PAC domain and coiled coil domains were identified. When aligned to the sequences in the NCBI database the closest hit was that for a CLK sequence of the prawn *Macrobrachium rosenbergii* (Accession No. AAX44045; (Yang *et al.*, 2006)).

QQHQQQQPQQHQQPQHPPQRPQEQQQQLQRNDQPEQNQPVFVGICRLEQPQLL**REMRLLERTNT**
EFVSRHSLEWKFLFLDQRASAIIGYLPFEVLGTSGYDYYHVDDLERVSTCHQFLIRTGKGS**SCY**
YRFLTKGHQWVWLQSHYYISYHQWNSKPEFVVCTNTVVSYDDIKAELNGSSTNYNDSSTNLQTS
SLTEDKTVSSSCPSQNCTFAEKIDPETKCKSEQNQRFFQKIQSFEEQCMNSSSRAEQSSS

Figure 3.26: Putatuve TalCLK partial sequence. Deduced from the Blast2GO annotated contig comp100688_c1_seq1. The PAS domain identified by SMART analysis is marked in red and the PAC domain shown in purple.

Besides the canonical clock genes, the present *T. saltator* neurotranscriptome was probed for homologs of clock-associated genes of which 22 were identified. Among these were the casein kinase II subunits α and β (CKIIα

and CKIIβ) both annotated by Blast2GO and are coded separately each on one single contig. The CKIIα sequence is 5,147 bp long and codes for a 353 amino acid protein. The sequence comprises a serine/threonine protein kinase catalytic domain and the closest alignment to sequences in the NCBI database was to the human CK2 A chain (Accession No. 1NA7_A; (Niefind *et al.*, 1998)) and the copepod *Paracyclpina nana* (Accession No. AII16523) CKIIα protein sequence. Similarly, for CKIIβ a single contig was identified containing a 1,567 bp long sequence coding for a 220 amino acid protein comprising a casein kinase regulatory subunit domain. In the NCBI database, the wood wasp *Orussus abietinus* CKIIβ (Accession No. XP_012287730) produced the closest alignment.

A contig coding for a putative *clockwork orange* (*cwo*) was found to be 503 nucleotides in length and coding of a 167 amino acid partial CWO protein. A bHLH domain and an Orange of the Hairy/E (SPL) family domain was identified in the sequence. The best alignment with sequences from the NCBI database was found to the mite *M. occidentalis* (Accession No. XP_003744690) uncharacterised protein but aligns to the FlyBase *D. melanogaster* CWO sequences with 55% amino acid identity. A 1,092 bp long contig was identified as coding for the DOUBLETIME (DBT) protein. When translated, the 310 amino acid long putative DBT protein sequence was shown to contain a serine/threonine protein kinase catalytic domain and sharing the highest alignment score with the *E. pulchra* DBT (Accession No. AGV28719; (Zhang *et al.*, 2013)).

A single transcript putatively coding for the *par domain protein 1ε* (*pdp1ε*) was identified exhibiting 3,423 bp in length. Translated, the sequence resulted in a 508 amino acid protein which comprises a basic leucine zipper domain and had the closest alignment to the hepatic leukaemia factor of the clonal raider ant *Cerapachys biroi* (Accession No. EZA50108; (Oxley *et al.*, 2014)). In the FlyBase databank the translated sequence dPDP1 (FlyBase No. FBpp0289727) was the closest hit.

For the *protein phosphatase 1* (*pp1*) a single 1,725 bp long contig was identified in the *T. saltator* transcriptome. The resulting protein, 357 aa in length inhabits a protein phosphatase 2Ac catalytic domain. The putative TalPP1 sequence most closely aligned to the PP1 of the jumping ant *Harpegnathos saltator* (Accession No. EFN86649; (Bonasio *et al.*, 2010)).

For the *protein phosphatase 2 a* (*pp2a*) contigs for three different catalytic subunits were identified, namely *microtubule star* (*mts*), *widerborst* (*wdb*) and *twins* (*tws*). A 2,981 bp contig was identified in the *T. saltator* transcriptome by using the

D. melanogaster MTS (dMTS, Accession No. AAF52567; (Adams *et al.*, 2000)) as a search term. The contig was annotated by Blast2GO as *serine threonine-protein phosphatase 2a catalytic subunit beta isoform-like.* The contig codes for a 309 amino acid putative TalPP2A subunit MTS and contains a protein phosphatase 2Ac catalytic domain. When aligned in the NCBI database, it most closely relates to a putative serine/threonine protein phosphatase PP-V found in the body louse *Pediculus humanus corporis* (Accession No. XP_002426726). Blast2GO annotated one contig as serine threonine-protein phosphatase 2a 56 kDa regulatory subunit alpha isoform-like which was determined to be the contig resembling the *Talpp2a widerborst* mRNA sequence. This 2,474 bp long contig codes for a partial 458 amino acid protein and contains B56 domains (serine/threonine-protein phosphatase 2A 56 kDa regulatory subunit epsilon) and returned the highest alignment score with the serine/threonine-protein phosphatase 2A 56 kDa regulatory subunit epsilon of the red flour beetle *T. castaneum* (Accession No. XP_971164) when used to search the NCBI database. The third of the contigs coding for TalPP2A subunits found was a 1,633 bp sequence assigned as *Talpp2a twins.* Blast2GO annotated the sequence as *protein phosphatase pp2a 55 kDa regulatory subunit-like isoform 2.* It codes for a 445 amino acid protein, which counts seven SMART identified WD40 domains. It aligns most closely to the mud crab *Scylla paramamosain* PP2A subunit B (Accession No. AFK24473) in the NCBI database.

A 4,413 bp contig was identified as probably coding for TalSHAGGY (SGG) and annotated by Blast2GO as *glycogen synthase kinase 3 beta* which is the mammalian shaggy orthologue. The contig codes for a 418 amino acid sequence containing a serine/threonine protein kinase catalytic domain. When aligned to the NCBI database the sequence shared the highest similarity with the glycogen synthase kinase-3 found in the turnip sawfly *Athalia rosae* (Accession No. XP_012256017).

A single contig was identified putatively coding for TalSUPERNUMARY LIMBS (SLIMB). The mRNA contig was 2,121 bp in length and coded for a 588

amino acid protein. Blast2GO annotated the contig as *f-box wd repeat-containing protein 1a* and a D domain of beta-TrCP, one F box and seven WD40 domains were found in the putative protein sequence. When the NCBI database was searched with the sequence, the highest alignment score was observed with the F-box/WD repeat-containing protein 1A of the termite *Z. nevadensis* (Accession No. KDR19729; (Terrapon *et al.*, 2014)).

A single 3,949 bp contig putatively coding for a 509 amino acid putative TalVRILLE (VRI) was discovered. The conceptual translation includes a basic region leucine zipper domain. Compared with the sequences in the NCBI database this putative TalVRI most closely aligned to the nuclear factor interleukin-3-regulated protein of the termite *Z. nevadensis* (Accession No. KDR19729; (Terrapon *et al.*, 2014)).

A 974 amino acid protein encoded by a 4,380 bp contig was determined to be TalEBONY. It contained several domain structures such as an AMP binding domain, one AMP binding C domain and one PP binding domain. When the sequence is used as a search term in the NCBI database it most closely aligns to the EBONY sequence of the cockroach *Periplaneta americana* described as β-alanyl conjugating enzyme (Accession No. CAI26307; (Blenau and Baumann, 2005)).

Declaration: The sequencing work described here on PDH was conducted by O'Grady but has been included here mentioned for completeness.

Two separate contigs were identified as coding for *T. saltator* PDH (I and II). One of which was 2,430 bp long and was identified through searching the transcriptome using the conserved NSELINS domain as a search term. The mined contig codes for a 129 amino acid TalPDH I prepropeptide and was extended by RACE PCR to 2,471 bp, including the5'UTR. The PDH-precursor –related peptide (PPRP) was determined to be 77 aa in length. A dibasic cleavage site at the end was identified as well a PDH domain was identified in the translated sequence by SMART analysis. A second transcript, 3,392 bp in length was determined to be *Talpdh II*. It codes for a 89 amino acid prepropeptide including a 23 amino acid long signal peptide. A dibasic cleavage site a residue 66 putatively enables the separation of the putative PPRP spanning from residue 24–66. The 23 amino acid mature TalPDH II peptide

end with an amidation signal and shares a 47.8% sequence identity with the *U. pugilator* ß-PDH sequence.

A single contig was identified to partially code for TalRORA. It was shown to be 2,217 bp long and exhibits a coding region translating to a 599 amino acid protein and included a single C4 zinc finger domain. When this sequence was used as a search term in the NCBI database the nuclear hormone receptor HR3 of the house fly *Musca domestica* (Accession No. XP_011290218) resembled the closest match. Blast2GO annotated the mRNA contig as *probable nuclear hormone receptor hr3.*

A candidate TalREVERB protein coding sequence was discovered, and coded by a 5,385 bp contig covering the full CDS of the 110 amino acid protein. The contig was annotated as *nuclear hormone receptor e75* in the Blast2GO analysis which is the *reverb* homolog of *Drosophila*. Two characteristic domains were identified in the sequence, namely a C4 zinc finger domain and a HOLI ligand binding domain. The best alignment in the NCBI database was observed with the nuclear hormone receptor E75 sequence found in the carpenter ant *Camponotus floridanus* (Accession No. XP_011259848).

Five different sequences were identified as potentially coding for Sirtuins, namely Sirt1, 2, 4, 6 and 7. A 4,033 bp contig was identified to be the *T. saltator* homologue of Sirt1. It was annotated by Blast2GO as *nad-dependent deacetylase sirtuin-1* and for a partial protein sequence of 955 aa in length. The *Talitrus sirt1* translated protein sequence aligned most closely to the trematode *Schistosoma mansoni* SIRT1 (Accession No. ABG78545) sequence when compared to the NCBI database. The second of the Sirtuins homolog identified for *T. saltator* is a 2,275 bp contig which was annotated as *nad-dependent deacetylase sirtuin.* and coding for a partial protein sequence of 376 aa and containing a SIR2 domain (identified by SMART analysis). When used as a term to search the NCBI database the best alignment match was a hypothetical protein (Accession No. EFA06770) of the red flour beetle *T. castaneum*. The contig sequences identified as coding for *sirt4, 6* and *7* are determined to be 2,977 bp, 1,209 bp and 5,180 bp long. They partially code for protein sequences 354, 402 and 948 aa long, respectively. All three sequences contain a SIR2 domain. When compared to the NCBI database, the TalSIRT4 sequence most closely aligned to the SIRT4 sequence of the Asian citrus psyllid *Diaphorina citri*

(Accession No. XP_008480918). When a similarity search was conducted with the TalSIRT6 sequence the hypothetical protein (Accession No. EFX74386) of the cladoceran *Daphnia pulex* showed the best alignment. Further, the TalSIRT7 sequence shoed to align most closely with the leafcutter bee *M. rotundata* SIRT7 protein sequence (Accession No. XP_012143211) in the NCBI database.

A single 2,454 bp long contig shown to code for a 458 amino acid partial protein sequence. The protein sequence contains an F-box domain and multiple leucine-rich repeat domains. When used to search the NCBI database the protein sequence most closely aligns so the F-box/LRR-repeat protein of the red flour beetle

T. castaneum (Accession No. XP_008193983). Similarity search with the *Drosophila* JETLAG sequence found this contig to represent the coding information of TalJETLAG.

3.4.5 Identification of rhythmically expressed transcripts

The sampling scheme (time-course sampling) for tissue used for the RNA-seq allowed a resolution of transcript expression levels over the circadian cycle. Time-course sequencing data files are available at the NCBI SRA data base, under the bioproject Accession No. 297565. To identify contigs that change in abundance over time and in a rhythmic fashion, the TPM values for each contig were analysed using the software package JTK_CYCLE (Hughes *et al.*, 2010; Kornacker and Hogenesch, 2010). In total, 67,262 entries were submitted to the analysis. 10,890 of the submitted contigs cycle with a period of 24 hrs which is about 83% of the cycling transcripts and 6.95% of the whole transcriptome, while the majority of the mRNA contigs, about 91.63% do not change expression level with the time of the day when measured in DD (see Table 3.3).

Table 3.3*:* Proportion of rhythmically expressed mRNA contigs in the *T. saltator* transcriptome according to JTK_cycle analysis. The percentage of transcripts which change in abundance over the time of the day is shown with their respective period (12 hrs, 21 hrs, 24 hrs and 27 hrs) are shown.

Period (τ)	**mRNAs cycling in DD**
24	6.95%
12	0.9%
21	0.14%
27	0.4%
Not rhythmic	91.63%

The results of the JTK_cycle analysis are graphically represented as heat maps in Figure 3.27. In 3.27 B the transcripts cycling with a 12 hrs period is shown. Compared to 3.27 A which shows the 24 hrs cycling transcripts the two expression maxima within the 24 hr period can be observed.

In addition to the JTK_cycle algorithm, the core clock and clock-associated genes were also analysed by one-way ANOVA for the relation of the expression level to the time of the day with significance threshold of p (ANOVA) or q (JTK_cycle) was < 0.05, respectively. The results of both analyses are summarised in Table 3.4.

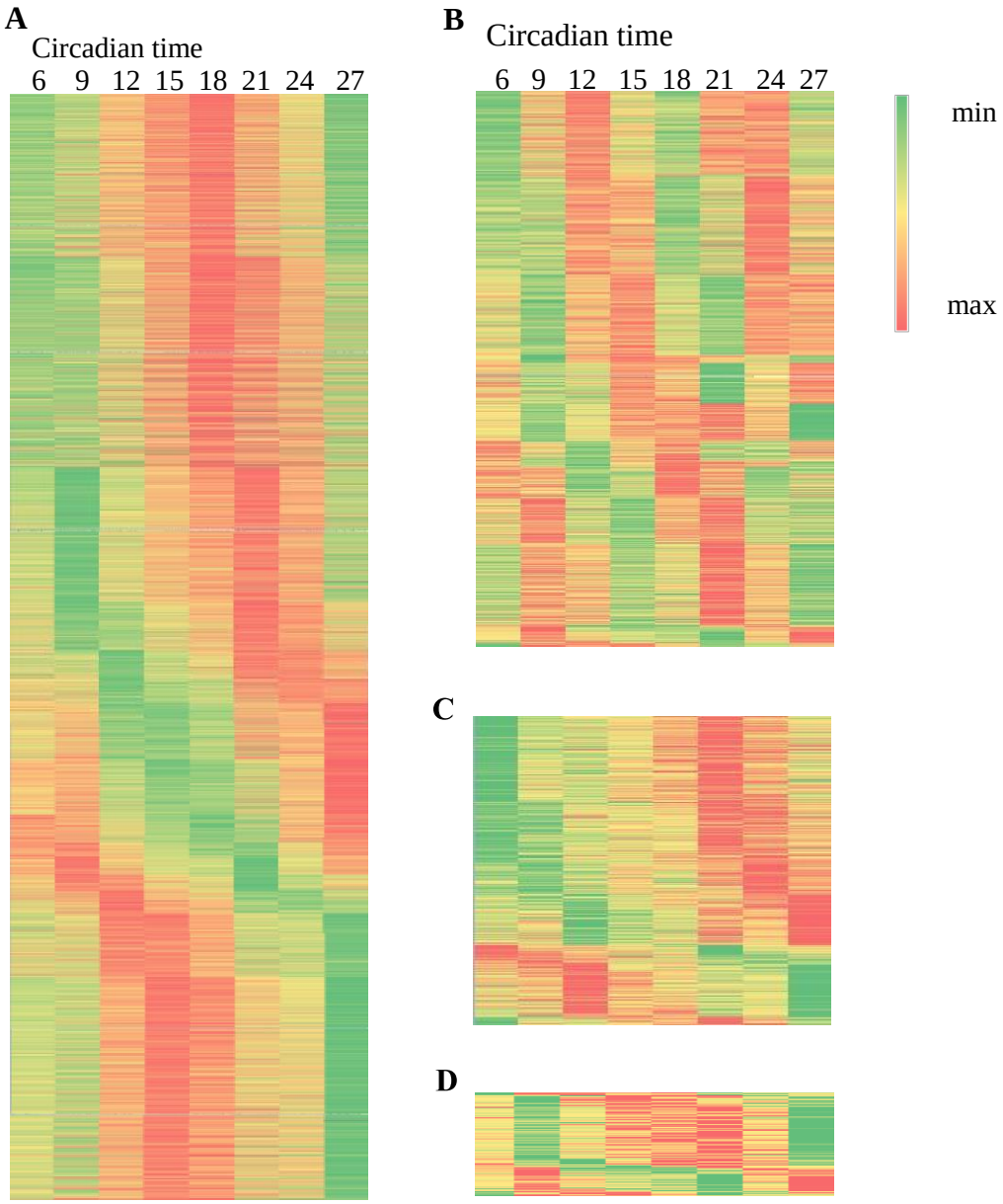

Figure 3.27: Heat maps of the circadian transcriptome. The TPM values were converted into heat maps for a period of 24 hrs (A) as well as for contigs cycling within 12 hrs (B), 27 hrs (C) and 21 hrs (D). Contigs included were reported by JTK cycle with a significance level of q<0.05 (n=4). Green=lowest expression; red=highest expression.

Of the core clock genes *Talper* and *Talbaml1/cyc* were expressed rhythmically according to the JTK_cycle algorithm both with a 24 hrs period and q < 0.00001 and q < 0.01 respectively. For the latter and *Talbmal1/cyc* it should be mentioned that the sequence information was divided among two contigs and both were analysed separately. The results reported herein concern the contig comp939723_c0_seq1.

One-way ANOVA confirmed that *Talper* and *TamBmal1/cyc* levels were depending on the time of the day (with $F_{7,30}=4.856$; $p=0.002$ and $F_{7,30}=2.445$; $p=0.049$) and also shows that one of the contigs coding for *Talcry2* namely comp102609_c0_seq3, changes in expression level depend of the time of the day ($F_{7,30}=2.745$; $p=0.032$). According to the JTK_cycle algorithm the clock associated genes *Talpdh* (contig comp939723_c0_seq1 with $q < 0.001$), *Talck2ß* ($q < 0.05$), *Talpp1* ($q < 0.05$), *Talsgg* ($q < 0.05$), *Talebony* ($q < 0.05$), *Talsirt1* ($q < 0.05$), *Talsirt7* ($q < 0.05$) and *Taljetlag* ($q < 0.05$) were rhythmically expressed. A phase of 24 hrs in change of expression level was reported for *Talcry2* (contig comp102609_c0_seq3), *Talper*, *Talbmal1/cyc*, *Talpdh*, *Talsgg*, *Talebony*, *Talsirt1*, *Talsirt7*, *Taljetlag* and *Talslimb*. For *Talck2ß* TPM values a period of *27 hrs* and for *Talpp1* a period of 21 hrs were determined. One-way ANOVA reveals that *Talck2ß* ($F_{7,30}=3.284$; $p=0.014$) *Talpp1*($F_{7,30}=3.987$; $p=0.005$) *Talslimb* ($F_{7,30}=3.187$; $p=0.016$) and *Talsirt1* ($F_{7,30}=4.905$; $p=0.002$) levels changed significantly throughout the subjective day/night cycle. *Talcwo* was excluded from the analysis because corresponding read levels obtained by RNAseq were suboptimal for the analysis.

The changes in TPM levels over the course of the sampling period is shown in Figure 3.28. The *Talcry2* transcripts levels peak with the onset of the subjective day and were measured to be the lowest just before the middle of the subjective night. In contrast to that, *Talper* peaks during the night and has its lowest expression level during expected midday. The *Talbmal1/cyc* contig is lowest in expression during the end of the subjective night phase and is highest expressed during the first half of the day. In total about 2/3 of the clock associated and core clock genes show their expression peaks during a time at the subjective light phase. The TPM values of the *Talpdh* (comp97165_c0_seq3) rise with the beginning of the subjective dark phase and fall with the beginning of the day. In contrast to this, the *Talck2ß* levels are the highest during the day especially during the end of the subjective day. A very similar picture is shown for the *Talpp1*, *Talebony*, *Talsirt1*, *Talsirt7* and *Talslimb* TPM values that are low during the subjective night and peaking during the subjective light phase, in most cases at the beginning of the light phase. The *Taljetlag* contigs TPM values are highest at CT27, which is three hrs after the beginning of the subjective light phase

Table 3.4: Summary of the core clock and clock associated gene transcripts rhythmicity analyses. The expression period (PER) and the phase (LAG) are reported by the JTK_cycle algorithm, as well as Benjamini-Hochberg q-values (B.HQ)) (corrected p-values). One-way ANOVA was performed additionally on the same data set. *Talcry2*, *Talbmal1*/*cyc* and *Talpdh* were represented with two contigs and they were analysed separately, thus two data points are available for these three clock genes. Genes with TPM levels that were statistically shown to cycle in DD (by JTK or ANOVA) are printed in bold.

Clock gene transcripts	**Trinity contig ID**	**JTK_cycle**			**One-way ANOVA**	
		B.HQ	**PER**	**LA**	**$F_{7,30}$**	**p**
Talcry2	comp100937_c0_seq1 **comp102609_c0_seq3**	1 **0.070657**	18 **2**	7.5 **0**	1.333 **2.745**	0.280 **0.032**
Talclk	comp100688_c1_seq1	0.212741	24	22.5	1.582	0.191
Talper	**comp102279_c0_seq7**	**1.69E-07**	**24**	**15**	**4.856**	**0.002**
Taltim	comp849619_c0_seq1	1	24	3	0.554	0.785
Talbmal1/ cyc	comp12103_c0_seq1 **comp939723_c0_seq1**	1 **0.001101**	24 **24**	3 **4.5**	1.323 2.445	0.284 **0.049**
Talpdh	comp92607_c0_seq2 **comp97165_c0_seq3**	0.872321 **0.000543**	24 **24**	0 **10.5**	1.937 1.972	0.110 0.104
Talck2α	comp102480_c0_seq1	0.256055	12	1.5	1.085	0.404
Talck2ß	**comp99101_c0_seq3**	**0.001738**	**27**	**1.5**	**3.284**	**0.014**
Taldbt/ck 1ε	comp87763_c0_seq1	1	27	25.5	1.512	0.213
Talpdp1ε	comp98345_c0_seq1	1	27	15	0.407	0.888
Talpp1	**comp97405_c0_seq1**	**0.023122**	**21**	**4.5**	**3.987**	**0.005**
Talpp2a-mst	comp98380_c0_seq1	1	27	25.5	2.132	0.081
Talpp2a-wdb	comp102157_c1_seq1	0.238745	24	0	2.173	0.076
Talpp2a-tws	comp99704_c0_seq3	1	24	22.5	1.217	0.334
Talsgg	**comp99811_c0_seq7**	**0.020999**	**24**	**22.5**	1.632	0.176
Talslimb	comp98870_c0_seq1	0.788187	24	22.5	**3.187**	**0.016**
Talvri	comp100474_c0_seq6	0.788187	27	19.5	2.184	0.074
Talebony	**comp99283_c0_seq2**	**0.027898**	**24**	**22.5**	1.580	0.191
Talrorα	comp99654_c0_seq3	1	12	3	0.868	0.545
Talreverb	comp101252_c0_seq2	1	27	15	1.477	0.224
Talsirt1	**comp101818_c1_seq1**	**0.001101**	**24**	**22.5**	**4.905**	**0.002**
Talsirt2	comp97450_c0_seq4	1	27	16.5	1.726	0.152
Talsirt4	comp92313_c0_seq2	1	27	25.5	0.640	0.719
Talsirt6	comp69157_c0_seq1	1	27	16.5	1.920	0.112
Talsirt7	**comp95761_c0_seq1**	**0.036551**	**24**	**22.5**	1.657	0.170
Taljetlag	**comp100423_c0_seq4**	**0.027898**	**24**	**22.5**	1.976	0.103

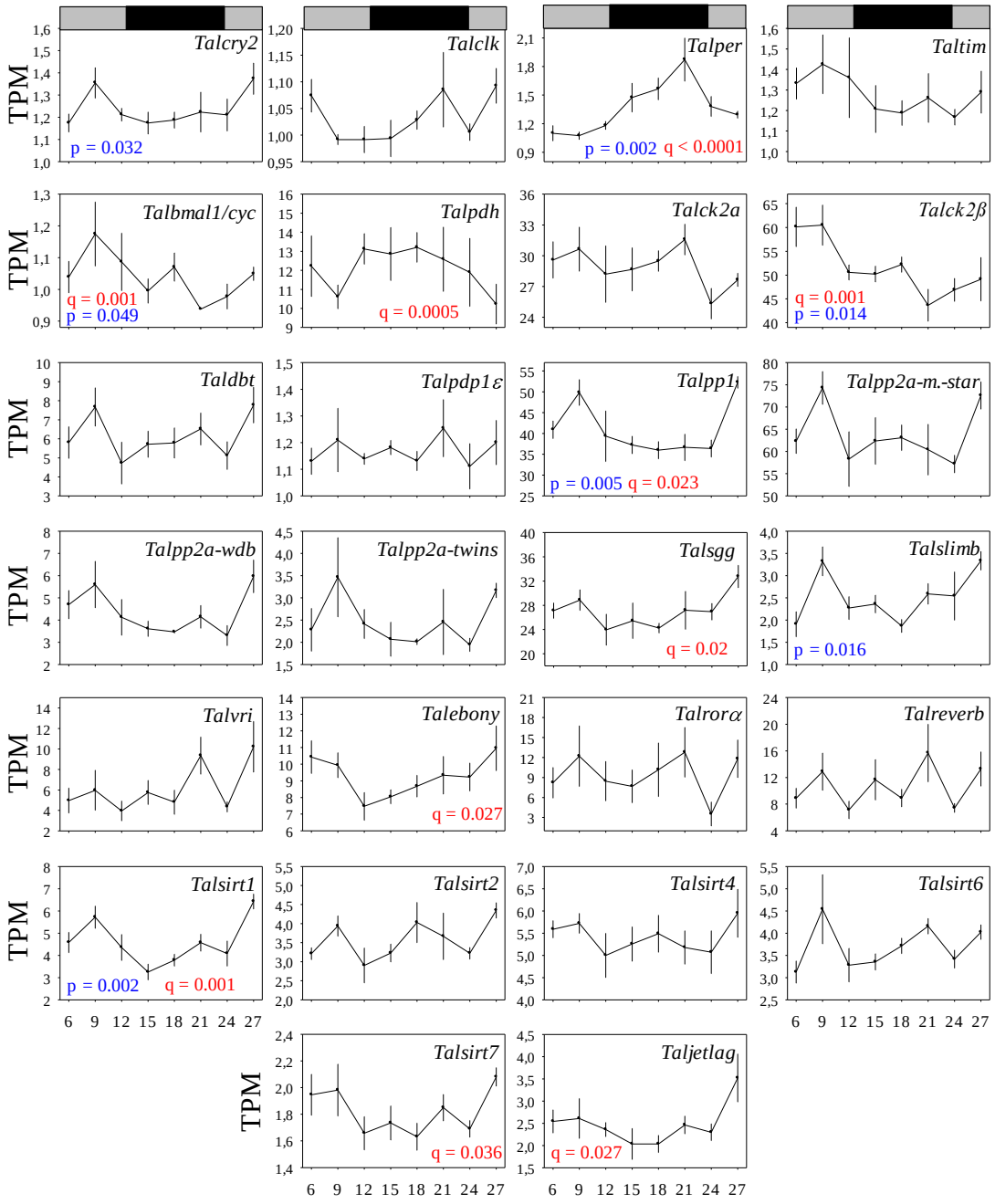

Figure 3.28: Expression dynamics of core clock and clock associated gene transcripts over a 24 hr DD period. TPM values (±SEM) are plotted against the tissue collection time points with n=4 except for CT18 (n=3). The grey and black bars above the graphs indicate the subjective day (grey) and dark (black) phase. One-way ANOVA p-values are displayed in blue and q-values from the JTK_cycle analysis are shown in red when they reached significance levels.

3.5 DISCUSSION

3.5.1 The *T. saltator* circadian transcriptome

Gene expression can fluctuate over time, throughout development of an organism and between individual tissues. A transcriptome represents a snapshot of the expressed genes at a given time at which the source tissue was collected. Therefore, the rationale in the current study was to maximise the coverage of mRNAs captured and enable temporal expression analysis to be done by sequencing samples acquired over a 24 h period and the sequenced reads indexed and pooled to make up a 'master' circadian transcriptome. In this way, clock genes and clock associated transcripts were identified and their expression dynamics, inferred by *in-silico* analysis throughout a circadian period. (In constant darkness 6.95% of the mRNAs in the present *T. saltator* transcriptome cycle in abundance with a period of 24 hrs). When compared with other published Blast2GO annotated transcriptomes the *T. saltator* annotation statistics are similar to other crustaceans (O'Grady, 2013; Lenz *et al.*, 2014). The *Asellus aquaticus* transcriptome annotation descriptive statistics, for instance the N50 statistic, sequence similarity and annotation values such as GO level are very similar (Stahl *et al.*, 2015). Unsurprisingly, the top BLAST hits were from arthropod species such as the crustacean

D. pulex and the insect *T. castaneum.* This outcome reflects also the relative paucity of reference genomes and annotated transcriptomes from crustacean species. This is probably also the reason for the large species variety in the top hits sequences the contigs most closely aligned to (see Figure 3.11). The sequence similarity with the top hits overall confirmed the robust identity of positive alignment hits whilst low sequence similarity cases were likely resulting from contigs that did not represent the complete gene sequence, such as seen for *Talcry2* and *Talbmal1/cyc*. An additional, albeit unlikely, reason and/or alternative interpretation is that the sequences available for comparison could be substantially diverged from those sequenced from *T. saltator*.

3.5.2 Identified clock and clock-associated genes

The high sequencing and annotation quality of the *T. saltator* transcriptome as well as the contig sequence identity coding for the core clock genes TalPER,

TalCRY2 and TalBMAL1/CYC were confirmed by cloning and manual sequencing and all showed 100% sequence alignment with the assembled contig(s). Motif searches revealed conserved functional domains in the translated protein sequences which were typical for the predicted putative proteins and which strengthens the inferred identity of the transcripts and the overall reliability of the Trinity assembly and downstream Blast2GO analysis.

The design of the sampling protocol used allowed us to map the numbers of transcriptome reads back to strictly defined time points. These measures, together with the JTK_cycle algorithm further allowed us to establish the global expression dynamics across the 24 hrs sampling period and thus identification of putatively rhythmically expressed transcripts. Importantly, tissue sampling from animals held in DD following LD entrainment and from bone-fide behaviourally rhythmic individuals permitted conclusions about the endogenous nature of transcript expression.

Similarities with other crustacean clock protein composition allow speculations about evolution of the crustacean circadian clock. In the *T. saltator,* circadian transcriptome a *Talcry2* contig was identified but no *Talcry1,* contrary to *D. melanogaster,* which harbours only the light sensitive CRY1. The monarch butterfly *D. plexxippus* carries both genes (Zhu *et al.*, 2005), the *Drosophila* –like, *cry1* which able to sense light and a mammalian-like *cry2* which the protein represses CLK/CYC mediated transcription (Yuan *et al.,* 2007). Genomes encoding both *cytochrome* genes are hypothesised to represent the ancestral condition (Sandrelli *et al.*, 2008). The lack of CRY1, in the *Talitrus* transcriptome is mirrored in the closely related peracaridean isopod *E. pulchra* (Zhang *et al.*, 2013) and a situation similar to that is observed in the insects *T. castaneum* and *Apis mellifera* which both also exhibit exclusively CRY2 (Rubin *et al.*, 2006; Yuan *et al.*, 2007). Thus, the TalCRY2 could potentially have functions similar to that described in *E. pulchra where* CRY2 serves as a negative repressor of the positive transcriptional regulators BMAL/CLK (Yuan *et al.*, 2007; Zhang *et al.*, 2013).

The contig putatively coding for the TalCLK only partially coded the complete coding region. Some of the commonly occurring domains such as the C-terminal transactivation domain and a bHLH domain (Bae *et al.*, 1998) were not detectable in

TalCLK which might lie in the part of the protein which has not yet been sequenced. Alternatively, TalCLK contig may have suffered some missassembly and require re-sequencing, via homology sequencing and RACE-PCR to clarify the full sequence. Nevertheless, given that the *Talclk* contig was the only one present in the *Talitrus* transcriptome that annotated as *clock* and the translated sequence showed several conserved domains there is confidence that the identified sequence represents the partial mRNA sequence coding for *Talclk*.

The TalPER sequence includes several characteristic protein domains including PAC and PAS domains as well as cytoplasmic localisation and nuclear localisation signals and are classical motifs in clock genes necessary for the protein to function in TTFLs. PAS domains occur across all phyla and occur in different signalling proteins (Taylor and Zhulin, 1999). The name PAS originates from the proteins they were found in which are Per (period circadian protein), Arnt (Ah receptor nuclear translocator protein) and Sim (single minded protein). These domains often appear to co-exist with PAC domains which are situated C-terminally of the PAS motif. Although separated in the primary protein structure, in the native protein the two structures unite forming the PAS domain fold (Borgstahl *et al.*, 1995; Ponting and Aravind, 1997; Zhulin *et al.*, 1997; Hefti *et al.*, 2004). The PAS domain is a binding site for other components in the biological clock. Through this action, PER can recruit clock proteins to target distinct DNA stretches (Ponting and Aravind, 1997). However, the functions of the deduced proteins described here are suppositional and require functional characterisation. The strategy would be using the *Drosophila* S2 cell luciferase assay (Stanewsky, 2007; Yu and Hardin, 2007; Asher *et al.*, 2008; Kadener *et al.*, 2008; Chappuis *et al.*, 2013; Tataroglu and Emery, 2014). Here, the *in vitro* function of the putative TalPER could be researched in cell culture. It would be intriguing to explore functional attributes of TalPER, for example whether it could rescue dPER knock-out in S2 cell cultures as well as to generally analyse the possible TalPER activity in cell cultures with luciferase reporter essays similarly as done for *E. pulchra* clock genes by (Zhang *et al.*, 2013).

Behavioural effects absent TalPER were attempted to be researched with RNAi of *Talper* similarly as performed in Zhang *et al.* (2013). To date, the RNAi of period in *T. saltator* has not yet been successfully accomplished. The *Taltim* contig only codes for a partial protein sequence and in a situation similar to that of putative

Talclk, some of the functionally conserved domains such as PAS domains and nuclear and cytoplasmic localisation domains were expected to be detected in the TalTIM sequence. The missing domains of the *Taltim* candidate may also be attributed to the fact that the contig only partially covers the CDS and the conserved domains reside in sequence regions not yet sequenced or assembled. At this juncture the identity of the mRNA contig rests only on the fact that the translated sequence was annotated by Blast2GO as *timeless*. Reassuringly however, the translated sequence contains a timeless domain which together with the NCBI BLAST hit permit us to draw the conclusion that the contig codes for the TIM homolog of *T. saltator*.

Blast2GO analysis and the identified structural motives lead to the conclusion that *T. saltator* expresses a mammalian-like *Bmal1* transcript rather than a *Drosophila-like cycle*. This is not an unusual finding, since the same situation has previously been reported for other crustaceans such as the closely related *E. pulchra, D. pulex* and *N. norvegicus* (Zhang *et al.*, 2013; Sbragaglia *et al.*, 2015). The *Talbmal* transcript sequence was assembled on two separate contigs but, when put together resulted in a continuous sequence, suggesting that this was an *in-silico* effect, rather than biologically relevant. The full CDS that has been identified for *Talbaml1* is 1,807 nucleotides long and codes for a 602 amino acid putative protein. The reported *N. norvegicus* homolog sequence is only partially available and is 222 nucleotides in length and comprises a 73 amino acid long putative sequence piece (Sbragaglia *et al.*, 2015). The TPM expression levels of *Talbmal1* follow a sinusoidal pattern over the time of the day and significantly dependent on the time as confirmed by all the analysis methods applied. Strikingly, the same expression pattern as for *T. saltator* was found in the firebrat *Thermobia domestica*, where qRT-PCR essays showed a rhythmically expressed *Tdcyc* which also shows the highest expression during the end of the subjective light phase and mRNA levels dropping during the subjective dark phase (Kamae *et al.*, 2010). In *E. pulchra* cell culture experiments showed the importance of a functional *Bmal1* as an ablated C-terminal transactivation domain impairs the functionality of the EpBMAL1:EpCLK dimers. As one of the primary driving elements of the circadian clock and given the close relatedness of *Talitrus* and *Eurydice* it is tempting to speculate that the BMAL1 homologs would have the same function in both species. To support that hypothesis, the cell based luciferase reporter essay experiment by Zhang *et al.*, (2013) might be repeated with the *T. saltator*

sequences.

For *Talpdh* two sequence contigs were identified individually. The first contig representing PDHI carries some prominent features such as a PDH domain and the mature peptide ehibits the conserved N- terminal NSE/ALINSSLLG sequence. It was perplexing however, that the sequence then continued further than the expected, and formerly considered highly conserved and characteristic 18 aa which would be expected for PDH. Moreover, the PDH found in our study also lacks an amidation signal. This latter however, is present in the second translated contig sequence that was identified as *TapdhII* but which also shows sequence features such as a 23 amino acid signal peptide and a 43 amino acid long *pigment-dispensing hormone* precursor-related peptide (PPRP). The occurrence of several *pdh* isoforms in one animal has been observed previously in the literature, incidentally reported for *Pandalus jordani* (Rao *et al.*, 1985), *Penaeus japonicas* (Yang, Aida and Nagasawa, 1999), *Callinectes sapidus* (Klein *et al.*, 1994) and *Penaeus vannamei* (Desmoucelles-Carette, Sellos and Van Wormhoudt, 1996). For *Euphasia crystallorophias* three PDH isoforms were reported, including an unusually long variant (PDH-Lß1&2, PDH-Lα) by Toullec *et al*. (2013). PDH-Lß1 has an extended C-terminus resulting in a mature, amidated peptide containing of 24 amino acids. Apart from the Ser2 being substituted for Ala2 the sequence of PDH-Lß2 is identical. In a laborious approach including immunochemical-identification, Edman microsequencing and cDNA cloning Wilcockson *et al*. in 2011 identified the *E. pulchra pdh* 249 amino acid long prepropeptide sequence which composition contains a putative signal peptide, the mature *pdh* sequence, and amidation signal and a dibasic cleavage site. Both *Talitrus* sequences show distinct PDH features and manual sequence confirmation by PCR and RACE PCR confirm the unusual mRNA identity of *TalpdhI* and *TalpdhII*. Further work is necessary to shed light on the makeup of *T. saltator* PDH proteins and the concomitant functional aspects. This would of course also resolve the issue of these unusually long PDH isoforms that are emerging since the advent of NGS sequencing efforts. *TalpdhII,* but not *TalpdhI* transcript expression levels change over a 24 h period in DD as revealed by JTK_cycle analysis, with a clear accumulation at the onset of the dark phase and decline when the subjective day time begins. In contrast, the peak of the *Eppdh* mRNA expression measured via qRT-PCR was shown to be at the end of the subjective dark phase. It has to be noted though, that

statistics did not confirm the mRNA levels as dependant on the time of the day. When comparing both animals it should also be taken into account that, as an intertidal animal *E. pulchra* is prone to environmental changes that come with the tides and its physiology is strongly adapted to that (Reid and Naylor, 1986; Wilcockson *et al.*, 2011; Zhang *et al.*, 2013). Naturally, anticipation of the changes though a circatidal clock should be of great advantage. How the circatidal and circadian crustacean clock are interlinked or if circatidally rhythmic behavioural phenotypes underlie a circalunar clock is currently one of the strongly researched and debated questions in marine invertebrate chronobiology (Tessmar-Raible *et al.*, 2011; Zantke *et al.*, 2013; Zhang *et al.*, 2013; Cheeseman *et al.*, 2017).

3.5.3 Rhythmically expressed transcripts

One-way ANOVA allowed an alternative analysis of individual transcripts. In contrast to JTK _cycle, One-way ANOVA easily identifies clock transcripts of which expression levels depended on the time of the day, but the expression pattern did not necessary follow a sinusoidal curve as expected of clock genes. Of the identified clock genes *Talper, Talbmal1/cyc, TalpdhI, Talck2ß, Talpp1, Talsgg, Talebony, Talsirt1, Talsirt7, Taljetlag* transcripts were changing in abundance in dependence of the subjective daytime. One-way ANOVA confirmed that mRNA abundance changed significantly over time for *Talper, Talbmal1, Talck2ß, Talpp1, Talsirt1* and, additionally, found the expression of *Talcry2* and *Talslimb* to be changing over the 24 hrs sampling period. However, detection of cycling mRNA does not necessarily allow us to draw the conclusion that the translated protein cycles in the same way. Indeed, circulating transcripts are not even essential for a functioning clock (Lakin-Thomas, 2006) but the identification of canonical core clock and clock associated genes by Blast2GO, and the finding of conserved typical protein domains together with changes in expression under free-running conditions strongly indicated that the transcripts are a functioning part of the *T. saltator* circadian clock, or controlled by the central oscillatory mechanism.

JTK_cycle algorithm helped to identify transcripts wich cycle in abundance in a circadian manner, namely *Talcry2, Talper, Talbaml1, TalpdhII, Talck2ß, Talpp1, Talsgg, Talslimb, Talebony, Talsirt1, Talsirt7 and Taljetlag.* The interplay between

the gene sequences of identified core clock and clock associated genes, their transcripts and proteins still need to be assessed. It is be too early to draw conclusions on the functions of the identified clock transcripts purely based on sequence homology and expression dynamics. It is even very plausible that *T. saltator* has some unique clock features that allow optimal adaptation to its environment. Nevertheless, the clock is an evolutionally ancient biological feature and the identification of so many clock genes in the transcriptome with a large variety of them expressed in a circadian rhythm is tantalising and broadens our scope for more penetrating functional analyses.

Data from this chapter allows us to probe the functionality of the proposed clock genes and work towards defining a model of crustacean clocks. The available transcriptome are the bases for manipulation of *Talitrus* in well establish behavioural paradigms such as their locomotor activity rhythms and orientation. Given the easy acquisition, husbandry, and extensive behavioural analysis and now clock gene information, position *Talitrus* as a future arthropod model organism. The data presented here, is a clear progress in breaking the limitation of crustacean non-model organism research. It is very probable, that in *T. saltator* genes and their products work together similarly as observed for *E. pulchra* or as for the model invertebrate *D. melanogaster* enabling anticipatory behaviour.

3.6 SUMMARY

A circadian mRNA transcriptome was sequenced and assembled *de novo* from neural cDNA of behaviourally rhythmic *T. saltator*. After identification and functional annotation of the mRNA contigs, the temporal expression profiles of the contigs were determined. Analysis showed that the data was reliable enabling expression analysis over time. As found for other species, a proportion of the transcriptome sequences were expressed in a circadian manner. Most of the expected clock transcript sequences were identified and subset of canonical core clock and clock-associated transcripts was characterised and compared to homolog sequences available.

CHAPTER 4: CELESTIAL NAVIGATION AND CLOCK GENE EXPRESSION

4.1 ABSTRACT

T. saltator utilizes clock-controlled time-compensated solar and lunar navigation for appropriate orientation on the beach (Edwards and Naylor, 1987; Homberg, 2004; Papi *et al.*, 2006; Meschini *et al.*, 2008). Whilst behavioural analysis has firmly established that the orientation behaviour is under clock control, the molecular basis of this has not been studied. It is demonstrated, that canonical circadian genes are likely involved in navigation; *Period* and *Timeless* mRNA show clear daily cycling in animals expressing circadian locomotor behaviour and time-compensated orientation. It was also hypothesised that, by analogy with insects such as monarch butterflies, key compass clock work would be located in the antennae (Merlin *et al.*, 2009). Removal of antennae had no effect on solar orientation suggesting that solar compass mechanisms operate independently from the antennae. However, when tested orientation behaviour at night, antennal ablation disrupted orientation. Thus, it is proposed, that lunar navigation is orchestrated by mechanisms located in the antennae. Data of this chapter is published in Ugolini *et al*., 2016.

4.2 INTRODUCTION

4.2.1 Solar navigation in *T. saltator*

During daytime, *T. saltator* stays buried in the sand along the strandline. At dusk, animals emerge from their burrows and migrate along the beach to forage. Just before dawn, animals retreat to the strandline to re-burry into the sand (Edwards and Naylor, 1987). Animals must have the competence to navigate across the land-sea axis during the night to find their feeding grounds and return home after feeding. Additionally, during the day, they must be able to quickly return to the burrowing zone when displaced from the sand especially during the summer where they are prone to desiccation (Williams, 1995).

Using astronomical cues for navigation is a common behaviour among higher animals (Homberg, 2004; Foster *et al.*, 2018). As the position of an astronomical body changes relative to the earth throughout time, animals utilizing these cues have to

constantly factor in this movement. Despite their small size, invertebrates navigate across large distances. To navigate successfully, animals have to orientate in their environment, chose a direction and then keep a bearing. Besides others, cues for orientation can be landmarks (Collett, *et al.*, 2013; Collett, 2014), skylight polarization (Labhart *et al.*, 2001), odometry (Wolf, 2011) and earth's magnetic field (O'Malley and Banks, 2008; Lohmann, *et al.*, 2012; Cresci *et al.*, 2017). Prominent orientation cues are celestial cues such as the sun and the moon (Dacke *et al.*, 2003; Homberg, 2004; Dacke *et al.*, 2014; Homberg *et al.*, 2015). Commonly, animals use more than one cue to navigate (Lohmann and Lohmann, 1996; Ugolini, 2001; Wehner *et al.*, 2016). Prominent examples of invertebrates that express navigation behaviour aided by celestial cues are the honeybee *A. mellifera* (Homberg, 2004; Towne *et al.*, 2017), the desert ant *Cataglyphis fortis* (Lebhardt and Ronacher, 2015; Pfeffer and Wittlinger, 2016) and of course the monarch butterfly *D. plexxippus.* The latter covers the longest distances and skilful experimental designs allowed the unravelling of the molecular biology behind the navigation behaviour to a large degree (Merlin *et al.*, 2009). The earliest proposal of a compass mechanism in *Talitrus* was in 1929 by Verwey and was subject to behavioural experimentation since the beginning of the 1960s (Williamson, 1951). Soon a connection between orientation abilities and circadian behaviour was drawn. *Talitrus* scototaxis for example was found to be prominent during the night with an onset just before dawn and persisted in constant darkness for seven days. The rhythm of orientation towards a light/dark boundary was shown to be subject to phaseal changes of the light regime (Edwards and Naylor, 1987). The sun compass mechanism in *Talitrus* was then established by Pardi and Papi in 1952. Ugolini and Macchi showed in 1988 that while a general direction of homing behaviour is innate, the animals also showed navigational plasticity and can learn a new navigational direction. These results match the findings of Gambineri and Scapini (2008) who experimented with two populations of *Talitrus* from two different beaches. They were able to show that especially for young animals the cues used to orientate (landscape, sun, scototaxis) depend on the geomorphology of the habitat they were born into (Gambineri and Scapini, 2008). Young *Talitrus* using the sun compass were found to be more dispersed than older experienced animals which supports the conclusion that behavioural plasticity fine tunes the compass orientation (Gambineri and Scapini, 2015). In the following, locomotor activity rhythms and solar orientation behaviour were discussed in concordance, as both behaviours were

found to be strongly dependent on the time of the day. This allowed the hypothesis that both behavioural traits are anchored in the same (circadian) internal timing system (Scapini *et al.*, 2005). Further, Ugolini *et al.* (2007) argued that phase shifted light conditions under which *T. saltator* were kept, were unable to dissociate the locomotor activity rhythm and the solar orientation behaviour and thus should both equally be subject the same chronometric mechanism. When *T. saltator* solar orientation was tested under various light regimes specifically different photoperiods, the results indicate that the compensation for the movement of the sun runs at a constant speed (indicating an involvement of the circadian clock) and depends on the light:dark-ratio in the day (Ugolini *et al.*, 2002).

In addition to locomotor activity rhythms (Ugolini, *et al.*, 2012), solar orientation behaviour was established as a behavioural biomarker of environmental contamination with trace metals (Ungherese and Ugolini, 2009). Here, the trace metals Hg, Cu, Cd and Zn had a dose dependent effect on the solar orientation ability of *Talitrids.* This allowed the conclusion, that these trace metals are toxic for *T. saltator* whilst disturbing the navigational abilities. Besides that, the seawater salinity influences the direction of orientation when tested under the sun (Ugolini *et al.*, 2015). Especially the Ca^{2+} concentration is a factor influencing the *T. saltator* sun compass functionality (Ugolini *et al.*, 2009). Recently, the wind direction was found to be an important orientation cue that influences sun compass orientation in *Talitrus* as animals released during onshore winds had a more precise direction of orientation than animals released during all other wind directions (Gambineri and Scapini, 2015). Besides the sun compass, the skylight intensity gradient is also used as a cue for navigation during the day. In an experimental setup were the spectral gradient and skylight polarisation were excluded as navigational cues with aid of dome shaped filters it was shown that the difference in skylight intensity between the dome and outside celestial factor in *Talitrus* orientation (Ugolini *et al.*, 2009). During the day, landmarks are also used as navigational cues. In an experiment with movable patterned walls, Ugolini demonstrated in 2014, that the optic flow *T. saltator* experiences during navigation has implication for the direction of orientation as the latter can be modified by lateral movements of wall patterns around the arena (Alberto Ugolini, 2014).

4.2.2 Lunar orientation in *T. saltator*

During the night, *T. saltator* is able to use the moon as a celestial cue for navigation. The lunar compass is independent of the moon phase or shape (Ugolini *et al.*, 1999; Ugolini *et al.*, 2007) or from earth's magnetic field (Ugolini *et al.*, 1999). The animals are able to compensate for the moon phase when it is not visible as the lunar compass continues to work after a new moon phase (Ugolini *et al.*, 2007). In their publication in 2008 Meschini *et al.* hypothesize that *Talitrus* lunar compass is guided by interacting internal circadian, circalunidian and circalunar rhythms which work together to keep the correct bearing during the night. They found that the moon compass can be shifted with artificial moon phases and that animals seem to have an internal "time of the moon" (Meschini *et al.*, 2008). As with the sun compass, the moon compass direction is innate (Ugolini *et al.*, 1999; Ugolini *et al.*, 2003; Ugolini *et al.*, 2005), inexperienced laboratory born animals orientated in accordance with their parental home beach direction when tested under the moon. Offspring whose parental generations originated from different beaches, chose an intermediate direction laying between the home beach directions of the parents. This strongly indicates a genetic or epigenetic component in the moon compass orientation mechanism (Ugolini *et al.*, 2003).

The earth magnetic field is commonly known to play an important role in long distance migrations of marine animals or birds but also arthropods such as *T. saltator* and the equatorial sandhopper *Talorchestia martensii* use the earth magnetic field for navigation (Arendse and Kruyswijk, 1981; Ugolini, 2001, 2006). An artificial magnetic field with a shifted north pole can be used for orientation in *T. saltator* (associated with a shift in orientation), whilst animals were unable to orientate in the absence of a magnetic field (Arendse and Kruyswijk, 1981).

Astonishingly, *T. saltator* can differentiate between the sun and the moon compass cue even when they are presented at an incorrect time of the day. Phase reversed sandhoppers were able to use the solar compass even though their internal time was night time and reciprocally were able to correctly orientate after the moon when their internal time was daytime (Ugolini *et al.*, 2012). In an laboratory based experimental setup, *T. saltator* was able to discriminate the artificial moon and sun (Ugolini *et al.*, 2005). Indications of a time- or "lunar phase"- compensated moon compass linked to the internal biological clock are given by the fact that the moon

orientation rhythm persist in DD but not under LL even when animals are collected from the beach at the new moon (Papi *et al.*, 2006).

4.2.3 Objective

The migratory monarch butterfly *D. plexxippus* utilises a time-compensated molecular clock to navigate across long distances following celestial cues (Froy *et al.*, 2003; Reppert, 2006). This solar compass clock is anatomically separated from the brain as the major molecular oscillator aiding navigation sits in the antennae (Merlin *et al.*, 2009). In the *Danaus* clock, CRY1 most probably mediates light induced TIM degradation as the monarch *cry1* is able to biochemically and behaviourally rescue cry^b *Drosophila* mutants (Zhu *et al.*, 2008). In contrast to *Drosophila* however, CRY2 is established as the major negative repressor of CLK:CYC mediated transcription as it co-localises with other clock proteins in specific brain structures (pars lateralis) and translocates into the neurons nucleus at a time coincident with transcriptional repression (Zhu *et al.*, 2008). As described above, *T. saltator* utilizes time-compensated solar, lunar and geo-magnetic compasses for orientation on the beach (Arendse and Kruyswijk, 1981; Scapini *et al.*, 1999; Ugolini *et al.*, 2002; Ugolini *et al.*, 2007; Meschini *et al.*, 2008). As the orientation mechanisms show circadian features the question arises if the biological clock tells time aiding in compensation for azimuthal changes when navigating with astronomical cues. The following chapter aims to shed light on the contribution of circadian core clock gene products to *T. saltator* celestial navigation behaviour and the involvement of the antennae therein. Specifically two questions were aimed to be answered: 1) Does the phase of canonical core clock genes expression correspond to a phenotype in locomotor activity and orientation? And further 2) Is there an extra-cerebral clock in the antennae in *T. saltator* as found in the monarch butterfly

4.3 MATERIALS AND METHODS

The escape direction of *T. saltator* was measured under the sun in animals accustomed to the natural onset of daylight and in animals with a 6 hrs phase shifted day phase. Neural clock gene transcripts were measured equally in both groups to determine if a shift in the onset of the day corresponds to a shift in the orientation direction as well as a shift in clock gene

expression. Further, the necessity of antennae for solar and lunar orientation was analysed.

4.3.1 Animal collection

T. saltator adult individuals were collected from three major sampling sites. These were Callelungo beach, Parc Regionale della Maremma, Grosseto (Albegna, southern Tuscany; 42°41'14.2"N 10°59'52.4"E), in the Natural Park of Migliarino, San Rossore, (Massaciuccoli, Pisa, Italy; 43°40'03"N, 10°20'29"E), and from Ynyslas Nature reserve (Ynyslas, UK; 52°31'49.6"N 4°03'26.3"W) between May and September.

Italian sandhoppers were placed in tanks filled with approximately 5 cm of damp sand taken from the sampling site with an ambient room temperature of 25°C and an L:D=12:12 photoperiod which was centred on the midday of the external photoperiod. Animals originating from the UK were kept as described in general methods 2.1.

4.3.2 Activity measurement

The locomotor activity of Italian animals was monitored with bespoke micro-wave radar activity measurement systems for 20 animals being recorded in one container as established by Ugolini *et al*. (2007) and established by Pasquali and Renzi in 2005. Animals were kept in tanks (17 x 11 x 12 cm) with a microwave radar device on top, 16 cm from the sand surface (Guardall MX950, 24 GHz, 20 m; Guardall Limited). A connected computer system allowed data collection and analysis of the locomotor activity data was performed by Vittorio Pasquali (Pasquali and Renzi 2005). Locomotor activity measurement of animals originating in the UK, was performed as described in 2.2.

4.3.3 Escape (orientation) behavior

To measure *T. saltator* solar orientation behaviour animals in groups of 10 were released into a Plexiglas bowl (15 cm diameter) as previously described by Ugolini *et*

al. (1988) (see Figure 4.1). The escape trajectory was read by an experimenter from an acetate compass attached to the bowl about 2 minutes after an initial introduction into the arena or video recorded from below and analysed from freeze- frame images and the mean resultant direction calculated. Experiments were conducted at solar midday and more than 100 km away from the beach on a tower in the absence of landmarks or alternative visual cues.

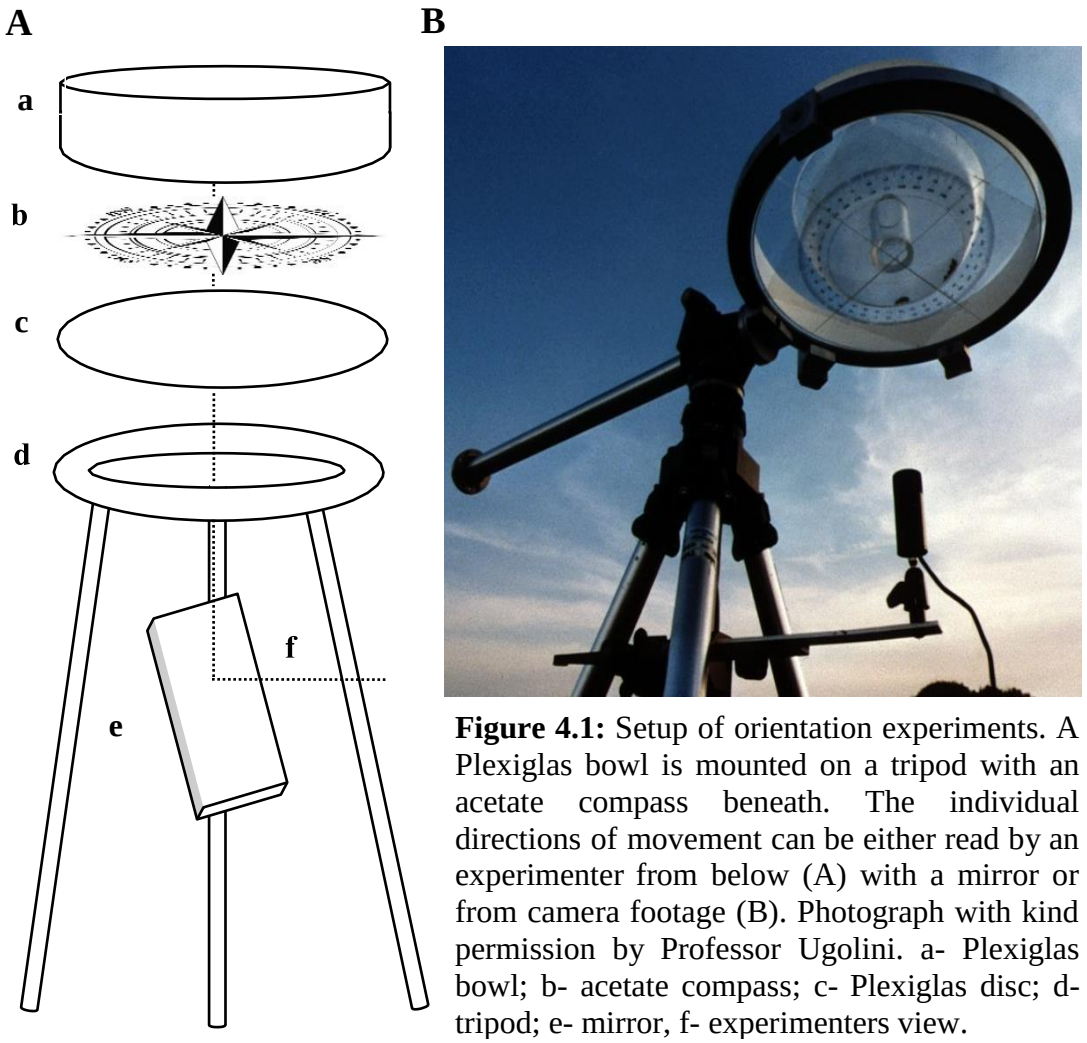

Figure 4.1: Setup of orientation experiments. A Plexiglas bowl is mounted on a tripod with an acetate compass beneath. The individual directions of movement can be either read by an experimenter from below (A) with a mirror or from camera footage (B). Photograph with kind permission by Professor Ugolini. a- Plexiglas bowl; b- acetate compass; c- Plexiglas disc; d- tripod; e- mirror, f- experimenters view.

Similarly, the lunar orientation behaviour was measured under 95% illuminated fraction. The Plexiglas bowl was filled with 0.5 cm seawater as it induces them to rapidly orientated towards their home beach. The escape behaviour was filmed from below with an infra-red camera and the trajectories analysed from freeze-frame images. As the earth's magnetic field is a common cue for orientation (Arendse and Kruyswijk, 1981). Its potential influence was reduced by a pair of battery driven

64 cm large Helmholtz coils, which could be regulated, via an electric rheostat which were mounted onto the tripod 35 cm away from the bowl. Night-time experiments were conducted in July 2015 away from the city in the absence of alternative light cues. Experiments on lunar orientation were conducted by Prof Dr Ugolini.

The distribution data was analysed according to Batschelet (1981). For each circular distribution, a mean vector was determined (direction and angle). The Rao's test was used to assess non-uniformity of the data distribution with probability levels of $p<0.05$ (Landler *et al.*, 2018).

A subgroup of animals was maintained in 6 hrs phase shifted light conditions. The onset of the light phase was 6 hrs advanced in relation to the control animals. It is well established, that the *T. saltator* homing behaviour shifts direction in accordance with a shift in the light phase they are kept in (Ugolini *et al.*, 2002). One hr of phase shift corresponds to 15° on the compass rose.

4.3.4 Antennal manipulation

To analyse the contribution of antennae to solar and lunar orientation, one experimental group of animals had antennae ablated with very fine micro scissors. Animals were allowed to recover from the operation for one week before experiments were conducted. Alternatively, the right pair of antennae were painted with black enamel (Rainbow) and tested for their orientation behaviour 24 hrs after.

4.3.5 Clock gene expression analysis

For tissue collection, animals were quickly decapitated with very fine micro scissors. A total number of 6 replicates were taken for each time point, containing 5 individual cephalic segments without antennae pooled and stored in 2 mL RNAlater® Solution (Ambion™) (Figure 4.2). The antennae were kept separately, treated the same as the brains. For a sufficient amount of tissue, all antennae from 30 animals were pooled into one sample. Samples were kept for 24 hrs at 4°C and consequently stored at -20°C.

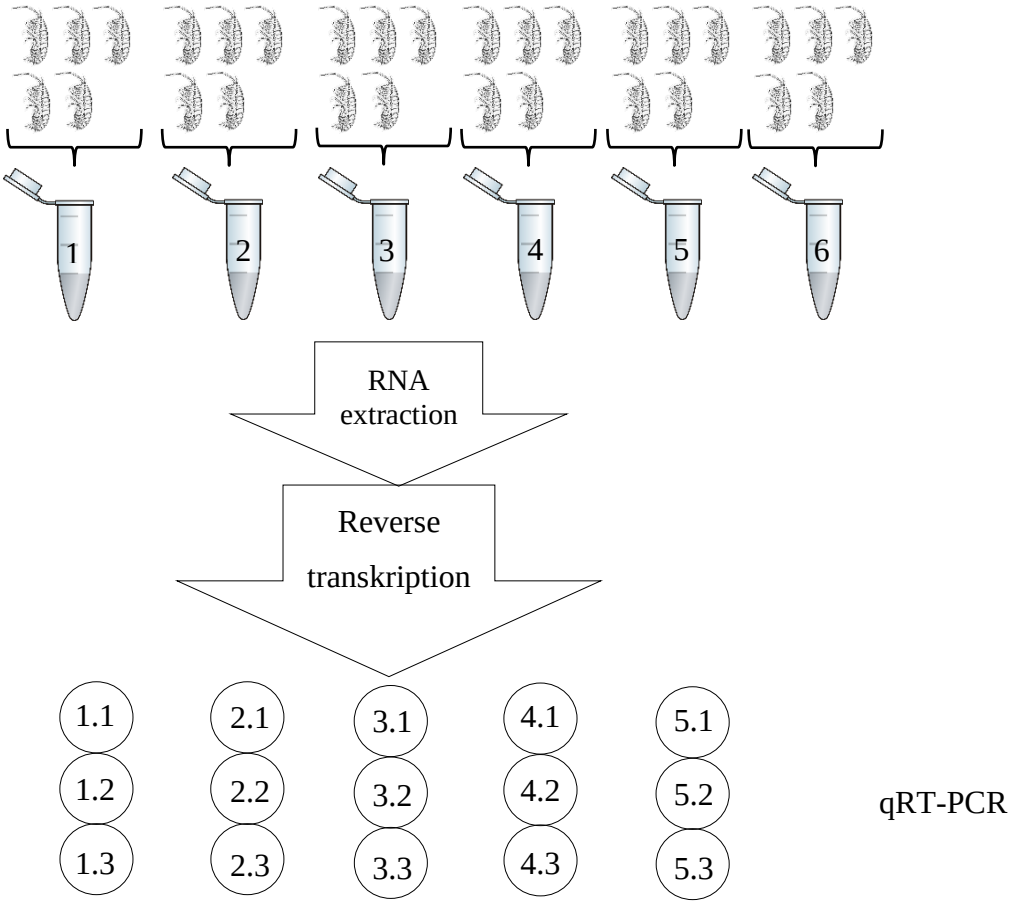

Figure 4.2: Tissue collection scheme and experimental pipeline. At each of the eight sampling time points, five animals were decapitated and the tissue pooled into one sample. Six samples were generated at each time point with antennae and head processed separately. To receive sufficient amounts of tissue, antennae of 30 animals were pooled to make up one sample. The RNA was then extracted and reverse transcribed into cDNA. Each of the six samples was measured in triplets in the qRT-PCR reaction. Reaction tube, free resource image: https://pixabay.com/en/vial-tube-fluid-laboratory-41375/; *T. saltator* body, side view, (public domain image) (Calman, 1911).

Total RNA was extracted using the RNeasy Mini Kit (Qiagen) according to manufacturer's instructions. Corresponding cDNA was obtained using the High-Capacity cDNA Reverse Transcription kit (Applied Biosystems®) with an input volume of 2 µL of total RNA likewise according to manufacturer's instructions.

As a preliminary analysis, the cDNA from brain, primary and secondary antennae was subjected to a PCR reaction with the respective primers for the clock genes *Talper*, *Taltim*, *Talclk*, *Talcry* and *Talbmal1* (see Table A.2 for oligonucleotide primer sequences used).

For the qRT-PCR, Taq-Man® hydrolysis probes for three core clock genes (*Talper, Talclk, Talcry2*) primers had already been designed and tested based on the mRNA transcriptome (O'Grady *et al.*, 2016). *Taltim* qRT-PCR primers, probes and cRNA standards were developed as described in the general methods 2.11 (oligonucleotide primer and probe sequences in Table A.3 in Appendix A).

Absolute quantification of the respective transcripts was accomplished in relation to previously quantified cRNA standards. Each biological replicate was measured in triplets. The PCR reactions were performed using the SensiFAST™Probe Lo-ROX Mix (Bioline Reagents) in the QuantStudio™12K Flex Real-Time PCR System (Applied Biosystems®). Expression values were normalized to the expression of the housekeeping gene *TalArginine kinase* (*TalAK*) which shows stable transcript levels along the circadian cycle *T. saltator*.

One-way ANOVA and students T-test were calculated with IMB SPSS Statistics 21 (IBM Corporation).

The Cosinor software (Refinetti *et al.*, 2007) was used to test for rhythmicity in mRNA expression levels throughout the 24 hrs circadian cycle using standard circadian settings (http://www.circadian.org/softwar.html).

4.4 RESULTS

To analyse if the neuronal clock gene expression is the basic chronometric mechanism for orientation, two groups of animals were tested for their escape direction. One group was accustomed to the onset of the day in accordance with the natural photoperiod. The other group was held under a light regime in which the onset of the day was shifted for 6 hours. The role of antennae in solar and lunar orientation was researched as well. Animals with ablated and enamel painted antennae were analysed for their escape behaviour under the sun during the day and under the moon light during the night.

4.4.1 Locomotor activity

The locomotor activity was measured to ensure and animals used for the experiments show expected activity during the dark phase despite out manipulation.

The animals kept in 6 hrs phase shifted conditions were adapted to the shift in light regime. Their activity patterns followed the new light regime with activity peaks during the dark phase and resting activity during the light phase (Figure 4.3). Activity under LD was unaffected by antennal ablation (Figure 4.3 B) and or shift in the onset of the dark phase (Figure 4.3 C).

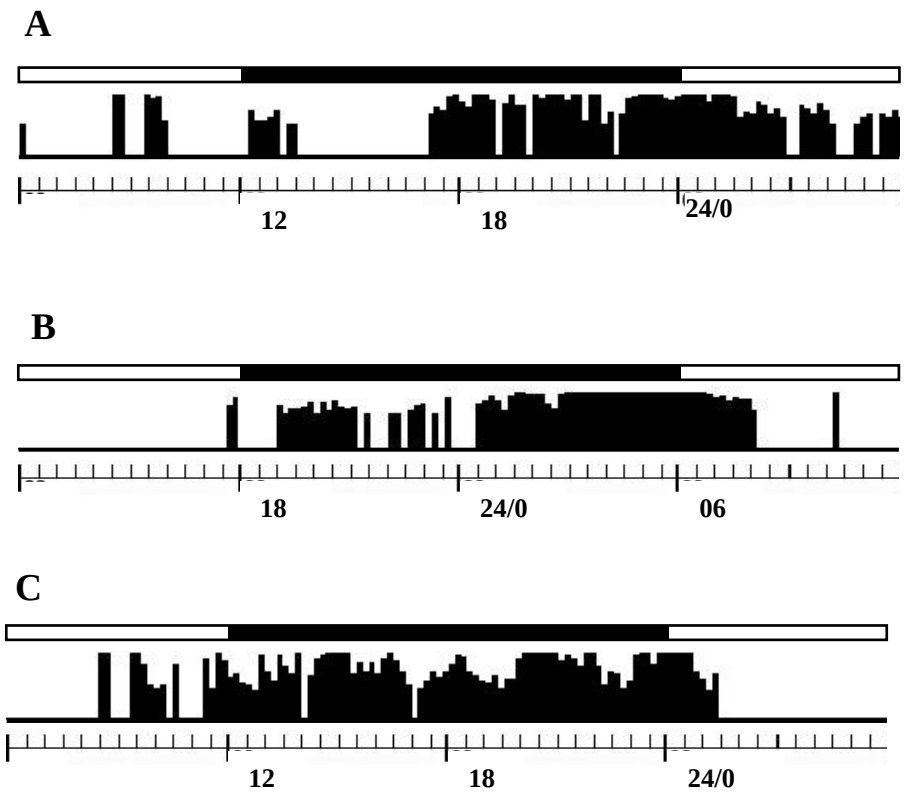

Figure 4.3: Average locomotor activity of 20 animals in one experimental chamber under 12:12 LD. Activity is presented in arbitrary units. The black and white bars on top of the graphs indicate the dark and light phase. (A) 6 hrs phase shifted; τ=23.8 hrs (B) Antennae ablated, τ=24.4 hrs (C) Antennae ablated and clock shifted by 6 hr, τ=23.6 hrs.

4.4.2 Orientation behaviour

The solar orientation behaviour with and without functional antennae was tested in *Talitrus* held in LD 12:12 in phase with the natural light cycle and in a 6 hrs phase shifted environment.

Control animals mean direction was 174° south when released in the absence of external cues (apart from the sun), with u=2,87 and p<0.01 (home beach direction=189°; Figure 4.4 A).

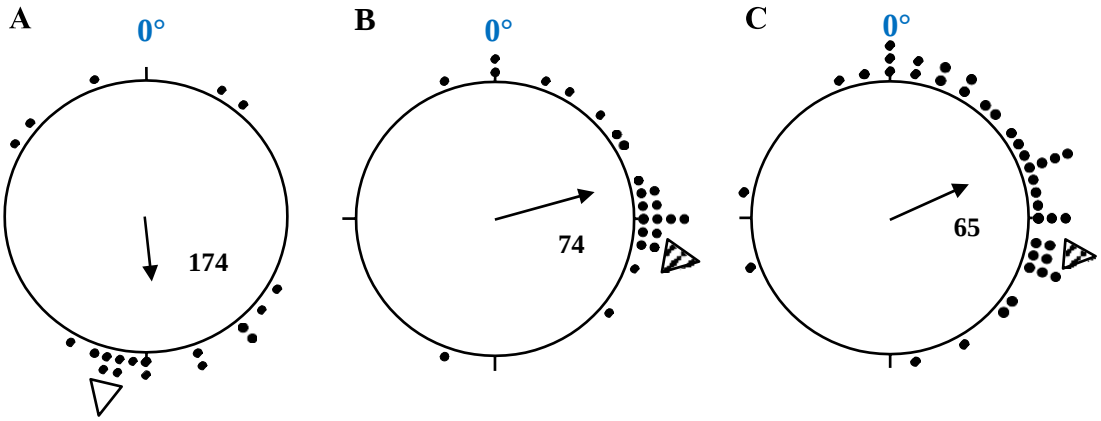

Figure 4.4: Orientation behaviour of *T. saltator* at solar midday (home beach direction=189°). Animals were released into a Plexiglas bowl. Each dot represents an individual with the position showing its escape direction. 0°=magnetic north. The triangle represents the expected direction of orientation i.e. home beach (blank) or home beach direction minus 90°C for the 6 hrs phase shifted animals (striped triangle). Arrow in the circle represents the mean vector and angle, Circle radius= maximal vector length=1. (A) Control, LD 12:12, mean direction of orientation was 174° S, n=20, u=2.87, p<0.01. (B) 6 hrs phase advanced to controls (n=24), mean angle of deflection was 74°, u=4.507 and p<0.001. (C) 6 hrs phase advanced to controls and 1^{ry} and 2^{ry} antennae ablated bilaterally (n=39), mean direction of orientation was 65°W with u=4.38 and p<0.001.

A shift in the light regime equally shifts the animals orientation direction as animals which were kept under a 6 hrs phase advanced light regime navigate towards 74° Western direction (u=4.507, p<0.001; see Figure 4.4 B). Functional antennae however are not necessary for the phase shift or the solar orientation as animals without antennae and kept under a shifted light cycle orientated towards 65° with u=4.38 and p<0.001 as seen in Figure 4.4. C, which is only 10° in difference.

The lunar orientation behaviour with and without intact antennae was tested in *Talitrus* held in LD 12:12 in phase with the natural light cycle. Animals were tested for their orientation under full moon light. *Talitrus* with intact antennae move along the sea land axis of their home beach between 91° and 271° with u=166.15 and p<0.001 (home beach direction=265°, Figure 4.5 A). With ablated antennae, animals

fail to find their home beach direction as they navigate towards 144° with u=149.79 and p>0.05 as shown in Figure 4.5 B. When the antennae are unilaterally (right side) obscured with black enamel, the animals move towards 207° equally unable to find their respective home beach direction (u=182.37, p>0.001) but displayed photopositive tendencies towards the moon light as seen in Figure 4.5 C.

To exclude all doubt about this difference in the experimental setup between sun and moon compass orientation, animals were also tested for their solar orientation in a Plexiglas bowl filled with water. Animals without antennae and with right antennae painted with black enamel both oriented in accordance with their expected home beach direction with u=180; p<0.005; n=28 and u=169.3; p<0,05; n=28 (only 14° ad 15° degrees difference, respectively). The only difference to the dry bowl solar orientation experiment was that control animals showed a bidirectional orientation across the sea land axis (100° and 280°) with n=40 and u=191 and p<0.001.

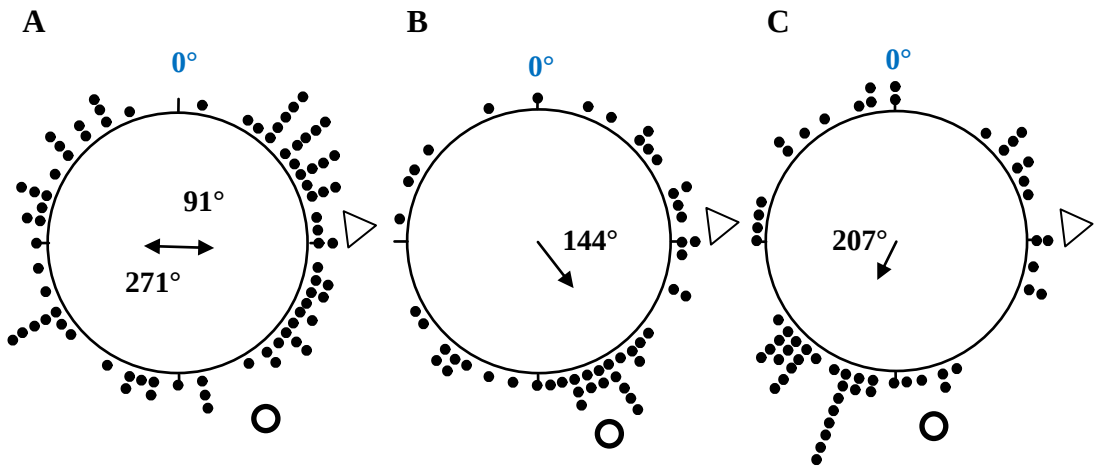

Figure 4.5: Lunar orientation behaviour under antennal manipulation. Home beach direction=265°. 0°= magnetic north, dots correspond to the orientation direction of one individual sandhopper; triangle expected direction of orientation; Arrow in the circle represents the mean vector and angle, Circle radius= maximal vector length=1. (A) Control animals, n=78, u=166.15, P<0.001 (B) antennae ablated (n=49, u=149.79 and p>0.05) and (C) right antennae painted with black enamel; n=59, u=182.37 and p<0.001.

4.4.3 Clock gene mRNA expression

The clock gene mRNA expression was measured in brain and antenna samples. Animals held in shifted and un-shifted light conditions were analysed to research the relation between the orientation mechanism and the circadian clock. Brain, primary and secondary antennae all express the core clock transcripts *Talper*, *Taltim*, *Talclk*, *Talcry2* and *Talbmal* as respective primers amplify cDNA of all three tissues in a PCR reaction (see Agarose gel Figure A.10 Appendix A).

The mRNA levels of four clock genes (*Talper*, *Taltim*, *Talclk* and *Talcry2*) in the brains and antennae of behaviourally rhythmic *T. saltator* were quantified along the circadian cycle using qRT-PCR. In the control group, animals were kept in 12:12 LD in phase with the natural photoperiod. Data for brain mRNA levels are shown in Figure 4.6. One-way ANOVA was performed in addition to the Cosinor analysis published. One-way ANOVA showed that the *Talper* and *Taltim* mRNA expression level depended on the hr of the day in constant conditions (Figure 4.6 A) with $F_{7,39}=15.39$ and $p<0.0001$ for *Talper* and $F_{7,39}=5.659$ and $p<0.0001$ for *Tatim* respectively. The *Talper* mRNA clearly shows higher levels during the subjective night phase with a maximum at CT15 and the minimum at CT 3 during the subjective light phase. Cosinor analysis additionally revealed this mRNA levels to cycle in abundance within the 24 hrs with $F_{2,5}=17.42$ and $p<0.01$. Similarly, *Talcry2* mRNA cycles in abundance with $F_{2,5}=18.84$ and $p<0.01$. However, one-way ANOVA did not show a dependence of the mRNA levels on the hrs of the day with $F_{7,39}=2.064$ and $p>0.05$. In contrast, the *Taltim* mRNA expression did change with the hrs of the day. *Taltim* mRNA levels were higher during the subjective day and low during the subjective night. The maximum expression level was determined at CT12 and the lowest at CT15. The *Talclk* mRNA expression level were not shown to depend on the time of the subjective day in DD nor expresses rhythmicity ($F_{7,39}=0.773$ and $p>0.05$). When animals were kept in 6 hrs phase shifted conditions (relative to the natural photoperiod at the day of collection), *Talper* and *Talcry2* mRNA levels were found to depend on the hr of the day ($F_{7,39}=4.388$, $p<0.01$ and $F_{7,39}=3.358$ and $p<0.01$; see Figure 4.6 B). *Talper* mRNA expression levels were higher during the subjective night phase and low during the subjective day with a maximum in expression level at CT24/0 and a minimum expression at CT12. The *Talcry2* mRNA expression level were highest at CT9 during the subjective light phase and lowest at

CT6 equally during the light phase. *Taltim* and *Talclk* mRNA expression levels were not shown to change with the hrs of the day, as one-way ANOVA results were $F_{7,39}=2.045$, $p>0.05$ and $F_{7,39}=0.937$, $p>0.05$ respectively. Figure 4.6 C also shows the mRNA levels of four clock genes *Talper*, *Taltim*, *Talcry2* and *Talclk* in *T. saltator* antennae . For none of the clock genes a dependence of the hrs of the day of the mRNA level was found by one-way ANOVA (respective F- and p-values can be found in Table A.4 in Appendix A). Cosinor analysis found *Talper* and *Talcry2* mRNA to cycle in expression within 24 hrs ($F_{2,5}=6.61$, $p<0.05$; $F_{2,5}=15.18$, $p<0.01$).

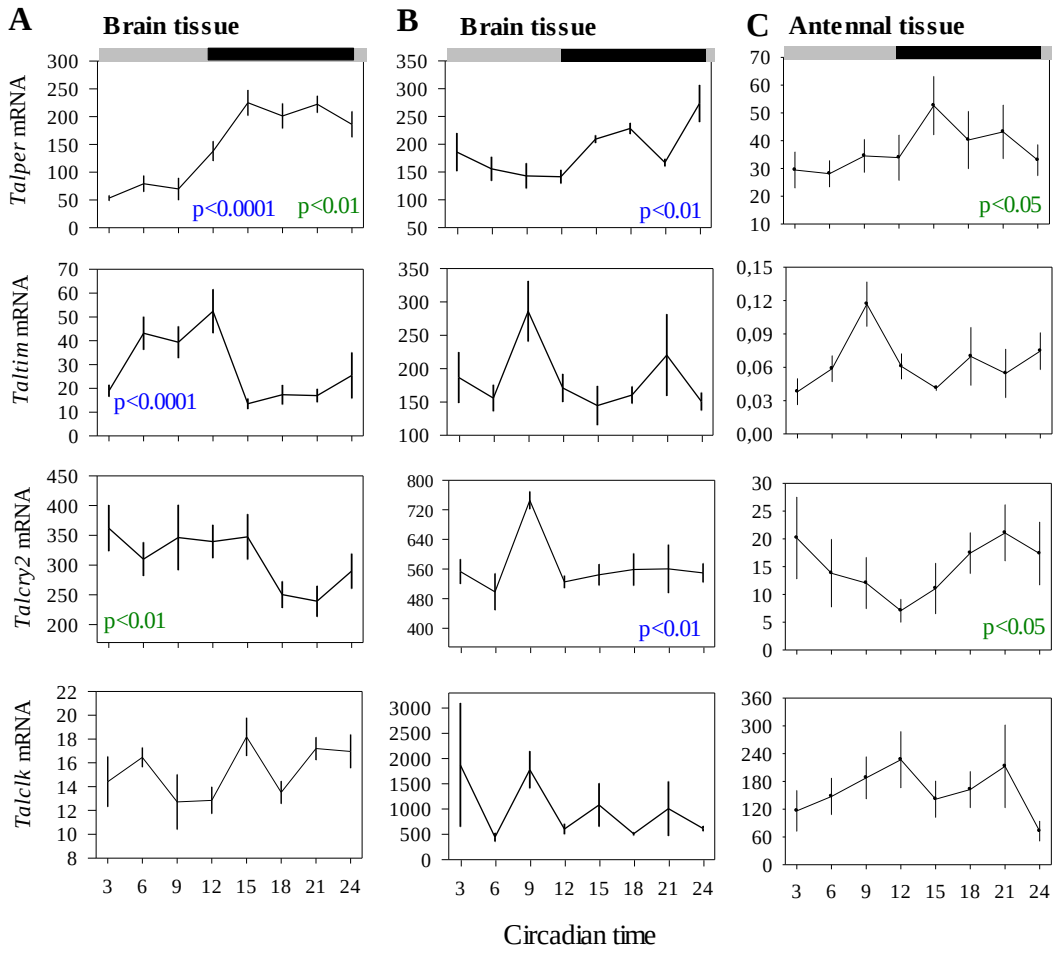

Figure 4.6: Cock gene mRNA levels in behaviourally rhythmic *T. saltator* brains (n =6). (A) Control, 12:12 LD in phase with natural onset of light phase. *Talper* and *Taltim* expression depend on the hr of the day ($F_{7,39}=15.39$, $p<0.00001$ and $F_{7,39}=5.659$, $p<0.0001$). *Talper* and *Talcry2* mRNA expression curves fitted a sinusoidal shape with $F_{2,}=17.33$, $p<0.01$ and $F_{2,5}=18.84$, $p<0.01$ are thus considered to cycling in a circadian rhythm. (B) 12:12 LD 6 hrs phase advanced in relation to the natural onset of light phase. *Talper* and *Talcry2* expression depend on the hr of the day ($F_{7,39}=4.388$, $p<0.01$ and $F_{7,39}=3.358$, $p<0.01$). (C) Clock gene mRNA levels in antennae of behaviourally rhythmic *T. saltator*. Animals were kept in 12:12 LD before 24 hrs in DD (n=6). Absolute mRNA values are presented as copy number of the respective clock gene per copy number of the house keeping gene *Talak* mRNA(*100). p-values for one-way ANOVA in blue and cosinor analysis in green.

4.5 DISCUSSION

4.5.1 Clock gene expression and orientation shifts

The aim of the work in this chapter was to research if a circadian clock in *T. saltator* is responsible for the time-compensation in the sun compass and if the sandhoppers exhibit an antennal sun compass clock anatomically discrete from a central brain clock as found for *D. plexxippus* (Reppert, 2007). Animals with and without functional antennae were tested for their locomotor activity, orientation behaviour and the mRNA expression of four canonical core clock genes were measured via qRT-PCR in the brain and antennae under control and clock shifted photoperiods. The locomotor activity of animals was not affected by antennal ablation and animals without antennae were able to entrain to a new, 6 hr shifted light regime. As previously reported in the literature (Ugolini *et al.*, 2002), the solar orientation direction was shifted in animals that underwent a phase shift. Associated with that, the expression profiles of *Talper*, *Taltim* and *Talcry2* showed shifts in the expression curves. For example, the *Talper* expression was higher during the subjective dark phase in control animals as well as in shifted animals. A shift in the time of the onset of the light phase was mirrored with a shift in the gene expression level.

Two of the clock gene transcript levels in the brains, *Talper* and *Taltim* display clear dependence on the time of the day under constant conditions. Similar findings were made for the invertebrate *D. plexxippus* where *period* and *timeless* mRNA were found to be the most reliably expressed and equally higher during the subjective night (Merlin *et al.*, 2009). The finding that *Talper* and *Taltim* both peak in mRNA expression during the early subjective night phase compares well with data from *D. melanogaster* circadian clock gene expression, where mRNA for both genes peaks in expression at the onset of the night (Hardin *et al.*, 1990; Young and Kay, 2001). In the antennae and brain, the *Talper* and *Talcry2* expression levels were found to cycle within 24 hrs and in the antennae the *Talper* expression levels are significantly higher during the night when data for the subjective light and dark phase are collapsed. The interval of measurement was every three hrs. With a higher resolution in sampling through more time points, a more precise dissection of the expression pattern could be obtained.

As already discussed in the previous chapter, the *Talitrus* clock is probably regulated on different levels but also the translation and protein activity of clock and clock-associated proteins account for a functioning circadian clock. Due to their small size, suitable methods to measure protein levels in *Talitrus in vivo* are currently not available (long standing experience in the group). Immunohistochemical analysis with clock protein specific antibodies to determine clock gene expressing cells (and maybe even subcellular localization) are the next logical step in the line of research.

Besides its role as a blue light sensor, CRY1 has been proposed to be magnetoreceptive in *Drosophila* (Gegear *et al.*, 2009). *Talitrus* population located closer to the equatorial plane are accounted to utilize the earth magnetic field for orientation (Arendse and Kruyswijk, 1981; Ugolini, 2006). Even though, a *Talcry1* could not be identified in transcriptome and a functioning circadian clock is not necessary for magnetoreception in *Drosophila* this throws up the question if an alternative part of the clock is responsible for magnetoreception in *Talitrus*.

4.5.2 A putative extra-cerebral lunar clock in the antennae

The second objective of the study was the analysis of the orientation behaviour in the light of a separate chronometric mechanism responsible for the sun compass following the example of the butterfly *D. plexxippus* where an anatomically discrete sun compass clock in the antennae is responsible for the time compensation mechanism of the animals solar orientation behaviour. The sun compass however, was found not to depend on intact or even present antennae. Amputating the antennae is an invasive procedure and leaves the animal missing an organ. The fact that solar orientation behaviour was not disturbed by it, speaks for the clear independence of the behavioural mechanism. Quick zonal recovery upon disruption on the beach should increase survival and thus, biological fitness. Behavioural plasticity is key to this and can also be found in *Talitrus* sun compass orientation. Whilst the general home beach direction is innate, the animals express navigational plasticity especially within the first 15 days after hatching (Ugolini and Macchi, 1988). In the summer days, the sand on Italian beaches can easily reach 45°C (Ugolini and Macchi, 1988). When dislocated from their burrows during the day, *Talitrids* have to quickly find their way back home to avoid the serious threat of desiccation (Williams, 1995). Because of this, the

sandhoppers are tested in a dry, empty Plexiglas bowl for their solar orientation behaviour. During the night however, animals show their strongest homing behaviour when they are tested in a bowl filled with water. A test of escape direction in sea water during the day confirmed the results of animals tested in a dry bowl.

Contrary to solar orientation, the lunar orientation was altered by ablated or painted antennae. When the antennae were painted, the sandhoppers showed a photopositive tendency moving towards the light source. The data strongly suggest a chronometric mechanism for moon orientation situated in these organs. It is stated that the antennae are essential for the correct usage of the moon as a celestial compass cue in *T. saltator* (Ugolini *et al.*, 2016). Nevertheless, a control experiment with antennae painted with clear enamel should be conducted to exclude any effect of the painting itself on the orientation.

Apart from the monarch butterfly, some other insect species have been demonstrated to harbour circadian oscillators in the antennae. A putative antennal clock was found in the cabbage moth *Mamestra brassicae*. *Mbper* and *Mbcry* are expressed in olfactory sensory neurons of the antennae which are known to be vital for the animals communication (Merlin *et al.*, 2006). Likewise, in another moth species *Spodoptera littoralis,* also known as the African cotton leaf worm, a circadian oscillator was found in the antennae. The mRNAs of *Per* and *Cry1* and *Cry2* were found to cycle in abundance within 24 hrs and these findings were linked to circadian rhythms in pheromone response (Merlin *et al.*, 2007). Some evidence for an antennal clock in form of immunostaining was shown in another moth species the tobacco hornworm *Manduca sexta,* were PER-positive olfactory receptor neurons were demonstrated. The corresponding mRNA was higher during the night (ZT15) then during the day (Schuckel *et al.*, 2007). In ablation studies, Tanoue *et al.*, demonstrated in 2004 that antennal neurons are responsible for olfactory rhythms in *Drosophila*. If antennae harbour a separate chronometric mechanism in form of a moon compass clock as found in *D. plexxippus* for sun compass clock remains to be investigated further. This could be accomplished with the methods used in this chapter. It would be very interesting to analyse the clock gene expression rhythm in moon-shifted *Talitrus*. The moon shift experiment has been published by Meschini *et al.* in 2008, even though it had been established previously that the moon compass time compensation mechanism functions independent from the sun (Ugolini *et al.*, 2007).

Similarly, a moon compass shift experiment is proposed where the ability to follow a shift in the moon phase of antennaeless animals would be researched. Additionally, the mRNA expression rhythms in the intact antennae of moon shifted *T. saltator* should be analysed. It would need to be established if and how an expression pattern of clock genes in the antennae of *Talitrus* changes with the lunar phase and if a potential detected expression rhythm detected corresponds to a natural and artificial change in the lunar phase.

The marine worm *Platynereis dumerilii* possesses a circalunar clock regulating reproductive timing which is entrained by nocturnal light similar to the lunar orientation mechanism in *T. saltator*. The circalunar clock situated in the forebrain of the worm seems to be independent from the circadian clock as CK1ε/δ inhibition disrupts the latter but not the circalunar behaviour (Zantke *et al.*, 2013). The isopod

E. pulchra exhibits and circatidal swimming behaviour and circadian rhythms in chromophore dispersion and clock gene expression (*Eptim*). The circadian clock can be disrupted molecularly with PF-670462 effecting circatidal behaviour indicating that both circadian and circatidal clock rely on CK1. Interestingly, RNAi knockdown of *Epper*, leaves tidal swimming rhythms unaffected (Zhang *et al.*, 2013). Both studies indicate that a circalunar (29.5 d) or circatidal (12.4 h) clock does not depend exclusively on the circadian clock. It would be very informative to see if a disruption of the circadian clock on a molecular level would equally disrupt sun orientation and leave the moon compass function unaffected. In both publications mentioned above the artificial pharmacological agent PF-67046 was used which is known to disturb the circadian clock by inhibiting CK1ε/δ (Eide *et al.*, 2005; Walton *et al.*, 2009; Zantke *et al.*, 2013). Preliminary experiments showed that animals become behaviourally arrhythmic when injected with 12.5 µM PF-4800567 (majorly inhibiting CK1ε) (see Figure A.4 in Appendix A) but solar orientation was deemed unaffected. Nevertheless high mortality rates did not allow explicit conclusions. This work can only be conducted after a successful application route has been found for *T. saltator*.

Rossano *et al.* (2009) found an additional bimodality to the rhythmic circadian locomotor behaviour of *T. saltator* collected from Atlantic beaches

(Brittany, France). This raises the question whether potential circatidal rhythms were also an important factor in this current research. In the Mediterranean, tides are relatively small and given that they live supralittoral, are not thought to influence their orientation behaviour. For animals collected from the British isles, they are subject to much larger tides but no bimodal rhythm in activity could be observed in agreement with the findings about French sandhoppers. It seems that the animals are very well adapted to their environments and exhibit finely tuned behavioural plasticity to ensure survival and increase biological fitness. In the equatorial sandhopper *T. martensii* for example the close relationship of the sun and magnetic compass was demonstrated. At a zenithal distance of the sun of less then 10°, the magnetic compass was given more weight while navigating (Ugolini, 2001).

Lunar orientation in arthropods is poorly researched. *Tylos europaeus* is the only other known crustacean isopod with antennae using a time compensated moon compass (Pardi, 2010; Ciofini and Ugolini, 2017). The wolf spider *Arctosa varania* does not have antennae but shows time-compensated lunar orientation (Tongiorgi, 1969). The ant *Formica rufa* and the earwig *Lapidura riparia* were shown to include celestial bodies in their way finding but a time-compensation of the mechanism still needs to be determined (Jander, 1957; Ugolini and Chiussi, 1996). The mRNA expression curves of *Talper* in brain and antennae are in phase, while they are antiphasic in *Talcry2*. In a scenario where *Talitrus* possesses an independent moon compass clock in the antenna, the clock transcripts could be regulated on a circalunar cycle. A direct role are a lunar light sensor has been proposed for *Cry2* in the branching stony coral *Acropora millepora* as the expression levels increase at full moon (Levy *et al.*, 2007). The moon phase effects *Per2* expression levels of the golden rabbitfish *Siganus guttatus* (Sugama *et al.*, 2008). A recent transcriptomic study in the acroporid coral *Acropora gemmifera* assessed the gene expression of clock and clock-associated genes during the night and day over the moon cycle. It was reported that expression levels change within the lunar cycle (Oldach *et al.*, 2017) and it would not be surprising to find differences in daily expression patterns depending on the phase of the moon. In the absence of experiments with free running animals any relation between clock gene levels and lunar phases remains speculative. To overcome that problem, clock gene transcripts should be measured over the lunar phase in free-running conditions and in lunar shift experiments to detect a direct dependence of clock transcripts by

the moon cycle.

It is proposed that the circadian time compensation mechanism utilised for the solar compass mechanism exhibited by *T. saltator* is governed by the animal's central circadian clock. A definite link between the two biological phenomena can be demonstrated using RNAi knock-down of involved clock genes and or pharmacological intervention with agents that are known to disturb the biological clock The current data provides unique insight into the crustacean circadian clock mechanisms and its relation to compass navigation behaviour. Further, it makes room for new and unexpected thought-provoking impulses about the versatile function of antennae in the orientation process.

4.6 SUMMARY

The data presented in this chapter indicates that *T. saltator* core clock genes are likely to be involved in the animal's navigation behaviour. Neuronal *Period* and *Timeless* mRNA show circadian rhythms in abundance in behaviourally rhythmic animals which also exhibit time-compensated solar home beach orientation. These clock gene expression patterns shift in accordance with a phase shift in the light regime. Equally, the orientation direction of the shifted animals corresponds with the amount of time the light regime was altered for, which further implicates the clock genes involvement in the animal's navigational capabilities. As opposed to other insects such as the monarch butterfly, *T. saltator* solar navigation behaviour does not rely on cycling clock genes in the antennae as amputation of these did not hinder successful home beach orientation. Concrete evidence for anatomically separate solar and lunar compasses is provided by the fact that lunar navigation was disturbed in animals without antennae.

CHAPTER 5: IMMUNOLOCALISATION OF CENTRAL PACEMAKER CELLS IN *T. SALTATOR* BRAINS

5.1 ABSTRACT

The primary aim of the study was the localisation of potential circadian pacemaker cells in the brain of *T. saltator*. To investigate the protein localisation in cerebral ganglia and possibly identify central pacemaker neurons, α-TalPER antisera were produced and qualified for whole mount immunohistochemical staining. Staining pattern showed distinct cells in the protocerebrum (PCRM) with at least two cells in each hemisphere present. Further, the abundance of PER protein was measured over the diurnal cycle and found to significantly depend on the time of the day. The current chapter provides a promising beginning of the identification and characterization of central pacemaker cells in *T. saltator* brains. Their localisation and determination of clock protein abundance over the course of a day and will help to understand the arthropod circadian clock.

5.2 INTRODUCTION

5.2.1 The core clock component *Period*

The *per* gene and protein have a key role in the transcription- translation feedback loop governing circadian rhythms (Reppert and Weaver, 2002). After translation PER molecules, translocate to the nucleus to dimerize with TIM, interact *period* promoter in a repressive manner leading to a regular fluctuation in transcript abundance. It is essential for functional rhythms as locomotor behaviour in several types of *Drosophila period* mutants mirror the mutant specific locomotor rhythm in PER abundance (Zerr *et al.*, 1990). Eclosion is similarly influenced by *period* mutations- a discovery that lead to the identification and classification of *period* as a clock gene (Konopka and Benzer, 1971). In *Drosophila*, *per* expression was identified in antennae, proboscis, eyes, optic lobes, central brain, thoracic ganglia, gut, Malpighian tubules and ovarian follicle cells (Liu *et al.*, 1988). In 1988, Siwicki *et al.* discovered groups of neurons in *Drosophila* eye and brain that showed a circadian rhythm in accumulation of PER. The overall staining appeared to be predominantly nuclear (Liu *et al.*, 1992) and peaks in intensity during the dark phase in *Drosophila*

and *Danaus* (Zwiebel *et al.*, 1991; Reppert, 2007). Hardin *et al.* showed in 1990 that dPER expression in the brain was preceded by an mRNA expression maximum by 5 hrs. In *Drosophila*, a nonsense *per* mutant did not exhibit cycling mRNA while this phenotype could be rescued with wild-type PER (Hardin *et al*., 1990). The hypothesis of a transcription-translation feedback loop with PER translocating to the nucleus and inhibiting its own transcription was formed and the idea of the circadian feedback loop was born. It was further supported by the discovery of a PAS domain in the PER sequence, which is common to transcription factors (Huang *et al*., 1993).

5.2.2 Invertebrate central pacemaker

In contrast to mammals, where the central circadian pacemaker sits in the suprachiasmatic nuclei (SCNi), invertebrate central pacemaker clock cells are more dispersed across the brain. In *Drosophila*, *per* expressing lateral neurons (LNs) are situated between the optic lobes and the central brain in both hemispheres. Two groups of 5 small ventrally located cells (s-LNv) and four large LNvs (l-LNv). They project to the dorsal PCRM and the second optic lobe neurophil. The l-LNv additionally project to the contralateral LNvs and the medulla. With *per*, the LNvs co-express *pdf* (Helfrich-Förster, 1995), which is crucial for rhythmic locomotor activity. A non-pdf expressing, third group of LNv, consists of 6 cells and lays more dorsally which are thus called LNd (Kaneko and Hall, 2000). Three groups of neurons in the dorsal brain called dorsal neurons DN1-3 also express-clock genes. DN1 consists of 15 cells, DN2 of 2 and DN3 of about 40 neurons. LNs and DN1 all terminate in the same dorsal brain region. Additionally, s-LNv cells also receive input from DN1 and DN3 neurons which results in an interconnected clock network (Kaneko and Hall, 2000; Helfrich-Förster, 2003). For a schematic overview of the *Drosophila* neuronal pacemaker cells see Figure 5.1.

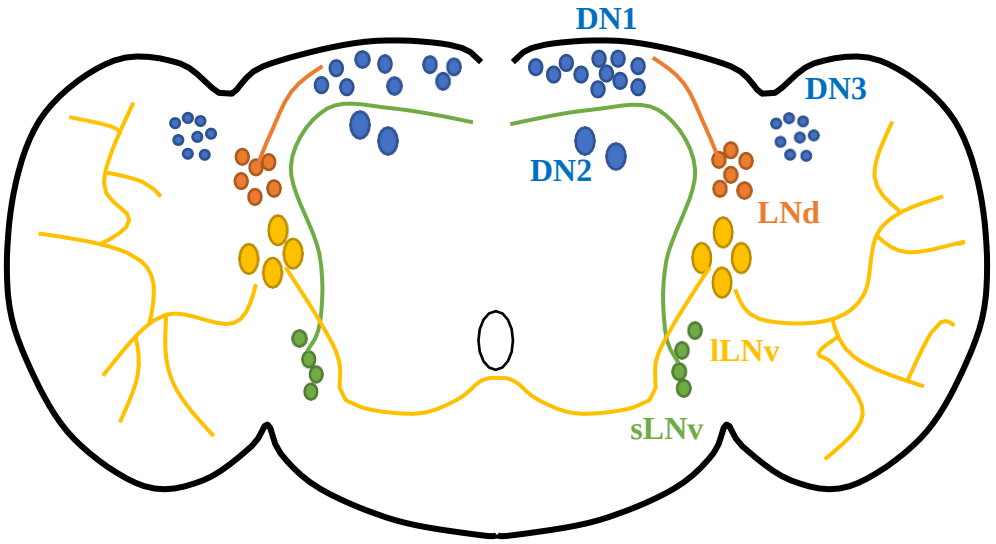

Figure 5.1: Schematic, simplified drawing of the *Drosophila* brain with clock cells and respective neuronal projections. DN=dorsal neurons, LNd=dorsolateral neurons, lLNv=large ventrolateral neurons, sLNv=small ventrolateral neurons. Modified after (Stanewsky, 002; Allada and Chung, 2010).

In the monarch, clock proteins (PER, TIM, CRY2, CRY1) are co-localised in two of the four cells of the pars lateralis (PL) in both hemispheres. These cells communicate with neurons of the pars intercerebralis (PI) and probably also with the central complex (Zhan *et al.*, 2011). Other cells in the brain express clock proteins and these potentially co-localise in some dorsal areas but the four cells of the PL are considered the central pacemaker brain clock cells (Reppert *et al.*, 2010). *E. pulchra* exhibits two dorsolateral cells which are PER positive, as well as one lateral cell close to the optic ganglia all three in each hemisphere (Zhang *et al.*, 2013). Immunofluorescent staining was reported to be intensive in the cytoplasm but weak in the nucleus. No differences were found for the staining intensity throughout the day but a stronger staining was observed during the night for the dorsolateral cells (Zhang *et al.*, 2013). In crayfish, beside other oscillators in the retinas of the eyes and in the X-organ sinus gland complex (XOSG), a putative central oscillators could be situated in the brain. This has not been identified yet, and a possible, less hierarchical model with different oscillator working together to govern biological rhythms in these animals are discussed (Strauss and Dircksen, 2010).

Many approaches have been made to characterize pacemaker neurons through PER-immunolocalisation. Anti-*drosophila* PER antibody used in *Homarus*

americanus tissues revealed positive immunoreactivity in the eyestalks which was highest during the mid of the dark phase (Grabek and Chabot, 2012). In *Procambarus clakii*, dPER also stained the retinal photoreceptors and cell bodies in the mania ganglionaris with axons running distally towards photoreceptors and proximally to other areas of the lamina (Aréchiga and Rodríguez-Sosa, 1998). Reppert and Sauman (1996) identified eight neurons expressing PER in the silkmoth *Antheraea pernyi*. Four cells were found in each hemisphere, one lateral pair and one medial pair in the dorsolateral region of each half of the brain. *Per* mRNA and protein both oscillate in antiphase in these cells but are suppressed by constant light (Sauman and Reppert, 1996).

5.2.3 *T. saltator* core clock component *Period*

Full sequence clarification was accomplished with a 8001 bp heavy contig containing a 1557 amino acid long putative PER protein (chapter 3.3). This aligns with a 29% sequence identity and a 50% similarity to *Drosophila* PER. The diverted protein contains two PAS domains and a PAC domain, an NES, cytoplasmic localization and nuclear localisation signal motivs. These are all common *Period* attributes as well as a CK1ε binding site sequence and a Period C domain (Zhang *et al.*, 2013). PCR analysis showed *Talper* transcript in brain, antennae (primary and secondary), pereiopods, ventral nerve cord as well as in the hepatopancreas ((O'Grady, 2013) and 4.4.3). The *Talper* mRNA expression was found to peak during the subjective dark phase in brain and antennae (chapter 4.4.3). In all measurements conducted in this thesis work, the *Talper* expression was rhythmic and depended on the time of the day. Taken together with what is known about the role of PER in crustaceans and invertebrate biological clocks, it is the most promising of the identified clock components to have a central role in the circadian clockwork. This makes it most suitable to identify the central pacemaker clock neurons in *T. saltator*. TalPER antisera were produced and tested via immunohistochemical staining. Antisera were applied on tissue harvested at different times of the day to identify potential rhythmicity in PER expression.

5.3 MATERIALS AND METHODS

5.3.1 Production of the TalPER antiserum

To localise putative central circadian pacemaker cells in the *T. saltator* brain, an antibody was produced against the TalPER sequence. The TalPER polyclonal rabbit antisera were produced from the deduced PER sequences shown in Table 5.1. The peptide sequences chosen, contained predicted hydrophilic regions. In the proteins native confirmation, these would be exposed to the outside of the molecule and thus can be recognized by the immune system of the rabbits used for antiserum production. Eurogentec in-house prediction software tools were used to identify the suitable sequences.

Table 5.1: Peptide sequences used for production of antisera.

	Peptide #1	**Peptide #2**
Sequence	C-FQSPEREHLSSNQSE	C-GSVDEAKSSSPKQQYC

Peptide production, immunization of rabbits and harvest of antisera was conducted by Eurogentec according to the 28+ days Speedy protocol visualised in Table 5.2 including 4 injections of both peptides. Two rabbits (#713, #714) were immunised at the same time. Animals were injected on day 0,7,10 and 18 and bled on day 0, 21 and finally at day 28. The final bleed after 28 days of incubation was used for the antisera tested here.

Table 5.2: Immunization protocol the rabbits were treated with to receive TalPER antisera.

Day	**0**	**7**	**10**	**18**	**21**	**28**
Injection	1st	2nd	3rd	4th		
Bleed	Pre-Immune				Medium	Final

The crude antisera were then cleaned though a column lined with an AF-Amino TOYOPEARL/MBS affinity matrix. After binding the antigen specific antibodies on the column, unrelated antibodies were washed-off with PBS and the purified antibody was eluted with 100 mM Glycine pH 2.5 and delivered with in PBS (1x), 0.01% w/v

thimerosal, 0.1% w/v BSA. Analysis of antiserum was accomplished via ELISA. The ELISA plate was coated with 5-15 µg/well peptide using 100 ng/well PBS as a carrier and incubated for 16 hrs at 4°C. Following this, the plate was blocked for 2 hrs at 25°C with 1 mg/mL BSA. Serum was then added in a serial dilution starting at 1:100 and incubated at 25°C for 2 hrs. Pre-immune serum (from the day 0 bleed) and serum from the final bleed (day 28) was also used. For detection a dilution of 1:2500 anti-rabbit-IgG-HRP conjugate antibody (Sigma-Aldrich) was applied and incubated for 2 hrs at 25°C The plate was then developed with 0.4 mg/mL o-phenylenediamine (OPD) for 20 minutes at 25°C. The reaction was stopped with 4 M H_2SO_4 and detection conducted at 492 nm.

5.3.2 Animal sampling protocol

Animals for these experiments were kept under LD as described in 2.1. Brains were harvested at ZT 0,6,12 and 18 (with ZT0 reflecting the onset of the light phase). Six brains harvested at ZT12 and ZT6 and 5 brains harvested at ZT0 and ZT18.

5.3.3 Whole mount immunofluorescent staining of *T. saltator* brains

To localise putative central pacemaker cells expressing TalPER in the brain, whole mount immunofluorescent staining was performed. *Talitrus* brains were dissected in ice-cold *Carcinus saline* under binoculars. The brains were then fixed in *Stephanini's fixative* solution for 12 -16 hrs at 4°C to allow the fixative to fully penetrate the tissue. Subsequently, the brains were washed in PTX (0.1M PBS (pH 7.5) containing 0.5% w/v Triton-X-100 + 0.025% NaN_3) on a shaker until the yellow colour of the fixative was washed out (about three to 6 hrs). Primary antibody incubation with a 1:500 concentration in PTX followed for 3 days at 4°C. Next, the brains were washed several times with PTX for a total time of 6 hrs and incubated for three days with a secondary antibody diluted 1:500 in PTX which was labelled with a fluorescent marker. Antibodies used were Alexaflour-488 goat-α-rabbit IgG (Molecular Probes) or Alexaflour-568 goat-α-rabbit IgG (Molecular Probes).The incubation and all following steps took place in the dark to avoid loss of fluorescence. After that, the brains were again washed in PTX for about 6 hrs and then incubated

in 1:1000 DAPI (Sigma-Aldrich) in PTX for 30 minutes to receive staining of nuclei. The brains were quickly washed again and incubated in one drop of Vectashield (Vectorlabs, Burlingame, CA, USA) for 10 minutes and mounted in 50 µL Vectashield on a microscope slide. The coverslip was sealed with clear nail polish.

A pre-absorption control was made to control for unspecific binding of the antibody in the tissue. For that, the antibody was incubated with the antigen it was directed against for 24 hrs and then used to stain whole mount brains as described above. Alongside, a positive control was run with the antibody only. Three to 5 brains were stained for each condition.

5.3.4 Image acquisition and analysis

Image acquisition is described in 2.12 and the following lenses were used: HCX PL APO lambda blue 1.25 OIL UV (40.0 x magnification), HCX PL APO lambda blue 1.40 OIL UV (63.0x magnification). Images were viewed with the LAS AF Lite Application Suite (http://leica-las-af-lite.software.informer.com/4.0/) and analysed with ImageJ (https://imagej.nih.gov/ij/) and as described in McCloy *et al*. (2014). Staining intensity (relative to the background) was calculated in the following: Corrected total cellular fluorescence (CTCF)=integrated density – (area of selected cell × mean fluorescence of background readings).

5.4 RESULTS

In this chapter, putative central circadian pacemaker cells in the *T. saltator* brain were investigated. These would be expected to express the core clock protein TalPER, which was localised through whole mount immunohistochemical staining of *T. saltator* brains with an anti-TalPER antibody. The staining intensity can hint towards higher or lower protein abundance. Thus, the staining intensity throughout the day and night phase was also researched to draw conclusions about the relative amount of protein thought the cycle.

5.4.1 Production of antisera

The quality and quantity assessments of the two TalPER antisera are displayed

in Table 5.3. When immunostainings with both antisera were compared, very poor or no staining was observed with antiserum #713 and thus the analyses and images shown were all acquired using TalPER #714.

Table 5.3: Quality and quantity assessment of the two TalPER antisera.

	Rabbit #713	**Rabbit #714**
Quantities (~)	3.2 mg	1.8 mg
Final volume	5 mL	3.8 mL
Antibody purity SDS- Page (BIOANALYSER)	92.9% (28.2 kDa light chain, 54.1 kDa heavy chain)	97.1% (29.5 kDA light chain, 54.7 kDa heavy chain)

5.4.2 Immunofluorescent labelling of TalPER cerebral ganglia

T. saltator brains were treated with the anti-TalPER antibody to identify putative central circadian pacemaker cells. To test if the TalPER antibody does not target other structures than PER, a preabsorbtion control was performed. The results is seen in Figure 5.2 A. Staining is absent in the brains were the antibody was preabsorbed with the peptide it was directed against. When brains were treated with antibody TalPER #714 alone, two cells in each hemisphere of the PCRM were visible (Figure 5.2 C).

To test whether TalPER levels and thus staining intensity changes over the 24 hr daily cycle, brains harvested at four different time points and then stained with the TalPER #714 antibody (Figure 5.2 B-H). At least two cells are visible in each hemisphere of the PCRM. Staining appears more intensive in structures seemingly resembling nuclei, but it rarely co-localised with DAPI (Figure 5.2 F & G). Well stained axons project posteriorly towards the deutocerebrum (Figure 4.2 B & C). In some brains, one single cell was stained in the anterior PCRM (not shown). This staining did not occur in all preparations. The two cells in the central PCRM and the one in the anterior PCRM could not be seen on the same transversal plane. A schematic overview of the staining is shown in Figure 5.3.

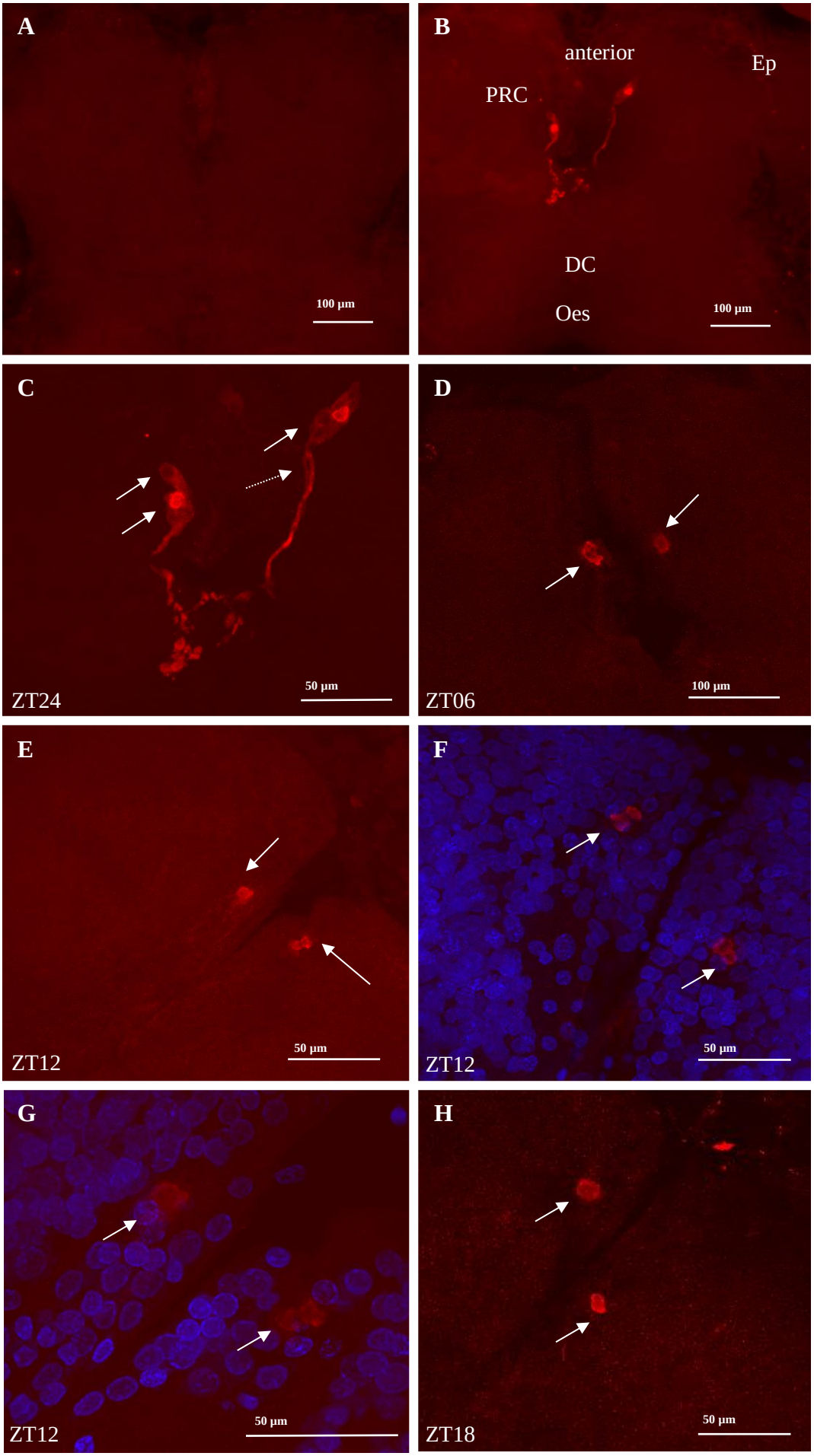
A
100 µm
B
anterior
Ep
PRC
DC
Oes
100 µm
C
ZT24
50 µm
D
ZT06
100 µm
E
ZT12
50 µm
F
ZT12
50 µm
G
ZT12
50 µm
H
ZT18
50 µm

Figure 5.2: Representative images of TalPER positive neurons in the *T. saltator* brain (red), nuclear DAPI staining=blue; White arrows indicate PER positive somata (A) Preabsorption control, overview over cerebral ganglia, 20x magnification (B) ZT24/0, overview without eye pedicles, at least two cells (white arrow) including axons (see dashed arrow) are visible, 20x magnification (C) ZT24/0, 40.0x magnification (D) ZT6 (E) ZT12 40.0x magnification (F) ZT12 40.0x magnification with DAPI (G) ZT12 with DAPI, 63.0x magnification (H) ZT18, 40.0x magnification. PCRM=Protocerebrum, De=Deutocerebrum, Oe=Oesophageal orifice, Ep=Eye pedicule.

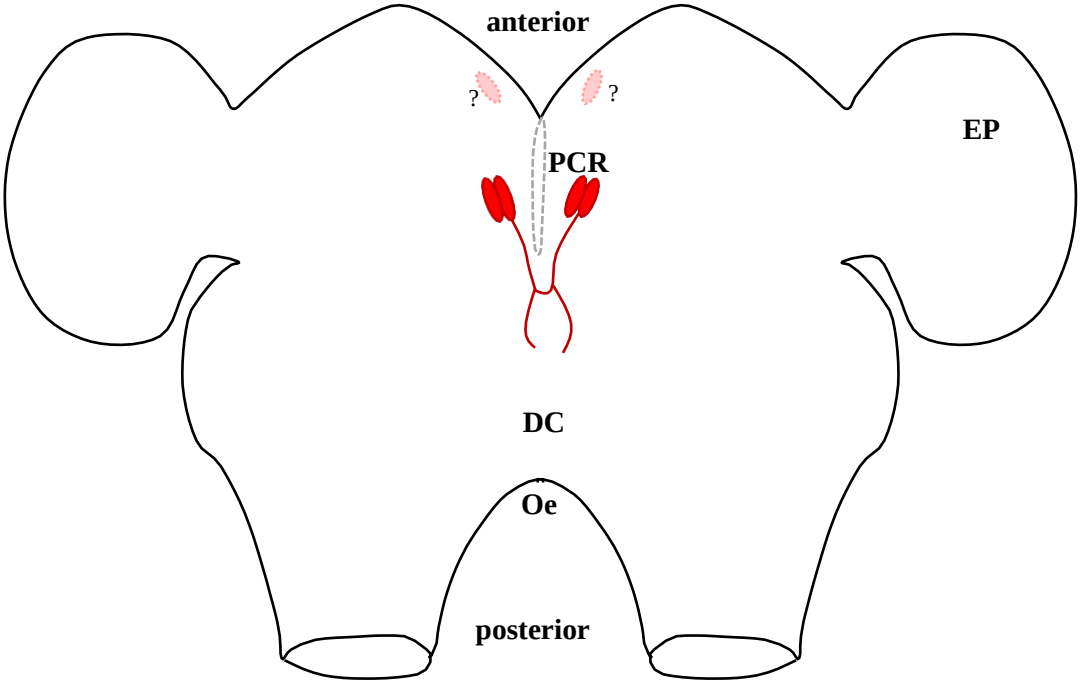

Figure 5.3: Schematic drawing of TalPER positive neurons in *T. saltator* cerebral ganglia. A group of at least two cells with axons in each hemisphere of the PCRM was stained (red). In some cases, an additional staining was visible in the anterior PCRM (rose). PCRM=Protocerebrum, EP=Eye pedicle, DC=Deutocerebrum, Oe=Oesophagus.

5.4.3 Diurnal rhythm of TalPER immunoreactivity

The staining intensity of TalPER positive neurons was analysed throughout the day at ZT0, ZT6, ZT12 and ZT18. The average CTCF (±*SEM)* is depicted in Figure 5.4. One-way ANOVA reported a dependence of the staining intensity on the time of the day ($F_{3,18}=3.1599$; $p<0.05$).

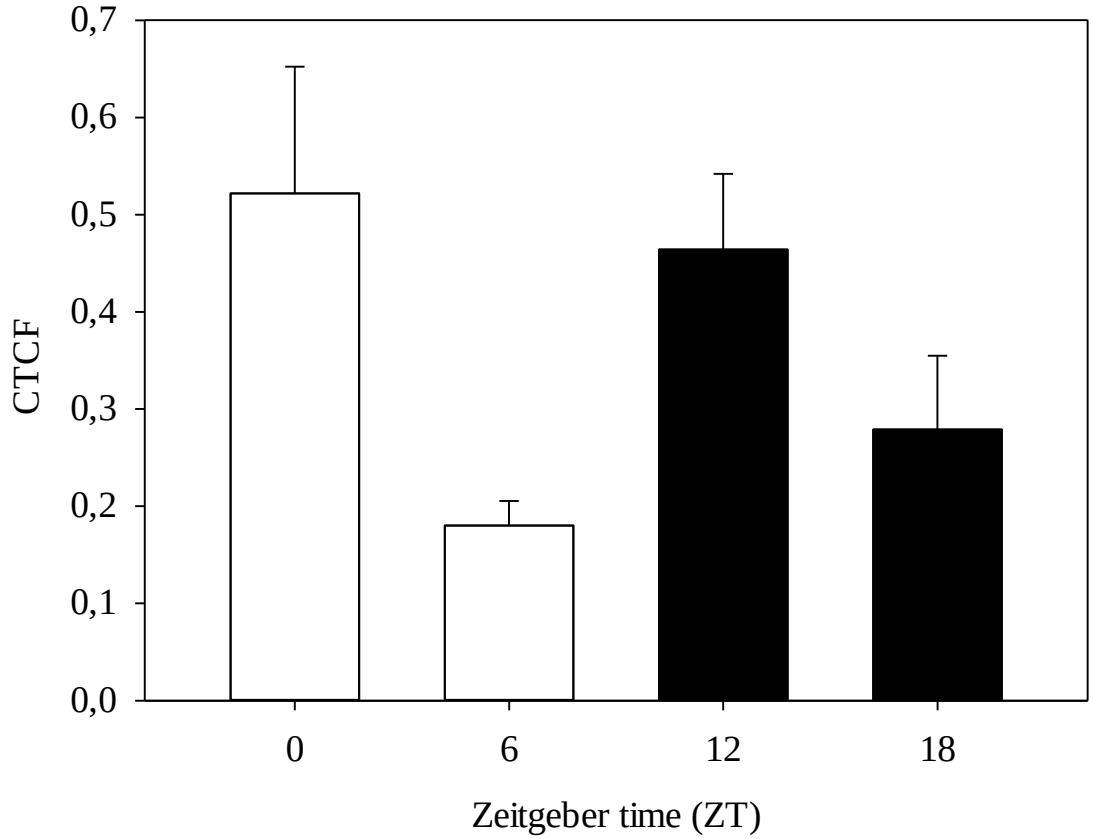

Figure 5.4: Analysis of diurnal TalPER staining intensity in cerebral ganglia. The staining intensity (CTCF±SEM) significantly depended on the time of the day with $F_{3,18}=3.1599$; $p<0.05$; ZT12 and ZT6 n=6, ZT0 and ZT18 n=5, respectively. The colour of the bars indicates brain samples taken during the dark phase (black) or day phase (white).

5.5 DISCUSSION

5.5.1 TalPER immunohistochemical staining of cerebral ganglia

Period, as the most promising clock gene to indicate circadian pacemaker neurons, was chosen to be further investigated. Polyclonal peptide antibodies were produced in rabbits and subsequently tested on whole mount immunohistological preparations of *T. saltator* brains. A preabsorption control indicated that the antibody did not bind to unspecific structures but did target TalPER protein. One of the antisera were found to be sufficient for further staining. It indicated at least two cells in close proximity to the midline with neurons projecting into the posterior PRC. In some brains one single cell was stained in the anterior PRC, even closer to the midline. This staining did not occur in all preparations and was not very well visible. This should

be investigated further. The two cells in the central PCRM and the one in the anterior PCRM could not be seen on the same transversal plane. It is suggested that, with other preparations methods (wax embedding, cryo-sectioning) transverse sections could be produced and cells made visible via Diaminobenzidine (DAB)-staining to locate the correct position and identity of all PER positive cells. The only similarity when compared to other animals is that in *E. pulchra* three cells are also PER positive (Zhang *et al.*, 2013). Position and projections do not compare to other images found in the literature. It has to be noted that the results shown here are very preliminary and it is maybe too early for a comparative analysis. Intracellular localisation of the staining appears mainly nuclear, but when images are overlaid with DAPI nuclear staining, this appears to accumulate in cytoplasmic structures. Further staining with more samples is necessary to clarify the PER subcellular localisation.

5.5.2 Diurnal rhythms of *Period* transcript and protein abundance

The staining intensity of the whole cell area differed significantly over the diurnal cycle. Even though the mRNA levels were determined in constant conditions and the PER staining intensity in 12:12 LD, with the mRNA analysis in chapter 3 and 4, a diagram with PER protein and mRNA expression levels was developed. The highest mRNA expression level was found between CT15 and CT21 (Figure 5.5), and is followed by a peak protein level at ZT24/0 which compares well to data from *Drosophila*, where the protein amount peaks 5 hrs after the expression levels (Zwiebel *et al.*, 1991). This comparison is done out of curiosity, and the TalPER accumulation in the sandhopper brain needs further research and results confirmation with alternative methods such as Western blot, before conclusions can be drawn and published under peer review.

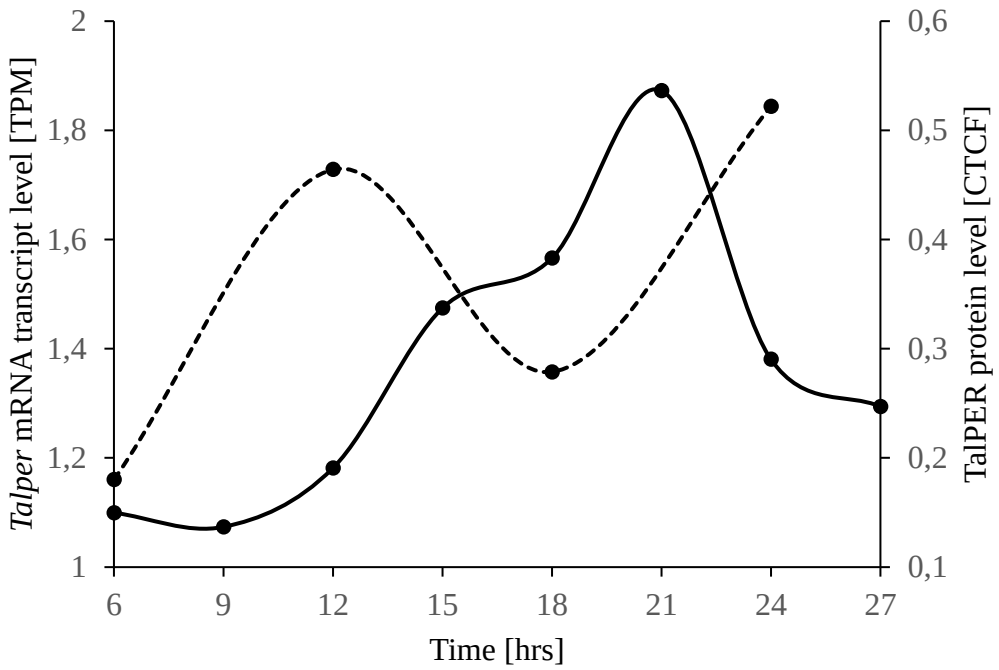

Figure 5.5*:* Period mRNA and protein levels in *T. saltator* brains. The mRNA expression levels are shown in the continuous line and the TalPER protein abundance as a striped line. The peak mRNA expression is followed by a peak in protein level about 5 hrs.

Staining intensity is only one indication for a rhythm in protein abundance. This finding should be confirmed via Western blot or ELISA. Preliminary experiments with both antisera (TalPER #713 and #714), could not confirm a suitability for Western blotting however. When compared to IHC with CHH antibodies, PER positive cells lay more ventral than CHH positive neurons and did not co-localise. Similar, when compared to PDH immunoreactivity (O'Grady, 2013), identified cells did not co- localise. In *Drosophila*, most of the circadian pacemaker cells co-express PER and PDF (Helfrich-Förster, 2003). This could be a hint for a differently constructed system to generate circadian locomotor activity in both animals and the role of PER and PDH/PDF therein. As soon as IHC is completely developed for brains, an antennal staining of *T. saltator* should be attempted. This could give insight into the potential moon compass clock of *T. saltator* (see chapter 4). Immunostaining with *E. superba* CRY2 antibodies should equally be driven forwards. Staining with two animals using the same protocol as for TalPER, showed immunoreactive cells in the posterior deutocerebrum. More specimens are necessary to confirm the results and identify the exact locations of the corresponding cells. In the future, antisera for

the other clock genes should be developed and tested using the protocols outlined here.

An alternative way to identify clock neurons would be *in situ* hybridisation with cRNA probes. In contrast to CHH (chapter 6) however, preliminary experiments were unsuccessful probably due to the low amount of transcript in the brain. A similarly unsuccessful approach was found for *E. pulchra* (pers. comm Dr Wilcockson).

5.6 SUMMARY

Polyclonal antibodies were developed against two different TalPER peptide sequences. In whole mount immunostainings of cerebral ganglia, one of the antibodies showed at least four immunoreactive cells in the PCRM of *T. saltator*. The overall staining intensity differed along the diurnal cycle with the strongest staining at ZT0/24. These results should be confirmed by alternative methods and further IHC analysis has to be conducted with more antisera. Co-localisation studies should be performed with antisera against other clock genes such as CRY2, TIM or CLK to confirm the identities of the found cells as circadian clock neurons. Nevertheless, a promising start was made to identify the central pacemaker in the *T. saltator* brain.

CHAPTER 6: CHARACTERISATION AND TEMPORAL EXPRESSION OF CRUSTACEAN HYPERGLYCAEMIC HORMONE

6.1 ABSTRACT

It is well established that rhythmically reoccurring behaviour such as periods of locomotor activity are clock controlled (Bregazzi and Naylor, 1972). Accordingly, provision of free glucose in the haemolymph anticipating the high metabolic demands during activity periods should be advantageous. Thus, blood glucose levels also have been thought to be under circadian control in crustaceans. The neurohormone, crustacean hyperglycaemic hormone (CHH) influences the abundance of free glucose in the haemolymph (Abramowitz *et al*., 1944) and its cyclic expression and or release into circulation, at least in diurnal species, has been hypothesised to be governed by the circadian clock (Kallen *et al*., 1988; Kallen *et al*., 1990; Nelson-Mora *et al.*, 2013). Consequently, the aim of this chapter was to fully sequence the *T. saltator chh* transcript, analyse its expression pattern and localise the corresponding protein in the brain to elucidate implications of the *T. saltator* circadian clock control in hormone physiology. Data presented here is published in Hoelters *et al*., 2016.

6.2 INTRODUCTION

6.2.1 Crustacean hyperglycaemic hormone

In 1944, Abramowitz and colleagues reported the occurrence of a diabetogenic factor in the eyestalks of the sand fiddler crab *U. pugilator*. When aqueous extracts of eyestalks were injected into the circulatory system of crabs an increased blood sugar level was noted (Abramowitz *et al*., 1944). This hyperglycaemia-inducing biological factor in the eyestalk was later called crustacean hyperglycaemic hormone. We now know that much of crustacean physiology is linked with neuropeptide control. One of the major groups of neuropeptides in crustaceans are members of the so called chh-superfamily which contains 80 family members from 40 different species (Webster, Keller and Dircksen, 2012; Watling and Thiel, 2013). Even though, first described in crustaceans (Abramowitz *et al*., 1944) CHH have evolved across the phylum of ecdysozoans (Laverdure *et al.*, 1994; Stockmann *et al*., 1997; Dai *et al*.,

2007; Drexler *et al.*, 2007; Christie, 2008; Dircksen *et al.*, 2008, 2011; Begum *et al.*, 2009; Montagné *et al.*, 2010; Christie *et al.*, 2011). CHH-family peptides are subdivided into two classes, type I and type II. CHH and ion transport peptides (ITPs) are type I class peptides and moult- inhibiting hormone (MIH), vitellogenesis inhibiting hormone (VIH), gonad-inhibiting hormone (GIH) and mandibular organ-inhibiting hormone (MOIH) belong to the second class (Lacombe *et al.*, 1999). In malacostran crustaceans the major site of CHH synthesis is the so-called X-organ (XO) (Watling and Thiel, 2013), located in the medulla terminals of the eyestalk (hence, MTXO). Axonal endings emanating from the XO form the sinus gland (SG) from where CHH is released by exocytosis. Outside the XO-SG complex, CHH is expressed in the pericardial organ (Keller *et al.*, 1985; Dircksen *et al.*, 2001; Chung and Zmora, 2008) and in paraneurons of the gut during premoult (Chung *et al.*, 1999; Webster *et al.*, 2000). CHH has also been described in retinal cells (Escamilla-Chimal *et al.*, 2001), the lateral and ventral nerve cord (Chang *et al.*, 1999) and cerebral ganglia (Nelson-Mora *et al.*, 2013).

6.2.2 Characteristics of the CHH transcript and protein sequences

The conserved CHH transcript core sequence is an about 40 amino acid long stretch containing most of the here listed features (Lacombe *et al.*, 1999; Chen *et al.*, 2005; Drexler *et al.*, 2007). Different CHH peptides can be made from the same gene by alternative splicing (Dircksen *et al.*, 2001) and post-translational isomerisation (Soyez *et al.*, 1994; Yasuda *et al.*, 1994; Bulau *et al.*, 2003; Bulau, 2004). The CHH mRNA and preprohormone is N-terminally flanked by a characteristic *CHH precursor related peptide* (CPRP) and separated from the mature CHH by a dibasic cleavage site (Webster *et al.*, 2012). The CPRP is co-released into the haemolymph in a stoichiometric fashion with CHH but its biological function is so far unclear (Wilcockson *et al.*, 2002).

The typical size for a type I CHH peptide is 72 aa in length (Edomi *et al.*, 2002; Nagaraju, 2011) and it invariably contains 6 cysteine (Cys) residues which allow the formation of three disulphide bonds in the resulting peptide secondary structure (Kegel *et al.*, 1989, 1991; Yasuda *et al.*, 1994; King *et al.*, 1999; Dircksen *et al.*, 2001). The peptide is C-terminally amidated which is thought to increase its bioactivity by making

it recalcitrant to degradation (Escamilla-Chimal *et al.*, 2001; Mosco *et al.*, 2008). Another common feature is a post-translational modification of the N-terminal glutamate to pyro-Glu which also seems to protect the active peptide from degradation (Chung and Webster, 1996; Chen *et al.*, 2004; Dircksen, 2009). The stereoisomer of the amino acid at position two or three which is most commonly phenylalanine (Phe) or tyrosine (Tyr) is important for biological activity (Gu, Yu and Chan, 2000; Katayama *et al.*, 2003; Katayama and Nagasawa, 2004; Zhao *et al.*, 2005; Mosco *et al.*, 2008). Regarding the hyperglycaemia-inducing effect the two enantiomers L-and D-Phe^3 CHH differ in *H. americanus* (Soyez *et al.*, 1994). The D-Phe^3 CHH stereoisomer also seems to be better protected from aminopeptidase degradation.

6.2.3 CHH release and receptor mechanism

Electron microscopic studies in crayfish identified serotonergic inputs into the MTOX (Scharrer *et al.*, 1991). The release of the CHH neuropeptide from the SG is stimulated by serotonin (5-HT) (Keller and Beyer, 1968; Lee *et al.*, 2000; Lee *et al.*, 2001; Santos *et al.*, 2001; Escamilla-Chimal *et al.*, 2002; Lorenzon *et al.*, 2005). In accordance with these findings the 5-HT reuptake inhibitor, fluoxetine provokes hyperglycaemia and elevated CHH titres in haemolymph (Santos *et al.*, 2001). In contrast, contradictory results have been found regarding the role of dopamine in CHH and the issue still needs further clarification through experiments (Sarojini *et al.*, 1995; Zou *et al.*, 2003). Enkephalins on the other hand inhibit CHH release (Rothe *et al.*, 1991). Activity provokes CHH release from the SG (Santos and Keller, 1993) but has also been measured in response to thermal, hypoxic, toxic and parasitic stress (Webster, 1996; Lorenzon *et al.*, 1997; Chang *et al.*, 1998; Kuo and Yang, 1999; Stentiford *et al.*, 2000; Stentiford *et al.*, 2001, 2002; Zou *et al.*, 2003; Chung and Webster, 2005; Chung and Zmora, 2008).

A receptor for CHH has not been sequenced to date but experiments using ^{125}I- labelled CHH, indicate specific and saturable binding sites in some tissues (Y-organ, hepatopancreas, gut, heart, gills and skeletal muscles) and specific CHH receptors have been hypothesised for many species including *Orconectes limosus* (Kummer and Keller, 1993), *C. maenas* (Kummer and Keller, 1993; Webster,

1993; Chung and Webster, 2006) and *C. sapidus* (Katayama and Chung, 2009). In *O. limosus,* the administration of CHH elevated the cGMP content in several tissues and this effect was observed to be time and dose dependent (Sedlmeier and Keller, 1981; Goy *et al.*, 1987; Goy, 1990; Chung and Webster, 2006). In *H. americanus* membrane preparations, CHH increases guanylyl cyclase activity and CHH effects are positively modulated by phosphodiesterase inhibitors. Thus, evidence suggests that CHH signalling is effected via a membrane bound guanylyl cyclase receptor (Sedlmeier and Keller, 1981).

6.2.4 CHH physiological effects

CHH induced hyperglycaemia typically occurs within about 15 min following CHH release and lasts for 1-3 hrs before returning to basal levels. However, since it's defining role of blood sugar elevation was discovered (Abramowitz *et al.*, 1944), CHH has been shown to exert many other physiological effects, some of which are site and tissue specific (Sedlmeier and Keller, 1981; Leuven *et al.*, 1982; Webster, 1993). The tissue specific effect of CHH in *O. limosus* can be observed in cyclic nucleotide levels. In the antennal gland and integumentary tissue, peak levels appear after 2 minutes post CHH injection while in heart and hepatopancreas it peaks after 5 min and even later in abdominal muscles (Sedlmeier and Keller, 1981). With regards to hyperglycaemia, the effect of CHH (or eyestalk extracts) differs between species. Interspecies studies showed that eyestalk extracts of *O. limosus* had limited and varied effects on elevating *Cancer pagurus, C. maenas, H. gammarus, N. norvegicus* blood glucose levels whereas the extracts of *O. limosus* and *Astacus leptodactylus* were interchangeable (Keller, 1969). Many of the physiological effects of CHH are linked to energy metabolism; e.g., CHH can facilitate the release of amylase in the midgut and an increase of free fatty acids and phospholipids (Sedlmeier, 1988; Santos *et al.*, 1997). Research of Sedlmeier and colleagues on the crayfish *O. limosus* shed light on the mechanism behind the hyperglycaemic effects of CHH by demonstrating that it can inhibit action of glycogen synthase and trigger phosphorylase activation. In both cases, a breakup of glycogen into free glucose is fostered and thus elevated blood glucose occurs (Sedlmeier and Keller, 1981; Sedlmeier, 1985, 1987). Reciprocally, administration of glucose has CHH inhibitory effects (Santos and Keller, 1993; Chung and Webster, 2005) suggesting a putative

feedback response. Further, CHH has been reported to be in involved in branchial ion transport, salt balance, osmoregulation as well as gamete maturation as well as inhibiting ecdysteroid synthesis form the y-organ (Eckhardt *et al.*, 1995; Coast, 1998; Chung, Dircksen and Webster, 1999; Spanings-Pierrot *et al.*, 2000; Serrano *et al.*, 2003; H.K. Tiu, He and Chan, 2007).

6.2.5 CHH as a circadian clock controlled gene?

It has been discovered that the *chh* mRNA levels oscillate with a circadian rhythm in *Procambarus clarkii* brains (Nelson-Mora *et al.*, 2013). Under LD, haemolymph CHH levels cycle daily with blood sugar levels rising at the beginning of the dark phase in *O. limosus* and *A. leptodactylus* (Kallen *et al.*, 1988; Kallen *et al.*, 1990). Under LD conditions, the nocturnally active *A. leptodactylus* and *O. limosus*, increased levels of CHH and subsequent hyperglycaemia were observed at the beginning of the dark phase (Gorgels-Kallen and Voorter, 1985; Kallen and Abrahamse, 1989; Kallen *et al.*, 1990). Cyclic hyperglycaemia mirrors elevated CHH titres in the haemolymph (Kallen *et al.*, 1990) resulting from synthesis, transport and release of CHH form the SGs 2 hrs in advance of the activity phase (Gorgels-Kallen and Voorter, 1985; Kallen *et al.*, 1990). The endogenous rhythmic hyperglycaemia was observed to be light entrainable in *A. leptodactylus* (Kallen *et al.*, 1988). In *U. pugilator*, Melatonin injections shifts cycling of haemolymph glucose (Tilden *et al.*, 2001). Other evidence for an implication of the circadian system in CHH production and release mechanisms stem from *P. clarkii* where *chh* transcripts in entrained animals (both LD and DD) follow circadian rhythm in abundance in the brain and optic lobe. Further, brain regions known to express canonical clock genes also exhibit immunostaining for CHH (Escamilla-Chimal *et al.*, 2010; Nelson-Mora *et al.*, 2013). CHH immune-positive cells were also reported in developing retinal cells of juvenile *P. clarkii* (Escamilla- Chimal *et al.*, 2001). The mentioned retinal cells exhibit daily rhythms in CHH immunoreactivity (Escamilla-Chimal *et al.*, 2001). The retinal cells which secrete CHH (about 25%) respond to the 5-HT concentration and the secretion dynamics seems to be modulated by neighbouring retinal tapetal cells (Escamilla-Chimal *et al.*, 2002). All these studies direct to the hypothesis that there is a connection between the circadian core oscillator and the pleiotropic neurohormone CHH.

6.2.6 Objective

The supralittoral amphipod *T. saltator* exhibits diurnal locomotor activity rhythms. This behaviour is under clock control to meet increased metabolic demands during phases of higher activity. We hypothesise that CHH levels show increase in anticipation of locomotor activity resulting in elevated haemolymph glucose to satisfy the need for more energy. Taken together, the literature provides a strong base indicative of links between the circadian pacemaker system and CHH signalling specifically. The objectives of the current work were the characterization the *Talchh* transcript sequence as a basis for further work. Also, the localisation of the mature peptide in the brain was to be achieved. Finally, the transcription dynamics of behaviourally rhythmic animals were studied in the brain. The *Talchh* mRNA transcript cycling in abundance over the 24 hrs of the day would be a strong indication for an implication of the circadian clock in neurohormonal control of the *T. saltator* physiology.

6.3 MATERIALS AND METHODS

As a putative clock controlled gene, the *Talchh* transcript was characterized. The corresponding expression rhythm in the brain over a period of 24 hrs was determined. The *Talchh* mRNA was localised in the brain using *in situ* hybridization and the TalCHH protein was localized in the brain via immunohistochemical staining with an anti-CHH antibody. If not stated otherwise explicitly, when using kits all experiments were carried out according to manufacturer's instructions.

6.3.1 Animal behaviour

To test if the experimental subjects were behaviourally rhythmic a subgroup of 35 animals was analysed for their locomotor activity rhythm prior to tissue collection as described in 2.2.

6.3.2 Obtaining *T. saltator* neural RNA

To be able to analyse the *Talchh* expression throughout the circadian cycle,

brain tissue was harvested over a 24 hr period. Animals were kept in DD for 24 hrs prior to tissue collection and then quickly decapitated and the heads flash frozen in liquid N_2. Tissues from 5 animals were pooled into one sample to obtain sufficient amounts of RNA for downstream applications (see sampling scheme in 3.21). Total RNA was extracted with Trizol® (Qiagen) according to proprietary instruction except that two ethanol washes were performed to ensure all traces of phenol were removed. Contaminating DNA was subsequently removed with 2U Turbo™ DNAse (Thermo Fisher Scientific). Sample quantity was determined with a Nanodrop ND2000 (Thermo Fisher Scientific).

6.3.3 *Talchh* full length sequencing

Sequence mining of the *Talitrus* transcriptome (see chapter 3 (O'Grady *et al.,* 2016) revealed a putative *Talchh* contig (comp96958_c1_seq1) which was annotated through Blast2GO as *crustacean hyperglycaemic hormone* (NCBI GenBank accession number KP898735). To confirm the assembled sequence identity and determine the full length cDNA we adopted a RACE-PCR strategy, using the putative *Talchh* against which to design primers. Template RNA was reverse transcribed using SuperScript™ III reverse transcriptase (Thermo Fisher Scientific) with 500 ng total RNA and using random hexamer primers. For the initial sequence confirmation a PCR was run using the GSPs Talchh F' and Talchh R' and AmpliTaq Gold™ 360 Master Mix (Thermo Fisher Scientific). All primer and probe nucleotide sequences used in this chapter are displayed in Table A.6 of the Appendix A and the PCR cycling conditions are described in 2.5. Resulting amplicons were separated on a 1.5% w/v agarose gel bands of expected size were excised and cleaned using Isolate II PCR and Gel kit (Bioline Reagents). The cleaned PCR fragments were cloned into pCR™4 vector (Thermo Fisher Scientific) and sequenced as described in 2.8.

To determine the 5' and 3' UTRs of the CHH transcript, RACE PCR was performed as described in the general methods section 2.7. All PCRs were done using AmpliTaq Gold™ 360 Master Mix and the oligonucleotide primer for 3' and 5' RACE PCRs can be found in Table A.6 of the Appendix A.

For the 3' RACE, an initial PCR was followed by two nested PCRs. For the

first round PCR, high quality template cDNA (general methods 2.4) was used with the GSP Talchh 3'RACE and the GeneRacer 3' Kit primer. The resulting PCR fragments served as template material for the second round PCR. Nested primers were used (GSP Talchh 3' RACE N1 and the GeneRacer 3' N primer). In the same fashion, the third PCR was conducted with Talchh 3' RACE N2 as a forward and GeneRacer 3' N as a reverse primer and template form the second round PCR but with 30 PCR cycles run to insure sequence integrity. Resulting amplicons were checked on an agarose gel, bands of expected size cut out, cleaned with the Isolate II PCR and Gel kit (Bioline Reagents) and cloned and sequenced as described in 2.8.

A similar approach was used for the 5' RACE PCR with the difference that specific 5'RACE mRNA was produced. A known priming site was introduced into the sequence through the ligation of an RNA oligonucleotide to the 5' end of decapped mRNA. First strand synthesis was performed with the GenRacer™ Oligo kit(Thermo Fisher Scientific). The cDNA for 5'RACE was provided by Dr. Wilcockson. A first round PCR using the GeneRacer 5' primer and the reverse Talchh 5' RACE primer was followed by a second round PCR using a nested reverse GSP (Talchh 5' RACE N) and the GeneRacer 5' primer as well as first round PCR as starting material for the reaction. Resulting amplicons were separated on an agarose gel, bands of the expected size were cut out and cleaned and sequences as described above.

SignalP 4.1 was used to determine putative signal peptides *in-silico* (Petersen *et al.*, 2011).

6.3.4 Quantification of *Talchh* mRNA transcripts

The expression of *Talchh* mRNA throughout the circadian cycle was analysed using qRT-PCR using TaqMan®MGB hydrolysis probes (Thermo Fisher Scientific) (as described in 2.11, Figure 4.2). Six biological replicates were measured for each sampling time point. Each of the six biological replicates was measured twice.

The qRT-PCR probe and primers were designed against the sequenced CHH transcript (GenBank accession number KP898735). *T. saltator arginine kinase* (*Talak)* was used as an internal reference and for *Talak* primers and probes were established by O'Grady (2013). Primer and probe sequences can be found in Table

A.6. PCR efficiencies were established using serial dilutions of each standard and corresponding graphs are displayed in Figures A.5 and A.6 of Appendix A.

6.3.5 Histological description of *Talchh* transcripts though *in situ* hybridization

The mRNA of *Talchh* was localised in the brain using Digoxygenin (DIG) labelled sense and antisense cRNA probes. These were synthesised by *in-vitro* transcription using PCR templates containing T7-phage promotor start sites. PCR templates were generated using AmpliTaq Gold™ 360 (Thermo Fisher Scientific) with the primers Talchh DIG F' and Talchh DIG T7 R' and Talchh DIG T7 F' and Talchh DIG R', respectively (oligonucleotide primer sequences can be found in Table A.6). Cycling conditions and reaction setup are described in 2.5. Amplicons were checked on a 1.5% w/v agarose gel and cleaned (Isolate II PCR and Gel kit, Bioline Reagents). The products were used as template for the transcription reaction using the MEGAshortcript™ kit (Thermo Fisher Scientific). Diverging from the manufacturer's instructions slightly, 0.7 µL of UTP were supplemented with 10 mM digoxygenin-11-UTP (Sigma-Aldrich). Residual template DNA was removed with the TURBO DNA-free™ kit (Thermo Fisher Scientific) and the DIG-labelled cRNA probes were quickly denatured at 95°C for 3 min and stored at -80°C over night. Next, the probes were extracted with Trizol® and quantified via Nanodrop ND2000 (Thermo Fisher Scientific).

To test the successful DIG-incorporation into the cRNA a dot blot was performed, where 1 µL of sense and antisense probe (including a number of 10-fold serial dilutions and a water control) were dotted on a nylon membrane (Hybond-N, GB Healthcare) and crosslinked on a UV table for 1 min at the maximum power. The membrane was washed in PBST 2 times for 5 min and then blocked with 2% w/v milk powder in 50 mM TBS for 30 min (see Appendix B for recipe). Subsequently, the membrane was incubated in α-digoxygenin-alkaline phosphatase fab fragments at 1:5000 dilution (Sigma-Aldrich) in TBS supplemented with 2% milk powder at room temperature for 30 min. Following incubation, the membrane was the washed 3 times for 10 min in PBST and 2 min in TNMT buffer. Visualisation was accomplished through incubation with 5 mL 4-nitroblue tetrazolium chloride/5-bromo-4-chloro-3-indolyl-phosphate (NBT/BCIP) solution (Sigma-Aldrich) made in

2% w/v in TNMT, in the dark until no further colour development was seen. The membrane was washed to terminate the reaction, 2 times for 5 min in PBST and documented using a digital camera.

To obtain brains for the *in-situ* hybridization experiment, animals were decapitated and brains quickly dissected in ice-cold physiological saline and fixed in 4% PFA (in 0.1M PBS) overnight. The samples were then dehydrated through a series of 30 min washes with 33%, 66% and 100% methanol and then stored in 100% methanol for 1 day at 4 C°. Subsequently, the brains were rehydrated through 10 min incubations in 33%, 66% and 100% PBST/methanol and then incubated with 200 µg/mL proteinase K in (Roche, Switzerland) for 2 min. The brains were then washed 2 times for 1 min in PBST and then 3 times for 5 min in PBST. A post fixation with 4% PFA was conducted for 30 min and the brains were washed again 3x10 min each in PBST. The tissue was pre-hybridized in 100 µL *in situ* hybridization solution (DakoCytomation) for 30 min at 50°C. The probe was denatured at 95°C for 5 min at a 1 µg/mL dilution in fresh hybridization solution (100µL volume per sample) and chilled on ice. Hybridization was performed at 50°C for 16 hrs. Following hybridization, tissues were washed 2 times with 2x SSC/50% formamide for 10 min at 50°C, then 2 times for 10 min in SSC (0.2x) at 50°C. These were followed by further washes at room temperature with 33%, 66% and 100% PBST in SSC (0.2x) for 5 min each. To minimize background staining, residual single stranded RNA was removed through treatment with ribonuclease A (Sigma-Aldrich). For this, samples were first washed 3 times for 10 min with TNE buffer and incubated in 20 µg/mL RNase A for 15 min. To avoid non-specific binding tissues were blocked with 1% w/v BSA (Sigma-Aldrich) in PBST for 90 min followed by an incubation with 1:2000 α-digoxygenin-alkaline phosphatase, fab fragments (Sigma-Aldrich) in blocking buffer (0.1x) overnight at room temperature. Tissues were then washed 6 times for 5 mins in PBST, 2 times for 10 min, 2 times for15 min, 2 times for 30 min and finally for 1 hr. The samples were first washed with TNMT for 10 min, equilibrated in TMN and developed in 0.2% NBT/BCIP w/v solution (Roche Holding AG) in TMN in the dark with regular microscopic examination until developed. Finally, the tissues were washed with water to stop the reaction. The brains were mounted in 50% v/v glycerol in PBS and imaged using a Leitz Dialux light microscope (Leitz) and imaged on a digital camera. Images were adjusted for size, cropping and contrast with Adobe

Photoshop CS6 (Adobe Systems Incorporated).

6.3.6 Immunolocalisation of CHH

The CHH peptides were visualised in whole mount immunohistochemical preparations of *T. saltator* brains. Brains were dissected in ice cold physiological saline and fixed at 4°C overnight in Stefanini's fixative (Stefanini *et al*., 1967). Following fixation, the tissue was washed with PTX 3 times for 10 min then 2 times for 30 min and finally for 2 hrs. Tissues were then incubated with anti- *C. maenas* CHH IgG 25 µg/µL made in rabbit (kindly supplied by Simon Webster (Chung and Webster, 2004)) at 1:5000 dilution in PTX over night at 4°C. The following day, brains were washed in PTX 3 times for 10 min and then 3 times for 30 min prior to incubation in secondary antibody, goat anti-rabbit Alexa Flour 488 or Alexa Flour 568, (Thermo Fisher Scientific) diluted 1:500 in PTX and incubation over night at 4°C. Subsequently, brains were washed extensively with PTX and mounted on glass slides in Vectashield mounting medium (Vector Laboratories Inc., Burlingame, CA, UK). Immunolabelling was visualised on a Leica TCS SP5 II confocal microscope using HCX PL APO CS 0.70 IMM UV (20.0x) and a HCX PL APO lambda blue 1.25 OIL UV (40.0x) objectives. Z-stack images of 15-25 optical sections were obtained at 1-2 µm intervals and images were analysed with the software suite Leica LAS AF Lite 2.6.3 (Leica Microsystems) and were edited for cropping, resizing and brightness/contrast with Adobe Photoshop CS6 (Adobe Systems Incorporated).

6.4 RESULTS

As a putative clock controlled gene and thus direct clock output, *Talchh* was analysed in *T. saltator* brains. The transcript was characterised vis sequencing and localised in the brain through in- situ hybridization. The expression rhythm of *Talchh* in the brain was researched though qRT-PCR. Further, the corresponding protein was localised in the brain through immunohistochemical staining.

6.4.1 CHH transcript characterization

The putative CHH sequence derived from previous work (O'Grady 2013) was confirmed by RT-PCR and RACE amplification of 3' and 5' termini. The sequenced cDNA comprised 1132 bp (NCBI GenBank accession number KP898735) and is schematically displayed in Figure 6.1. The *T. saltator* CHH sequence contains a 404 bp open reading frame (ORF) which encodes a preprohormone with a deduced 75 aa CHH mature peptide, N-terminally flanked by a 24 aa signal peptide (determined by SignalP 4.1 (Petersen *et al.*, 2011)) and a 56 aa CHH precursor related peptide (CPRP). The CPRP and mature CHH are departed by a typical dibasic cleavage site (KR). At its C-terminal end, the mature CHH exhibits an amidation signal (GKK). The amino acid sequence is shown in Figure 6.2 with the peptide sequence shown in capital letters. The *Talchh* sequence exhibits 64% sequence identity with the *E. pulcha Epchh* transcript sequence (Hoelters *et al.*, 2016).

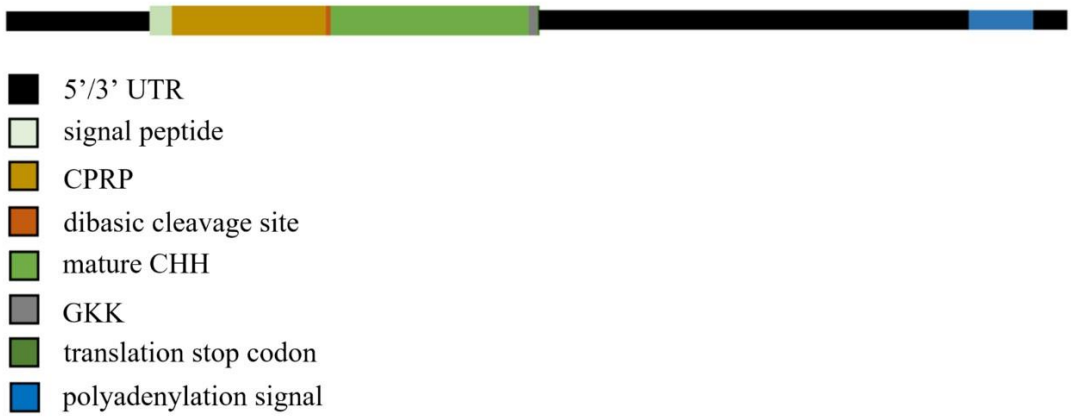

Figure 6.1: Schematic depiction of the *T. saltator* CHH mRNA transcript. Functional sequences such as the coding regions for the CPRP and the sequence coding for the mature CHH are colour coded. The nucleotide and CHH preprohormone amino acid sequence is displayed in Figure 6.2.

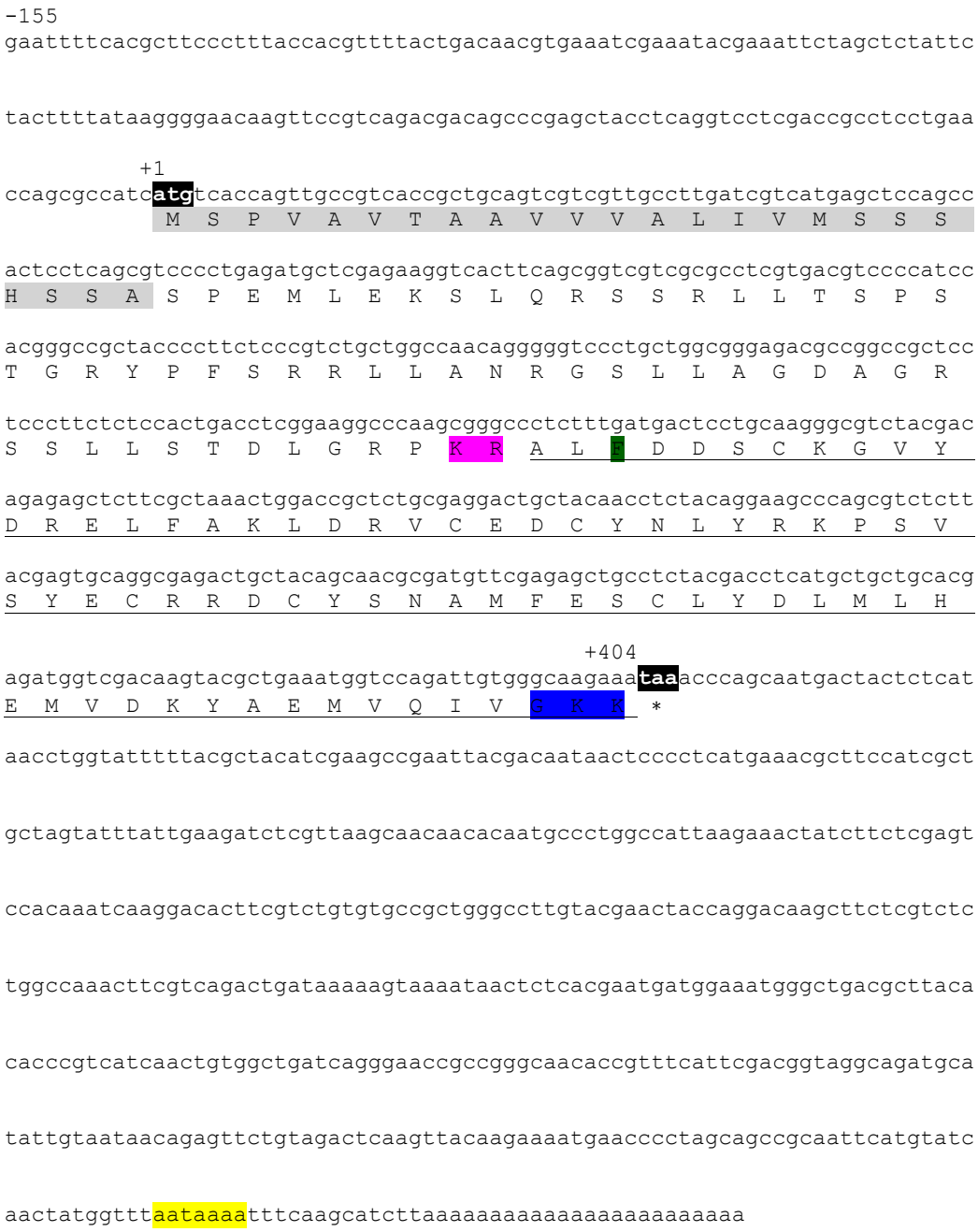

Figure 6.2: *T. saltator* CHH cDNA sequence. Nucleotide sequence is shown in lower-case letters. The sequence is shown from the 5' UTR -155 nucleotides from the translation start site (+1). Start (atg) and stop codons (taa, +404) are marked in black boxes. The polyadenylation signal is marked in yellow. The deduced amino acid sequence is shown in capital letters and the putative signal peptide is shown in grey. The mature CHH sequence is underlined with the amidation signal (GKK) and its end and the dibasic cleavage site (KR) are marked in blue and pink, respectively. The phenylalanine (F) at position three is marked in green.

6.4.2 Locomotor activity analysis

Animals used for the experiments were tested for behavioural rhythmicity in a setup detailed in 2.2. Animals showed clear, endogenously driven nocturnal activity when held in DD with peak locomotor activity observed during the subjective night (CT17-18) with a period of 24.18 hrs (±0.3 SEM, n=7; Figure 6.3).

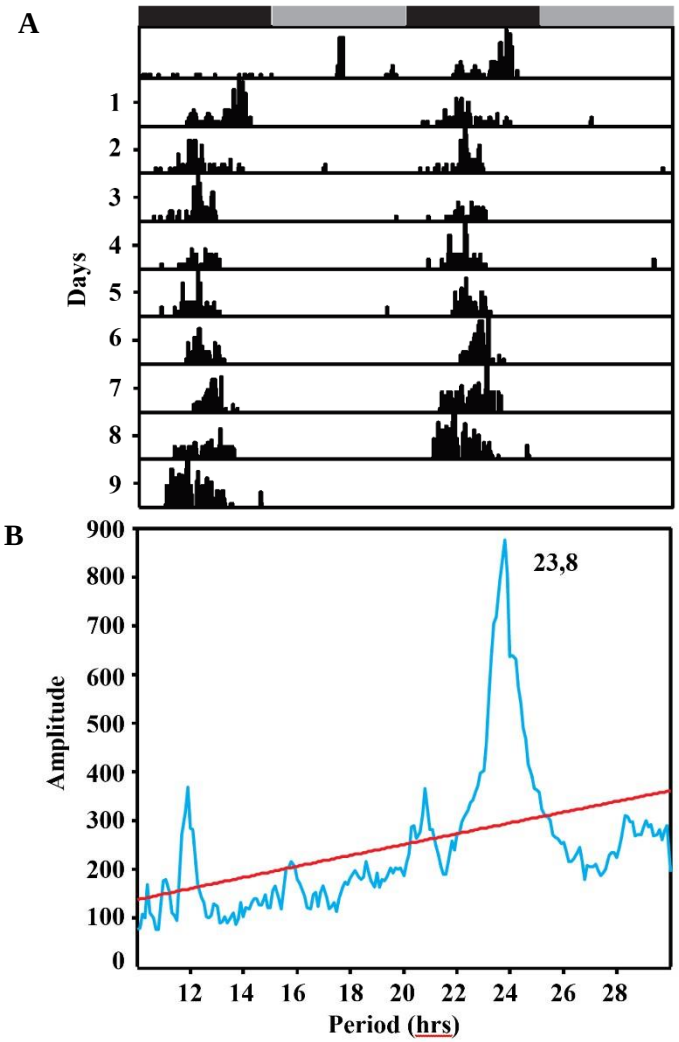

Figure 6.3: *T. saltator* activity rhythms in DD. (A) Actogram representing the free running locomotor activity of 5 animals. The black and grey bars above indicate the respective day and night periods. (B) Activity data was analysed to reveal an activity period of tau=23.8 hrs and resulting chi-squared periodogram is shown.

6.4.3 Temporal expression of neural CHH mRNA

The *Talchh* mRNA expression rhythm over 24 hrs were analysed using qRT-PCR. Animals used were dropped into DD 24 hrs prior to the experiment. When a

subsample of these animals (n=6) were assayed for changes in CHH transcript abundance, no significant changes throughout the 24 hr period sampled were recorded (Figure 6.4., ANOVA, $F_{8,53}$=0.72; p=0.67).

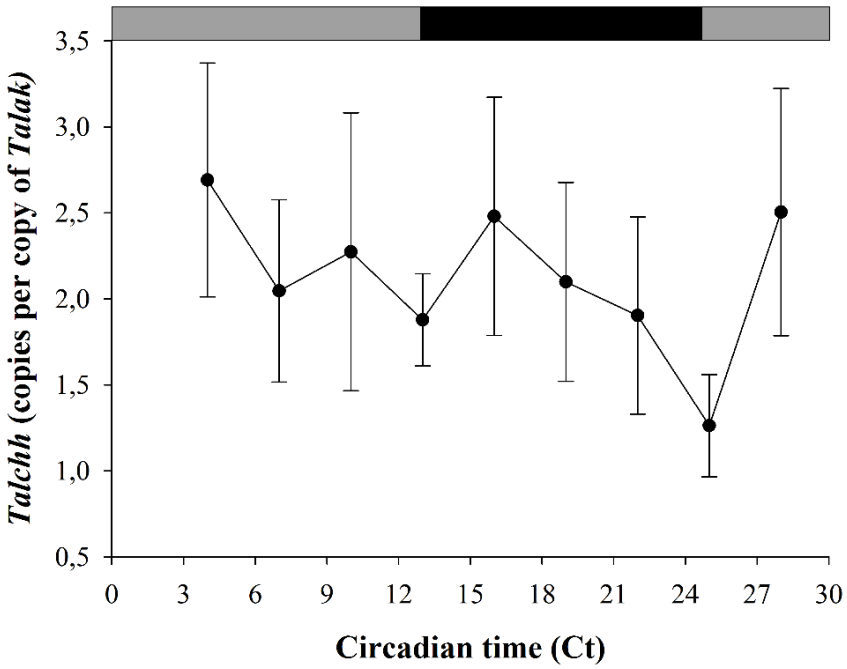

Figure 6.4: CHH transcript abundance in the brain quantified with qRT-PCR (n=6, measured in triplets, with 5 heads pooled for each biological replicate). Grey and black bars indicate the subjective day and subjective night time points, respectively. Animals were kept in constant darkness (DD) 24 hrs prior to tissue collection. Expression values are shown as copies per copy of internal reference gene (*Talak*) (±SEM). One-way ANOVA did not reveal any dependence of the *Talchh* expression level on the time of the subjective day $F_{8,53}$=0.72; p=0.67.

6.4.4 Histological description of CHH mRNA and protein

The CHH peptide was visualised in the brain by whole mount immunofluorescent labelling using a highly specific and high affinity antiserum (Chung and Webster, 2004). Two cell groups were stained in each hemisphere of the anterior margin of the PCR. Each group contained 6 distinct cell bodies, three large ones (35 µm +- 4 µm) and three small cells (23µm +- 4 µm, white arrowheads in Figure 6.5 A-D) all projecting axons form a primary axonal tract. A close-up view image of the 6 perikaria can be seen in Figure 6.5 C and D (40.0x magnification) where the cytoplasmic staining appears granular. Axons emanating from these cells

unite to form one axonal tract that runs to the posterior PCR where it bifurcates and one branch is directed laterally, to the optic lobe and end to form the SG. Axonal endings making up the SG appear bulbar. The other axonal branch travels posteriorly through the deutocerebrum and into the tritrocerebrum where it appears to terminate in very fine dendritic fields adjacent to the margins of the oesophageal foramen (marked with an asterisk in Figure 6.5 A, B, E).

The CHH mRNA transcript localisation was examined through *in situ* hybridisation. Hybridization with antisense probes confirmed the result of the antibody staining by revealing two groups (large and small) containing three cells each in each hemisphere of the anterior PRC. Each group contained three cells each with three larger cells closer to the midline and three smaller cells positioned lateral to the midline group of larger cells with the same size proportions as seen in the confocal images (Figure 6.5 G). The incubation with sense probes did not shown any specific staining (images not presented), thus confirming the specificity of the observed hybridisation patterns.

Figure 6.5: Immunolocalisation of the CHH peptide in *T. saltator* cerebral ganglia. (A-F). Whole mount confocal laser microscopic images of anti-CHH immunorpositive neurons. (B), (D), (F) Alexafluor 488 coupled 2^{ry} antibody; (A), (C), (E)=Alexafluor 568 coupled 2^{ry} antibody. (A) & (B) Overview of the whole mount preparations. Two groups of cells in the anterior PCR each containing three cells (triangles). Axons stemming from the cell groups join to form an axonal tract (white arrow) that bifurcates (dashed circle) and one of the branches travels toward the optic lobe (filled arrowhead) and ends to form the SG. The other branch of axonal tract travels posteriorly to end in the tritrocerebrum in fine branches (dashed arrow & asterisk).(C) & (D) Two groups of cells in the anterior PCR. (F) Sinus gland, bulbar structures are clearly visible. (F) Whole-mount CHH in situ hybridisation. Two groups of cells in each hemisphere of the PCR are clearly visible and they can be distinguished by size and shape (large cell group -red arrows with white filling, small cell group- red arrow heads). Oe=esophargal orifice, SG=sinus gland, PCR=protocerebrum.

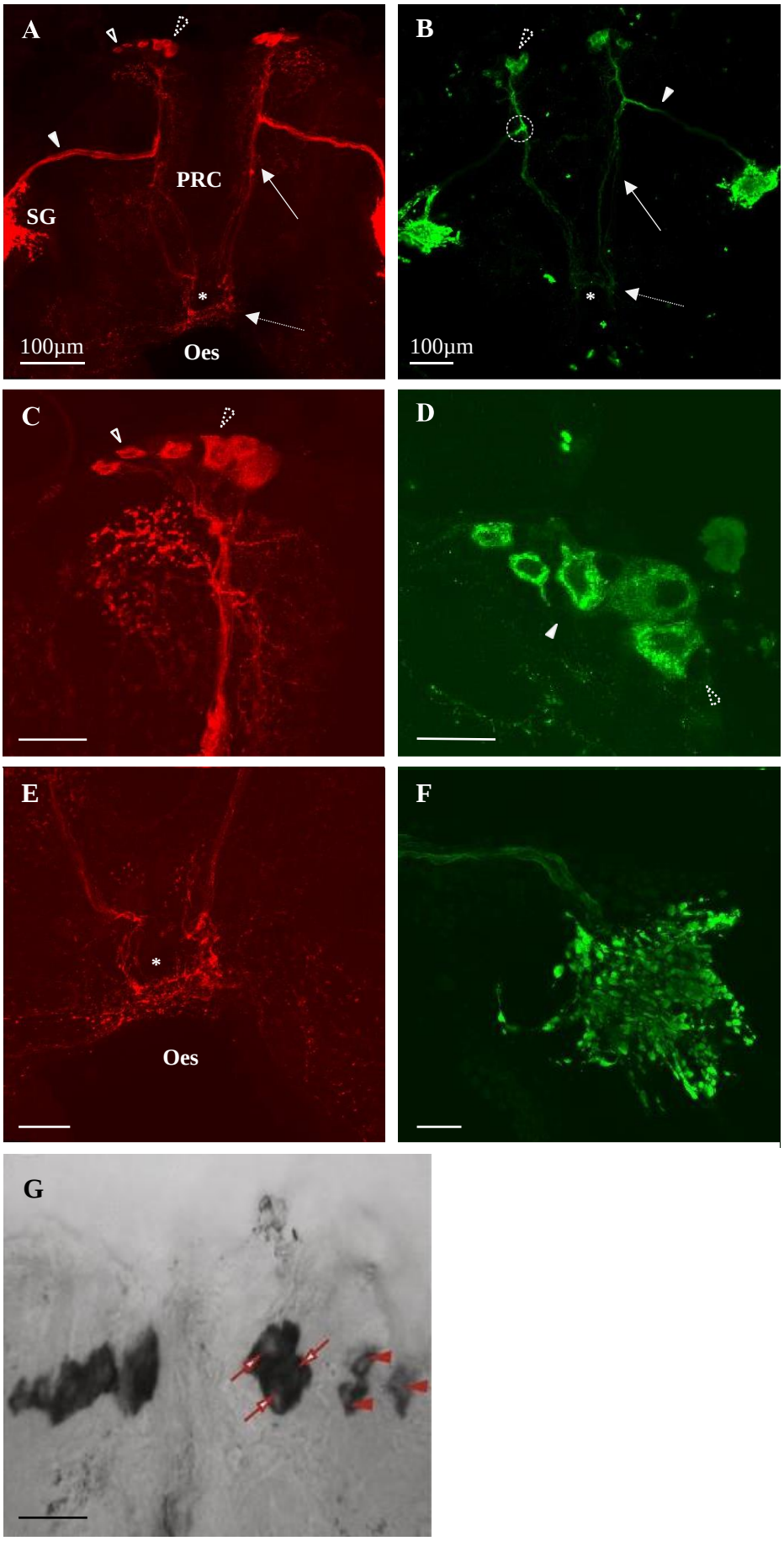
A
PRC
SG
*
100µm
Oes
B
*
100µm
C
D
E
*
Oes
F
G

6.5 DISCUSSION

6.5.1 CHH transcript sequencing

The sequencing work revealed one single transcript comprising all characteristic features of a type I CHH, compared to for example *C. maenas* and *O. limulus* CHH sequences (Kegel *et al.*, 1989, 1991; Webster *et al.*, 2012). An alignment of the mature CHH peptide sequences of *T. saltator* and *E. pulchra* is shown below in Figure 6.6. A phylogenetic tree showing the relation of several CHH peptide sequences is shown in Figure 6.7 below. It graphically represents the evolutionally similarity of the sequences.

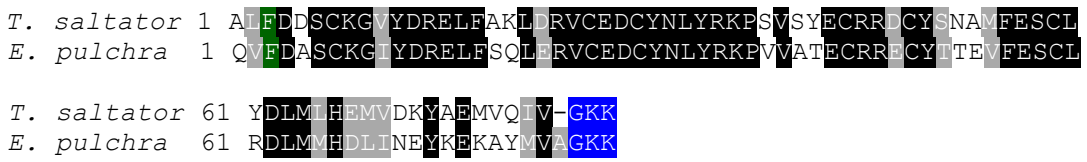

Figure 6.6: Alignment of mature CHH peptide sequences of *T. saltator* and *E. pulchra* (NCBI Accession number: JF927891). Black boxes mark matching aa and grey boxes indicate similar amino acids. The phenylalanine at position three, which is probably subject to stereoisomerization, is marked in green and the amidation signal at the end of the sequence is marked in blue.

The cDNA comprises a 404 bp spanning open reading frame (ORF) including coding for a 24 amino acid long signal peptide and a 75 amino acid CHH propeptide. The translated sequence contains the characteristic 6 Cys residues predicted to form disulphide bridges at positions 7 and 43, 23 and 39 and 26 and 52. At the N-terminal flank of the CHH lies a 56 amino acid long sequence, separated from the main CHH by a dibasic cleavage site. This flanking peptide is most likely a CPRP. The biological function of CPRPs is so far unclear. It is hypothesised however, that the TalCHH preprohormone is a zymogen, which is activated among cleavage at the dibasic cleavage site by a specific enzyme. In that fashion, large quantities of preprohormone could be synthesised and activated at once. The CPRPs' main function would be to render the effective CHH inactive until need (Foster *et al.*, 1990; Rholam and Fahy, 2009). Analysis of the sites and patterns of CPRP release in the edible crab *C. pagurus* revealed that the CPRP peptide circulates in the haemolymph and released simultaneously with CHH from the SG (Wilcockson *et al.*, 2002).

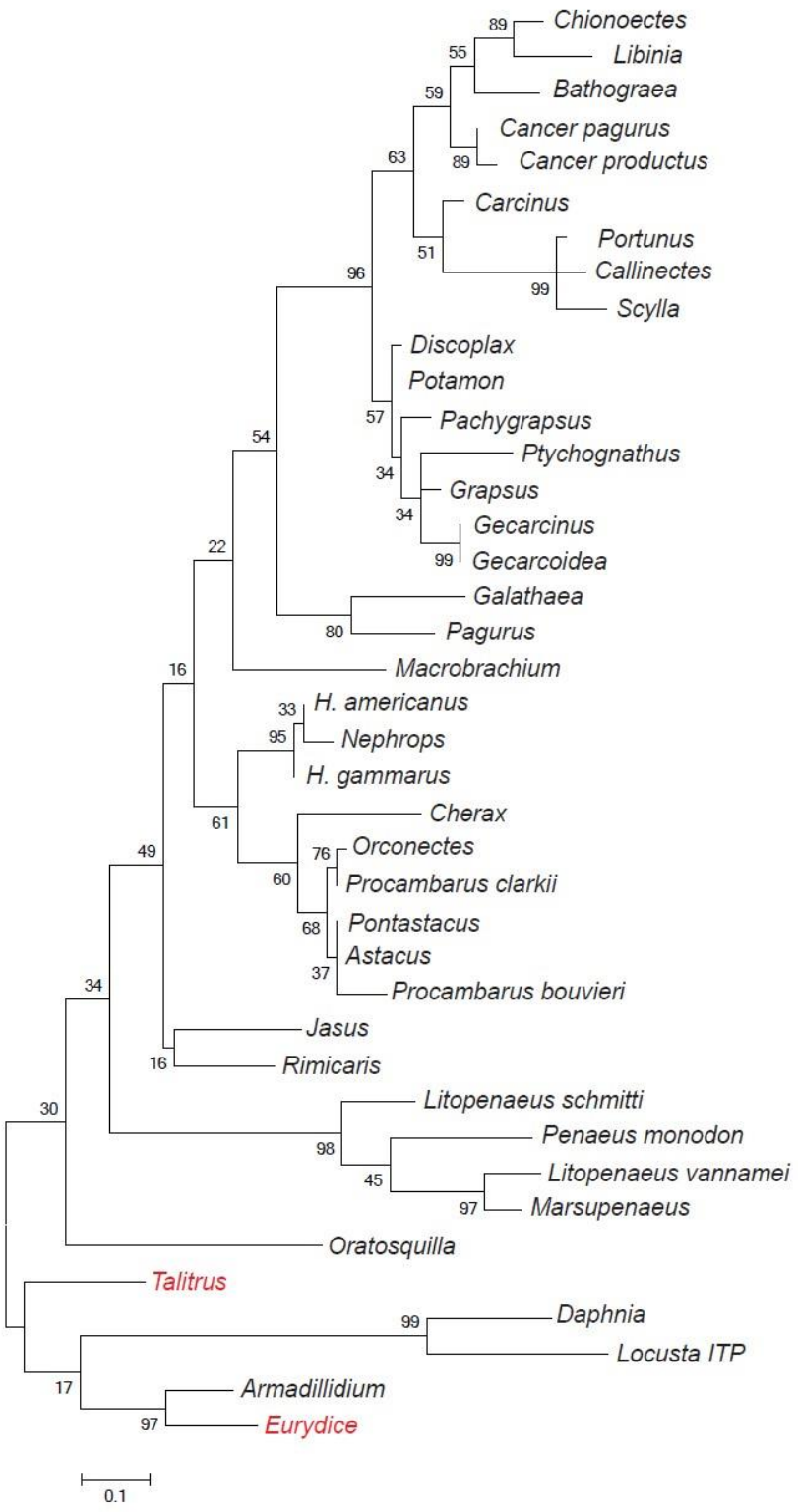

Figure 6.7: Phylogenetic analysis of CHH sequences (accession numbers used are available in Hoelters et al., 2016). The Maximum Likelihood Method with 1000 bootstrap replications was used to deduce the relation of the CHH sequences. The branches signify bootstrap support values. Image composed by Dr O'Grady.

A phenylalanine is coded at amino acid position three of the mature *T. saltator* CHH peptide. In CHHs from other species this amino acid residue usually undergoes post-translational stereoisomierisation (Soyez *et al.*, 1994, 1998, 2000; Yasuda *et al.*, 1994). Both isoforms differ in biological activity with the D-Phe³ CHH isomer showing prolonged biological activity (Gallois *et al.*, 2003). Furthermore, stereoisomer-specific antibodies have been observed to label distinct cell types in the XO-SG-complex. The cells seem to be harbouring one or both isomers of CHH and VIH (for which similar stereoisomers have been observed), can be epimer specific (Ollivaux *et al.*, 2009). Even though more research needs to be conducted, results so far suggest the potential for different functions of the two forms or an alternative mechanism for protein regulation. Indeed, it has been shown. in *A. leptodactylus* only the D-Phe³-CHH evokes increased osmolality in the haemolymph (Serrano *et al.*, 2003) and has stronger effects on glucose levels and gene expression in hepatopancreas cells after injection (Manfrin *et al.*, 2013). In *P. clarkii* both L and D isoforms have been shown to have distinct functionality with the D-form having a stronger hyperglycaemic effect and the L-form rather repressing ecdysteroid synthesis (Yasuda *et al.*, 1994). Against this background and given the inclusion of the Phe^3 residue in it's deduced sequence, it is possible, that the *T. saltator* CHH could equally undergo post-translational stereoisomierisation and warrants further investigation. This could be investigated via immunohistochemical studies with epimer specific antisera as done by Ollivaux *et al.*, (2009).

6.5.2 CHH immunoreactivity in cerebral ganglia

Labelling of whole mount brain preparations using a highly specific anti-*C. maenas* IgG revealed cell groups with each 6 cells project axons from the anterior PCR towards the caudally situated tritocerebrum proximal to the oesophageal foramen. Here, they end in a finely structured net. After one third of the way the axons bifurcate and travel to the optic lobes to from the sinus glands with their axonal endings. This neuroarchitecture is strikingly similar to that identified in the peracaridean isopod *E. pulchra* (Hoelters *et al.*, 2016) although in *E. pulchra* the distinct cell groups with different sized cells were not identified. Staining in the PCR of a group of cells and intense labelling of the SG has also been demonstrated in the

terrestrial isopods *Armadillidium vulgare* (Azzouna *et al.*, 2003), *Porcellio dilatatus* (Martin, Jaros, *et al.*, 1984), *Oniscus asellus* (Nussbaum and Dircksen, 1995). It has to be mentioned, that the crustaceans mentioned do not possess protruding eyes in eyestalks. In crustacean species having ommatophore eyestalks the neurosecretory XO-SG system resides in the eyestalk with the XO in the proximoventral side of the medulla terminalis and the SG in the connection of the medulla interna and the medulla externa (Bliss, 1982; Hartenstein, 2006). In the immunofluorescent CHH staining in *E. pulchra* or *T. saltator* the perikaria of the neurosecretory cells are located in the PCR which is likely the ancestral morphology.

The protocerebral neurosecretory cells seen in the terrestrial isopods were subgrouped in to β-cells (subgroups β1 and β2), B-cells and γ-cells by Martin in 1988 based on a terminology introduced by Matsumoto in 1959. Antisera raised against crude extracts of *C. maenas* SGs are known to label so-called ß1-cells in the woodlouse *P. dilatatus* (Martin, Keller, *et al.*, 1984) whilst *A. vulgare* CHH positive cells neurons also resemble characteristics of β-cells (Azzouna *et al.*, 2003) and *O. asellus* CHH staining reveal neurons classified as ß1-cells (Nussbaum and Dircksen, 1995). In addition to ß1-cells, ß2- cells were found in the sea slater *Ligia oceanica* (Martin *et al*., 1983). The protocerebral CHH immune-positive cells found in *T. saltator* form two size groups harbouring three cells each (large and small). The cells that were observed to be "large" (35µM ± 4µM) exhibit features of ß1- and ß2-cells. Their polygonal appearance is a feature of ß1-cells and their spherical nuclei would be typical for ß2-cells. The smaller cells (23µM ± 4µM) similarly resemble characteristics of both of ß1- and ß2-cells. According to Martin (1988), ß1-cells exhibit nuclei which appear ovoid in shape. This feature can be observed in our preparations for the small cells equally. Nevertheless, they also show a feature of ß2-cells as the soma are observed to be tear shaped. It should be remembered, however, that these observations and comparisons could also be artefacts of the preparation protocols. Further staining and a comparison with other preparation methods would be necessary to clarify this issue. Considering functionality of the two cell groups, it has been hypothesised that the different groups of cells described above are responsible for processing and release of the different Phe^3-stereorisomers of CHH (Ollivaux *et al.*, 2009). Given that the stereoisomierisation also occurs in *T. saltator* it could be possible that either of the groups of cells is specific for one of the CHH

stereoisomers. To test that hypothesis a similar approach as to Ollivaux and colleagues could be followed. CHH-Phe^3 isomer- specific antisera could help to answer the question if the CHH expressing cells identified here, harbour specific isomers. Additionally immunogold-electron microscopy could be used to conduct a localisation study of the two epimers in the axonal endings of the SG. Confocal microscopic studies in *P. clarkii* revealed CHH positive staining in the same areas where canonical clock proteins were reported which suggests a close relationship between in the two protein systems (Nelson-Mora *et al.*, 2013). In *T. saltator*, the neural staining of clock proteins other than PER still has to be carried out to uncover a potential similarity with the *P. clarkii* brain. The PER positive cells in *T. saltator* are much closer to the midline and situated rather caudally when compared to the CHH immune-positive cells shown in this chapter (preliminary experiments). So a co-localisation of PER and CHH or a very close proximity of cells expressing both is excluded. It yet has to be uncovered where other canonical clock genes such as TIM, CRY2 and BMAL1 are expressed in the *T. saltator* brain. Again, in *P.clarkii*; developing retinal cells show a rhythm in CHH immunostaining which follows the time of the day. Even though, the animals were not held in constant conditions but in 12:12 LD, this supports the hypothesis that CHH is regulated in a circadian manner (Escamilla-Chimal, Van Herp and Fanjul-Moles, 2001). To follow this study up in *T. saltator*, a simple time series of CHH brain staining could be conducted. Naturally, the whole 24 hr day should be covered and subjects held under constant conditions.

6.5.3 Temporal expression of CHH mRNA in the brain

CHH is rhythmically transcribed in extracts of the optic lobe and central brain of *P. clarkii* (Nelson-Mora *et al.*, 2013). In *A. leptordactylus* the CHH expression has been shown to follow cyclic release dynamics (Gorgels-Kallen and Voorter, 1985). The CHH releasing cells are thought to receive a stimulus 2 hrs before the onset of the dark phase, upon which CHH is transported into axons. At the beginning of the dark phase the CHH peptide is released into the haemolymph (Gorgels-Kallen and Voorter, 1985). In *O. limosus* blood glucose and CHH levels follow a circadian rhythm and raise with the onset of darkness (Kallen *et al*., 1990).

It was aimed to explore the expression dynamic of CHH mRNA in *T. saltator*

because it has very robust circadian activity patterns. We hypothesised that *chh* mRNA should show corresponding cycles of expression to meet the metabolic demands of episodic activity. However, the CHH mRNA transcription levels in behaviourally rhythmic *T. saltator* do not change with the time of the subjective day as determined by qRT-PCR. This finding resonates with that shown in the circatidal isopod of *E. pulchra* (Hoelters *et al.*, 2016). Whilst it is acknowledged, that pooled head tissue samples were used in these studies, other transcript levels have been shown to change with the circadian cycle, including canonical clock genes *Talper and Taltim*. Thus, there is confidence in the results to be accurately displaying the CHH mRNA expression. Nevertheless, whilst CHH is not rhythmically transcribed, it does not preclude the cyclic translation of post-translational process or release as has been demonstrated for the migratory locust *Locusta migratoria*, where synthesis and release of adipokinetic hormone (AKH) seem to be uncoupled (Harthoorn *et al.*, 2001).

Taking into account that TalCHH could also be a zymogen it is unsurprising that the mRNA is not expressed in a rhythmic fashion. Here, the rhythmic activity of the enzyme processing the preprohormone at the dibasic cleavage site would be the key factor for a circadian activity of the mature CHH protein in *T. saltator*. To analyse this further, a Western blot using the CmCHH antibody introduced in this chapter would result in a larger band representing the preprohormone and a smaller band showing the mature CHH. The abundance of both bands over a 24 hr cycle should be examined and if done with tissue of animals kept in DD would be a clear indication for a circadian regulation of CHH on a protein level.

In a similar fashion, it is thought that only freshly synthesised CHH peptide is released from the SG (Chung and Webster, 2004). Thus, it is still possible that CHH underlies a circadian regulation, which we could not detect with our methods. To explore this possibility the protein synthesis and the release patterns could be analysed by a fine time series of immunohistological staining as performed for *A. leptodactylus* (Gorgels-Kallen and Voorter, 1985). The size of *T. saltator* and *E. pulchra* make collection and assay of temporally collected blood samples impossible at present.

6.6 SUMMARY

CHH transcript sequence, abundance over the 24 hr cycle and protein localisation in the brain of *T. saltator* was analysed to test whether it functions as a part of the circadian clock machinery output. The complete *chh* transcript of *T. saltator* has been characterised with qRT-PCR and RACE-PCR. The sequence showed all classical features of CHH commonly found in crustaceans. Whole mount immunostaining with a *C. maenas* α-CHH antibody, revealed a staining pattern that agrees, with immunological studies on other peracaridean species. Apart from the classic axon tracts to the sinus gland, labelling revealed an additional descending fibre tract leading caudally and ending close to the esophargal foramen the significance of which is undetermined. The hypothesis that *Talchh* mRNA expression is under cyclic control was explored but no evidence could be seen in robustly rhythmic animals.

CHAPTER 7: GENERAL DISCUSSION

The present work aimed to dissect the biological clock of *T. saltator* on a molecular and behavioural level. Invertebrate chronological research has largely been focused on the model organism *D. melanogaster*. The molecular and cellular structure of the *Drosophila* circadian clock served as a background for this research. The clock components are highly conserved among diverse phylogenetic groups but functional relationships of clock genes can be redundant (Zhu *et al.*, 2008; Beckwith *et al.*, 2011). The study of *T. saltator* circadian machinery is important from a functional and evolutionarily comparative perspective. Besides all advantages of established model systems, recent developments in invertebrate chronobiology have shown its limitations. For example, the *Drosophila* clock gene elements have been researched in great detail, but when compared to other invertebrate clocks they can greatly differ. Such as in the Monarch butterfly, where CRY2 instead of PER is the major keyplayer of the negative feedback loop. This example illustrates the diversity of invertebrate clock systems and shows the necessity of researching other clock systems. Non-model research is under-represented in the literature, but of great interest in the lay public which provides the large quantity of research funding. It is obvious that researchers have to turn to less prominent study subjects to understand the fundamental clock mechanisms behind lunar and or tidal clocks.

7.1 CIRCADIAN CLOCK GENE EXPRESSION IN *T. SALTATOR*

One primary objective of the thesis was the sequence determination and temporal dissection of *T.saltator* circadian clock genes. Cycling clock genes and clock-associated genes were identified in the following way: a circadian transcriptome was generated via RNA-sequencing and identified expression levels of clock and clock–associated genes submitted to JTK_cycle analysis. *Talper, Talbmal1, Talpdh, Talck2ß, Talpp1, Talsgg, Talebony, Talsirt1, Talsirt7* and *Taljetlag* were found to cycle in abundance through the circadian cycle as well an analysis of the transcriptome TPM levels by ANOVA revealed *Talcry2, Talper, Talbmal1, Talck2ß, Talpp1, Talslimb* and *Talsirt1* expression levels to depend on the time of the subjective day. Even tough cycling mRNA transcripts are not a necessary predicament of functioning circadian clocks (Reddy *et al.*, 2006), the data represent a very promising progression

in the analysis of the circadian clock components and their interplay. Cycling clock gene transcripts have been reported in the literature as arguments for clock participation (Kojima *et al.*, 2011). Full length cDNA sequences were generated by RACE PCR or were fully identified though RNA-seq and are now available for *Talcry2, Talper, Talbmal1, Talpdh I&II, talck2α, Talck2ß, Taldbt, Talpdp1ε, Talpp1, Talpp2a-su microtubule star, Talpp2a-su widerborst, Talppp2a-su twins, Talsgg, Talslimb, Talvrille* and *Talrev-erb* and the sequences for the residual genes of interest could be determined by the same methodology.

The overall composition of the transcriptome compares well with data found for other crustaceans. In the *C. finmarchicus* transcriptome, for example, a similar set of clock genes and clock associated genes was identified with *per, tim, cry2* and *clk* as the major core clock genes (Christie *et al.*, 2013, Häfker *et al*., 2017). *Cry1*, which is found in *Danaus* and *Drosophila* is also absent in *Calanus*. CRY1, which in other invertebrates serves as a sensor for light input aiding the resetting of the clock (Koh, Zheng and Sehgal, 2006). This is mediated in *Drosophila* via TIM and JETLAG, which bother were identified for *Talitrus*. It would be intriguing to find out how the *Talitrus* circadiannclock can be entrained by light. A start to this, could be a similarity search with other photolyase/cry blue-light photoreceptor sequences in the *T. saltator* transcriptome. Besides its role as a blue light sensor, CRY1 has been proposed to be magnetoreceptive in *Drosophila* (Gegear *et al.*, 2009). *Talitrus* population located closer to the equator are proposed to utilize the earth magnetic field for orientation (Arendse and Kruyswijk, 1981; Ugolini, 2006). Even though, a *Talcry1* could not be identified in transcriptome and a functioning circadian clock is not necessary for magnetoreception in *Drosophila* this raises the question if an alternative part of the clock is responsible for magnetoreception in *T. saltator*. Earth's magnetic field is known to not only play an important role in long distance migrations of marine animals or birds but also arthropods such as *T. saltator* and the equatorial sandhopper *T. martensii* (Arendse and Kruyswijk, 1981; Ugolini, 2001, 2006). An artificial magnetic field with a shifted north pole can be used for orientation in *T. saltator* (associated with a shift in orientation), whilst animals were unable to orientate in the absence of a magnetic field (Arendse and Kruyswijk, 1981). However, it is not known how *Talitrus* utilize or sense the magnetic field. A sequence similarity search with the transcript sequence motif responsible for magnetoreception of

Drosophila cry1 could be a first start to research this.

Light entrained animals that show robust daily rhythms were dissected and brain and antennae tissue harvested at three-hr intervals. These samples were be used to assess the temporal expression patterns of identified clock genes by qRT-PCR using TaqMan® assays. In the brain, *Talper* and *Taltim* mRNA cycled in abundance over 24 hrs as well as the *Talcry2* levels, which were found to depend on the subjective time of the day. To further this investigation, TaqMan® primers and probes for other clock genes and clock associated genes could be synthesised, now that sufficient transcript sequence data is available.

It was planned to evaluate the differential roles of the clock genes and their interplay by silencing selected clock genes via RNA interference (RNAi) and analysis of the resulting behavioural and molecular phenotypes as described in Zhang *et al.* (2013). dsRNA probes for *Talper* were generated by *in vitro* transcription. Preliminary experiments however showed that the application route (microinjection) for *Talitrus* is not technically mature and needs further development before more trails with RNAi can be accomplished. Then, dsRNAs of target genes including Clock, Cycle and Cry2 could be readily developed and tested.

One could argue, that clock gene mRNA should be attempted to be localised by whole mount *in situ* hybridisation as done for CHH. As in *E. pulchra* the transcript abundance was deemed too low to be detected and trials with *Talitrus* brains were equally unsuccessful.

The transcriptional regulation of clock genes may be investigated in cell culture of *Drosophila* S2 cells that are co-transfected with an E-box-luciferase (E-box-luc) reporter as done for *E. pulchra* (Zhang *et al.*, 2013). The measured promoter activity could tell the time of expression of a certain gene. Deletion of putative functional domains should limit the activation of the reporter and thus could be used to prove the functionality of proposed sequences. Further, a successful rescue of *Drosophila* null mutants of clock genes with *Talitrus* clock sequences could hint to a similar function in *Talitrus*.

As already mentioned, cycling mRNA is not necessary for circadian clocks. For example in the unicellular alga *Ostreococcus,* the oxidation of peroxiredoxin

proteins functions as a sufficient rhythmic biomarker and is also rhythmic in mammals (O'Neill *et al.*, 2011). Similar, in red blood cells which do not contain a nuclear membrane, circadian rhythms are generated by peroxyredoxins which undergo a 24~ hrs redox cycles, which persist under constant conditions, are entrainable and temperature compensated (O'Neill and Reddy, 2011). In *E. pulchra*, the overoxydation of peroxyredoxin exhibits a 12.4 hrs circatidal pattern and not a circadian one but is discussed as following the metabolic cycle of the animal (O'Neill *et al.*, 2015). Recent work by Bodvard and colleagues gave rise to new possibilities in the purpose of peroxyredoxin in biological rhythms. They showed that yeast peroxisomal oxidase converters light into hydrogen peroxide with can be sensed und further transduced by a peroxyredoxin (Bodvard *et al.*, 2017). Authors propose that via this mechanism light could be sensed (and thus used to reset the biological clock) in animals that do not express specific photoreceptors. Given that Blast2GO analysis identified 6 transcripts as peroxydasin homologs, three peroxyredoxins and two peroxyredoxin- like sequences this could be a start to further investigate the role of redox-states as potential light sensors and their possible involvement in the biological clock system of *T. saltator*.

The transcript abundance of four core clock genes were measured with two different methods, RNA-seq and qRT-PCR. *Talper* shows a very similar expression curve in both studies with peak levels during the subjective dark phase. All statistical test applied to the data clearly state that the expression pattern is rhythmic (follows a sinusoidal curve) and depends on the time of the day. With certainty, it can be stated that the *Talper* mRNA is expressed in a circadian manner. *Taltim* was measured to be rhythmically expressed in qRT-PCR data but not in RNA-seq data. *Talclk* levels were neither found to be dependent on the time of day nor does the expression curve fit a sinusoidal shape. Thus, it is concluded that the *Talclk* mRNA expression does not exhibit any rhythmicity. *Talcry2* again, was shown to be expressed higher during the day in both methods and the levels were shown to follow a rhythmicity through the diurnal cycle. It is proposed that the *Talcry2* is also expressed in a circadian manner.

7.2 CLOCK PROTEINS IN *T. SALTATOR*

Another aim of the current work was the localization of the core oscillator cells and confirmation of nucleic acid data on protein levels. Two antisera against TalPER were developed and tested on *T. saltator* whole brains. A specific subgroup of 2 cells was identified expressing this protein, with a higher abundance at ZT0/24 at the onset of the light phase. Additionally, primary experiments were conducted using an α-*E. superba (Es)Cry2* antibody, which identified two cells in the posterior deutocerebrum of the brain (data not shown). This immunohistochemical analysis of the *T. saltator* clock is in its very beginnings and more antisera also for other clock proteins and more experiments with greater numbers of brains are necessary for publishable conclusions. Nevertheless, the preliminary experiments showed, that the immunostaining is a suitable method to research clock protein abundance in the sandhopper brains and can aid to identify putative (central) clock cells governing the circadian rhythms in the animals. Data from all IHC studies in *T. saltator* cerebral ganglia is schematically represented in Figure 7.1. The data about PDHir was taken from O'Gray (2013).

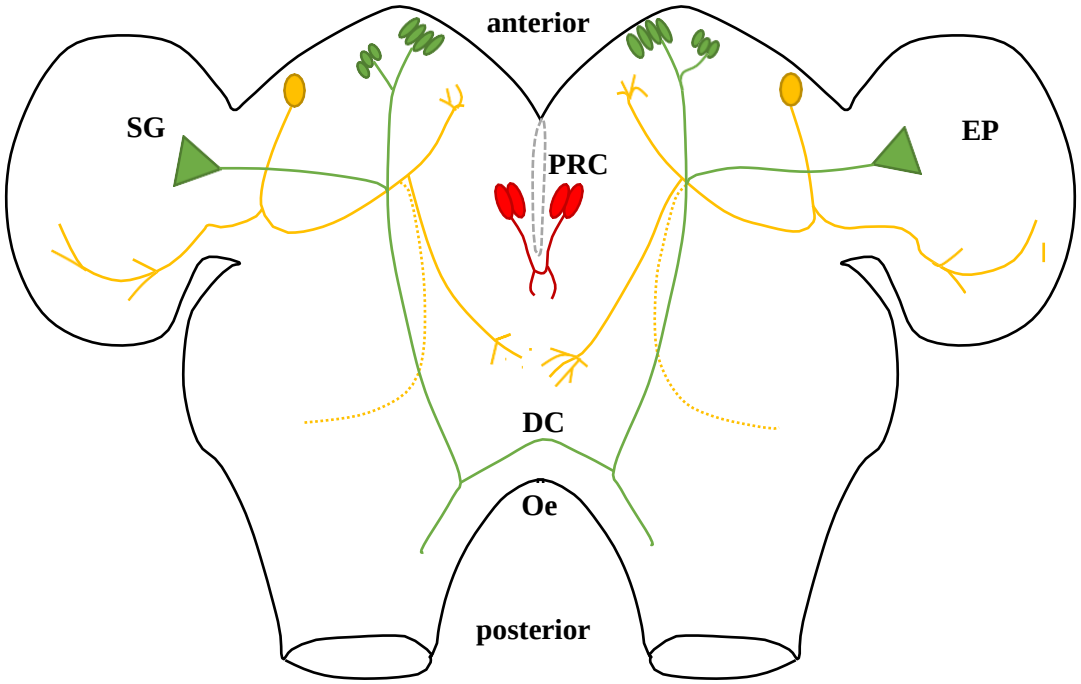

Figure 7.1: Schematic drawing of the *T. saltator* brain. red=TalPER positive neurons, green=CmCHH positive neurons, yellow=TalPDH positive neurons, modified after O'Grady, 2013. SG=sinus gland, EP=eye pedicule, PRC=protocerebrum, DC=deutocerebrum, Oe=Oesophargus.

The mentioned antisera could also be used in Western blots, with brain extracts gathered at different times of the day (or lunar phase) to measure protein amount in the *T. saltator* brain at given times of the cycle.

The target sequences of the core clock genes could be identified with Chromatin ImmunoPrecipitation (ChIP) DNA sequencing, where a DNA region of interest is targeted by a specific antibody against the protein of interest (TalPER, TalCRY2, TalCLK and TalBMAL1/CYCLE). This would be then followed by co-IP and sequencing of the DNA sequence the protein was bound to. When done in a time resolved manner maybe even so far unpredicted promoter sites of clock protein action could be identified (Pett *et al.*, 2016).

7.3 CLOCK CONTROLLED GENES IN *T. SALTATOR*

CHH is rhythmically expressed in other crustaceans (Nelson-Mora et al. 2013) and known for its hyperglycaemic effects (Webster, Keller and Dircksen, 2012), which ties the hormone to energy metabolism which usually anticipates rhythmic environmental changes for optima energyusage. In *T. saltator* however, CHH mRNA does not cycle in abundance within the time of the day. This does not conclude a non-rhythmicity in its functional protein. The *Talchh* transcript sequence contained the majority of CHH motifs including a putative CPRP, which allows the hypothesis that the preprohormone is a zymogen and that putative rhythmic activation is rather regulated on a protein level.

7.4 LOCOMOTOR ACTIVITY RHYTHM

Circadian rhythms are plastic and prone to modulation by abiotic factors enhancing an individual's adaptability to environmental changes. Diel activity rhythms have been analysed in various crustacean species from giant robber crabs *Birgus latro* to diminutive isopods such as *E. pulchra* (Krieger *et al.*, 2012; Naylor, 2013). The sandhoppers used in the present work expressed robust locomotor activity rhythms under constant conditions. This gives confidence that the rhythms were actually generated intrinsically (and not light induced) and thus, true circadian. In LD, activity rhythms did not rely on functional antennae. Further scheduled

manipulations of environmental factors (light/ temperature regimes) combined with molecular approaches such as RNAi knock-down for example will uncover differential roles of clock genes and their interplay in governing rhythmic behaviour.

7.5 CELESTIAL COMPASS NAVIGATION

Sandhoppers express time compensated solar and lunar orientation towards the home beach. The sun compass however, was independent from the animal antenna in contrast to *D. plexxippus*, where antennae harbour a sun compass clock. Evidence was found for an anatomically discrete moon compass in the antennae as animals lacking these lost their competence to orientate at night. This, needs further investigation. A start could be the measurement of clock mRNAs in the antennae through the lunar cycle to identify potentially rhythmic transcripts. Further, moon shift experiments could be conducted as executed by Papi *et al.(*2006) and Meschini *et al*. (2008) and a shift in clock gene expression phase could be a strong indication for an independent oscillator in the organ. It could also be that the overall expression of clock genes in the antennae does not change through the synodical month but effects could be seen in daily changes in the expression rhythm throughout the month. Then, following Merlin *et al.* (2009) antennae could be held in culture and free-running clock gene rhythms could be determined. The problem with this is, that monarch antennae only survive for a limited amount of days and the synodical month is definitely too long for the tissue to survive (Merlin *et al.,* 2009).

Further, it would be interesting to understand how the innate orientation direction of *Talitrus* is coded into its DNA. It is proposed, that the orientation direction is coded via epigenetic mechanism as these provide the necessary scope for plasticity. Very recently, examples for clock genes that modulate chromatin activity and vice versa have achieved prominence in the literature and epigenetic modulation may ensure evolutionary flexibility (Orozco-Solis and Sassone-Corsi, 2014; Masri *et al.,* 2015; Yue *et al.,* 2017; Denhardt, 2018). Circadian clock components directly modify chromatin composition and thereby regulate gene activity of non-clock and clock components (Bellet and Sassone-Corsi, 2010; Ripperger and Merrow, 2011; Li *et al.*, 2012; Pirooznia *et al.*, 2012; Egg *et al.*, 2013; Masri *et al.*, 2013). Nevertheless, epigenetic modifications are poorly understood in crustaceans (Federman *et al.,*

2009, 2012; Vandegehuchte *et al.*, 2010; Simon *et al.*, 2011). Bisulfite sequencing could show if *Talitrus* utilizes DNA methylation as gene regulation and patterns therein. Alternatively, patterns in methylation could be detected via methyl- sensitive enzymatic digestion (methyl-sensitive RFLP) and then sequencing of the resulting fragments. Regions of interest could be quantified across the circadian cycle using methylation specific real-time PCR (Cottrell *et al.*, 2004). Acetylation of distinct lysine residues on histones is a further common mechanism of chromatin remodelling (Federman, Fustiñana and Romano, 2009), that could be assessed via Western Blot. Joined by gene knock-down this analysis will clarify circadian gene function and the epigenetic regulation of the *T. saltator* genome. Only approximaly twenty publications are available on epigenetic mechanisms of any type in crustaceans and thus, this area presents a fertile area for rhythms research in this class. The clock gene functions in the integration of temporally gated phenotypes, potential epigenetic modulations and their role in ecological flexibility such as the compass behaviour should be investigated.

7.6 SUMMARY

The proposed project aimed to analyse the biological clock(s) of the coastal crustacean *T. saltator* (Montagu, 1808). *T. saltator* displays astonishing precision in timing and orientation while navigating on the beach. In the literature, time-compensated orientation mechanisms using celestial cues, Earth's magnetic field, visual landmarks and wind direction have been proposed for sandhoppers whilst navigating on the beach. Precise timing of their behaviour suggests a molecular circadian mechanism modulates rhythmic activity. Evidence was presented for an anatomically discrete moon compass clock situated in the antennae, while the sun compass clock seems to function antennae independent. The isolation, identification and quantification of neurogenetic clock components was a primary objective of this project. A circadian transcriptome of brain tissue was prepared and analysed for clock gene sequences and their cycling in abundance within constant conditions. Clock gene sequences were further characterised and compared to published sequences. A start was made to localise central clock cells in the brain and an analysis of clock protein levels over the day were presented. The elucidation of *T. saltator* biological

rhythms will serve as a model for other coastal organisms. The thesis presented here is a highly valuable contribution to the understanding of biological rhythms in marine environments and key behaviours such as animals navigation.

References

Burnet, A. M. R. (1965) ‘Observations on the spawning migrations of Galaxias attenuatus (Jenys)’, *NZ Jl. Sci.*, 8, pp. 79–87.

Abdelrhman, K. F. A. *et al.* (2017) ‘Exploring the bacterial gut microbiota of supralittoral talitrid amphipods’, *Research in Microbiology*, 168(1), pp. 74–84.

Abelló, P., Reid, D. G. and Naylor, E. (1991) ‘Comparative locomotor activity patterns in the portunid crabs Liocarcinus holsatus and L. depurator’, *Journal of the Marine Biological Association of the United Kingdom*. Cambridge University Press, 71(1), p. 1.

Abramowitz, A. A. *et al.* (1944) ‘The occurance of a diabetogenic factor in the exestalks of crustaceans’, *The Biological Bulletin*. Marine Biological Laboratory, 86(1), pp. 1–5.

Abramowitz, A. A., Hisaw, F. L. and Papandrea, D. N. (1944) ‘The occurance of a diabetogenic factor in the eyestalks of crustaceans’, 86(1).

Adams, M. D. *et al.* (2000) ‘The Genome Sequence of Drosophila melanogaster’, *Science*, 287(5461).

Adhub-Al, a. H. Y. and Naylor, E. (2009) ‘Emergence rhythms and tidal migrations in the brown shrimp Crangon crangon (L.)’, *Journal of the Marine Biological Association of the United Kingdom*, 55(4), p. 801.

Agrawal, T., Sadaf, S. and Hasan, G. (2013) ‘A Genetic RNAi Screen for IP3/Ca2+ Coupled GPCRs in Drosophila Identifies the PdfR as a Regulator of Insect Flight’, *PLoS Genetics*. Edited by P. H. Taghert. Public Library of Science, 9(10), p. e1003849.

Aguilar Soto, N. *et al.* (2008) ‘Cheetahs of the deep sea: deep foraging sprints in short-finned pilot whales off Tenerife (Canary Islands).’, *The Journal of animal ecology*, 77(5), pp. 936–47.

Albrecht, U. (2012) ‘Timing to Perfection : The Biology of Central and Peripheral Circadian Clocks’, *Neuron*. Elsevier Inc., 74(2), pp. 246–260.

Alheit, J. and Naylor, E. (1976) ‘Behavioural basis of intertidal zonation in Eurydice pulchra Leach’, *Journal of Experimental Marine Biology and Ecology*, 23(2), pp.

135–144.

Allada, R. and Chung, B. Y. (2010) ‘Circadian Organization of Behavior and Physiology in *Drosophila*’, *Annual Review of Physiology*. NIH Public Access, 72(1), pp. 605–624.

Ando, H., Shahjahan, M. and Hattori, A. (2013) ‘Molecular neuroendocrine basis of lunar-related spawning in grass puffer.’, *General and comparative endocrinology*, 181, pp. 211–4.

Andrews, S. (2010) *Babraham Bioinformatics - FastQC A Quality Control tool for High Throughput Sequence Data*.

Aréchiga, H. and Rodríguez-Sosa, L. (1998) 'Circadian clock function in isolated eyestalk tissue of crayfish.', *Proceedings. Biological sciences*. The Royal Society, 265(1408), pp. 1819–23.

Arendse, M. C. and Kruyswijk, C. J. (1981) 'Orientation of Talitrus saltator to magnetic fields', *Netherlands Journal of Sea Research*. Elsevier, 15(1), pp. 23–32.

Aschoff, J. (1954) 'Zeitgeber der tierischen Tagesperiodik', *Die Naturwissenschaften*. Springer-Verlag, 41(3), pp. 49–56.

Asher, G. *et al.* (2008) 'SIRT1 Regulates Circadian Clock Gene Expression through PER2 Deacetylation', *Cell*. Cell Press, 134(2), pp. 317–328.

Au, W. W. L. *et al.* (2013) 'Nighttime foraging by deep diving echolocating odontocetes off the Hawaiian islands of Kauai and Ni'ihau as determined by passive acoustic monitors.', *The Journal of the Acoustical Society of America*, 133(5), pp.

3119–27.

Au, W. W. L. and Benoit-Bird, K. J. (2008) 'Broadband backscatter from individual Hawaiian mesopelagic boundary community animals with implications for spinner dolphin foraging.', *The Journal of the Acoustical Society of America*. Acoustical Society of America, 123(5), pp. 2884–94.

Axmann, I. M. *et al.* (2014) 'Diversity of KaiC-based timing systems in marine Cyanobacteria.', *Marine genomics*, 14(April), pp. 3–16.

Azzouna, A. *et al.* (2003) 'Localization of crustacean hyperglycemic and vitellogenesis-inhibiting hormones in separate cell types in the protocerebrum of the woodlouse Armadillidium vulgare (Crustacea, Isopoda)', *General and Comparative Endocrinology*, 131(2), pp. 134–142.

Bae, K. *et al.* (1998) 'Circadian regulation of a Drosophila homolog of the mammalian Clock gene: PER and TIM function as positive regulators.', *Molecular and cellular biology*. American Society for Microbiology, 18(10), pp. 6142–51.

Bae, Y. M. and Hastings, J. W. (1994) 'Cloning, sequencing and expression of dinoflagellate luciferase DNA from a marine alga, Gonyaulax polyedra.', *Biochimica et biophysica acta*, 1219(2), pp. 449–56.

Bandyopadhyay, M. *et al.* (2016) 'Drosophila Protein Kinase CK2: Genetics, Regulatory Complexity and Emerging Roles during Development', *Pharmaceuticals*, 10(1), p. 4.

Barca-Bravo, S. *et al.* (2008) 'The effect of human use of sandy beaches on developmental stability of Talitrus saltator (Montagu, 1808) (Crustacea, Amphipoda). A study on fluctuating asymmetry', *Marine Ecology*. Blackwell Publishing Ltd, 29(s1), pp. 91–98.

Batschelet, E. (1981) *Circular statistics in biology*, Academic Press.

Beckwith, E. J. *et al.* (2011) 'Functional conservation of clock output signaling between flies and intertidal crabs.', *Journal of biological rhythms*. SAGE PublicationsSage CA: Los Angeles, CA, 26(6), pp. 518–29.

Begum, K. *et al.* (2009) 'Functions of ion transport peptide and ion transport peptide-like in the red flour beetle Tribolium castaneum', *Insect Biochemistry and Molecular Biology*, 39(10), pp. 717–725.

Belden, W. J. and Dunlap, J. C. (2008) 'SIRT1 is a circadian deacetylase for core clock components.', *Cell*. NIH Public Access, 134(2), pp. 212–4.

Bellet, M. M. and Sassone-Corsi, P. (2010) 'Mammalian circadian clock and metabolism - the epigenetic link', *Journal of Cell Science*, 123(22), pp. 3837–3848.

Benoit-Bird, K. J., Cowles, T. J. and Wingard, C. E. (2009) 'Edge gradients provide evidence of ecological interactions in planktonic thin layers', *Limnology and Oceanography*, 54(4), pp. 1382–1392.

Berge, J. *et al.* (2009) 'Diel vertical migration of Arctic zooplankton during the polar night', *Biology Letters*, 5(1), pp. 69–72.

Biscontin, A. *et al.* (2017) 'Functional characterization of the circadian clock in the Antarctic krill, *Euphausia superba', Scientific REPORTS*, 7(1), p. 17742.

Biuw, M. *et al.* (2010) 'Effects of hydrographic variability on the spatial, seasonal and diel diving patterns of southern elephant seals in the eastern Weddell Sea.', *PloS one*, 5(11), p. e13816.

Blenau, W. and Baumann, A. (2005) 'Molecular characterization of the ebony gene from the American cockroach, *Periplaneta americana*.', *Archives of insect biochemistry and physiology*, 59(3), pp. 184–95.

Bliss, D. E. (1982) *The Biology of Crustacea*. Academic Press.

Bodvard, K. *et al.* (2017) 'Light-sensing via hydrogen peroxide and a peroxiredoxin', *Nature Communications*. Nature Publishing Group, 8, p. 14791.

Bonasio, R. *et al.* (2010) 'Genomic Comparison of the Ants Camponotus floridanus and Harpegnathos saltator', *Science*, 329(5995).

Borgstahl, G. E., Williams, D. R. and Getzoff, E. D. (1995) '1.4 A structure of photoactive yellow protein, a cytosolic photoreceptor: unusual fold, active site, and chromophore.', *Biochemistry*, 34(19), pp. 6278–87.

Bregazzi, P. K. (1972) 'The Effects of Low Temperature Upon the Locomotor Activity Rhythm of Talitrus Saltator (Montagu) (Crustacea: Amphipoda)', *Journal of Experimental Biology*, 57(2).

Bregazzi, P. K. and Naylor, E. (1972) 'The Locomotor Activity Rhythm Of Talitrus Saltator (Montagu) (Crustacea, Amphipoda)', *J. Exp. Biol.*, 57(1967), pp. 375–391.

Bulau, P. *et al.* (2003) 'Two genetic variants of the crustacean hyperglycemic hormone (CHH) from the Australian crayfish, Cherax destructor: detection of chiral isoforms due to post-translational modification.', *Peptides*, 24(12), pp. 1871–9.

Bulau, P. (2004) 'Identification of Neuropeptides from the Sinus Gland of the Crayfish Orconectes limosus Using Nanoscale On-line Liquid Chromatography Tandem Mass Spectrometry', *Molecular & Cellular Proteomics*, 3(6), pp. 558–564.

Calman, W. T. (1911) *The life of Crustacea*. New York: The Macmillan company.

Cardon, Z. G. (2018) 'A model suite of green algae within the Scenedesmaceae for investigating contrasting desiccation tolerance and morphology', *Journal of Cell Science*, (131) jcs212233.

Caspers, H. (1984) 'Spawning periodicity and habitat of the palolo worm *Eunice viridis* (Polychaeta: Eunicidae) in the Samoan Islands', *Marine Biology*, (79), pp. 229-236.

Chang, E. S. *et al.* (1999) 'Crustacean hyperglycemic hormone in the lobster nervous system: localization and release from cells in the subesophageal ganglion and thoracic second roots.', *The Journal of comparative neurology*, 414(1), pp. 50–6.

Chang, E. S., Keller, R. and Chang, S. A. (1998) 'Quantification of Crustacean Hyperglycemic Hormone by ELISA in Hemolymph of the Lobster,Homarus americanus,Following Various Stresses', *General and Comparative Endocrinology*, 111(3), pp. 359–366.

Chappuis, S. *et al.* (2013) 'Role of the circadian clock gene Per2 in adaptation to cold temperature', *Molecular Metabolism*. Elsevier, 2(3), pp. 184–193.

Cheeseman, J. F. Fewster, R. M. R. M. and Walker, M. M. M. (2017) 'Circadian and circatidal clocks control the mechanism of semilunar foraging behaviour', *Scientific Reports*, 7(1), p. 3780.

Chen, S.-H., Lin, C.-Y. and Kuo, C. M. (2004) 'Cloning of two crustacean hyperglycemic hormone isoforms in freshwater giant prawn (Macrobrachium rosenbergii): evidence of alternative splicing.', *Marine biotechnology (New York, N.Y.)*, 6(1), pp. 83–94.

Chen, S. H., Lin, C. Y. and Kuo, C. M. (2005) 'In Silico Analysis of Crustacean Hyperglycemic Hormone Family', *Marine Biotechnology*, 7(3), pp. 193–206.

Christie, A. E. (2008) 'Neuropeptide discovery in Ixodoidea: An in silico investigation using publicly accessible expressed sequence tags', *General and Comparative Endocrinology*, 157(2), pp. 174–85.

Christie, A. E. *et al.* (2011) 'Bioinformatic prediction of arthropod/nematode-like peptides in non-arthropod, non-nematode members of the Ecdysozoa', *General and Comparative Endocrinology*, 170(3), pp. 480–486.

Christie, A. E. *et al.* (2013) 'Prediction of the protein components of a putative Calanus finmarchicus (Crustacea, Copepoda) circadian signaling system using a de

novo assembled transcriptome.', *Comparative biochemistry and physiology. Part D, Genomics & proteomics*. NIH Public Access, 8(3), pp. 165–93.

Chung, J. S., Dircksen, H. and Webster, S. G. (1999) 'A remarkable, precisely timed release of hyperglycemic hormone from endocrine cells in the gut is associated with ecdysis in the crab Carcinus maenas.', *Proceedings of the National Academy of Sciences of the United States of America*. National Academy of Sciences, 96(23), pp. 13103–7.

Chung, J. S. and Webster, S. G. (1996) 'Does the N-terminal pyroglutamate residue have any physiological significance for crab hyperglycemic neuropeptides?', *European journal of biochemistry*, 240(2), pp. 358–64.

Chung, J. S. and Webster, S. G. (2005) 'Dynamics of in vivo release of molt-inhibiting hormone and crustacean hyperglycemic hormone in the shore crab, Carcinus maenas.', *Endocrinology*, 146(12), pp. 5545–51.

Chung, J. S. and Webster, S. G. (2006) 'Binding sites of crustacean hyperglycemic hormone and its second messengers on gills and hindgut of the green shore crab, Carcinus maenas: a possible osmoregulatory role.', *General and comparative endocrinology*, 147(2), pp. 206–13.

Chung, J. S. and Zmora, N. (2008) 'Functional studies of crustacean hyperglycemic hormones (CHHs) of the blue crab, Callinectes sapidus - the expression and release of CHH in eyestalk and pericardial organ in response to environmental stress'.

Blackwell Publishing Ltd, 275(4), pp. 693–704.

Chung, S. J. and Webster, S. G. (2004) 'Expression and release patterns of neuropeptides during embryonic development and hatching of the green shore crab, Carcinus maenas', *Development (Cambridge, England)*, 131(19), pp. 4751–61.

Ciofini, A. and Ugolini, A. (2017) 'Sun and moon compasses in *Tylos europaeus* (Crustacea Isopoda)', *Ethology Ecology & Evolution*. Taylor & Francis, pp. 1–10.

Claydon, J. A. B., McCormick, M. I. and Jones, G. P. (2014) 'Multispecies spawning sites for fishes on a low-latitude coral reef: spatial and temporal patterns.', *Journal of fish biology*, 84(4), pp. 1136–63.

Coast GM, W. S. (eds) (1998) 'Neuropeptides inhibiting growth and repro- duction in crustaceans.', in *Recent advances in arthropod endocrinology*. Cambridge University Press, Cambridge, pp. 33–53.

Costa, R., Peixoto, A. A, Barbujani, G., Kyriacou, C. P. (1992) 'A latitudinal cline in a Drosophila clock gene.', *Proceedings. Biological sciences / The Royal Society* (250), pp. 43-9.

Collett, M. (2014) 'A desert ant's memory of recent visual experience and the control of route guidance.', *Proceedings. Biological sciences / The Royal Society*, 281(1787).

Collett, M., Chittka, L. and Collett, T. S. (2013) 'Spatial Memory in Insect Navigation', *Current Biology*, 23(17), pp. R789–R800.

Conesa, A. *et al.* (2005) 'Blast2GO: a universal tool for annotation, visualization and analysis in functional genomics research.', *BIOINFORMATICS APPLICATIONS NOTE*, 21(18), pp. 3674–3676.

Conesa, A. and Götz, S. (2008) 'Blast2GO: A Comprehensive Suite for Functional Analysis in Plant Genomics', *International Journal of Plant Genomics*, 2008, pp. 1–12.

Cottrell, S. E. *et al.* (2004) 'A real-time PCR assay for DNA-methylation using methylation-specific blockers.', *Nucleic acids research*. Oxford University Press, 32(1), p. e10.

La Cour, T. *et al.* (2004) 'Analysis and prediction of leucine-rich nuclear export signals', *Protein Eng. Des. Sel.*, 17(6), pp. 527–36.

Cresci, A. *et al.* (2017) 'Glass eels (Anguilla anguilla) have a magnetic compass linked to the tidal cycle.', *Science advances*. American Association for the Advancement of Science, 3(6), p. e1602007.

Cyran, S. A. *et al.* (2003) 'vrille, Pdp1, and dClock form a second feedback loop in the Drosophila circadian clock.', *Cell*. Elsevier, 112(3), pp. 329–41.

Dacke, M. *et al.* (2003) 'Insect orientation to polarized moonlight', *Nature*. Nature Publishing Group, 424(6944), pp. 33–33.

Dacke, M. *et al.* (2014) 'The role of the sun in the celestial compass of dung beetles.', *Philosophical transactions of the Royal Society of London. Series B, Biological sciences*, 369(1636), p. 20130036.

Dai, L., Zitnan, D. and Adams, M. E. (2007) 'Strategic expression of ion transport peptide gene products in central and peripheral neurons of insects.', *The Journal of comparative neurology*, 500(2), pp. 353–67.

Darlington, T. K. *et al.* (1998) 'Closing the circadian loop: CLOCK-induced transcription of its own inhibitors *per* and *tim*.', *Science (New York, N.Y.)*, 280(5369), pp. 1599–603.

Denhardt, D. T. (2018) 'Effect of stress on human biology: Epigenetics, adaptation, inheritance, and social significance', *Journal of Cellular Physiology*, 233(3), pp.

1975–1984.

Desmoucelles-Carette, C., Sellos, D. and Van Wormhoudt, A. (1996) 'Molecular Cloning of the Precursors of Pigment Dispersing Hormone in Crustaceans', *Biochemical and Biophysical Research Communications*, 221(3), pp. 739–743.

Dircksen, H. *et al.* (2001) 'Crustacean hyperglycaemic hormone (CHH)-like peptides and CHH-precursor-related peptides from pericardial organ neurosecretory cells in the shore crab, Carcinus maenas, are putatively spliced and modified products of multiple genes.', *The Biochemical journal*, 356(Pt 1), pp. 159–70.

Dircksen, H. *et al.* (2008) 'Ion transport peptide splice forms in central and peripheral

neurons throughout post-embryogenesis of Drosophila melanogaster', *The Journal of Comparative Neurology*, 509(1), pp. 23–41.

Dircksen, H. (2009) 'Insect ion transport peptides are derived from alternatively spliced genes and differentially expressed in the central and peripheral nervous system', *Journal of Experimental Biology*, 212(3), pp. 401–412.

Dircksen, H. *et al.* (2011) 'Genomics, Transcriptomics, and Peptidomics of Daphnia pulex Neuropeptides and Protein Hormones', *Journal of Proteome Research*, 10(10), pp. 4478–504.

Drexler, A. L. *et al.* (2007) 'Molecular characterization and cell-specific expression of an ion transport peptide in the tobacco hornworm, Manduca sexta.', *Cell and tissue research*, 329(2), pp. 391–408.

Dubruille, R. and Emery, P. (2008) 'A Plastic Clock: How Circadian Rhythms Respond to Environmental Cues in Drosophila', *Molecular Neurobiology*. Humana Press Inc, 38(2), pp. 129–145.

Dunlap, J. C. (1999) 'Molecular Bases for Circadian Clocks Review', 96, pp. 271–290.

Eckhardt, E. *et al.* (1995) 'Stimulation of osmoregulating processes in the perfused gill of the crab Pachygrapsus marmoratus (Crustacea, Decapoda) by a sinus gland peptide.', *General and comparative endocrinology*, 99(2), pp. 169–77.

Edomi, P. *et al.* (2002) 'Gonad-inhibiting hormone of the Norway lobster (Nephrops norvegicus): cDNA cloning, expression, recombinant protein production, and immunolocalization.', *Gene*, 284(1–2), pp. 93–102.

Edwards, J. M. and Naylor, E. (1987) 'Endogenous Circadian changes in orientational behaviour of Talitrus saltator', pp. 17–26.

Egg, M. *et al.* (2013) 'Linking Oxygen to Time: The Bidirectional Interaction Between the Hypoxic Signaling Pathway and the Circadian Clock', *Chronobiology International*, 30(4), pp. 510–529.

Eide, E. J. *et al.* (2005) 'Control of Mammalian Circadian Rhythm by CKI - Regulated Proteasome-Mediated PER2 Degradation', *Molecular and Cellular Biology*, 25(7), pp. 2795–2807.

Escamilla-Chimal, E. G. *et al.* (2002) 'Serotonin Modulation of CHH Secretion by Isolated Cells of the Crayfish Retina and Optic Lobe', *General and Comparative Endocrinology*, 125(2), pp. 283–290.

Escamilla-Chimal, E. G. *et al.* (2010) 'Putative pacemakers of crayfish show clock proteins interlocked with circadian oscillations.', *The Journal of experimental biology*, 213(Pt 21), pp. 3723–33.

Escamilla-Chimal, E. G. E. G., Van Herp, F. and Fanjul-Moles (2001) 'Daily variations in crustacean hyperglycaemic hormone and serotonin immunoreactivity during the development of crayfish.', *The Journal of experimental biology*, 204(Pt

6), pp. 1073–81.

Escande, M. (2010) ‘Integration of Light Signals by the Retinoblastoma Pathway in the Control of S Phase Entry in the Picophytoplanktonic Cell Ostreococcus’, 6(5).

Fang, Y., Sathyanarayanan, S. and Sehgal, A. (2007) ‘Post-translational regulation of the Drosophila circadian clock requires protein phosphatase 1 (PP1).’, *Genes & development*. Cold Spring Harbor Laboratory Press, 21(12), pp. 1506–18.

Federman, N., Fustiñana, M. S. and Romano, A. (2009) ‘Histone acetylation is recruited in consolidation as a molecular feature of stronger memories.’, *Learning & memory (Cold Spring Harbor, N.Y.)*, 16(10), pp. 600–6.

Federman, N., Fustiñana, M. S. and Romano, A. (2012) ‘Reconsolidation involves histone acetylation depending on the strength of the memory.’, *Neuroscience*, 219, pp. 145–56.

Fernlund, P. (1976) ‘Structure of a light-adapting hormone from the shrimp, Pandalus borealis.’, *Biochimica et biophysica acta*, 439(1), pp. 17–25.

Fialkowski, W. *et al.* (2009) ‘The sandhopper Talitrus saltator (Crustacea: Amphipoda) as a biomonitor of trace metal bioavailabilities in European coastal waters.’, *Marine pollution bulletin*, 58(1), pp. 39–44.

Foster, J. J. *et al.* (2018) ‘How animals follow the stars’, *Proc. R. Soc. B*. The Royal Society, 285(1871), p. 20172322.

Froy, O. *et al.* (2003) ‘Illuminating the circadian clock in monarch butterfly migration.’, *Science (New York, N.Y.)*, 300(5623), pp. 1303–5.

Fu, Q. *et al.* (2005) ‘Hormone complement of theCancer productus sinus gland and pericardial organ: An anatomical and mass spectrometric investigation’, *The Journal of Comparative Neurology*, 493(4), pp. 607–626.

Gallois, D. *et al.* (2003) ‘Post-translational isomerization of a neuropeptide in crustacean neurosecretory cells studied by ultrastructural immunocytochemistry’, *European journal of cell biology*, 82(8), pp. 431–40.

Gambineri, S. and Scapini, F. (2008) ‘Importance of orientation to the sun and local landscape features in young inexpert Talitrus saltator (Amphipoda: Talitridae) from two Italian beaches differing in morphodynamics, erosion or stability’, *Estuarine, Coastal and Shelf Science*, 77(3), pp. 357–368.

Gambineri, S. and Scapini, F. (2015) ‘Sandhopper orientation under natural conditions: Comparing individual tracks’, *Behavioural Processes*, 113, pp. 13–23.

Gamble, F. W. and Keeble, F. (1903) ‘The Bionomics of Convoluta roscoffensis, with Special Reference to its Green Cells’, *Journal of Cell Science*, (s2-47), pp.363-431.

Gasteiger, E. *et al.* (2003) ‘ExPASy: The proteomics server for in-depth protein knowledge and analysis.’, *Nucleic acids research*, 31(13), pp. 3784–8.

Gaten, E. *et al.* (2008) 'Is vertical migration in Antarctic krill (Euphausia superba) influenced by an underlying circadian rhythm?', *Journal of genetics*, 87(5), pp. 473–483.

Gegear, R. J. *et al.* (2009) 'CRYPTOCHROME mediates light-dependent magnetosensitivity in Drosophila', *Nature*, 454(7207), pp. 1014–1018.

Geppetti, L. and Tongiorgi, P. (1967a) 'Nocturnal Migrations of Talitrus Saltator (Montagu) (Crustacean, Amphipoda).', *Monitore Zoologico Italiano - Italian Journal of Zoology*. Taylor & Francis, 1(1), pp. 37–40.

Geppetti, L. and Tongiorgi, P. (1967b) 'Nocturnal migrations of *Talitrus saltator* (Montagu)(Crustacea Amphipoda)', *Bolletino di zoologia*, 1(1), pp. 139–160.

Giebultowicz, J. M. (2000) 'Molecular Mechanism and Cellular Distribution of Insect Circadian Clocks', *Annual Review of Entomology*, 45(1), pp. 769–793.

Gorgels-Kallen, J. and Voorter, C. M. (1985) 'The secretory dynamics of the CHH-producing cell group in the eyestalk of the crayfish, Astacus leptodactylus, in the course of the day/night cycle', *Cell and Tissue Research*. Springer-Verlag, 241(2), pp. 361–366.

Gotz, S. *et al.* (2008) 'High-throughput functional annotation and data mining with the Blast2GO suite', *Nucleic Acids Research*, 36(10), pp. 3420–3435.

Goy, M. F. (1990) 'Activation of membrane guanylate cyclase by an invertebrate peptide hormone.', *The Journal of biological chemistry*, 265(33), pp. 20220–7.

Goy, M. F., Mandelbrot, D. A. and York, C. M. (1987) 'Identification and Characterization of a Polypeptide from a Lobster Neurosecretory Gland that Induces Cyclic GMP Accumulation in Lobster Neuromuscular Preparations', *Journal of Neurochemistry*. Blackwell Publishing Ltd, 48(3), pp. 954–966.

Grabek, K. R. and Chabot, C. C. (2012) 'Daily Rhythms of PERIOD protein in the eyestalk of the American lobster,Homarus americanus.', *Marine and freshwater behaviour and physiology*. NIH Public Access, 45(4), pp. 269–279.

Grabherr, M. G. *et al.* (2011) 'Full-length transcriptome assembly from RNA-Seq data without a reference genome.', *Nature biotechnology*, 29(7), pp. 644–52.

Green, C. B., Takahashi, J. S. and Bass, J. (2008) 'The Meter of Metabolism', *Cell*, 134(5), pp. 728–742.

Grima, B. *et al.* (2004) 'Morning and evening peaks of activity rely on different clock neurons of the Drosophila brain.', *Nature*, 431(7010), pp. 869–73.

Grossmann, G. *et al*. (2018) 'Green light for quantitative live-cell imaging in plants ', *Journal of Cell Science*, (131), jcs209270

Gu, P.-L. L., Yu, K. L. and Chan, S.-M. M. (2000) 'Molecular characterization of an additional shrimp hyperglycemic hormone: cDNA cloning, gene organization, expression and biological assay of recombinant proteins.', *FEBS letters*, 472(1), pp.

122–128.

Guerra, P. A., Gegear, R. J. and Reppert, S. M. (2014) ‘A magnetic compass aids monarch butterfly migration’, *Nature Communications*, 5, p. 4164.

H.K. Tiu, S., He, J.-G. and Chan, S.-M. (2007) ‘The LvCHH-ITP gene of the shrimp (Litopenaeus vannamei) produces a widely expressed putative ion transport peptide (LvITP) for osmo-regulation’, *Gene*, 396(2), pp. 226–235.

Haas, B. J. *et al.* (2013) ‘De novo transcript sequence reconstruction from RNA-seq using the Trinity platform for reference generation and analysis’, *Nature Protocols*. Nature Research, 8(8), pp. 1494–1512.

Häfker, N. S. *et al.* (2017) ‘Circadian Clock Involvement in Zooplankton Diel Vertical Migration’, *Current Biology*, 27(14), p. 2194–2201.e3.

Halberg, F. *et al.* (2003) ‘Transdisciplinary unifying implications of circadian findings in the 1950s’, *Journal of Circadian Rhythms*. Ubiquity Press, 1(0), p. 2.

Hall (1999) ‘BioEdit: a user-friendly biological sequence alignment editor and analysis program for Windows 95/98/NT’, *Nucleic Acids Symposium Series*, 41.

Hardin, P. E., Hall, J. C. and Rosbash, M. (1990) ‘Feedback of the Drosophila period gene product on circadian cycling of its messenger RNA levels’, *Nature*. Nature Publishing Group, 343(6258), pp. 536–540.

Hardin, P. E., Hall, J. C. and Rosbash, M. (1990) ‘Feedback of the Drosophila period gene product on circadian cycling of its messenger RNA levels’, *Nature*, 343(6258), pp. 536–540.

Harding, L. W. and Heinbokel, J. F. (1984) ‘Periodicities of photosynthesis and cell division : behavior of phase-lagged replicate cultures of Ditylum brightwellii in a diurnally varying pho tic regime’, 15(1971), pp. 225–232.

Hartenstein, V. (2006) ‘The neuroendocrine system of invertebrates: a developmental and evolutionary perspective’, *Journal of Endocrinology*, 190, pp. 555–570.

Harthoorn, L. *et al.* (2001) ‘Absence of coupling between release and biosynthesis of peptide hormones in insect neuroendocrine cells’, *European Journal of Cell Biology*, 80(7), pp. 451–457.

Hastings, M. H. and Naylor, E. (1980) ‘Ontogeny of an endogenous rhythm in Eurydice pulchra’, *Journal of Experimental Marine Biology and Ecology*, 46(2), pp. 137–145.

Hauenschild, C. (1968) ‘Untersuchungen am pazifischen Palolowurm Eunice viridis (Polychaeta) in Samoa‘, *Helgoländer wissenschaftliche Meeresuntersuchungen*, (18), pp. 254-295.

Hefti, M. H. *et al.* (2004) ‘The PAS fold. A redefinition of the PAS domain based upon structural prediction.’, *European journal of biochemistry*, 271(6), pp. 1198–208.

Helfrich-Förster, C. (1995) ‘The period clock gene is expressed in central nervous system neurons which also produce a neuropeptide that reveals the projections of circadian pacemaker cells within the brain of Drosophila melanogaster.’, *Proceedings of the National Academy of Sciences of the United States of America*. National Academy of Sciences, 92(2), pp. 612–6.

Helfrich-Förster, C. (2003) ‘The neuroarchitecture of the circadian clock in the brain of *Drosophila melanogaster*’, *Microscopy Research and Technique*, 62(2), pp. 94–102.

Helfrich-Förster, C. *et al.* (2007) ‘The Lateral and Dorsal Neurons of Drosophila melanogaster: New Insights about Their Morphology and Function’, in *Cold Spring Harbor Symposia on Quantitative Biolog*. Cold Spring Harbor Laboratory Press, pp. 517–525.

Helfrich-Förster, C. and Homberg, U. (1993) ‘Pigment-dispersing hormone-immunoreactive neurons in the nervous system of wild-type *Drosophila melanogaster* and of several mutants with altered circadian rhythmicity’, *Journal of Comparative Neurology*, 337(2), pp. 177–190.

Hoelters, L. *et al.* (2016) ‘Characterization, localization and temporal expression of crustacean hyperglycemic hormone (CHH) in the behaviorally rhythmic peracarid crustaceans, Eurydice pulchra (Leach) and Talitrus saltator (Montagu)’, *General and Comparative Endocrinology*, 237, pp. 43–52.

Homberg, U. (2004) ‘In search of the sky compass in the insect brain’,

Naturwissenschaften, 91(5), pp. 199–208.

Homberg, U. *et al.* (2015) ‘Sky Compass Orientation in Desert Locusts—Evidence from Field and Laboratory Studies’.

Hsu, Y.-W. A. *et al.* (2008) ‘Cloning and differential expression of two β-pigment-dispersing hormone (β-PDH) isoforms in the crabCancer productus: Evidence for authentic β-PDH as a local neurotransmitter and β-PDH II as a humoral factor’, *The Journal of Comparative Neurology*, 508(2), pp. 197–211.

Huang, X. and Miller, W. (1991) ‘A Time-Efficient, Linear-Space Local Similaritiy Algoryhtm’, *Advances in Applied Mathematics*, 12, pp. 337–357.

Huang, Z. J., Edery, I. and Rosbash, M. (1993) ‘PAS is a dimerization domain common to Drosophila Period and several transcription factors’, *Nature*, 364(6434), pp. 259–262.

Hughes, M. E., Hogenesch, J. B. and Kornacker, K. (2010) ‘JTK_CYCLE: an efficient nonparametric algorithm for detecting rhythmic components in genome-scale data sets.’, *Journal of Biological Rhythms*. NIH Public Access, 25(5), pp. 372–380.

Hut, R. a and Beersma, D. G. M. (2011) ‘Evolution of time-keeping mechanisms: early emergence and adaptation to photoperiod.’, *Philosophical transactions of the Royal Society of London. Series B, Biological sciences*, 366(1574), pp. 2141–2154.

HyperLadder Selection Chart (2017).

Jander, R. (1957) 'Die optische Richtungsorientierung der roten Waldameise (Formica rufa)', *Zeitschrift für vergleichende Physiologie*, 40, pp. 162–238.

Jankauskienė, R. and Safonovienė, A. (2009) 'Distribution of sand hoppers (Talitrus saltator, Montagu, 1808) on the beach of the Lithuanian Baltic Sea', *EKOLOGIJA*, 55, pp. 3–4.

Jenouvrier, S. *et al.* (2005) 'Evidence of a shift in the cyclicity of Antarctic seabird dynamics linked to climate.', *Proceedings. Biological sciences / The Royal Society*, 272(1566), pp. 887–95.

Kadener, S. *et al.* (2007) 'Clockwork Orange is a transcriptional repressor and a new Drosophila circadian pacemaker component.', *Genes & development*. Cold Spring Harbor Laboratory Press, 21(13), pp. 1675–86.

Kadener, S. *et al.* (2008) 'Circadian Transcription Contributes to Core Period Determination in Drosophila', *PLoS Biology*. Edited by J. B. Hogenesch. Public Library of Science, 6(5), p. e119.

Kaiser, T. S. and Heckel, D. G. (2012) 'Genetic architecture of local adaptation in lunar and diurnal emergence times of the marine midge Clunio marinus (Chironomidae, Diptera).', *PloS one*, 7(2), p. e32092.

Kaiser, T. S., Neumann, D. and Heckel, D. G. (2011) 'Timing the tides: genetic control of diurnal and lunar emergence times is correlated in the marine midge Clunio marinus.', *BMC genetics*. BioMed Central Ltd, 12(1), p. 49.

Kallen, J. L., Abrahamse, S. L. and Van Herp, F. (1990) 'cccccc', *Biol. Bull.*, 179, pp. 351–357.

Kallen, J. L., Rigiani, N. R. and Trompenaars, H. J. A. J. (1988) 'Aspects of Entrainment of CHH Cell Activity and Hemolymph Glucose Levels in Crayfish*', *Reference: Biol. Bull*, 175, pp. 137–143.

Kallen J., L. and Abrahamse S., L. (1989) 'Functional aspects of the hyperglycemic hormone producing system of the crayfish orconectes limosus in relation to its day night rhythm', *General & Comparative Endocrinology*, 74(2), p. 262.

Kamae, Y., Tanaka, F. and Tomioka, K. (2010) 'Molecular cloning and functional analysis of the clock genes, Clock and cycle, in the firebrat Thermobia domestica', *Journal of Insect Physiology*. Pergamon, 56(9), pp. 1291–1299.

Kaneko, M. and Hall, J. C. (2000) 'Neuroanatomy of cells expressing clock genes in Drosophila: transgenic manipulation of the period and timeless genes to mark the perikarya of circadian pacemaker neurons and their projections.', *The Journal of comparative neurology*, 422(1), pp. 66–94.

Katayama, H. *et al.* (2003) 'The Solution Structure of Molt-inhibiting Hormone from the Kuruma Prawn Marsupenaeus japonicus', *Journal of Biological Chemistry*, 278(11), pp. 9620–9623.

Katayama, H. and Chung, J. S. (2009) ‘The specific binding sites of eyestalk- and pericardial organ-crustacean hyperglycaemic hormones (CHHs) in multiple tissues of the blue crab, Callinectes sapidus’, *Journal of Experimental Biology*, 212(4), pp. 542–549.

Katayama, H. and Nagasawa, H. (2004) ‘Effect of a Glycine Residue Insertion into Crustacean Hyperglycemic Hormone on Hormonal Activity’, *Zoological Science*, 21(11), pp. 1121–1124.

Kegel, G. *et al.* (1989) ‘Amino acid sequence of the crustacean hyperglycemic hormone (CHH) from the shore crab, *Carcinus maenas*’, *FEBS Letters*, 255(1), pp. 10–14.

Kegel, G. *et al.* (1991) ‘Amino acid sequence of crustacean hyperglycemic hormone (CHH) from the crayfish, Orconectes limousus: Emergence of a novel neuropeptide family’, *Peptides*, 12(5), pp. 909–913.

Keller, R. (1969) ‘Untersuchungen zur Artspezifität eines Crustaceenhormons’, *Zeitschrift fuer Vergleichende Physiologie*. Springer-Verlag, 63(2), pp. 137–145.

Keller, R. and Beyer, J. (1968) ‘Zur hyperglykämischen Wirkung von Serotonin und Augenstielextrakt beim Flußkrebs Orconectes limosus’, *Zeitschrift fuer Vergleichende Physiologie*. Springer-Verlag, 59(1), pp. 78–85.

Keller, R., Jaros, P. P. and Kegel, G. (1985) ‘Crustacean Hyperglycemic Neuropeptides’, *American Zoologist*, 25(1), pp. 207–221.

Kim, W. J., Jan, L. Y. and Jan, Y. N. (2013) ‘A PDF/NPF Neuropeptide Signaling Circuitry of Male Drosophila melanogaster Controls Rival-Induced Prolonged Mating’, *Neuron*, 80(5), pp. 1190–1205.

King, D. S. *et al.* (1999) ‘Biological actions of synthetic locust ion transport peptide (ITP).’, *Insect biochemistry and molecular biology*, 29(1), pp. 11–8.

Kivimäe, S. *et al.* (2008) ‘Activating PER Repressor through a DBT-Directed Phosphorylation Switch’, *PLoS Biology*. Edited by U. Schibler. Elsevier, 6(7), p. e183.

Klein, J. M. *et al.* (1994) ‘Molecular Cloning of Two Pigment-Dispersing Hormone (PDH) Precursors in the Blue Crab Callinectes sapidus Reveals a Novel Member of the PDH Neuropeptide Family’, *Biochemical and Biophysical Research Communications*, 205(1), pp. 410–416.

Koh, K., Zheng, X. and Sehgal, A. (2006) ‘JETLAG Resets the Drosophila Circadian Clock by Promoting Light-Induced Degradation of TIMELESS’, *Science (New York, N.Y.)*. NIH Public Access, 312(5781), pp. 1809–12.

Kojima, S., Shingle, D. L. and Green, C. B. (2011) ‘Post-transcriptional control of circadian rhythms.’, *Journal of cell science*. Company of Biologists, 124(Pt 3), pp. 311–20.

Konopka, R. J. and Benzer, S. (1971) ‘Clock mutants of Drosophila melanogaster.’,

Proceedings of the National Academy of Sciences of the United States of America, 68(9), pp. 2112–6.

Kornacker, K. and Hogenesch, J. (2010) *HughesLab:JTK Cycle - OpenWetWare*.

Krieger, J. *et al.* (2012) 'Giant Robber Crabs Monitored from Space : GPS-Based Telemetric Studies on Christmas Island (Indian Ocean)', *PloS one*, 7(11), p. e49809.

Kumar, S., Stecher, G. and Tamura, K. (2016) 'MEGA7: Molecular Evolutionary Genetics Analysis Version 7.0 for Bigger Datasets', *Molecular Biology and Evolution*, 33(7), pp. 1870–1874.

Kummer, G. and Keller, R. (1993) 'High-affinity binding of crustacean hyperglycemic hormone (CHH) to hepatopancreatic plasma membranes of the crab Carcinus maenas and the crayfish Orconectes limosus.', *Peptides*, 14(1), pp. 103–8.

Kunst, M. *et al.* (2014) 'Calcitonin gene-related peptide neurons mediate sleep-specific circadian output in Drosophila.', *Current biology : CB*. NIH Public Access, 24(22), pp. 2652–64.

Kuo, C. M. and Yang, Y. H. (1999) 'Hyperglycemic responses to cold shock in the freshwater giant prawn, Macrobrachium rosenbergii', *Journal of Comparative Physiology B: Biochemical, Systemic, and Environmental Physiology*. Springer-Verlag, 169(1), pp. 49–54.

Kyriacou, C. P. and Rosato, E. (2000) 'Squaring up the E-box.', *Journal of biological rhythms*, 15(6), pp. 483–90.

Labhart, T., Petzold, J. and Helbling, H. (2001) 'Spatial integration in polarization-sensitive interneurones of crickets: a survey of evidence, mechanisms and benefits.', *The Journal of experimental biology*, 204(Pt 14), pp. 2423–30.

Lacombe, C., Grève, P. and Martin, G. (1999) 'Overview on the sub-grouping of the crustacean hyperglycemic hormone family', *Neuropeptides*, 33(1), pp. 71–80.

Lakin-Thomas, P. L. (2006) 'Transcriptional Feedback Oscillators: Maybe, Maybe Not...', *Journal of Biological Rhythms*. Sage Publications, Sage CA: Thousand Oaks, CA, 21(2), pp. 83–92.

Lam, V. H. and C. J. C. (2017) 'Evolution and Design of Invertebrate Circadian Clocks', *The Oxford Handbook of Invertebrate Neurobiology*.

Lampert, W. (1989) 'The Adaptive Significance of Diel Vertical Migration of Zooplankton', *Functional Ecology*, (3), p. 21.

Last, K. S. *et al.* (2016) 'Moonlight Drives Ocean-Scale Mass Vertical Migration of Zooplankton during the Arctic Winter', *Current Biology*, 26, pp. 244–251.

Laurent, G. *et al.* (2013) 'SIRT4 represses peroxisome proliferator-activated receptor α activity to suppress hepatic fat oxidation.', *Molecular and cellular biology*.

American Society for Microbiology, 33(22), pp. 4552–61.

Laverdure, A. M. *et al.* (1994) 'Neuropeptides and related nucleic acid sequences detected in peneid shrimps by immunohistochemistry and molecular hybridizations.', *Neuroscience*, 60(2), pp. 569–79.

Lebhardt, F. and Ronacher, B. (2015) 'Transfer of directional information between the polarization compass and the sun compass in desert ants', *Journal of Comparative Physiology A*, 201(6), pp. 599–608.

Lee, C. Y. *et al.* (2000) 'Serotonergic regulation of blood glucose levels in the crayfish, Procambarus clarkii: site of action and receptor characterization.', *The Journal of experimental zoology*, 286(6), pp. 596–605.

Lee, C., Yang, P. and Zou, H. (2001) 'Serotonergic Regulation of Crustacean Hyperglycemic Hormone Secretion in the Crayfish, *Procambarus clarkii*', *Physiological and Biochemical Zoology*, 74(3), pp. 376–382.

Lenz, P. H. *et al.* (2014) 'De Novo Assembly of a Transcriptome for Calanus finmarchicus (Crustacea, Copepoda) – The Dominant Zooplankter of the North Atlantic Ocean', *PLoS ONE*. Edited by A. Ianora. Public Library of Science, 9(2), p. e88589.

Letunic, I., Doerks, T. and Bork, P. (2015) 'SMART: recent updates, new developments and status in 2015', *Nucleic acids research*. Oxford University Press, 43(Database issue), pp. D257-60.

Leuven, R. S. *et al.* (1982) 'Species or group specificity in biological and immunological studies of crustacean hyperglycemic hormone.', *General and comparative endocrinology*, 46(3), pp. 288–96.

Levy, O. *et al.* (2007) 'Light-responsive cryptochromes from a simple multicellular animal, the coral Acropora millepora.', *Science (New York, N.Y.)*, 318(5849), pp.

467–70.

Li, C. *et al.* (2012) 'Epigenetic Control of Circadian Clock Operation during Development', *Genetics Research International*, 2012, pp. 1–8.

Li, W. *et al.* (2015) 'The EMBL-EBI bioinformatics web and programmatic tools framework', *Nucleic Acids Research*. Oxford University Press, 43(W1), pp. W580–W584.

Li, W. and Godzik, A. (2006) 'Cd-hit: a fast program for clustering and comparing large sets of protein or nucleotide sequences', *Bioinformatics*. Oxford University Press, 22(13), pp. 1658–1659.

Li, W., Jaroszewski, L. and Godzik, A. (2001) 'Clustering of highly homologous sequences to reduce the size of large protein databases.', *Bioinformatics (Oxford, England)*, 17(3), pp. 282–3.

Lim, C. *et al.* (2007) 'Clockwork orange encodes a transcriptional repressor important for circadian-clock amplitude in Drosophila.', *Current biology : CB*. NIH Public Access, 17(12), pp. 1082–9.

Linneweber, G. A. *et al.* (2014) 'Neuronal Control of Metabolism through Nutrient-Dependent Modulation of Tracheal Branching', *Cell*, 156(1–2), pp. 69–83.

Liu, S.-H. (2003), 'Diel vertical migration of zooplankton following optimal food intake under predation', *Journal of Plankton Research,* (25), pp. 1069-1077.

Liu, X. *et al.* (1988) 'Spatial and temporal expression of the period gene in Drosophila melanogaster.', *Genes & development*, 2(2), pp. 228–38.

Liu, X. *et al.* (1992) 'The period gene encodes a predominantly nuclear protein in adult Drosophila.', *The Journal of neuroscience : the official journal of the Society for Neuroscience*, 12(7), pp. 2735–44.

Lohmann, K. J. and Lohmann, C. M. F. (1996) 'Orientation and open-sea navigation in sea turtles', *J. Exp. Biol.*, (199), pp. 73–81.

Lohmann, K. J., Putman, N. F. and Lohmann, C. M. (2012) 'The magnetic map of hatchling loggerhead sea turtles', *Current Opinion in Neurobiology*, 22(2), pp. 336–342.

Lorenzon, S. *et al.* (2005) 'Role of biogenic amines and cHH in the crustacean hyperglycemic stress response', *Journal of Experimental Biology*, 208(17).

Lorenzon, S., Giulianini, P. G. and Ferrero, E. A. (1997) 'Lipopolysaccharide-Induced Hyperglycemia Is Mediated by CHH Release in Crustaceans', *General and Comparative Endocrinology*, 108(3), pp. 395–405.

Manfrin, C. *et al.* (2013) 'Application of D-Crustacean Hyperglycemic Hormone Induces Peptidases Transcription and Suppresses Glycolysis-Related Transcripts in the Hepatopancreas of the Crayfish Pontastacus leptodactylus — Results of a Transcriptomic Study', *PLoS ONE*, 8(6).

Marques, J. C. *et al.* (2003) 'Comparison of Talitrus saltator (Amphipoda, Talitridae) biology, dynamics, and secondary production in Atlantic (Portugal) and Mediterranean (Italy and Tunisia) populations', *Estuarine, Coastal and Shelf Science*. Academic Press, 58, pp. 127–148.

Marsden, I. D. D., Rainbow, P. S. S. and Smith, B. D. D. (2003) 'Trace metal concentrations in two New Zealand talitrid amphipods: effects of gender and reproductive state and implications for biomonitoring', *Journal of Experimental Marine Biology and Ecology*, 290(1), pp. 93–113.

Martin, G., Keller, R., *et al.* (1984) 'The hyperglycemic neuropeptide of the terrestrial isopod, Porcellio dilatatus. I. Isolation and characterization', *General and Comparative Endocrinology*, 55(2), pp. 208–216.

Martin, G., Jaros, P. P., *et al.* (1984) 'The hyperglycemic neuropeptide of the terrestrial isopod, Porcellio dilatatus. II. Immunocytochemical demonstration in neurosecretory structures of the nervous system', *General and Comparative Endocrinology*, 55(2), pp. 217–226.

Martin, G. (1988) 'Immunocytochemistry and ultrastructure of crustacean endocrine

cells', in *Thorndyke, M.C., Goldsworthy, G.J. (Eds.), Neurohormones in Invertebrates Seminar Series*. vol. 33. Cambridge University Press, pp. 79–96.

Martin, G., Maissiat, R. and Girard, P. (1983) 'Ultrastructure of the sinus gland and lateral cephalic nerve plexus in the isopod Ligia oceanica (Crustacea Oniscoidea).', *General and comparative endocrinology*, 52(1), pp. 38–50.

Martinek, S. *et al.* (2001) 'A role for the segment polarity gene shaggy/GSK-3 in the Drosophila circadian clock.', *Cell*, 105(6), pp. 769–79.

Masri, S. *et al.* (2013) 'Circadian acetylome reveals regulation of mitochondrial metabolic pathways', *Proceedings of the National Academy of Sciences*, 110(9), pp. 3339–3344.

Masri, S., Kinouchi, K. and Sassone-Corsi, P. (2015) 'Circadian clocks, epigenetics, and cancer', *Current Opinion in Oncology*, 27(1), pp. 50–56.

Masri, S. and Sassone-Corsi, P. (2014) 'Sirtuins and the circadian clock: Bridging chromatin and metabolism', *Science Signaling*, 7(342).

Matsumoto, A. *et al.* (2007) 'A functional genomics strategy reveals clockwork orange as a transcriptional regulator in the Drosophila circadian clock.', *Genes & development*. Cold Spring Harbor Laboratory Press, 21(13), pp. 1687–700.

McWilliam, H. *et al.* (2013) 'Analysis Tool Web Services from the EMBL-EBI.', *Nucleic acids research*, 41(Web Server issue), pp. W597-600.

Meissner, R.-A. *et al.* (2008) 'TIMELESS is an important mediator of CK2 effects on circadian clock function in vivo.', *The Journal of neuroscience : the official journal of the Society for Neuroscience*. NIH Public Access, 28(39), pp. 9732–40.

Mercier, A. *et al.* (2011) 'Lunar rhythms in the deep sea: evidence from the reproductive periodicity of several marine invertebrates.', *Journal of biological rhythms*, 26(1), pp. 82–6.

Merlin, C. *et al.* (2006) 'Evidence for a putative antennal clock in Mamestra brassicae: Molecular cloning and characterization of two clock genes -period and cryptochrome- in antennae', *Insect Molecular Biology*, 15(2), pp. 137–145.

Merlin, C. *et al.* (2007) 'An Antennal Circadian Clock and Circadian Rhythms in Peripheral Pheromone Reception in the Moth *Spodoptera littoralis*', *Journal of Biological Rhythms*, 22(6), pp. 502–514.

Merlin, C., Gegear, R. J. and Reppert, S. M. (2009) 'Antennal circadian clocks coordintae sun compass orientation in migratory monarch butterflies.', *Science (New York, N.Y.)*, 325(5948), pp. 1700–4.

Meschini, E., Gagliardo, A. and Papi, F. (2008) 'Lunar orientation in sandhoppers is affected by shifting both the moon phase and the daily clock', *Animal Behaviour*, 76(1), pp. 25–35.

Meyer-Bernstein, E. L. and Sehgal, A. (2001) 'Molecular Regulation of Circadian

Rhythms in Drosophila and Mammals', *The Neuroscientist*, 7(6), pp. 496–505.

Miyazaki, M. *et al.* (2011) 'Age-Associated Disruption of Molecular Clock Expression in Skeletal Muscle of the Spontaneously Hypertensive Rat', *PLoS ONE*. Edited by S. Yamazaki, 6(11), p. e27168.

Mohawk, J. A., Green, C. B. and Takahashi, J. S. (2012) 'Central and Peripheral Circadian Clocks in Mammals', *Annual Review of Neuroscience*, 35(1), pp. 445–462.

Montagné, N. *et al.* (2010) 'Molecular evolution of the crustacean hyperglycemic hormone family in ecdysozoans', *BMC Evolutionary Biology*. BioMed Central, 10(1), p. 62.

Morgan, E. (1991) 'An appraisal of tidal activity rhythms.', *Chronobiology international*, 8(4), pp. 283–306.

Mortazavi, A. *et al.* (2008) 'Mapping and quantifying mammalian transcriptomes by RNA-Seq.', *Nature methods*. Nature Publishing Group, 5(7), pp. 621–628.

Mosco, A. *et al.* (2008) 'Functional aspects of cHH C-terminal amidation in crayfish species', *Regulatory Peptides*, 147(1–3), pp. 88–95.

Myhre, S. *et al.* (2006) 'Additional Gene Ontology structure for improved biological reasoning', *Bioinformatics*. Morgan Kaufmann, San Fransisco, USA, 22(16), pp. 2020–2027.

Nagaraju, G. P. C. (2011) 'Reproductive regulators in decapod crustaceans: an overview', *Journal of Experimental Biology*, 214(1), pp. 3–16.

Nakagawa, T. and Guarente, L. (2014) SnapShot: Sirtuins, NAD, and Aging. *Cell Metabolism*, pp.192-192.

Nakahata, Y. *et al.* (2008) 'The NAD+-Dependent Deacetylase SIRT1 Modulates CLOCK-Mediated Chromatin Remodeling and Circadian Control', *Cell*, 134(2), pp. 329–340.

Nardi, M., Morgan, E. and Scapini, F. (2003) 'Seasonal variation in the free-running period in two Talitrus saltator populations from Italian beaches differing in morphodynamics and human disturbance', *Estuarine, Coastal and Shelf Science*, 58, pp. 199–206.

Nässel, D. R. *et al.* (1993) 'Pigment-dispersing hormone-like peptide in the nervous system of the flies Phormia and Drosophila: immunocytochemistry and partial characterization.', *The Journal of comparative neurology*, 331(2), pp. 183–98.

Naylor, E. (1958) 'Tidal and diurnal rhyhtms of locomotor activity in Carcinus maenas (L .)'. Journal of Expreimental Biology, 35: pp. 602-610.

Naylor, E. (1963) 'Temperature relationships of the locomotor rhythm of Carcinus.', *Journal of Experimental Biology*, (40), pp. 669–679.

Naylor, E. (1985) 'Tidally rhythmic behaviour of marine animals.', *Symposia of the*

Society for Experimental Biology, 39, pp. 63–93.

Naylor, E. (1996) 'Crab clockwork: the case for interactive circatidal and circadian oscillators controlling rhythmic locomotor activity of Carcinus maenas.', *Chronobiology international*, 13(3), pp. 153–61.

Naylor, E. (1997) 'Crab clocks rewound.', *Chronobiology international*, 14(4), pp. 427–30.

Naylor, E. (2013) *Chronobiology of Marine Organisms*. Cambridge: Cambridge University Press (Book).

Naylor, E. and Atkinson, R. J. (1972) 'Pressure and the rhythmic behaviour of inshore marine animals.', *Symposia of the Society for Experimental Biology*, 26, pp. 395–415.

Naylor, E. and Rejeki, S. R. I. (1996) 'Tidal migrations and rhythmic behaviour of sandbeach Crustacea'. Revista Chilena de Historia Natural, 69: pp. 475-484.

Nelson-Mora, J. *et al.* (2013) 'Putative pacemakers in the eyestalk and brain of the crayfish Procambarus clarkii show circadian oscillations in levels of mRNA for crustacean hyperglycemic hormone', *PLoS ONE*, 8(12).

Nesbit, K. T. and Christie, A. E. (2014) 'Identification of the molecular components of a Tigriopus californicus (Crustacea, Copepoda) circadian clock', *Comparative Biochemistry and Physiology Part D: Genomics and Proteomics*. Elsevier, 12, pp. 16–44.

Neumann, D. (1966) 'Die lunare und tägliche Schlüpfperiodik der Mücke Clunio', *Journal of Comparative Physiology*, 61, pp. 1–61.

Neumann, D. (1989) 'Circadian Components of Semilunar and Lunar Timing Mechanisms', *Journal of Biological Rhythms*, 4(2), pp. 173–182.

Newby, L. M. and Jackson, F. R. (1991) 'Drosophila ebony mutants have altered circadian activity rhythms but normal eclosion rhythms.', *Journal of neurogenetics*, 7(2–3), pp. 85–101.

Nguyen Ba, A. N. *et al.* (2009) 'NLStradamus: a simple Hidden Markov Model for nuclear localization signal prediction', *BMC Bioinformatics*, 10(1), p. 202.

Niefind, K. *et al.* (1998) 'Crystal structure of the catalytic subunit of protein kinase CK2 from Zea mays at 2.1 A resolution.', *The EMBO journal*, 17(9), pp. 2451–62.

Nussbaum, T. and Dircksen, H. (1995) 'Neuronal Pathways of Classical Crustacean Neurohormones in the Central Nervous System of the Neuronal pathways of classical crustacean neurohormones in the central nervous system of the woodlouse, Oniscus asellus (L.)', *Biological Sciences*, 347(1320), pp. 139–154.

O'Grady, J. F. (2013) *Molecular biology of timekeeping in the beach amphipod Talitrus saltator (Montagu). PhD Thesis*, Aberystwyth University.

O'Grady, J. F. *et al.* (2016) 'Identification and temporal expression of putative circadian clock transcripts in the amphipod crustacean Talitrus saltator', *PeerJ*, 4, p. e2555.

O'Malley, K. G. *et al.* (2013) 'Adaptive genetic markers discriminate migratory runs of Chinook salmon (Oncorhynchus tshawytscha) amid continued gene flow.', *Evolutionary applications*, 6(8), pp. 1184–94.

O'Malley, K. G. and Banks, M. a (2008) 'A latitudinal cline in the Chinook salmon (Oncorhynchus tshawytscha) Clock gene: evidence for selection on PolyQ length variants.', *Proceedings. Biological sciences / The Royal Society*, 275(1653), pp. 2813–2821.

O'Neill, J. S. *et al.* (2011) 'Circadian rhythms persist without transcription in a eukaryote', *Nature*, 469(7331), pp. 554–558.

O'Neill, J. S. *et al.* (2015) 'Metabolic molecular markers of the tidal clock in the marine crustacean Eurydice pulchra', *Current Biology*, 25(8), pp. R326–R327.

O'Neill, J. S. and Reddy, A. B. (2011) 'Circadian clocks in human red blood cells', *Nature*, 469(7331), pp. 498–503.

Olabarria, C. *et al.* (2009) 'Intraspecific diet shift in Talitrus saltator inhabiting exposed sandy beaches'. Estuarine, Coastal and Shelf Science, 84, pp. 282-288.

Oldach, M. J. *et al.* (2017) 'Transcriptome dynamics over a lunar month in a broadcast spawning acroporid coral', *Molecular Ecology*, 26(9), pp. 2514–2526.

Ollivaux, C. *et al.* (2009) 'Molecular and cellular specificity of post-translational aminoacyl isomerization in the crustacean hyperglycaemic hormone family', *FEBS Journal*. Blackwell Publishing Ltd, 276(17), pp. 4790–4802.

Orozco-Solis, R. and Sassone-Corsi, P. (2014) 'Circadian clock: linking epigenetics to aging', *Current Opinion in Genetics & Development*, 26, pp. 66–72.

Orozco-Solis, R. and Sassone-Corsi, P. (2014) 'Epigenetic control and the circadian clock: Linking metabolism to neuronal responses', *Neuroscience*, 264, pp. 76–87.

Oxley, P. R. *et al.* (2014) 'The Genome of the Clonal Raider Ant Cerapachys biroi', *Current Biology*, 24(4), pp. 451–458.

Pachter, L. (2011) 'Models for transcript quantification from RNA-seq'.

Palluault, M. (1954) 'Notes ecologiques sur le Talitrus saltator L.', *Archives de Zoologie Experimentale et Generale*, 91, pp. 105–129.

Papi, F., Gagliardo, A. and Meschini, E. (2006) 'Moon orientation in sandhoppers: effects of lighting treatments on the persistence of orientation ability', *Marine Biology*, 150(5), pp. 953–965.

Pardi, L. (1960) 'Innate components in the solar orientation of littoral amphipods.', *Cold Spring Harbor symposia on quantitative biology*. Cold Spring Harbor

Laboratory Press, 25, pp. 395–401.

Pardi, L. (2010) ‘Über die Orientierung von Tylos latreillii Aud. & Sav. (Isopoda terrestria)’, *Zeitschrift für Tierpsychologie*. Blackwell Publishing Ltd, 11(2), pp. 175–181.

Pardi, L. and Grassi, M. (1955) ‘Experimental modification of direction-finding in Talitrus saltator (Montagu) and Talorchestia deshayesei (Aud.) (Crustacea-Amphipoda).’, *Experientia*, 11(5), pp. 202–5.

Pardi, L. and Papi, F. (1952) ‘Die Sonne als Kompaß bei Talitrus saltator (Montagu), (Amphipoda, Talitridae)’, *Die Naturwissenschaften*. Springer-Verlag, 39(11), pp. 262–263.

Parisky, K. M. *et al.* (2008) ‘PDF Cells Are a GABA-Responsive Wake-Promoting Component of the Drosophila Sleep Circuit’, *Neuron*, 60(4), pp. 672–682.

Pegoraro, M. and Tauber, E. (2011) ‘Animal clocks: a multitude of molecular mechanisms for circadian timekeeping’, *Wiley Interdisciplinary Reviews: RNA*. John Wiley & Sons, Inc., 2(2), pp. 312–320.

Peschel, N. *et al.* (2009) ‘Light-Dependent Interactions between the Drosophila Circadian Clock Factors Cryptochrome, Jetlag, and Timeless’, *Current Biology*, 19(3), pp. 241–247.

Petersen, T. N. *et al.* (2011) ‘SignalP 4.0: discriminating signal peptides from transmembrane regions’, *Nature Methods*, 8(10), pp. 785–786.

Pett, J. P. *et al.* (2016) ‘Feedback Loops of the Mammalian Circadian Clock Constitute Repressilator.’, *PLoS computational biology*. Public Library of Science, 12(12), p. e1005266.

Pfeffer, S. E. and Wittlinger, M. (2016) ‘How to find home backwards? Navigation during rearward homing of *Cataglyphis fortis* desert ants’, *The Journal of Experimental Biology*, 219(14), pp. 2119–2126.

Pirooznia, S. K. *et al.* (2012) ‘Epigenetic Regulation of Axonal Growth of *Drosophila* Pacemaker Cells by Histone Acetyltransferase Tip60 Controls Sleep’, *Genetics*, 192(4), pp. 1327–1345.

De Pittà, C. *et al.* (2013) ‘The Antarctic Krill Euphausia superba Shows Diurnal Cycles of Transcription under Natural Conditions’, *PLoS ONE*. Edited by N. S. Foulkes. Public Library of Science, 8(7), p. e68652.

Ponting, C. P. and Aravind, L. (1997) ‘PAS: a multifunctional domain family comes to light.’, *Current biology : CB*, 7(11), pp. R674-7.

Powell, B. L. (1962) ‘Studies on Rhythmical Behaviour in Crustacea . I . Persistent Locomotor Activity in Juvenile *Carcinus maenas* (L.) and in *Ligia oceanica* (L .)’, *Crustaceana*, 4(1), pp. 42–46.

R_Core_Team (2013) ‘R: A language and environment for statistical computing.’, *R*

Foundation for Statistical Computing, Vienna, Austria.

Rainbow, P. S., Fialkowskit, W. and Smith, B. D. (1998) 'The Sandhopper *Talitrus saltator* as a Trace Metal Biomonitor in the Gulf of Gdansk , Poland', 2(3), pp. 193–200.

Ralph, M. R. *et al.* (1990) 'Transplanted suprachiasmatic nucleus determines circadian period.', *Science (New York, N.Y.)*, 247(4945), pp. 975–8.

Ramalho, C. B., Hastings, J. W. and Colepicolo, P. (1995) 'Circadian Oscillation of Nitrate Reductase Activity in *Gonyaulax polyedra* is Due to Changes in Cellular Protein Levels', (1 995), pp. 225–231.

Rao, K. R. *et al.* (1985) 'Characterization of a pigment-dispersing hormone in eyestalks of the fiddler crab *Uca pugilator*.', *Proceedings of the National Academy of Sciences of the United States of America*, 82(16), pp. 5319–22.

Rao, K. R. R. (2009) 'Crustacean Pigmentary-Effector Hormones: Chemistry and Functions of RPCH, PDH, and Related Peptides', *Oxford University Press*, 41(3), pp. 364–379.

Rao, K. R. and Riehm, J. P. (1989) 'The Pigment-Dispersing Hormone Family: Chemistry, Structure-Activity Relations, and Distribution', *The Biological Bulletin*. Marine Biological Laboratory, 177(2), pp. 225–229.

Reddy, A. B. *et al.* (2006) 'Circadian Orchestration of the Hepatic Proteome',

Current Biology, 16(11), pp. 1107–1115.

Refinetti, R., Lissen, G. C. and Halberg, F. (2007) 'Procedures for numerical analysis of circadian rhythms', *Biol Rhythm Res.*, 38(4), pp. 275–325.

Reid, D. G. and Naylor, E. (1989) 'Are there separate circatidal and circadian clocks', 52, pp. 1–6.

Reitzel, A. M., Tarrant, A. M. and Levy, O. (2013) 'Circadian clocks in the cnidaria: environmental entrainment, molecular regulation, and organismal outputs.', *Integrative and comparative biology*, 53(1), pp. 118–30.

Renn, S. C. *et al.* (1999) 'A *pdf* neuropeptide gene mutation and ablation of PDF neurons each cause severe abnormalities of behavioural circadian rhythms in *Drosophila*.', *Cell*, 99(7), pp. 791–802.

Reppert, S. M. (2006) 'A colourful model of the circadian clock.', *Cell*, 124(2), pp. 233–6.

Reppert, S. M. (2007) 'The ancestral circadian clock of monarch butterflies: Role in time-compensated sun compass orientation', *Cold Spring Harbor Symposia on Quantitative Biology*, 72(1), pp. 113–118.

Reppert, S. M., Gegear, R. J. and Merlin, C. (2010) 'Navigational mechanisms of migrating monarch butterflies.', *Trends in neurosciences*. NIH Public Access, 33(9),

pp. 399–406.

Reppert, S. M. and Weaver, D. R. (2002) ‘Coordination of circadian timing in mammals’, *Nature*, 418(6901), pp. 935–941.

Rice, P., Longden, I. and Bleasby, A. (2000) ‘EMBOSS: the European Molecular Biology Open Software Suite.’, *Trends in genetics : TIG*. Elsevier, 16(6), pp. 276–7.

Richier, B. *et al.* (2008) ‘The Clockwork Orange *Drosophila* Protein Functions as Both an Activator and a Repressor of Clock Gene Expression’, *Journal of Biological Rhythms*. Sage PublicationsSage CA: Los Angeles, CA, 23(2), pp. 103–116.

Ripperger, J. A. and Merrow, M. (2011) ‘Perfect timing: Epigenetic regulation of the circadian clock’, *FEBS Letters*, 585(10), pp. 1406–1411.

Robinson, R. (2008) ‘In monarchs, Cry2 is king of the clock.’, *PLoS biology*. Public Library of Science, 6(1), p. e12.

Roenneberg, T. (1995) ‘The effects of light on the *Gonyaulax* circadian system.’,

Ciba Foundation symposium, 183, pp. 117-27-33.

Roenneberg, T. and Taylor, W. (1994) ‘Light-induced phase responses in *Gonyaulax* are drastically altered by creatine.’, *Journal of biological rhythms*, 9(1), pp. 1–12.

Rothe, H. *et al.* (1991) ‘Purified crustacean enkephalin inhibits release of hyperglycemic hormone in the crab *Carcinus maenas* L.’, *Comparative Biochemistry and Physiology Part C: Comparative Pharmacology*, 99(1–2), pp. 57–62.

Rothschild, L. J. (1994) ‘Elevated CO2: impact on diurnal patterns of photosynthesis in natural microbial ecosystems.’, *Advances in space research : the official journal of the Committee on Space Research (COSPAR)*, 14(11), pp. 285–9.

Rubin, E. B. *et al.* (2006) ‘Molecular and phylogenetic analyses reveal mammalian-like clockwork in the honey bee (*Apis mellifera*) and shed new light on the molecular evolution of the circadian clock.’, *Genome research*, 16(11), pp. 1352–65.

Rutila, J. E. *et al.* (1998) ‘CYCLE is a second bHLH-PAS clock protein essential for circadian rhythmicity and transcription of *Drosophila period* and *timeless*.’, *Cell*, 93(5), pp. 805–14.

Saez, L. and Young, M. W. (1996) ‘Regulation of nuclear entry of the *Drosophila* clock proteins period and *timeless*.’, *Neuron*, 17(5), pp. 911–20.

Sales, G. *et al.* (2017) ‘KrillDB: A de novo transcriptome database for the Antarctic krill (*Euphausia superba*)’, *PLOS ONE*. Edited by C. Bertolucci, 12(2), p. e0171908.

Sandrelli, F. *et al.* (2008) ‘Comparative analysis of circadian clock genes in insects’, *Insect Molecular Biology*, 17(5), pp. 447–463.

Santos, E. A. *et al.* (1997) ‘Evidence for the involvement of the crustacean hyperglycemic hormone in the regulation of lipid metabolism.’, *Physiological*

zoology, 70(4), pp. 415–20.

Santos, E. A. *et al.* (2001) 'Effects of serotonin and fluoxetine on blood glucose regulation in two decapod species.', *Brazilian journal of medical and biological research=Revista brasileira de pesquisas medicas e biologicas*, 34(1), pp. 75–80.

Santos, E. A. and Keller, R. (1993) 'Regulation of circulating levels of the crustacean hyperglycemic hormone: evidence for a dual feedback control system', *J Comp Physiol B*, 163, pp. 374–379.

Sarojini, R., Nagabhushanam, R. and Fingerman, M. (1995) 'Dopaminergic and Enkephalinergic Involvement in the Regulation of Blood Glucose in the Red Swamp Crayfish, *Procambarus clarkii*', *General and Comparative Endocrinology*, 97(1), pp. 160–170.

Sathyanarayanan, S. *et al.* (2004) 'Post-translational regulation of *Drosophila* PERIOD protein by protein phosphatase 2A.', *Cell*, 116(4), pp. 603–15.

Sauman, I. and Reppert, S. M. (1996) 'Circadian clock neurons in the silkmoth *Antheraea pernyi*: novel mechanisms of Period protein regulation.', *Neuron*, 17(5), pp. 889–900.

Sbragaglia, V. *et al.* (2015) 'Identification, Characterization, and Diel Pattern of Expression of Canonical Clock Genes in *Nephrops norvegicus* (Crustacea: Decapoda) Eyestalk', *PLOS ONE*. Edited by C. Bertolucci. Public Library of Science, 10(11), p. e0141893.

Scapini, F. *et al.* (1999) 'Solar orientation of adult and laboratory-born juvenile sandhoppers: inter- and intra-population variation', *Journal of Experimental Marine Biology and Ecology*. Elsevier, 238(1), pp. 107–126.

Scapini, F. *et al.* (2005) 'The role of the biological clock in the sun compass orientation of free-running individuals of *Talitrus saltator*', *Animal Behaviour*. Academic Press, 69(4), pp. 835–843.

Scapini, F., Campacci, F. and Audoglio, M. (1999) 'Variation among Natural Populations of *Talitrus saltator* (Amphipoda): Morphometric Analysis', *Crustaceana*. Brill, pp. 659–672.

Scharrer, B., Florey, E. and Stefano, G. B. (1991) *Comparative aspects of neuropeptide function*. Manchester University Press.

Schuckel, J., Siwicki, K. K. and Stengl, M. (2007) 'Putative circadian pacemaker cells in the antenna of the hawkmoth *Manduca sexta'*, *Cell and Tissue Research*, 330(2), pp. 271–278.

Schultz, J. *et al.* (1998) 'SMART, a simple modular architecture research tool: identification of signaling domains.', *Proceedings of the National Academy of Sciences of the United States of America*, 95(11), pp. 5857–64.

Sedlmeier, D. (1985) 'Mode of Action of the Crustacean Hyperglycemic Hormone', *American Zoologist*, 25(1), pp. 223–232.

Sedlmeier, D. (1987) ‘The role of hepatopancreatic glycogen in the action of the crustacean hyperglycemic hormone (CHH)’, *Comparative Biochemistry and Physiology Part A: Physiology*, 87(2), pp. 423–425.

Sedlmeier, D. (1988) ‘The crustacean hyperglycemic hormone (CHH) releases amylase from the crayfish midgut gland.’, *Regulatory peptides*, 20(2), pp. 91–8.

Sedlmeier, D. and Keller, R. (1981) ‘The mode of action of the crustacean neurosecretory hyperglycemic hormone: I. Involvement of cyclic nucleotides’, *General and Comparative Endocrinology*, 45(1), pp. 82–90.

Sehgal, A. *et al.* (1994) ‘Loss of circadian behavioral rhythms and per RNA oscillations in the *Drosophila* mutant timeless.’, *Science (New York, N.Y.)*, 263(5153), pp. 1603–6.

Sehgal, A. (1995) ‘Genetic dissection of the circadian clock: A timeless story’, *Seminars in Neuroscience*. Academic Press, 7(1), pp. 27–35.

Serrano, L. *et al.* (2003) ‘Putative involvement of crustacean hyperglycemic hormone isoforms in the neuroendocrine mediation of osmoregulation in the crayfish Astacus leptodactylus.’, *The Journal of experimental biology*, 206(Pt 6), pp. 979– 988.

Shafer, O. T. *et al.* (2006) ‘Reevaluation of *Drosophila melanogaster’s* neuronal circadian pacemakers reveals new neuronal classes.’, *The Journal of comparative neurology*. NIH Public Access, 498(2), pp. 180–93.

Shafer, O. T. and Yao, Z. (2014) ‘Pigment-dispersing factor signalling and circadian rhythms in insect locomotor activity’, *Current Opinion in Insect Science*, 1, pp. 73–80.

Shang, Y., Griffith, L. C. and Rosbash, M. (2008) ‘Light-arousal and circadian photoreception circuits intersect at the large PDF cells of the *Drosophila* brain’,

Proceedings of the National Academy of Sciences, 105(50), pp. 19587–19594.

Sheeba, V. *et al.* (2008) ‘Large ventral lateral neurons modulate arousal and sleep in Drosophila.’, *Current biology : CB*, 18(20), pp. 1537–45.

Simon, J.-C. *et al.* (2011) ‘Genomics of environmentally induced phenotypes in 2 extremely plastic arthropods.’, *The Journal of heredity*, 102(5), pp. 512–25.

Siwicki, K. K. *et al.* (1988) ‘Antibodies to the period gene product of *Drosophila* reveal diverse tissue distribution and rhythmic changes in the visual system.’, *Neuron*, 1(2), pp. 141–50.

Solt, L. A. *et al.* (2012) ‘Regulation of circadian behaviour and metabolism by synthetic REV-ERB agonists.’, *Nature*. NIH Public Access, 485(7396), pp. 62–8.

Solt, L. A., Kojetin, D. J. and Burris, T. P. (2011) ‘The REV-ERBs and RORs: molecular links between circadian rhythms and lipid homeostasis.’, *Future medicinal chemistry*. NIH Public Access, 3(5), pp. 623–38.

Sonnenberg, A., Watt, F. M. (2009) ‘Integrin Special Issue‘, *Journal of Cell Science’,* (122), p. 157.

Soyez, D. *et al.* (1994) ‘Evidence for a conformational polymorphism of invertebrate neurohormones. D-amino acid residue in crustacean hyperglycemic peptides.’, *The Journal of biological chemistry*, 269(28), pp. 18295–18298.

Soyez, D. *et al.* (1998) ‘Demonstration of a cell-specific isomerization of invertebrate neuropeptides.’, *Neuroscience*, 82(3), pp. 935–42.

Soyez, D. *et al.* (2000) ‘L to D amino acid isomerization in a peptide hormone is a late post-translational event occurring in specialized neurosecretory cells.’, *The Journal of biological chemistry*, 275(48), pp. 37870–5.

Spanings-Pierrot, C. *et al.* (2000) ‘Involvement of Crustacean Hyperglycemic Hormone in the Control of Gill Ion Transport in the Crab Pachygrapsus marmoratus’, *General and Comparative Endocrinology*, 119(3), pp. 340–350.

Stahl, B. A. *et al.* (2015) ‘A Transcriptomic Analysis of Cave, Surface, and Hybrid Isopod Crustaceans of the Species Asellus aquaticus.’, *PloS one*. Public Library of Science, 10(10), p. e0140484.

Stanewsky, R. (2002) ‘Clock mechanisms in Drosophila.’, *Cell and tissue research*, 309(1), pp. 11–26.

Stanewsky, R. (2007) ‘Analysis of Rhythmic Gene Expression in Adult Drosophila Using the Firefly Luciferase Reporter Gene’, in. Humana Press, pp. 131–142.

Stefanini, M., De Martino, C. and Zamboni, L. (1967) ‘Fixation of ejaculated spermatozoa for electron microscopy.’, *Nature*, 216(5111), pp. 173–4.

Stentiford, G. . *et al.* (2001) ‘Carbohydrate Dynamics and the Crustacean Hyperglycemic Hormone (CHH): Effects of Parasitic Infection in Norway Lobsters (Nephrops norvegicus)’, *General and Comparative Endocrinology*, 121(1), pp. 13–22.

Stentiford, G. . *et al.* (2002) ‘Infection by a Hematodinium-like parasitic dinoflagellate causes Pink Crab Disease (PCD) in the edible crab Cancer pagurus’, *Journal of Invertebrate Pathology*, 79(3), pp. 179–191.

Stentiford, G., Neil, D. and Coombs, G. (2000) ‘Alterations in the biochemistry and ultrastructure of the deep abdominal flexor muscle of the Norway lobster Nephrops norvegicus during infection by a parasitic dinoflagellate of the genus Hematodinium’, *Diseases of Aquatic Organisms*, 42(2), pp. 133–141.

Stockmann, R., Laverdure, A. M. and Breuzet, M. (1997) ‘Localization of a crustacean hyperglycemic hormone-like immunoreactivity in the neuroendocrine system of Euscorpius carpathicus (L.) (Scorpionida, Chactidae).’, *General and comparative endocrinology*, 106(3), pp. 320–6.

Stoleru, D. *et al.* (2004) ‘Coupled oscillators control morning and evening locomotor behaviour of Drosophila’, *Nature*, 431(7010), pp. 862–868.

Strauss, J. and Dircksen, H. (2010) ‘Circadian clocks in crustaceans: identified neuronal and cellular systems’, *Frontiers in bioscience (Landmark edition)*, 15, pp. 1040–74.

Sugama, N. *et al.* (2008) ‘Moonlight affects nocturnal Period2 transcript levels in the pineal gland of the reef fish Siganus guttatus.’, *Journal of pineal research*, 45(2), pp. 133–41.

Suh, J. and Jackson, F. R. (2007) ‘Drosophila Ebony Activity Is Required in Glia for the Circadian Regulation of Locomotor Activity’, *Neuron*. NIH Public Access, 55(3), pp. 435–47.

Takemura, A. (2001) ‘Lunar-synchronised spawning rhythm in coral reef fishes’, pp. 19–22.

Talsma, A. D. *et al.* (2012) ‘Remote control of renal physiology by the intestinal neuropeptide pigment-dispersing factor in *Drosophila*’, *Proceedings of the National Academy of Sciences*, 109(30), pp. 12177–12182.

Tamura, K. *et al.* (2011) ‘MEGA5: molecular evolutionary genetics analysis using maximum likelihood, evolutionary distance, and maximum parsimony methods.’, *Molecular biology and evolution*. Oxford University Press, 28(10), pp. 2731–9.

Tamura, K. *et al.* (2013) ‘MEGA6: Molecular Evolutionary Genetics Analysis version 6.0.’, *Molecular biology and evolution*. Oxford University Press, 30(12), pp. 2725–9.

Tataroglu, O. and Emery, P. (2014) ‘Studying circadian rhythms in Drosophila melanogaster.’, *Methods (San Diego, Calif.)*. NIH Public Access, 68(1), pp. 140–50.

Taylor, B. L. and Zhulin, I. B. (1999) ‘PAS domains: internal sensors of oxygen, redox potential, and light.’, *Microbiology and molecular biology reviews : MMBR*, 63(2), pp. 479–506.

Terrapon, N. *et al.* (2014) ‘Molecular traces of alternative social organization in a termite genome’, *Nature Communications*, 5(2).

Teschke, M. *et al.* (2011) ‘A circadian clock in Antarctic krill: an endogenous timing system governs metabolic output rhythms in the euphausid species Euphausia superba.’, *PloS one*. Edited by M. N. Nitabach, 6(10), p. e26090.

Tessmar-Raible, K., Raible, F. and Arboleda, E. (2011) ‘Another place, another timer: Marine species and the rhythms of life.’, *BioEssays : news and reviews in molecular, cellular and developmental biology*, 33(3), pp. 165–72.

Thuiller, W. (2007) ‘Biodiversity: climate change and the ecologist.’, *Nature*, 448(7153), pp. 550–2.

Tilden, A. *et al.* (2001) ‘Effect of melatonin on hemolymph glucose and lactate levels in the fiddler crab Uca pugilator.’, *The Journal of experimental zoology*, 290(4), pp. 379–83.

Tilden, A. R. *et al.* (2011) 'Genomic identification of a putative circadian system in the cladoceran crustacean Daphnia pulex.', *Comparative biochemistry and physiology. Part D, Genomics & proteomics*. NIH Public Access, 6(3), pp. 282–309.

Toma, D. P. *et al.* (2002) 'Identification of genes involved in Drosophila melanogaster geotaxis, a complex behavioral trait', *Nature Genetics*, 31(4), pp. 349–353.

Tomioka, K. and Matsumoto, A. (2010) 'A comparative view of insect circadian clock systems', *Cellular and Molecular Life Sciences*. SP Birkhäuser Verlag Basel, 67(9), pp. 1397–1406.

Tongiorgi, P. (1969) 'Evidence of a moon orientation in the wolf spider, Arctosa variana CL Koch (Araneae, Lycosidae)', *Bulletin du Muséum national d'histoire naturelle*, (41), pp. 243–249.

Towne, W. F. *et al.* (2017) 'Honeybees use the skyline in orientation', *The Journal of Experimental Biology*, 220(13), pp. 2476–2485.

Ugolini, A. (2001) 'Relationship between compass systems of orientation in equatorial sandhoppers', *Animal Behaviour*, 62(2), pp. 193–199.

Ugolini, A. *et al.* (2004) 'Mediterranean Talitrus saltator (Crustacea, Amphipoda) as a biomonitor of heavy metals contamination.', *Marine pollution bulletin*, 48(5–6), pp. 526–532.

Ugolini, A. *et al.* (2005) 'Moon orientation in adult and young sandhoppers under artificial light.', *Proceedings. Biological sciences / The Royal Society*, 272(1577), pp. 2189–2194.

Ugolini, A. (2006) 'Equatorial sandhoppers use body scans to detect the earth's magnetic field.', *Journal of comparative physiology. A, Neuroethology, sensory, neural, and behavioral physiology*, 192(1), pp. 45–49.

Ugolini, A. *et al.* (2007) 'Locomotor activity rhythm and sun compass orientation in the sandhopper Talitrus saltator are related.', *Journal of comparative physiology. A, Neuroethology, sensory, neural, and behavioral physiology*, 193(12), pp. 1259–63.

Ugolini, A. *et al.* (2008) 'The amphipod Talitrus saltator as a bioindicator of human trampling on sandy beaches.', *Marine environmental research*, 65(4), pp. 349–57.

Ugolini, A. *et al.* (2009) 'Seawater Ca2+ concentration influences solar orientation in Talitrus saltator (Crustacea, Amphipoda).', *The Journal of experimental biology*, 212(Pt 6), pp. 797–801.

Ugolini, A., Pasquali, V., *et al.* (2012) 'Behavioural responses of the supralittoral amphipod Talitrus saltator (Montagu) to trace metals contamination.', *Ecotoxicology (London, England)*, 21(1), pp. 139–147.

Ugolini, A., Perra, G., *et al.* (2012) 'Sandhopper Talitrus saltator (Montagu) as a bioindicator of contamination by polycyclic aromatic hydrocarbons.', *Bulletin of environmental contamination and toxicology*, 89(6), pp. 1272–6.

Ugolini, A. (2014) ‘Optic flow and sea-land orientation in the sandhopper Talitrus saltator.’, *The Journal of experimental biology*, 217(Pt 12), pp. 2041–3.

Ugolini, A. (2014) ‘Optic flow and sea - land orientation in the sandhopper Talitrus saltator (Montagu).’, *The Journal of experimental biology*, 217(April), pp. 2041–3.

Ugolini, A. *et al.* (2015) ‘Salt concentration and solar orientation in two supralittoral sandhoppers: Talitrus saltator (Montagu) and Talorchestia ugolinii Bellan Santini and Ruffo.’, *Journal of comparative physiology. A, Neuroethology, sensory, neural, and behavioral physiology*, 201(5), pp. 455–60.

Ugolini, A., Castellini, C. and Mercatelli, L. (2007) ‘Moon orientation on moonless nights’, *Animal Behaviour*, 73(3), pp. 453–456.

Ugolini, A. and Chiussi, R. (1996) ‘Astronomical orientation and learning in the earwig Labidura riparia.’, *Behavioural processes*, 36(2), pp. 151–61.

Ugolini, A., Fantini, T. and Innocenti, R. (2003) ‘Orientation at night: an innate moon compass in sandhoppers (Amphipoda: Talitridae).’, *Proceedings. Biological sciences*, 270(1512), pp. 279–81.

Ugolini, A., Galanti, G. and Mercatelli, L. (2009) ‘Difference in skylight intensity is a new celestial cue for sandhopper orientation (Amphipoda, Talitridae)’, *Animal Behaviour*. Elsevier Ltd, 77(1), pp. 171–175.

Ugolini, A., Galanti, G. and Mercatelli, L. (2012) ‘The skylight gradient of luminance helps sandhoppers in sun and moon identification.’, *The Journal of experimental biology*, 215(Pt 16), pp. 2814–9.

Ugolini, A. and Macchi, T. (1988) ‘Learned component in the solar orientation of Talitrus saltator Montagu (Amphipoda: Talitridae)’, *Journal of Experimental Marine Biology and Ecology*. Elsevier, 121(1), pp. 79–87.

Ugolini, A., Melis, C. and Innocenti, R. (1999) ‘Moon orientation in adult and young sandhoppers’, *Journal of Comparative Physiology A: Sensory, Neural, and Behavioral Physiology*. Springer-Verlag, 184(1), pp. 9–12.

Ugolini, A., Tiribilli, B. and Boddi, V. (2002) ‘The sun compass of the sandhopper Talitrus saltator: the speed of the chronometric mechanism depends on the hours of light.’, *The Journal of experimental biology*, 205(Pt 20), pp. 3225–30.

Ungherese, G. *et al.* (2010) ‘Trace metal contamination of Tuscan and eastern Corsican coastal supralittoral zones: The sandhopper Talitrus saltator (Montagu) as a biomonitor.’, *Ecotoxicology and environmental safety*. Elsevier, 73(8), pp. 1919–1924.

Ungherese, G. *et al.* (2012) ‘PBDEs in the supralittoral environment: the sandhopper Talitrus saltator (Montagu) as biomonitor?’, *Chemosphere*. Elsevier Ltd, 86(3), pp. 223–227.

Ungherese, G. and Ugolini, A. (2009) ‘Sandhopper solar orientation as a behavioural biomarker of trace metals contamination.’, *Environmental pollution (Barking,*

Essex :1987). Elsevier Ltd, 157(4), pp. 1360–4.

Vandegehuchte, M. B. *et al.* (2010) 'Direct and transgenerational impact on Daphnia magna of chemicals with a known effect on DNA methylation', *Comparative Biochemistry and Physiology Part C: Toxicology & Pharmacology*, 151(3), pp. 278–285.

Vandegehuchte, M. B. and Janssen, C. R. (2011) 'Epigenetics and its implications for ecotoxicology.', *Ecotoxicology (London, England)*, 20(3), pp. 607–24.

Vitaterna, M. H. *et al.* (1994) 'Mutagenesis and mapping of a mouse gene, Clock, essential for circadian behavior.', *Science (New York, N.Y.)*, 264(5159), pp. 719–25.

Vosshall, L. B. *et al.* (1994) 'Block in nuclear localization of period protein by a second clock mutation, timeless.', *Science (New York, N.Y.)*, 263(5153), pp. 1606–9.

W.D. Hoyt (1927) 'The periodic fruiting of Dictyota and its relation to th envirnonment.', *Am J Bot*, (14), pp. 592–619.

Wagner, G. P., Kin, K. and Lynch, V. J. (2012) 'Measurement of mRNA abundance using RNA-seq data: RPKM measure is inconsistent among samples.', *Theory in biosciences=Theorie in den Biowissenschaften*, 131(4), pp. 281–5.

Walther, G.-R. *et al.* (2002) 'Ecological responses to recent climate change', *Nature*, 416(6879), pp. 389–395.

Walton, K. M. *et al.* (2009) 'Selective inhibition of casein kinase 1 epsilon minimally alters circadian clock period.', *The Journal of pharmacology and experimental therapeutics*. American Society for Pharmacology and Experimental Therapeutics, 330(2), pp. 430–9.

Watling, L. and Thiel, M. (2013) *The natural history of the Crustacea*. Oxford University Press.

Way, M. (2016) Journal of Cell Science is going green, *Journal of Cell Science*, (129), p. 3519.

Webster (1996) 'Measurement of crustacean hyperglycaemic hormone levels in the edible crab Cancer pagurus during emersion stress', *The Journal of experimental biology*, 199(Pt 7), pp. 1579–85.

Webster, S. G. (1993) 'High-Affinity Binding of Putative Moult-Inhibiting Hormone (MIH) and Crustacean Hyperglycaemic Hormone (CHH) to Membrane-Bound Receptors on the Y-Organ of the Shore Crab Carcinus maenus', *Proceedings of the Royal Society of London B: Biological Sciences*, 251(1330).

Webster, S. G., Dircksen, H. and Chung, J. S. (2000) 'Endocrine cells in the gut of the shore crab Carcinus maenas immunoreactive to crustacean hyperglycaemic hormone and its precursor-related peptide.', *Cell and tissue research*, 300(1), pp. 193–205.

Webster, S. G., Keller, R. and Dircksen, H. (2012) 'The CHH-superfamily of

multifunctional peptide hormones controlling crustacean metabolism, osmoregulation, moulting, and reproduction', *General and Comparative Endocrinology*, 175(2), pp. 217–233.

Wehner, R. *et al.* (2016) 'Steering intermediate courses: desert ants combine information from various navigational routines', *Journal of Comparative Physiology A*, 202(7), pp. 459–472.

Welsh, D. K. *et al.* (1995) 'Individual neurons dissociated from rat suprachiasmatic nucleus express independently phased circadian firing rhythms.', *Neuron*, 14(4), pp. 697–706.

Wilcockson, D. C. *et al.* (2002) 'Is crustacean hyperglycaemic hormone precursor-related peptide a circulating neurohormone in crabs?', *Cell and Tissue Research*. Springer-Verlag, 307(1), pp. 129–138.

Wilcockson, D. C. *et al.* (2011) 'A Novel Form of Pigment-Dispersing Hormone in the Central Nervous System of the Intertidal Marine Isopod, Eurydice pulchra (Leach)', *The Journal of Comparative Neurology*, 519(3), pp. 562–575.

Wilcockson, D. and Zhang, L. (2008) 'Circatidal clocks', *Current biology*, 18(17), p. pR753–R755.

Williams, J. A. (1978) 'The annual pattern of reproduction of Talitrus saltator (Crustacea: Amphipoda: Talitridae)', *Journal of Zoology*. Blackwell Publishing Ltd, 184(2), pp. 231–244.

Williams, J. A. (1980a) 'Environmental influence on the locomotor activity rhythm of Talitrus saltator (Crustacea: Amphipoda)', *Marine Biology*. Springer-Verlag, 57(1), pp. 7–16.

Williams, J. A. (1980b) 'The effect of dusk and dawn on the locomotor activity rhythm of Talitrus saltator (Montagu) (Crustacea: Amphipoda)', *Journal of Experimental Marine Biology and Ecology*. Elsevier, 42(3), pp. 285–297.

Williams, J. A. (1982) 'A circadian rhythm of oxygen consumption in the sand beach amphipod Talitrus saltator (Montagu)', *Journal of Experimental Marine Biology and Ecology*, 57(2–3), pp. 125–134.

Williams, J. A. (1983) 'The endogenous locomotor activity rhythm of four supralittoral peracarid crustace', *Journal of the Marine Biological Association of the United Kingdom*. Cambridge University Press, 63(2), p. 481.

Williams, J. A. (1985) 'The role of photoperiod in the initiation of breeding and brood development in the amphipod Talitrus saltator Montagu', *Journal of Experimental Marine Biology and Ecology*. Elsevier, 86(1), pp. 59–72.

Williams, J. A. (1995) 'Burrow-Zone Distribution of the Supralittoral Amphipod Talitrus saltator on Derbyhaven Beach, Isle of Man: A Possible Mechanism for Regulating Desiccation Stress?', *Journal of Crustacean Biology*. Oxford University PressThe Crustacean Society, 15(3), p. 466.

Williamson, D. I. (1951) ‘Studies in the biology of Talitridae (Crustacea, Amphipoda): visual orientation in Talitrus saltator’, *Journal of the Marine Biological Association of the United Kingdom*. Cambridge University Press, 30(1), pp. 91–99.

Wolf, H. (2011) ‘Odometry and insect navigation.’, *The Journal of experimental biology*, 214(Pt 10), pp. 1629–41.

Yang, J.-S. *et al.* (2006) ‘Molecular cloning of Clock cDNA from the prawn, Macrobrachium rosenbergii’, *Brain Research*, 1067(1), pp. 13–24.

Yang, W.-J. J., Aida, K. and Nagasawa, H. (1999) ‘Characterization of Chromatophorotropic Neuropeptides from the Kuruma PrawnPenaeus japonicus’, *General and Comparative Endocrinology*, 114(3), pp. 415–424.

Yasuda, A. *et al.* (1994) ‘Characterization of Crustacean Hyperglycemic Hormone from the Crayfish (Procambarus clarkii): Multiplicity of Molecular Forms by Stereoinversion and Diverse Functions’, *General and Comparative Endocrinology*, 95(3), pp. 387–398.

Young, M. W. and Kay, S. A. (2001) ‘Time zones: a comparative genetics of circadian clocks.’, *Nature reviews. Genetics*, 2(9), pp. 702–15.

Young, M. W. and Kay, S. A. (2001) ‘Time zones: a comparative genetics of circadian clocks.’, *Nature reviews. Genetics*, 2(9), pp. 702–715.

Yu, W. and Hardin, P. E. (2007) ‘Use of Firefly Luciferase Activity Assays to Monitor Circadian Molecular Rhythms In Vivo and In Vitro’, in *Methods in molecular biology (Clifton, N.J.)*, pp. 465–480.

Yuan, Q. *et al.* (2007) ‘Insect Cryptochromes: Gene Duplication and Loss Define Diverse Ways to Construct Insect Circadian Clocks’, *Molecular Biology and Evolution*. Sinauer Associates, Sunderland (MA), 24(4), pp. 948–955.

Yue, M. *et al.* (2017) ‘Genetic and epigeneticregulations of mammalian circadian rhythms.’, *Yi chuan=Hereditas*, 39(12), pp. 1122–1137.

Zantke, J. *et al.* (2013) ‘Circadian and circalunar clock interactions in a marine annelid.’, *Cell reports*. The Authors, 5(1), pp. 99–113.

Zerr, D. M. *et al.* (1990) ‘Circadian fluctuations of period protein immunoreactivity in the CNS and the visual system of Drosophila.’, *The Journal of neuroscience : the official journal of the Society for Neuroscience*, 10(8), pp. 2749–62.

Zhan, S. *et al.* (2011) ‘The Monarch Butterfly Genome Yields Insights into Long-Distance Migration’, *Cell*, 147(5), pp. 1171–1185.

Zhang, L. *et al.* (2013) ‘Dissociation of circadian and circatidal timekeeping in the marine crustacean Eurydice pulchra.’, *Current biology : CB*. Elsevier, 23(19), pp. 1863–73.

Zhao, Y. *et al.* (2005) ‘Mutational analysis of the n-terminus inSchistocerca gregaria ion-transport peptide expressed inDrosophila Kc1 cells’, *Archives of Insect*

Biochemistry and Physiology. Wiley Subscription Services, Inc., A Wiley Company, 58(1), pp. 27–38.

Zheng, X. *et al.* (2009) 'An isoform-specific mutant reveals a role of PDP1 epsilon in the circadian oscillator.', *The Journal of neuroscience : the official journal of the Society for Neuroscience*. NIH Public Access, 29(35), pp. 10920–7.

Zhu, H. *et al.* (2005) 'The two CRYs of the butterfly.', *Current biology : CB*. Elsevier, 15(23), pp. R953-4.

Zhu, H. *et al.* (2008) 'Cryptochromes define a novel circadian clock mechanism in monarch butterflies that may underlie sun compass navigation', *PLoS Biology*, 6(1), pp. 0138–0155.

Zhulin, I. B., Taylor, B. L. and Dixon, R. (1997) 'PAS domain S-boxes in Archaea, Bacteria and sensors for oxygen and redox.', *Trends in biochemical sciences*, 22(9), pp. 331–3.

Zordan, M. A. and Sandrelli, F. (2015) 'Circadian Clock Dysfunction and Psychiatric Disease: Could Fruit Flies have a Say?', *Frontiers in Neurology*. Frontiers, 6, p. 80.

Zou, H.-S. *et al.* (2003) 'Dopaminergic regulation of crustacean hyperglycemic hormone and glucose levels in the hemolymph of the crayfishProcambarus clarkii', *Journal of Experimental Zoology*, 298A(1), pp. 44–52.

Zwiebel, L. J. *et al.* (1991) 'Circadian oscillations in protein and mRNA levels of the period gene of Drosophila melanogaster'.

APPENDIX A

Additional Figures and Tables

Table A.1: Commonly used oligonucleotide primer sequences.

Primer name	**Oligonucleotide sequence**
M13 forward	GTAAAACGACGGCCAG
M13 reverse	CAGGAAACAGCTATGAC
T7	TAATACGACTCACTATAGG

Table A.2: Oligonucleotide primers used for full length sequence confirmation for the *T. saltator* core clock gene transcripts.

Experiment	**Primer name**	**Oligonucleotide sequence**
Sequence confirmation		
Talclk	TS_Clk 1 F	CCCAGCTGCTGAGGGAGAT
	TS_Clk 1R	CGAAGCTTTGGATTTTCTGG
	TS_Clk 2F	CCAAAGCTTCGAAGAACAATG
	TS_Clk 2R	GAAGCATTGGGTCACTCTCTG
	TS_Clk 3F	CCCAATGCTTCTGAGCAGC
	TS_Clk 3R	GAGGAGCAATCGATCGAAGA
	TS_Clk4F	GATTGCTCCTCTATCAGAAAACTATGA
	TS_Clk4R	GGGGGACTATTACTTCTTCTTTTG
	TS_Clk5F	AATAGTCCCCCTGAAATCTCAAA
	TS_Clk5R	GATTCTGCTGCCGAGAATTT
	TS_Clk6F	GCAGCAGAATCTTGCTCAAC
	TS_Clk6R	ATCCCATCAAAGGAGCCAT
	TS_Clk7F	TTTGATGGGATCTGGTGATG
	TS_Clk7R	CAGGATTAAATCCCTTATTTTTTCG
	TS_Clk8F	ATTTAATCCTGCTGATGATTTTTTTG
	TS_Clk8R	GACCATGATTGTCCTCAAAATC
	TS_Clk9F	CAATCATGGTCAAAAACATAATACTTC
	TS_Clk9R	GCCGAGCCGATGAATTTC
	TS_Clk10F	GGAGAAATTCATCGGCTCG
	TS_Clk10R	TCTAGATAGATGACTGGTTTCTTCAAC
Taltim	Tim f1 forward	CACTGCTTGTCTTCCATCAG
	Tim f1 reverse	GTAGTAGGTGCCACCAAACC
	Tim f2 forward	TCGCAAGCATTACAATGC
	Tim f2 reverse	ATCCATAGCAGAGAGGGACA
Talcry2	TalDegen Cry2 F	GARGARYTIGGNTTYGAYAC
	TalDegen Cry2 F	GARMGIAARGCNTGGGTNGC
	TalDegen Cry2 R	ATRWARTCICCRTTNGGRTC
	TalDegen Cry2 R	ACYTTCATNCCYTCYTCCCA
	TS Cry2 Seq F1	GAAAGTTAAAATGTCACCAAATAAAA
	TS Cry2 Seq R1	AAAGGCTCAGGGTCTTCCTC
	TS Cry2 Seq F2	CCATGGTTTGCAGGATCTTC
	TS Cry2 Seq R2	GTCTCCCCTCCCTTCCATAC
	TS Cry2 Seq F3	CTGAAACACGCGTACACTCC
	TS Cry2 Seq R3	AATCCATGGGAACCCAGTCT
	TS Cry2 Seq F4	GACCACATGAAAGGCAATCC
	TS Cry2 Seq R4	GGTCCACCATGGGCAGAG
	TS Cry2 Seq F5	TCATTCGCACGTATCTACCG
	TS Cry2 Seq R5	TGTCGGTATTACATCATTTATTCTACG
Talbaml1/cyc	TS Cyc RACE 3a F1 JO	TGTGTCTGAGAGCGTCACCCCCTT
	Ts Cyc rev fragment 1	GTCCACGTACCCAGACTCTAACT
	Ts Cyc fwd fragment 2	TCTTCGATGTCCACGTACCC
	Ts Cyc rev fragment 2	GCGACGCTTCTAGTTAGGAGT

	Ts cyc fwd fragment 3	ACCTCAACAAAAAGATTTCAACAG
	Ts Cyc rev fragment 3	ATTCCAACCCAACCGAAAC
	TS Cyc RACE 3a F1 JO	TGTGTCTGAGAGCGTCACCCCCTT
	TS Cyc RACE 3a F2 JO	AGATTGACTACATTCATGCGGCCTCAG
Talper	Tal period 4 R	TACCCAAGAGGCAATGGAAG
	primer6R	CTTCTGTGGTACCTGGTGC
	Primer7F	CTGTGAGTAGTTCGTGCCG
	primer6F	CAAGCCCCTTATTTCTTCC
	Tal period 2 R	CAGCAGCCATCAACAACTC
	Tal period 1 R	TCTCGAGCAGACCATGTCAC
	Primer5R	CTCTGCACACAACCCATGG
	TalUK Per RNAi rev	CTGTCGACCTATTCAGAGGAA
	TS PER RACE 5a R2	TTCCCTGAAGATATGGTGGTCGGCC
	TS PER RACE3a F1	GATCGTCAGCGGAATGAGCCTCTTCA
Talbmal1/cyc 3'RACE	Ts Cyc fwd fragment 3	ACCTCAACAAAAAGATTTCAACAG
Talbmal1/cyc 5'RACE	TS Cyc RACE 5aR1 JO	CATGAATGTAGTCAATCTGCGGTGAGTG A
	TS Cyc RACE 5aR2 JO	GCTGGTCAAGAAATGGTGCACGTCCTGA
Taltim 3'RACE	Tim 3'RACE Nested	CGCGAGTGCAAGAGCACGACGAGTC
	Tim 3'RACE	CGCACAAGCCCGTAGCAGACGTCAA
Talper 3'RACE	TS_UKPer3RACE lsh8	CGAAGAAGG CGCGGTCGTCTCGAT
	TS_UKPer3RACENest	CTGCAATTCCTCCTCCGGACTTGTCAAT
Talper 5'RACE	Tal period 5’ gspN	CTGGAAGAAGCGGGCAACCAAAGCTTAC
	TS_UKPer5RACENest	CCAAGAGGCAATGGAAG TGCTGCCC
Talcry2 3' RACE	TalCry2 3’ RACE F4	GAGTTTTTCTACACGGCAGCCACCAACA
	TalCry2 3’ RACE F5	ACGGCAGCCACCAACAACCCCAAA
	TalCry2 3’ RACE F6	GACCACATGAAAGGCAATCCCATATG
Talclk 3' RACE	TalClk 3’ RACE F2	GAGGGCCTCTGCAATCATCGGTTA
	TalClk 3’ RACE F3	ATGTGGACGACCTGGAACGGGTGTCTAC
	TS_Clk 3 RACE	ATCTATCTAGACAATGTACAACACGGT
Talcry2 5' RACE	TalCry2 5’4 RACE R8	CAGGCGAACAACGATTGTGGTGTCAT
	TalCry2 5’ RACE R9	CCGAACGAGGCGACCCAGGCTTT
	TalCry2 5’ RACE R8	CAGGCGAACAACGATTGTGGTGTCAT
	TalCry2 5’ RACE R9	CCGAACGAGGCGACCCAGGCTTT
	TalCry2 3’ RACE F4	GAGTTTTTCTACACGGCAGCCACCAACA
	TalCry2 3’ RACE F5	ACGGCAGCCACCAACAACCCCAAA
	TalCry2 3’ RACE F6	GACCACATGAAAGGCAATCCCATATG
Talpdh 3' RACE	TalPDH 3’ RACE F1	TGGGGCTGCCAAAGTTTTTGAGGGAG
	TalPDH 3’ RACE F2	GACAAGAGGAACTCGGAGCTCATCAACT C
Talpdh 5' RACE	TalPDH 5’ RACE R1	GAGTTGATGAGCTCCGAGTTCCTCTTGT C
	TalPDH 5’ RACE R2	CTCCCTCAAAAACTTTGGCAGCCCCA
	GeneRacer™ 5’	CGACTGGAGCACGAGGACACTGA
	GeneRacer™ 5’ Nested	GGACACTGACATGGACTGAAGGAGTA
	Adapter Gene Racer™ RNA Oligo	CGACUGGAGCACGAGGACACUGACAUG GACUGAAGGAGUAGAAA

Table A.3: Primers & probes used for TaqMan® qPCR; primers abbreviated "Stand" were used to synthesize the qPCR standards. All 3’ non-fluorescent quenchers were MGB.

Use	**Oligonucleotide**	**Sequence**
cRNA standard	TalAKTaqStandF1	TATTTGGGGGCACAATTTGA
	TalAKTaqStandR1	CCAAGGCCAGTTTTCTTGTC
	TalClkTaqStandF1	TTCCTGTTCCTAGACCAGAGG
	TalClkTaqStandR1	ATTCTGGCTTGCTGTTCCAC
	TalCry2TaqStandF1	TGTTTGGAGGATGTGGACAA

	TalCry2TaqStandR1	ATGACTTCGATGCCCATCTC
	TalPerTaqStandF1	CTCGAGATTCGGTGCATTTT
	TalPerTaqStandR1	GCCATCACCTCTTCTTCCAA
	TalTimTaqStandF1	TGCACTTGGCCGGCATA
	TalTimTaqStandR1	TGCACTTGGCCGGCATA
	and respective T7 coupled versions see A.1.	
qRT-PCR	TalAKTaqF1	TCGAGGAACGGCTGTCCTT
	TalAKTaqR1	AGCAGCGTCAACCATTTTGTT
	TalClkTaqF1	TCGGTTACCTGCCATTCGA
	TalClkTaqR1	CAGGTCGTCCACATGGTAGTAAT
	TalCry2TaqF1	GCGCTCCCGCAGCTT
	TalCry2TaqR1	GGTCTTCCTCGAAACTCAGAACT
	TalPerTaqF1	GCCTCATGCCTCCATTCTACTG
	TalPerTaqR1	CGCAGAGGCTTGGTAGCATT
	TalTimTaqF1	TGCACTTGGCCGGCATA
	TalTimTaqR1	CTCGTCCGTCGACGTAGACA
qRT-PCR probes	TalAKTaqProbe	NED-CCTGAGCCAAGACAG
	TalClkTaqProbe	TGCTAGGTACCTCAGGTTA
	TalCry2TaqProbe	TCAAGGAGTGGAATACG
	TalPerTaqProbe	CGAGTTCGCGAGAAC
	TalTimTaqProbe	CGGACCTGCTCTTG

Table A.4: Statistical analysis of mRNA expression levels of *Talper, Taltim, Talcry2* and *Talclk* in *Talitrus* heads (n=6) and antennae (n=6 for DD and n=1 for DD 6 hrs phase advanced).

Head tissue		**One-way ANOVA**	
Name	**Light Conditions**	**F 7,39**	**p**
Talper	DD	15.390	<0.000
Taltim	DD	5.659	<0.000
Talcry2	DD	2.064	>0.05
Talclk	DD	0.773	>0.05
Talper	DD 6 hrs phase advanced	4.388	<0.01
Taltim	DD 6 hrs phase advanced	2.045	>0.05
Talcry2	DD 6 hrs phase advanced	3.358	<0.01
Talclk	DD 6 hrs phase advanced	0.937	>0.05
Antennae tissue			
Talper	DD	1.027	<0.05
Taltim	DD	2.143	>0.05
Talcry2	DD	0.984	>0.05
Talclk	DD	1.988	>0.05

Table A.5: Cosinor analysis of clock gene mRNA expression measurement. Absolute mRNA levels of four clock genes were analysed throughout the circadian cycle and under clock-shifted conditions for a cyclic expression pattern. Cosinor performs a sinusoidal curve fit to estimate cyclicity.

Name	**Tissue**	**Light conditions**	**F2,5**	**p**
Talper	heads	DD control	17,33	<0.01
Taltim	heads	DD control	3,82	>0.05
Talcry2	heads	DD control	18.84	<0.05
Talclk	heads	DD control	0,734	>0.05
Talper	antennae	DD control	6,41	<0.05
Taltim	antennae	DD control	0,333	>0.05

Talcry2	antennae	DD control	12,73	<0.05
Talclk	antennae	DD control	1,444	>0.05
Talper	heads	DD shifted	2,291	>0.05
Taltim	heads	DD shifted	0,284	>0.05
Talcry2	heads	DD shifted	0,282	>0.05
Talclk	heads	DD shifted	0,344	>0.05
Talper	antennae	DD shifted	0	>0.05
Taltim	antennae	DD shifted	0,859	>0.05
Talcry2	antennae	DD shifted	0,44	>0.05
Talclk	antennae	DD shifted	1,535	>0.05

Table A.6: Oligonucleotide sequences used in chapter 6.

Reaction	**Primer name**	**Oligonucleotide sequence**
Sequencing	Talchh F'	CTCCCTTCTCTCCACTGACCT
Sequencing	Talchh R'	GGACTCACTGACGAAGTTTGG
In situ	Talchh DIG T7 F'	T7-CTCCCTTCTCTCCACTGACCT
In situ	Talchh DIG T7 R'	T7-GGACTCACTGACGAAGTTTGG
In situ	Tal CHH DIG F'	CTCCCTTCTCTCCACTGACCT
In situ	Talchh DIG R'	GGACTCACTGACGAAGTTTGG
qRT-PCR	Talchh TaqMan F'	GCTACAGCAACGCGATGTTC
qRT-PCR	Talchh TaqMan R'	TTTCAGCGTACTTGTCGACCAT
qRT-PCR	Talchh TaqMan probe	6-FAM-CTGCCTCTACGACCTTATGCTGCACGA
qRT-PCR	TalAK TaqMan F'	TCGAGGAACGGCTGTCCTT
qRT-PCR	TalAK TaqMan R'	AGCAGCGTCAACCATTTTGTT
qRT-PCR	TalAK TaqMan	NED-CCTGAGCCAAGACAG
qRT-PCR cRNA standard	Talchh STD T7 F'	T7-CTCCCTTCTCTCCACTGACCT
qRT-PCR cRNA standard	Talchh STD T7 R'	T7-GGACTCACTGACGAAGTTTGG
qRT-PCR cRNA standard	TalAK STD F'	TATTTGGGGGCACAATTTGA
qRT-PCR cRNA standard	TalAK STD R'	T7-CCAAGGCCAGTTTTCTTGTC
5´ RACE	Talchh 5' RACE	GGGCCTTCCGAGGTCAGTGGA
5´ RACE	Talchh 5' RACE N	TGTTGGCCAGCAGACGGGAGA
3' RACE	Talchh 3' RACE	GACACTTCGTCTGTGTGCCGCTGGG
3' RACE PCR	Talchh 3' RACE N1	ACCAGGACAAGCTTCTCGTCTCTGGCCA
3' RACE	Talchh 3' RACE N2	CTGGGCCTTGTACGAACTACCAGGAC
Sequencing	Talchh Full 1F'	TTCACGCTTCCCTTTACCAC
Sequencing	Talchh Full 1R'	CCCACAATCTGGACCATTTC
Sequencing	Talchh full 3F'	CCAGATTGTGGGCAAGAAAT
Sequencing	Talchh full 3R'	GGCTGCTAGGGGTTCATTTT
Cloning	M13 forward	GTAAAACGACGGCCAG
Cloning	M13 reverse	CAGGAAACAGCTATGAC

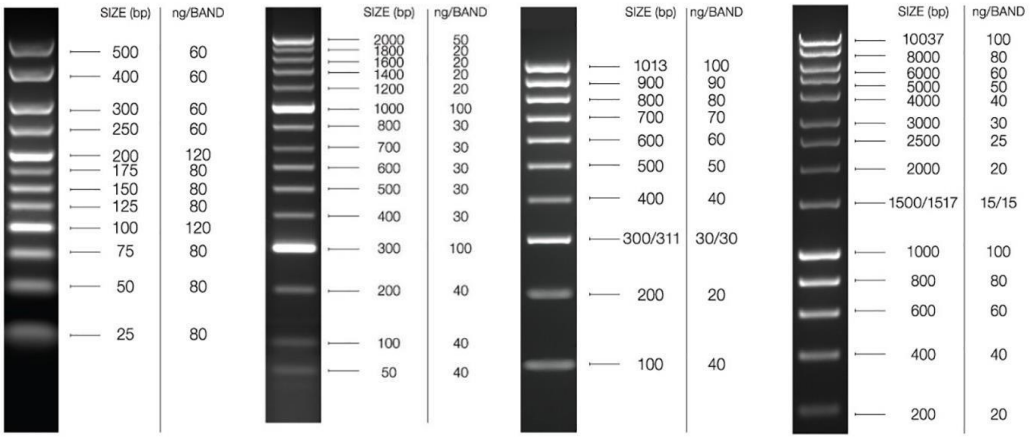

Figure A.1: HyperLadder™ series used for agarose gel electrophoresis. The ladders are shown in the following order: HyperLadder™ 25 bp, HyperLadder™ 50 bp, HyperLadder™ 100 bp, HyperLadder™ 1 kb (HyperLadder Selection Chart, 2017).

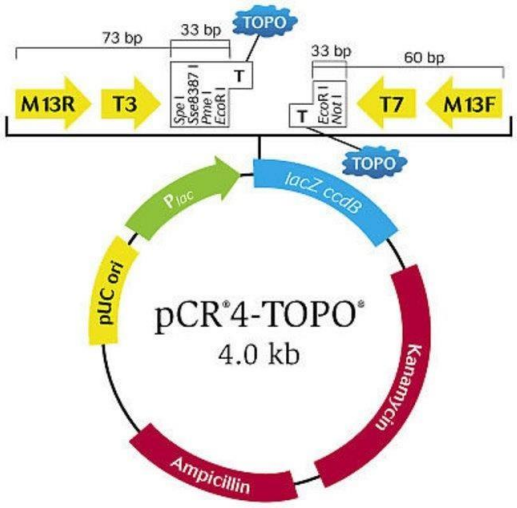

Figure A.2: pCR™4-TOPO® Vector map The multiple cloning site (MCS) is flanked by M13 forward and reverse priming sites and the vector contains an ampicillin resistance gene as well as a *lacZ* ccdB necessary for blue-white screening (http://www.thermofisher.com/order/catalog/product/K457502).

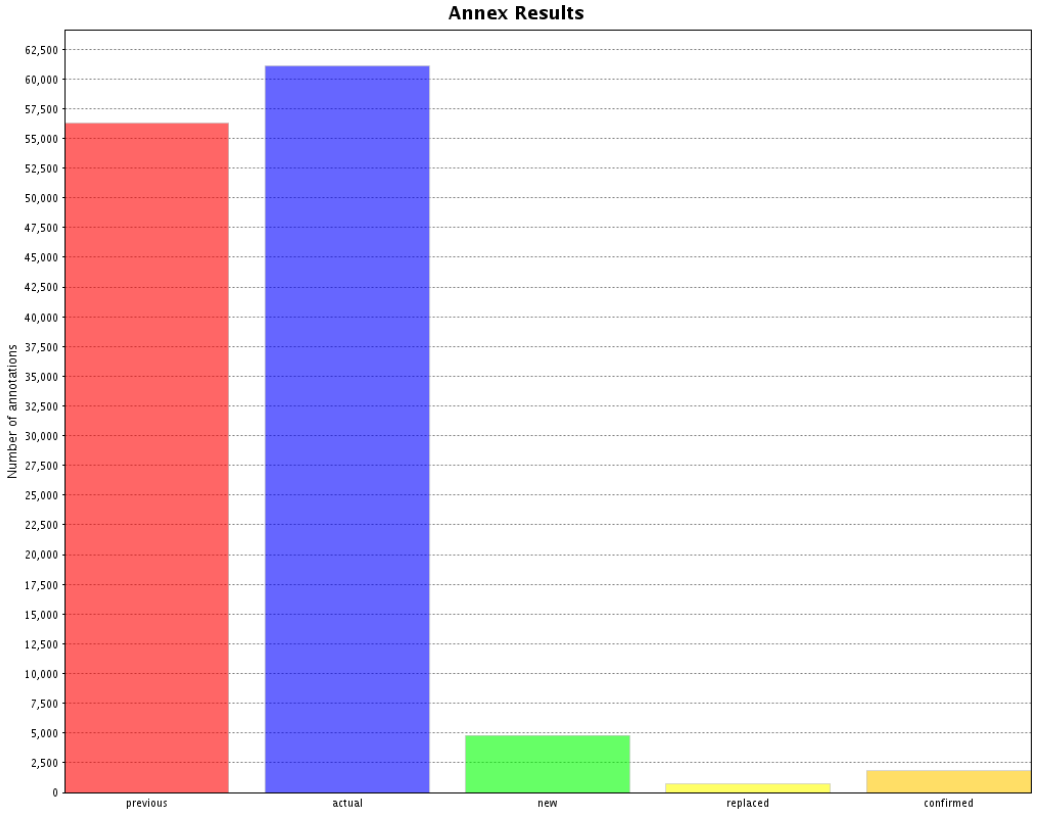

Figure A.3: Annex results. The bar graph displays the number of anotations that were made previous to the Annex run, the actual annotations, the new annotations made thourgh Annex, the replaced anotations and the confirmed annotations.

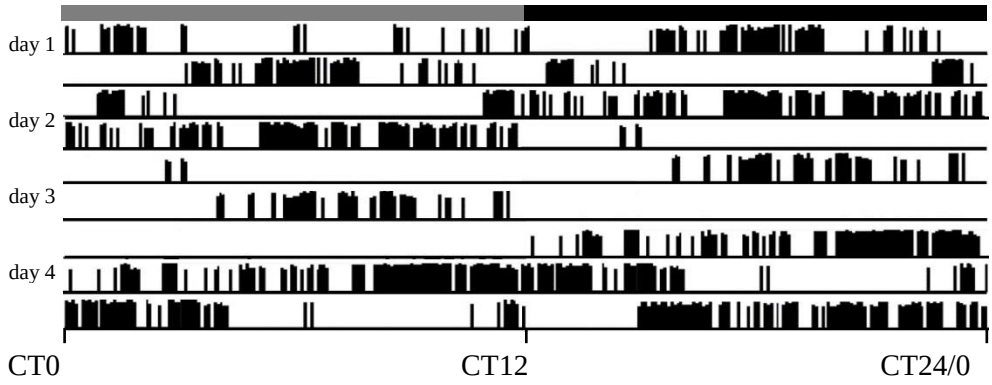

Figure A.4: Activity measurement of 10 animals. 12,5 µM PF-480056 (in crustacean saline) was injected with a towed, fine glass capillary at the end of a syringe. Animals' activity was radiographically recorded for 10 successive days and is displayed in arbitrary units. Despite previous behavioural rhythmicity, (data not shown) animals become arrhythmic upon injections.

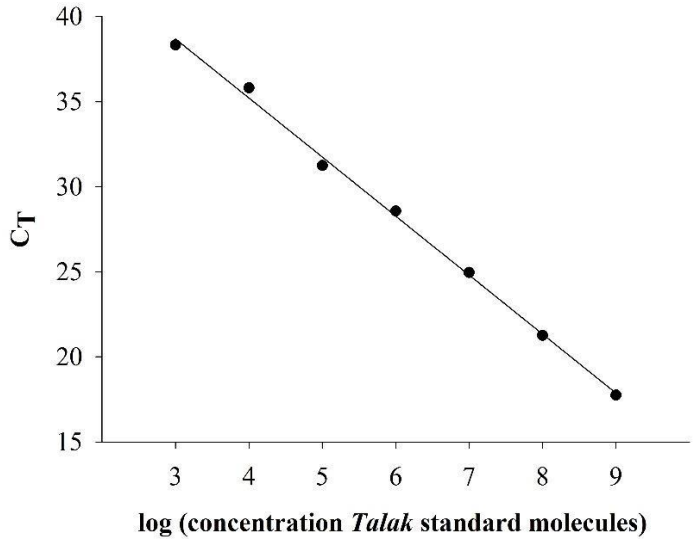

Figure A.5: qRT-PCR standard curve for *Talak* cRNA standards. The amount of standards used (log(concentration)) is plotted against the average CT values. The PCR reaction efficiency is 94.17% and the R^2 value 0.9997.

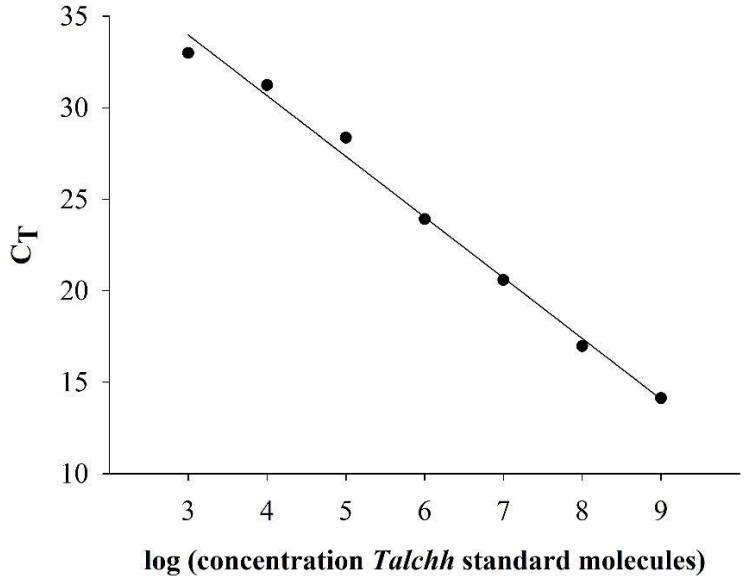

Figure A.6: qRT-PCR standard curve for *Talchh* standards. The amount of standards used (log(concentration) is plotted against the average CT values. The PCR reaction efficiency is 100.13% and the R^2 value 0.9918.

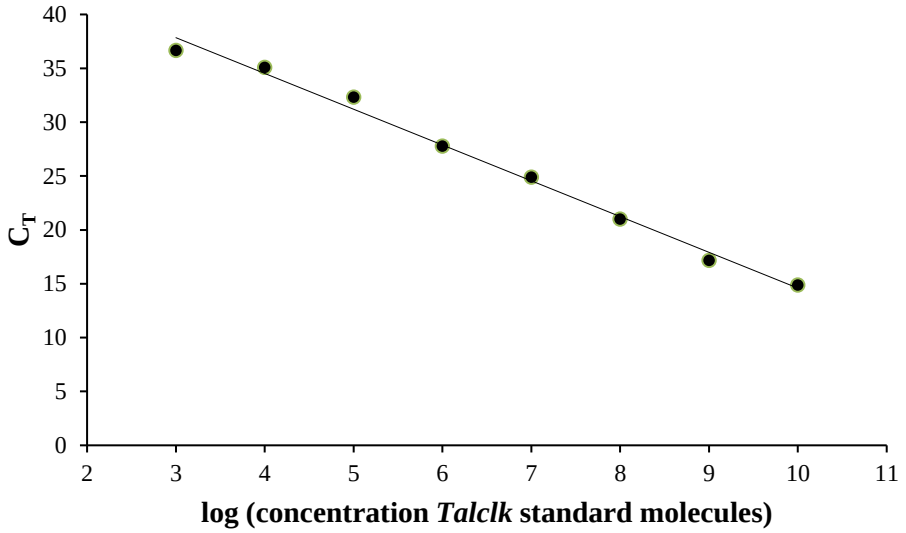

Figure A.7: *q*RT-PCR standard curve for *Talclk* cRNA standards. The amount of standards used (log(concentration)) is plotted against the average CT values. The PCR reaction efficiency is 100.03% and the R^2 value 0.9919.

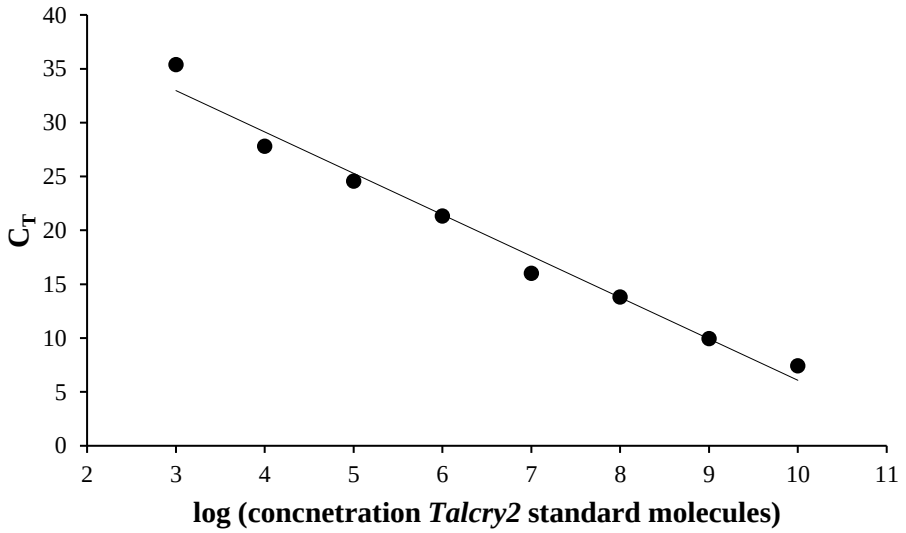

Figure A.8: qRT-PCR standard curve for *Talcry2* cRNA standards. The amount of standards used (log(concentration)) is plotted against the average CT values. The PCR reaction efficiency is 99.53% and the R^2 value 0.932.

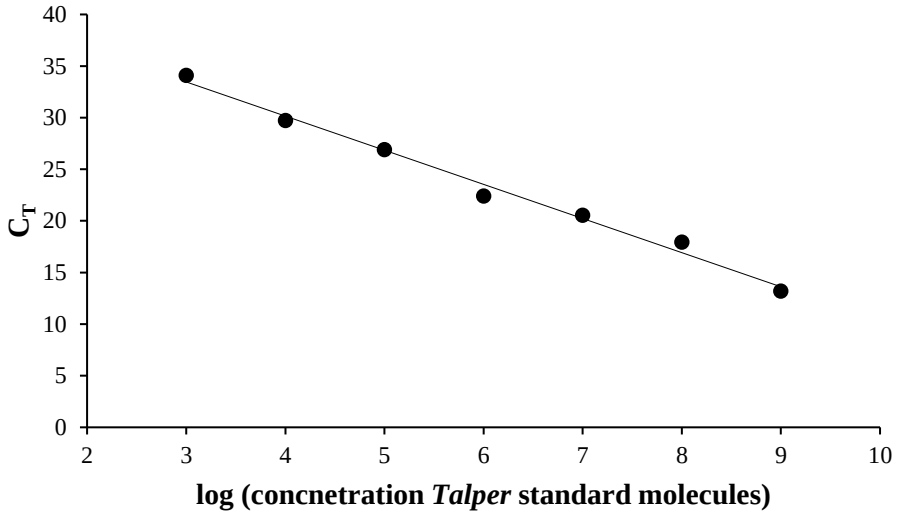

Figure A.9: qRT-PCR standard curve for *Talper* cRNA standards. The amount of standards used (log(concentration)) is plotted against the average CT values. The PCR reaction efficiency is 100.6% and the R^2 value 0.9897.

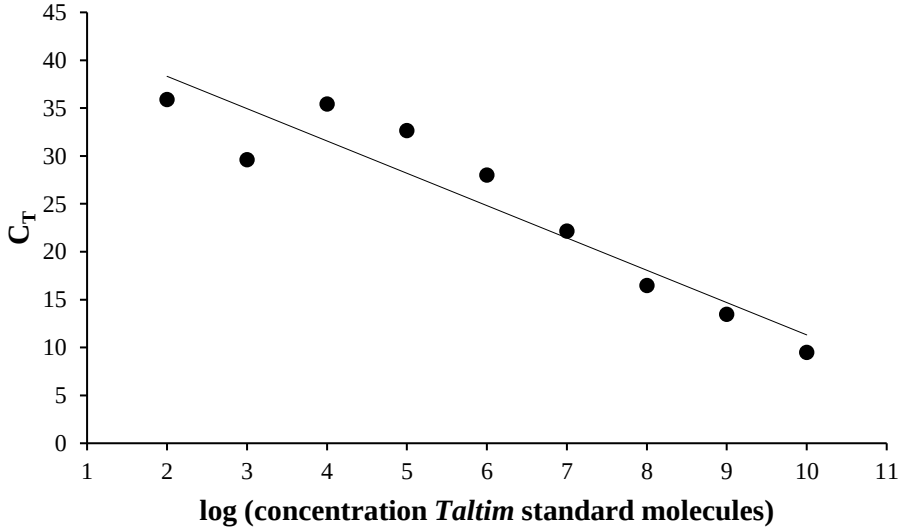

Figure A.10: qRT-PCR standard curve for *Taltim* cRNA standards. The amount of standards used (log(concentration)) is plotted against the average CT values. The PCR reaction efficiency is 97.8% and the R^2 value 0.8866.

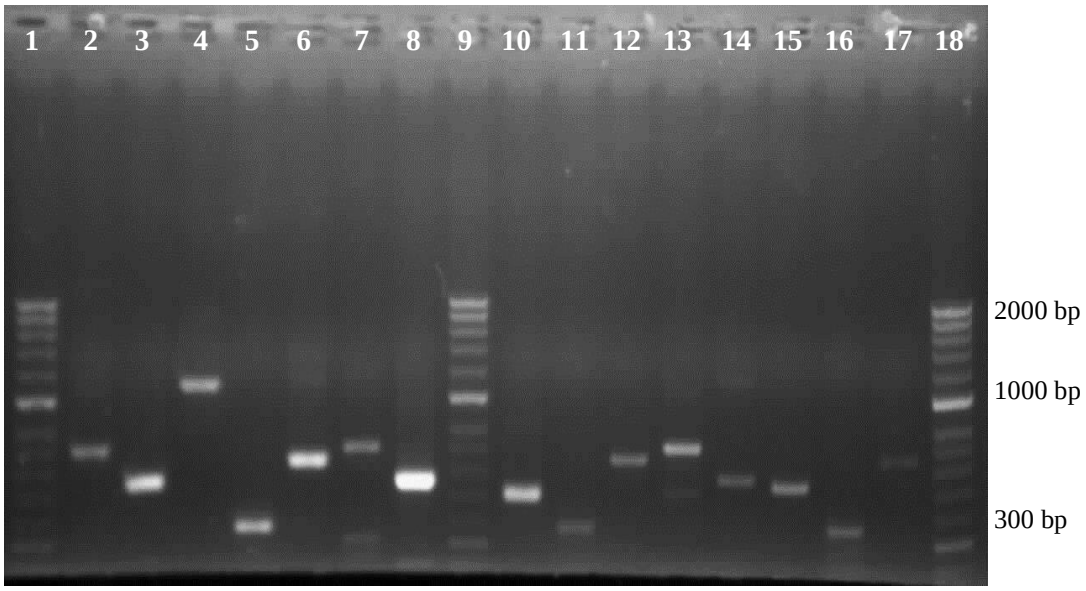

Figure A.10: Template cDNA from brain, primary and secondary antennae were incubated with primers for *T. saltator* core clock genes. PCR conditions are shown in Table 2.1. Tissue, clock gene and expected band sizes are given for each sample lane: 1=Hyperladder II, 2=*Talbmal1*-heads-~700bp, 3=*Talclk*- heads-551 bp, 4=*Talcry2*-heads-1125, 5=*Talper*-heads- 369 bp, 6=*Taltim*-heads-571 bp, 7=*Talbmal1*-primary antennae-~700 bp, 8=*Talclk*-primary antennae-561 bp, 9=Hyperladder II, 10=*Talcry2*-primary antennae-499 bp, 11=*Talper*- primary antennae-369 bp, 12=*Taltim* -primary antennae-571 bp, 13=*Talbmal1*-secondary antennae-~700 bp, 14=*Talclk*-secondary antennae-561 bp, 15=*Talcry2*-secondary antennae-530 bp, 16=*Talper* -secondary antennae-369 bp, 17=*Taltim*-secondary antennae- 571 bp, 18=Hyperladder II

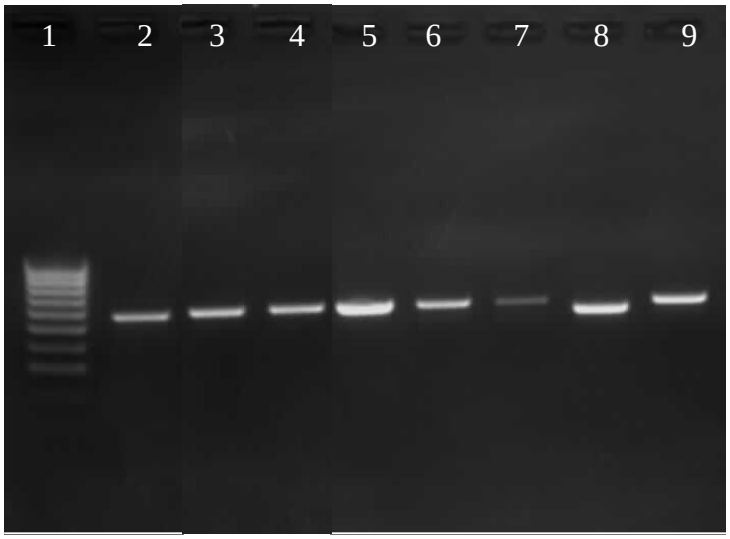

Figure A.11: Agarose gel for *Talclk* sequencing PCRs Fragments 1, 3-4, 6-10. Primers used were (sequences shown in Tab. A.2): 1=Hyperladder II, 2=TS Clk F1/R1 (561 bp), 3=TS Clk F3/R3 (550 bp), 4=TS Clk F4/R4 (551 bp), 5=TS Clk F6/R6 (551bp), 6=TS Clk F7/R7 (551 bp), 7=TS Clk F8/R8 (551 bp), 8=TS Clk F9/R9 (501 bp), 9=TS Clk F10/R10 (561 bp)

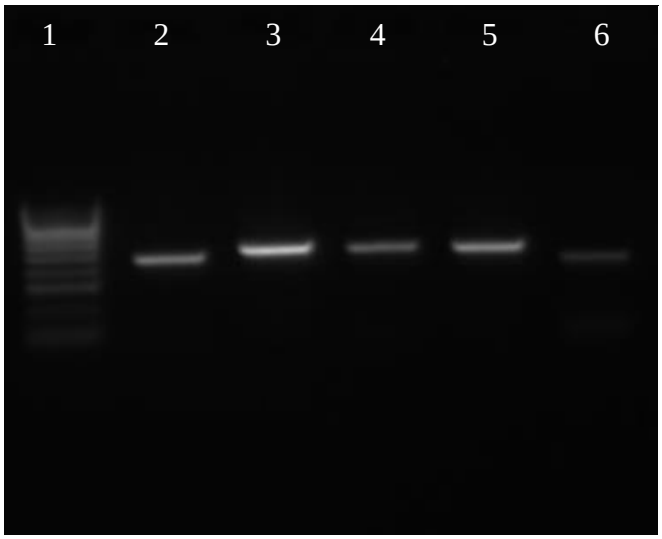

Figure A.12: Agarose gel for *Talcry2* sequencing PCRs Fragement 1-5. Primers used were (sequences shown in Table A.2): 1=Hyperladder II, 2=TS Cry2 seq F1/R1 (468 bp), 3= TS Cry2 seq F2/R2 (530 bp), 4= TS Cry2 seq F3/R3 (595 bp), 5= TS Cry2 seq F4/R4 (499 bp), 6= TS Cry2 seq F5/R5 (395 bp)

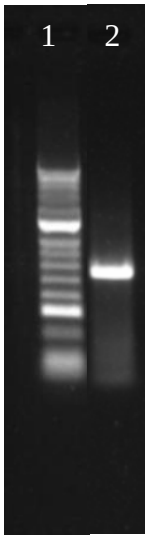

Figure A.13: Agarose gel for *Taltim* sequencing PCR Fragment 1. Primers used were (sequences shown in Table A.2): 1=Hyperladder II, 2=Tal TIM f1 fwd/rev (575 bp)

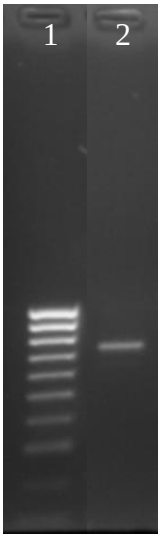

Figure A.14: Agarose gel for *Taltim* sequencing PCR Fragment 2. Primers used were (sequences shown in Table A.2): 1=Hyperladder III, 2=Tal TIM f2 fwd/rev (643 bp)

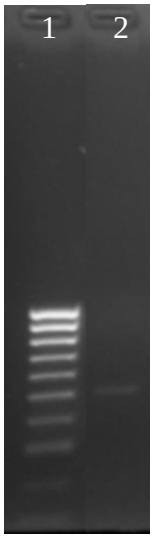

Figure A.15: Agarose gel for *Talclk* sequencing PCR Fragment 2. Primers used were (sequences shown in Table A.2): 1=Hyperladder III, 2= TS Clk F1/R1 (551 bp)

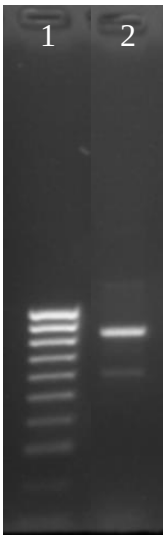

Figure A.16: Agarose gel for *Talbmal1/cyc* sequencing PCR Fragment 1. Primers used were (sequences shown in Table A.2): 1=Hyperladder III, 2= F1/R1 (bp)

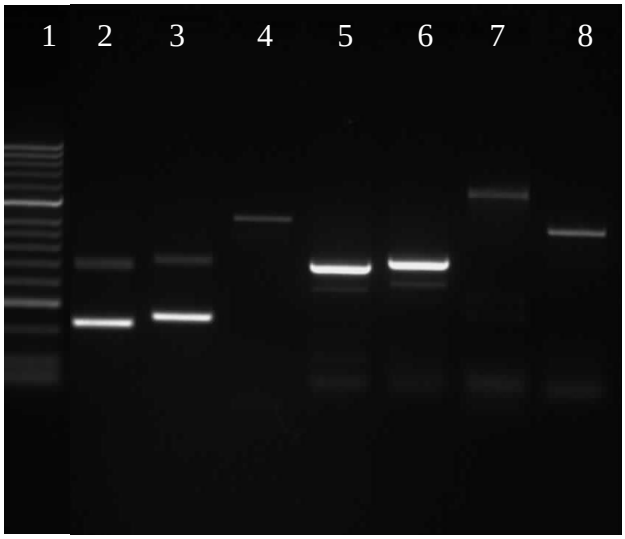

Figure A.17: Agarose gel for *Talper* sequencing PCRs Fragments 1, 3-4, 6-10. Primers used were (sequences shown in Tab. A.2): 1=Hyperladder II, 2=Tal period 3R/TS PER RACE 5aR1 (228 bp), 3=Tal period 3R/ Tal Per Taq R1 (254 bp), 4=Tal period 3R/TS period RNAi R (830 bp), 5=primer 6R/TS PER RACE 5aR1 (507 bp), 6=primer 6R/Tal Per Taq R1 (533 bp), 7=primer 6R/TS period RNAiR (1109 bp), 8=TS_UK Per RNAi fwd/Tal period 3F (769 bp)

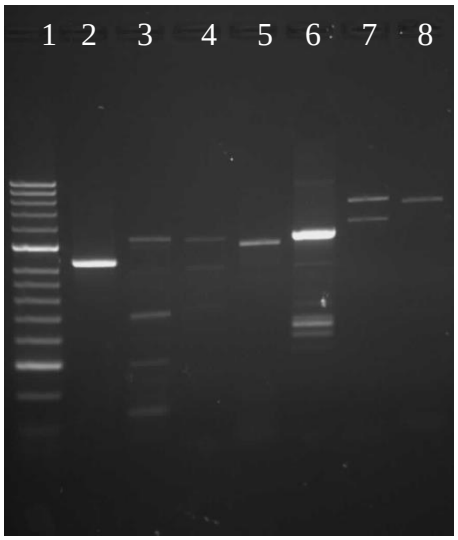

Figure A.18: Agarose gel for *Talper* sequencing PCRs Fragments. Primers used were (sequences shown in Tab. A.2): 1=Hyperladder II, 2=TS_UK Per RNAi fwd/primer 6F (856 bp), 3=TS PER RACE 3a R2JO/Tal period 3F (?-> RACE PCR to determine 5' ends), 4=TS period RNAiR/primer 6F (?-> RACE PCR to determine 5' ends), 5=Tal Per Taq F1/Tal period 3F (964 bp), 6= Tal Per Taq F1/primer 6F (1051 bp), 7=primer 5R/Tal period 1F (1438 bp), Tal period 1R/Tal period 1F (1379 bp)

Table A.7: NCBI Blast search results of *T. saltator* putative clock transcript and protein sequences

Putative clock protein	**Tblastn (Accession #)**	**Species**	**E-value**	**% aa identity/ similarity**	**Tblastp (Accession #)**	**Species**	**E-value**	**% aa identity/ similarity**
TalCRY2	KC885970	*Eurydice pulchra*	0.0	78/89	AGV28717	*Eurydice pulchra*	0.0	78/98
TalCLK	AY842303	*Macrobrachium rosenbergii*	3,00E-64	76/90	AAX44045	*Macrobrachium rosenbergii*	2,00E-67	71/84
TalPER	KC885967	*Eurydice pulchra*	3,00E-121	44/64	AGV28714	*Eurydice pulchra*	0.0	37/53
TalTIM	XM_009048115	*Lottia gigantea*	3,00E-108	49/68	KDR17447	*Zootermopsis nevadensis*	6,00E-139	52/72
TalBMAL1	JQ670886	*Pacifasticus leniusculus*	4,00E-139	43/55	AFV39705	*Macrobrachium rosenbergii*	2,00E-154	43/57
TalPDH I	AB073368	*Marsupenaeus japonicus*	0.073	90/95	BAB91011	*Marsupenaeus japonicus*	0.041	90/95
TalPDH II	-	-	-	-	BAD13514	*Meimuna opalifera*	0.091	34/48
TalCK2α	XM_011140473	*Harpegnathos saltator*	0.0	92/97	1NA7_A	*Homo sapiens*	0.0	88/94
TalCK2ß	XM_012208415	*Atta cephalotes*	5,00E-124	82/90	XP_012287730	*Orussus abietinus*	8,00E-144	86/94
TalCWO	XP_003744690	*Metaseiulus occidentalis*	8,00E-80	82/89	XP_003744690	*Metaseiulus occidentalis*	2,00E-80	82/89
TalDBT	KC885972	*Eurydice pulchra*	0.0	95/97	AGV28719	*Eurydice pulchra*	0.07e-37	95/97
TalPDP1ε	XM_012203776	*Atta cephalotes*	2,00E-35	70/85	EZA50108	Cerapachys biroi	0.0	68/82
TalPP1	XM_011065955	*Acromyrmex echinatior*	0.0	79/85	XP_011136198	*Harpegnathos saltator*	0.0	94/97
TalMTS	XM_002426681	*Pediculus humanus corporis*	0.0	95/98	XP_002426726	*Pediculus humanus corporis*	0.0	95/98
TalWBT	XM_008197190	*Tribolium castaneum*	0.0	88/94	XP_971164	*Tribolium castaneum*	**0.0**	88/94
TalTWS	JQ867383	*Scylla paramamosain*	0.0	86/92	AFK24473	*Scylla paramamosain*	**0.0**	87/93
TalSGG	XM_012400594	*Athalia rosae*	0.0	79/86	XP_012256017	*Athalia rosae*	**0.0**	80/87
TalSLIMB	XM_012405697	*Athalia rosae*	0.0	82/90	KDR19729	*Zootermopsis nevadensis*	0.0	84/92
TalVRI	JQ011276	*Clunio marinus*	6,00E-41	64/91	KDR16467	*Zootermopsis nevadensis*	3,00E-46	50/64
TalEBONY	XM_008199683	*Tribolium castaneum*	7,00E-85	39/56	CAI26307	*Periplantea americana*	1,00E-95	39/57
TalRORα	XM_001987136	*Drosophila grimshawi*	3,00E-71	68/77	XP_011290218	*Musca domestica*	2,00E-75	70/80
TalREV-ERB	AM710419	*Blattella germanica*	2,00E-102	45/64	XP_011259848	*Camponotus floridanus*	1,00E-105	48/65
TalSIRT1	XM_008555996	*Microplitis demolitor*	2,00E-81	69/84	ABG78545	Schistosoma mansoni	1,00E-115	47/62
TalSIRT2	XM_963962	*Tribolium castaneum*	5,00E-130	62/75	EFA06770	*Tribolium castaneum*	4e—141	60/73
TalSIRT4	XM_002605838	*Branchiostoma floridae*	4,00E-110	57/69	XP_008480918	*Diaphorina citri*	8,00E-116	57/72
TalSIRT6	XM_011552750	*Plutella xylostella*	3,00E-120	55/71	EFX74386	*Daphnia plurex*	2,00E-123	50/67
TalSIRT7	XM_012287821	*Megachile rotundata*	3,00E-144	56/71	XP_012143211	*Megachile rotundata*	8,00E-147	56/71
TalJET	XM_012430170	*Orussus abietinus*	0.0	65/77	XP_008193983	*Tribolium castaneum*	0.0	63/78

APPENDIX B

Buffers and Solutions

Agar plates	Dissolve 15 g Bacto Agar in 1 L water by autoclaving. When the medium has cooled down to 50 °C add ampicillin (50µg/mL working concentration) and mix gently. Pour into sterile plates carefully and allow to cool down. Store reversed at 4°C. I fused for blue-white screening, one hr before use bring plates to 37°C in the incubator and add IPTG in a final concentration for 0.2 mM and X-gal in a final concentration of 40 µg/mL.
Crustacean physiological saline (low K^+)	NaCl 29 g, KCl 0.71 g, $MgSO_4$ * 7 H_2O 3,16 g; $CaCl_2$*2H_2O 2.38 g; $MgCl_2$*6H_2O 0,17 g, $NaHCO_3$ 0.5g, HEPES (10 mM) 2.38 g add 500 mL water pH to 7.4 and treat with DEPC.
DTT (1 M)–20 ml	Dissolve 3.085 g DTT in 20 mL 10 mM sodium acetate (pH 5.2). Aliquots à 1 ml.
Ethidium bromide solution for PAGE gel	EtBr (15µL in 100mL TBE (0.5x))
IPTG (0.1 M)–50 ml	Dissolve 1.19 g IPTG in 40mL H_2O.Adjust volume to 50mL with H_2O. Aliquot à 5 mL and sterilize by filtration. Store at –15 to –25°C; stable up to 4 months.
LB (Luria Broth) medium	10 g Bactor Tryptone, 5 g Bacto Yeast extract, 10 g NaCl in 900 mL H_2O. Adjust pH to 7.0 and fill up to 1L. Sterilize by autoclaving.
PBS (Phosphate Buffered Saline) 10 x	Dissolve 80 g NaCl, 2 g KCl, 26.8 g Na_2HPO_4 – $7H_2O$ and 2.4 g KH_2PO_4 in 800 mL H_2O and adjust pH to 7.4. Adjust volume to 1 L and store at room temperature (+15 to +25°C).
PBST	1 mL Tween 20 dissolved in 1 L PBS buffer.
PFA (4%)	Add 40 g paraformaldehyde to 1L of 0.1M phosphate buffer and heat up to 65°C while stirring. Add 1M NaOH until solution clears. Cool down to room temperature and filter solution. Store at 4°C.
PTX	0.1% (v/v) Triton-X-100 and 0.02% NaN_3 in PBS.
RNA elution buffer (PAGE-gel)	0.5M ammonium acetate, 1mM EDTA 0,2 % SDS.

SSC 20x	Dissolve 175.3 g NaCl and 88.2 g sodium citrate–$2H_2O$ in 800 mL H_2O. Adjust pH to 7.0 and the volume to 1 L. Aliquot and autoclave. Store at room temperature (+15 to +25°C).
Stephanini's fixative	Combine 12.5 mL 4% w/v paraformaldehyde solution (from 16% w/v stock solution) and 15 mL picric acid (saturated aqueous), stirring on a heat plate under the hood. Add 10 M NaOH solution until clear. Filter. Make up to 100 mL with 0.1 M phosphate buffer. Adjust to pH 7.3 if necessary.
TAE (Tris-acetate) 50x:	Dissolve 242 g Tris in 500 mL H_2O. Add 100 mL 0.5 M Na_2EDTA (pH 8.0) and 57.1 mL glacial acetic acid. Adjust volume to 1 L with H_2O. Store at room temperature (+15 to +25°C).
TBE (Tris-borate; 0,5x as running buffer) 10x*	Dissolve 108 g Tris and 55 g boric acid in 900 mL H_2O. Add 40 mL 0.5 M Na_2EDTA (pH 8.0) and adjust volume to 1 L. Store at room temperature (+15 to +25°C).
TBS (Tris buffered saline) 1x	Dissolve 6.05 g Tris (50 mM) and 8.76 g NaCl (150 mM) in 800 mL H_2O and adjust pH to 7.5. Adjust volume to 1 L.
TBST (Tris buffered saline-Tween) 1x	1 mL Tween 20 dissolved in 1 L TBS buffer.
TE (Tris-EDTA) 1x	Dissolve 10 mL 1 M Tris (pH 8.0, 7.6 or 7.4) and 2 mL 0.5 M Na_2EDTA (pH 8.0) in 800 mL H_2O. Mix and adjust volume to 1 L. Store at room temperature (+15 to +25°C).
TMN	100 mM NaCl, 50 mM $MgCl_2$, 100 mM Tris-HCl (pH 9.5) in H_2O.
TMNT	0.05% (v/v) Tween 20 in TMN buffer.
TNE	Dissolve 50 mM Tris-HCl (pH 7.4) in 100 mM NaCl solution and add 0.1 mM EDTA.
Tris (1 M)	Dissolve 121.14 g Tris in 800 mL H_2O. Adjust pH and add water H_2O to make 1L. Store at room temperature (+15 to +25°C).
X-gal (20 mg/ml) 20 ml*	Dissolve 400 mg X-gal in 20 mL N,N'-dimethylformamide. Aliquot à 500 µl and store protected from light at –15 to –25°C. Stock solution is stable for up to 4 months.

APPENDIX C

List of Origins (consumables)

ActiMetrics, Wilmette, IL, USA

Adobe Systems Incorporated, San Jose, CA, USA

Ambion™, Thermo Fisher Scientific, Waltham, MA, USA

Applied Biosystems®, Thermo Fisher Scientific, Waltham, MA, USA

Bioline Reagents, London, UK

DakoCytomation, Carpinteria, CA, USA

Eurogentec, Seraing, Belgium

GB Healthcare, Amersham, Buckingham, UK)

Guardall Limited, Newbridge, UK

IBM Corporation, Armonk, NY, USA

Illumina®, Inc., San Diego, CA, USA

Invitrogen™, Thermo Fisher Scientific, Waltham, MA, USA

Leica Microsystems, Wetzlar, Deutschland

Leitz, Wetzlar, Germany

Life Technologies™, Thermo Fisher Scientific, Waltham, MA, USA

Microsoft, Microsoft Redmond Campus Redmond, Washington, USA

Molecular Probes, Eugene, OR, USA

Qiagen N.V., Venlo, Netherlands

Rainbow, Maimeri S.p.A., Mediglia Milano, Italy

Roche Holding AG, Basel, Switzerland

Sigma-Aldrich, St. Louis, MO, USA

Tetra, Melle, Germany

Thermo Fisher Scientific, Waltham, MA, USA

TriKinetics Inc, Waltham, MA, USA